

Genetic and Epigenetic Factors Determining Centromere Structure and Function in *Candida* Species

A thesis Submitted for the degree of

Doctor of Philosophy

By

Jitendra Thakur



**Molecular Biology and Genetics Unit,
Jawaharlal Nehru Centre for Advanced Scientific Research,
(A deemed University)
Jakkur, Bangalore- 560064, India**

July 2011

.....TO MY FAMILY

DECLARATION

I hereby declare that this thesis entitled “**Genetic and Epigenetic Factors Determining Centromere Structure and Function in *Candida* Species**” is an authentic record of research work carried out by me under the supervision of **Dr. Kaustuv Sanyal** at the Molecular Biology and Genetics Unit, Jawaharlal Nehru Centre for Advanced Scientific Research, Bangalore-560064, India and that this work has not been submitted elsewhere for the award of any other degree. In keeping with the norm of reporting scientific observations, due acknowledgements have been made whenever the work described was based on the findings of other investigators. Any omission, which might have occurred by oversight or misjudgment, is regretted.

Jitendra Thakur

Place Bangalore

Date :

Certificate

This is to certify that the work described in this thesis entitled “**Genetic and Epigenetic Factors Determining Centromere Structure and Function in *Candida* Species**” is the result of the investigations carried out by **Ms. Jitendra Thakur** in the Molecular Biology and Genetics Unit, Jawaharlal Nehru Centre for Advanced Scientific Research, Bangalore, India under my guidance, and that the results presented in this thesis have not previously formed the basis for the award of any other diploma, degree or fellowship.

Kaustuv Sanyal

Molecular Biology and Genetics Unit

Jawaharlal Nehru Centre for Advanced Scientific Research

Bangalore 560064

Place: Bangalore

Date:

Acknowledgements

I acknowledge the presence of almighty GOD for His kind benedictions and blessings and His unseen hand over my head to make me feel that He is always with me. Before I start thinking close to home I want to express my gratitude to all those who helped me achieve what I have today.

I express my sincere thanks to Prof. Kaustuv Sanyal for his guidance and for providing necessary facilities to undertake studies presented in this thesis.

I greatly admire Prof. C. N. R. Rao, the founding President of JNCASR, for establishing this extraordinary research institute. I am grateful to the president, Prof. M.R.S Rao for his continuous support. I acknowledge scientific (JNCASR Colloquium) and non scientific (Hostel Day) insights that he provided us during his seminars.

I would like to take this opportunity to thank Prof. Anuranjan Anand, the Chairman, MBGU, JNCASR, for his continuous encouragement throughout my PhD. I owe special thanks to Prof. Namita Surolia for her constant encouragement and the affection she has bestowed on me. Her generous and appreciating behavior is one of those things due to which I am highly attached to the department. I would like to thank Prof. Tapas Kundu, Prof. Uday Kumar Ranga, Prof. Hemlatha Balaram and Prof. Maneesha Inamdar for providing a stimulating environment in the department. I highly appreciate Prof. Chandrabhas Narayana for his special efforts in making me understand organic spectroscopy course in my first year. I also thank short term fellows Prof. Dharni Dhar Dubey, Dr. Deepti Jain, Dr. Jonathan, and Dr. Indrani Bose whose presence in the lab made it a better place to work. I acknowledge timely help rendered by Suma (Confocal facility), Anitha (Sequencing facility), Roopa (Mass spec facility), Dr. Suresh, Dr. Prakash (Animal house facility), Sukanaya ma'am, Princy ma'am (Academic section), library staff, computer lab staff and administrative staff.

Candida albicans, the model system I worked on, deserves special thanks for being highly versatile and so different from other yeasts in many aspects that made the work presented in this study interesting. I thank Prof. Judith Berman, Prof. Joachim Morschhauser, Prof. Parag Sadhale, Suzanne Noble and Peter Koetter for their generosity in sharing *C. albicans* strains and other reagents with us.

I acknowledge Sreedevi Padamanabhan and Prof. Rahul Siddharthan for their indispensable contribution in work on *C. dubliniensis* centromeres. I am highly grateful to the Department of

Biotechnology, Ministry of Science and Technology, India for the financial support during my MSc. and PhD courses.

I am indebted to all my teachers from schools and college especially Urmila Kapoor, Neelam Ma'am, Dr. Kishori Lal, Dr. U. D. Sankhyan, and Dr. Jaswant Singh for their remarkable teaching, encouragement, blessings and support. I am grateful to my graduation batchmates and friends Priyanka Thakur, Ajay Deepak Verma, Surender Singh Rana, Chirag Sharma and Rupesh Malhotra for providing highly stimulating environment. I thank all my juniors in college and hostel whose constant admiration has helped me expanding my knowledge and improving my personality to keep up with their expectations.

I am grateful to everybody in the department of Biotechnology, Summer Hills, Shimla for providing a wonderful ambience during my MSc. course. The day I joined the department has been the happiest day of my life so far and memories of that day are still so fresh in my mind. Prof. T. C. Bhalla (the Dean, Faculty of Life Sciences, HPU, Shimla) has been a fatherly figure and a great source of inspiration. I will always miss his constant support and observation that he showed during my MSc. tenure in Shimla. I sincerely thank my MSc. project Supervisor Prof. S. S Kanwar (Chairman, Dept of Biotechnology HPU, Shimla) for his guidance, keen interest in my work and most importantly for helping me in finishing my MSc. project work on time. I am truly grateful to my MSc. batchmates Nandana Bhardwaj, Shilpa Raghuvanshi, Asha Minz and Sunita Nayak for their unconditional support and affection. Most memorable moments spent during MSc. were joint study sessions with Shilpa at Advance studies, Summer Hills Railway Station and many other places around Summer Hills. I thank all my seniors and grand seniors for their great care and invaluable help both in the department as well as in the hostel.

I express my sincere gratitude for Dr. Sanjay Kumar (Scientist F, Biotech division, Institute of Himalayan Bioresources and Technologies, Palampur) who let me work in his well equipped, highly disciplined and stimulating lab for my MSc. project training. I am highly indebted to all the members of his lab for being so generous. I highly appreciate Hitesh Thakur, Anu Sharma and Ravi Shankar Singh who discussed with me many aspects of research with a great enthusiasm.

Himani Joshi, Sivani Vempati and Nishtha Pandey are the part of most memorable moments that I spent in JNC. Himani and Sivani have been close pals and great well-wishers. Nishtha, my constant companion for the discussions related to work presented in this thesis had been very critical about speculations that I made related to my odd and even results (however odds were always favorite to both of us). I always had to think hard to convince her about my explanations

which made things better for me in every possible way. I would never forget the moments we laughed to madness on my funny description of few real life events (which mostly were stretched up a little by me only to make stories sound funnier). I thank 1st batch of POBE students- Deepti Ramachandran, Taruni Roy, Sonal Jain, Sneha Shah, Jatin Nagpal, Vineet jain, Tejaswi Satpute and Swathi Srivathsa for being my wonderful companions during their POBE tenure in JNC. Deepti Ramachandran, an intelligent POBE student who worked with me during her POBE tenure, Anuja C, a summer student during my first year of PhD and Taruni Roy who worked in the opposite lab have been great friends ever since.

I am grateful to Sivani Vempati (my junior) and Pushpa Thakur (my sister) for their invaluable suggestions and help during my thesis writing. I sincerely thank Sreedevi Padamanabhan, Vikram Naik, Laxmi S. Rai, Tanmoy Chakraborty and Nagraj for their unconditional desire to help me whenever I needed one. I acknowledge Garima Verma, Selvi R, Mangai A, Aparna G and Meenakshi Sharma for helpful discussions on various topics. I express my sincere thanks to my PhD batchmates – Himani Joshi, Abhishek Sinha, Deepak Jha, Mukti Mishra, Mahesh B, Laxmi Mishra and Libin Abraham for good discussions on various course work subjects and all the help and support thereafter.

To enunciate gratitude to my parents will be a futile exercise as words fail to express their contribution in my life. They are the embodiment of love, pride, sacrifice and self respect. They worked harder than I have worked on me so everything I have achieved so far and what lies in future for me to achieve is solely their accomplishment. My parents have given me all the freedom in life but more importantly, at the same time they taught me how to make best use of this freedom. Memories of childhood spent with my sister and brother are overloaded in my heart that make me nostalgic so often. These memories have bound us together and we shall always be there for each other.

Jitendra

July14, 2011

Table of content

1. INTRODUCTION.....	1-44
1. Introduction.....	1
1.1 Cell Cycle, chromosome segregation, human diseases associated with it.....	2
1.2 Centromeres.....	3
1.3 Types of centromeres.....	4
<i>1.3.1 Point centromeres.....</i>	<i>4</i>
<i>1.3.2 Regional centromeres.....</i>	<i>5</i>
<i>1.3.3 Intermediate centromeres.....</i>	<i>7</i>
<i>1.3.4 Diffused centromeres.....</i>	<i>7</i>
1.4 Neocentromeres.....	8
1.5 Epigenetic behavior of centromeres in three different classes of centromeres	10
1.6 Factors controlling centromere formation.....	12
1.6 .1 Genetic.....	12
<i>1.6 .1.1 DNA sequence motifs.....</i>	<i>12</i>
<i>1.6 .1.2 Centromere replication.....</i>	<i>12</i>
<i>1.6 .1.3 Recombination at centromeres.....</i>	<i>13</i>
<i>1.6 .1.4 Gene conversion.....</i>	<i>14</i>

1.6 .2 Epigenetic.....	16
1.6 .2 .1 <i>CENP-A</i>	16
1.6 .2 .1 .1 <i>CENP-A loading</i>	17
1.6 .2 .1 .2 <i>Organization of CENP-A nucleosomes</i>	18
1.6 .2 .1 .3 <i>CENP-A Overexpression</i>	19
1.6 .2 .2 <i>RNA interference</i>	20
1.6 .2 .3 <i>Chromatin organization</i>	21
1.6 .2 .4 <i>Transcriptional silencing</i>	22
1.6 .2 .5 <i>Chromatin modifications</i>	22
1.6 .2 .6 <i>DNA methylation</i>	24
1.7 Centromere Evolution.....	25
1.8 Evolution of CENH3.....	26
1.9. Kinetochore.....	28
1.9. 1.1 <i>Inner kinetochore</i>	29
1.9. 1.2 <i>Middle kinetochore</i>	29
1.9. 1.3 <i>Outer kinetochore</i>	29

1.9.2 Kinetochore assembly.....	30
1.9.3 Kinetochore clustering.....	31
1.10 Chromosome segregation.....	32
1.10 .1 Types of mitosis.....	32
1.10 .2 Spindle length regulation.....	33
1.10 .3 Spindle assembly checkpoint.....	34
1.10 .4 Dam1 complex.....	36
1.11 <i>Candida albicans</i>.....	38
1.11 .1 Classification.....	38
1.11 .2 Diseases.....	38
1.11 .3 Ploidy, Aneuploidy and chromosomal rearrangements.....	40
1.11 .4 Cell cycle, Chromosome segregation, Centromeres and kinetochores.....	41
1.12. <i>Candida dubliniensis</i>.....	42
1.13 Summary of present study.....	42
2. RESULTS.....	44-100
A. Rapid evolution of CENP-A/Cse4p-rich centromeric DNA sequences in closely related pathogenic yeasts, <i>Candida albicans</i> and <i>Candida dubliniensis</i>.....	44
A1. Synteny of Centromere-Adjacent Genes Is Maintained in <i>C. albicans</i> and <i>C. dubliniensis</i>	46
A2. The Centromeric Histone Protein of <i>C. dubliniensis</i> (<i>CdCse4</i>) is Localized at the Kinetochore.....	49
A3. Centromeric Chromatin on Various <i>C. dubliniensis</i> Chromosomes Is Restricted to a 3- to 5-kb Region.....	50
A4. The Evolutionarily Conserved Kinetochore Protein CENP-C Homolog in <i>C. dubliniensis</i> , <i>CdMif2</i> Binds Preferentially to <i>CdCse4</i> -Associated DNA.....	52

<i>A5. Comparative Sequence Analysis between C. albicans and C. dubliniensis Reveals That Cse4-Rich Centromere Regions Are the Most Rapidly Evolving Loci of the Chromosome.....</i>	<i>55</i>
--	-----------

B. DYNAMICS OF CENTROMERE AND NEOCENTROMERE FORMATION IN C. ALBICANS59

<i>B1. Integration Centromeric chromatin assembles on a marker gene when integrated at CEN7.</i>	<i>59</i>
<i>B2. Centromeric DNA sequences are necessary (if not sufficient) to assemble centromeric chromatin on URA3 integrated at CEN7.....</i>	<i>61</i>
<i>B3. Neocentromere formation is programmed in C. albicans-replacement of core CENP-A-rich cen7 sequence with URA3 revealed two hot spots of neocentromeres on chromosome 7, adjacent to native CEN7 locus.</i>	<i>63</i>
<i>B4. Replacement of a 6.5 kb or a 30 kb regions spanning CEN7 again leads to formation of neocentromeres adjacent to replaced regions.</i>	<i>63</i>
<i>B5. Neocentromeres formation on chromosomes 1 also takes place at CEN adjacent regions.</i>	<i>66</i>
<i>B6. Proximity to a native centromere defines neocentromere formation in C. albicans.....</i>	<i>70</i>
<i>B7. Chromosomal location defines centromere/neocentromere formation in Candida species.</i>	<i>71</i>
<i>B8. Gene conversion at C. albicans centromeres.</i>	<i>72</i>
<i>B9. Inactivation of neocentromere by native CEN7 acquired by gene conversion.....</i>	<i>75</i>

C. THE ESSENTIALITY OF THE FUNGAL SPECIFIC DAM1 COMPLEX IS CORRELATED WITH 1MT/1KT INTERACTION PRESENT THROUGHOUT THE CELL CYCLE, INDEPENDENT OF THE NATURE OF A CENTROMERE.....77

<i>C1. The Dam1 complex is localized to the kinetochore throughout the Cell Cycle in C. albicans.</i>	<i>77</i>
<i>C2. Kinetochore recruitment of the Dam1 complex is independent of presence of microtubules.</i>	<i>78</i>
<i>C3. The Dam1 Complex is Essential for Viability and required for G2/M Progression and Completion of Mitosis in C. albicans.....</i>	<i>80</i>

<i>C4. Depletion of an essential kinetochore protein in C. albicans leads to severe spindle defects.....</i>	<i>81</i>
<i>C5. Subunits of the Dam1 complex maintain dynamics of interpolar and astral MTs.</i>	<i>83</i>
<i>C6. Dad2 is localized also at the spindle midzone.</i>	<i>84</i>
<i>C7. The spindle assembly checkpoint (SAC) monitors KT-MT interaction mediated by the Dam1 complex.</i>	<i>86</i>
<i>C8. Dam1 complex-dependent KT-MT interaction restricts spindle length in pre-mitotic cells to avoid premature chromosome segregation.....</i>	<i>87</i>

D. A COORDINATED INTERDEPENDENT PROTEIN CIRCUITRY STABILIZES KINETOCHORE ENSEMBLE THAT PROTECTS CENP-A IN HUMAN PATHOGENIC YEAST CANDIDA ALBICANS.....89

<i>D1. The kinetochore super-complex is stabilized by an interdependent coordinated process.</i>	<i>90</i>
<i>D2. Integrity of a kinetochore is independent of KT-MT interaction.....</i>	<i>93</i>
<i>D3. KT clustering ensures integrity of individual KTs in C. albicans.....</i>	<i>94</i>
<i>D4. Nuclear peripheral localization is maintained in unclustered kinetochores.....</i>	<i>96</i>
<i>D5. Kinetochore ensemble maintains centromeric chromatin.....</i>	<i>97</i>
<i>D6. Stabilization of centromeric chromatin by kinetochore ensemble protects CENP-A.....</i>	<i>99</i>

3. DISCUSSION.....101-111

3.1 Rapid evolution of centromeric DNA sequences in closely related pathogenic yeasts, *Candida albicans* and *Candida dubliniensis*.....102

3.2 Physical location determines centromere/neocentromere formation in *Candida* sp.....103

3.3 Native centromere suppresses other potential neocentromeres by lateral inhibition.....104

3.4 Dam1 complex is essential for 1MT-1KT interaction.....105

3.5 Localization dependency of proteins at the KT is species-specific.....108

3.6 Clustered KT stabilize integrity of an individual KT in <i>C. albicans</i>	109
3.7 An intact KT maintains centromeric chromatin and protects CENP-A from degradation	110
4. MATERIALS AND METHODS	112-149
4.1 Sequence analysis	113
4.1.1 <i>Identification of orthologous ORF</i>	113
4.1.2 <i>Identification of CdCse4p and CdMif2p</i>	113
4.1.3 <i>Homology Detection and Mutation Rate Measurement</i>	113
4.1.4 <i>Data Availability</i>	114
4.2 Strain construction	115
4.2.1 <i>Construction of CAKS3b</i>	115
4.2.2 <i>Construction of CDM1 Carrying C-Terminally TAP-Tagged CdMIF2</i>	116
4.2.3 <i>Construction of centromeric deletion strains</i>	116
4.2.4 <i>Expression of MycMif2 in neocentromere containing clones</i>	118
4.2.5 <i>Construction of conditional mutants of DAM1, ASK1, SPC19 and DAD2</i>	118
4.2.6 <i>Construction of the mad2 null mutant and conditional double mutants of the Dam1 complex proteins in the mad2 null mutant background</i>	119
4.2.7 <i>Construction of Protein A tagged strains</i>	119
4.2.8 <i>Construction of Dam1 and Ask1 conditional mutants expressing Mtw1 GFP</i>	120
4.2.9 <i>Construction of Dam1 and Ask1 conditional mutants expressing Mtw1 GFP</i>	120
4.3 Media and growth conditions	121
4.4 Viability assays	121
4.5 DAPI staining, calcoflour staining and FACS analysis	121
4.6 Nocodazole treatment	122

4.7 Subcellular immunolocalization and image analysis.....	122
4.8 Microscopy, image capture and image processing.....	123
4.9 Chromatin Immunoprecipitation assay.....	123
4.10 Pulsed field gel electrophoresis.....	126
4.11 Generation of polyclonal antibodies against Dad2 in rabbits.....	126
4.12 Western blot analysis.....	127
4.13 Antibodies.....	127
4. REFERENCES.....	150-172
5. LIST OF PUBLICATIONS.....	173

LIST OF FIGURES

1. INTRODUCTION.....	1-44
1. A schematic showing various stages of the cell cycle.....	2
2. Sister chromatids attached to spindle microtubules at kinetochores assembled on centromeres.....	4
3. CEN organization in different organisms.....	8
4. Mechanisms of gene conversion.....	15
5. Schematic showing structural domains of CenH3.....	17
6. Mechanism of pericentric heterochromatin formation by RNAi.....	21
7. Histone modifications present at the centromeric and pericentromeric DNA of various organisms...	24
8. A model proposed by Henikoff and colleagues to explain co evolution of centromeres and CenH3....	28
9. Schematic showing regulation of metaphase-anaphase transition.....	36
10. Phylogenetic tree showing evolution of Ascomycetes including <i>S. cerevisiae</i> , <i>Candida</i> species and <i>S. pombe</i>	39
11. Various morphological forms of <i>C. albicans</i>	40
2. RESULTS.....	45-99
A. Rapid evolution of CENP-A/Cse4p-rich centromeric DNA sequences in closely related pathogenic yeasts, <i>Candida albicans</i> and <i>Candida dubliniensis</i>	
A1. Comparative analysis of the orthologous regions spanning CEN6 in <i>C. albicans</i> and <i>C. dubliniensis</i>	46
A2. The centromeric histone in <i>C. dubliniensis</i> , CdCse4, is localized at the kinetochores throughout the cell cycle.....	49
A3. Two evolutionarily conserved key kinetochore proteins, CdCse4/CENP-A and CdMif2/CENP-C co localize on CENs of different <i>C. dubliniensis</i> chromosomes.....	53
A4. The CENP-C homolog in <i>C. dubliniensis</i> (CdMif2) is localized at the kinetochores throughout the cell cycle.....	54
A5. Orthologous Cse4p-rich CEN regions in <i>C. albicans</i> and <i>C. dubliniensis</i>	54
A6. Conserved blocks in the pericentric regions of various chromosomes of <i>C. dubliniensis</i> and <i>C. albicans</i>	58

B. DYNAMICS OF CENTROMERE AND NEOCENTROMERE FORMATION IN *C. ALBICANS*.

<i>B1. CENP-A chromatin assembles on the non-centromeric URA3 sequence integrated at CEN7 locus.....</i>	<i>60</i>
<i>B2. Replacement of CENP-A binding region on chromosome 7 with URA3.....</i>	<i>61</i>
<i>B3. Replacement of pericentric regions spanning CEN7 with URA3.....</i>	<i>64</i>
<i>B4. Neocentromere formation is programmed (non random) to CEN adjacent regions in C. albicans.....</i>	<i>67</i>
<i>B5. Neocentromere formation on chromosome1 takes place at CEN1 adjacent region.....</i>	<i>68</i>
<i>B6. Proximity to a native centromere determines neocentromere formation in C. albicans.....</i>	<i>71</i>
<i>B7. Relative chromosomal positions of CENP-A binding regions in C. albicans and C. dubliniensis.....</i>	<i>72</i>
<i>B8. Gene conversion occurs at C. albicans centromeres.....</i>	<i>74</i>
<i>B9. Established neocentromere is suppressed laterally in the presence of a native centromere.....</i>	<i>76</i>

C. THE ESSENTIALITY OF THE FUNGAL SPECIFIC DAM1 COMPLEX IS CORRELATED WITH 1MT/1KT INTERACTION PRESENT THROUGHOUT THE CELL CYCLE, INDEPENDENT OF THE NATURE OF A CENTROMERE

<i>C1. The Dam1 complex is localized to the kinetochore throughout the cell cycle in C. albicans.....</i>	<i>78</i>
<i>C2. Kinetochore localization of Dad2 does not dependent on the integrity of kinetochore-microtubule interaction in C. albicans.....</i>	<i>79</i>
<i>C3. The Dam1 complex is essential for viability in C. albicans.....</i>	<i>80</i>
<i>C4. The Dam1 complex is required for G2/M progression through cell cycle and completion of mitosis.....</i>	<i>82</i>
<i>C5. Depletion of an essential kinetochore protein in C. albicans leads to severe spindle defects.....</i>	<i>83</i>
<i>C6. Dam1 and Ask1, two subunits of the Dam1 complex, maintain the polymerization/depolymerization dynamics of interpolar and astral microtubules.....</i>	<i>84</i>
<i>C7. Dad2 is also localized at the spindle midzone.....</i>	<i>85</i>
<i>C8. The function of the Dam1 complex is under the surveillance of Mad2-mediated spindle assembly checkpoint in C. albicans.....</i>	<i>87</i>
<i>C9. The Dam1 complex restricts spindle length in premitotic cells to avoid precocious chromosome separation.....</i>	<i>88</i>

D. A COORDINATED INTERDEPENDENT PROTEIN CIRCUITRY STABILIZES KINETOCHORE ENSEMBLE THAT PROTECTS CENP-A IN HUMAN PATHOGENIC YEAST CANDIDA ALBICANS

D1. The process of kinetochore assembly is interdependent and coordinated in C. albicans.....91

D2. Kinetochores are unclustered in the absence of as essential KT protein.....92

D3. Kinetochore integrity is independent of KT-MT interaction.....94

D4. Kinetochore clustering prevents kinetochore disassembly.....96

D5. Nuclear peripheral localization is maintained in unclustered KTs.....97

D6. KT ensemble maintains centromeric chromatin.....98

D7. CENP-A is protected by kinetochore ensemble.....100

3. Discussion.....101

E1. Reductive evolution of the Dam1 complex.....107

E2. A coordinated interdependent protein circuitry maintains kinetochore ensemble that protects CENP-A in a functional kinetochore.....111

LIST OF TABLES

1. INTRODUCTION.....1-44

Table 1. Budding yeast kinetochore and spindle- checkpoint components.....35

2. RESULTS.....45-100

A. RAPID EVOLUTION OF CENP-A/CSE4P-RICH CENTROMERIC DNA SEQUENCES IN CLOSELY RELATED PATHOGENIC YEASTS, CANDIDA ALBICANS AND CANDIDA DUBLINIENSIS

Table A1. Comparison of the amino acid (aa) sequence homology of the ORFs flanking the CEN regions in C. albicans and C. dubliniensis.....46

Table A2. Sequence coordinates of the Cse4- binding and the pericentric regions in all the chromosomes of C. albicans and C. dubliniensis.....51

Table A3. Comparison of mutation rates in Cse4-binding and other genomic non-coding regions in C. albicans and C. dubliniensis.....56

B. DYNAMICS OF CENTROMERE AND NEOCENTROMERE FORMATION IN C. ALBICANS

Table B1. Chromosome loss frequency in RM1000AH/CEN7::URA3 , RM1000AH/cen7Δ-4.5kb, RM1000AH/cen7Δ-6.5kb, RM1000AH/cen7Δ-30kb, RM1000AH/cen1Δ-4.2kb transformants.....69

3. Discussion.....101

4. MATERIALS AND METHODS.....112

Table M1. Details of construction of cassettes for the deletion of centromeric and pericentric regions.....117

Table M2. Table summarizing the details of Southern strategies used for the confirmation of deletions of centromeric regions.....117

Table M3. Candida albicans strains used in present study.....128

Table M4. Primers used in present study.....134

ABBREVIATIONS

bp	base pair
BSA	Bovine Serum Albumin
DAPI	4', 6-Diamino-2-phenylindole
DNA	Deoxyribonucleic Acid
DTT	Dithiothreitol
EDTA	Ethylene diamine tetra-acetic acid
EGTA	Ethylene glycol tetra acetic acid
h	hour
kb	kilobasepairs
µg	Microgram
µl	Microlitre
ml	Millilitre
mM	Millimolar
min	minutes
ORF	Open reading frame
PAGE	Polyacrylamide gel electrophoresis
PBS	Phosphate buffered saline
PCR	Polymerase Chain Reaction
RNA	Ribonucleic Acid
rpm	Revolution per minute
RT	Room temperature
SDS	Sodium Dodecyl Sulphate
Sec	Second
TE	Tris-EDTA
UV	ultraviolet

Introduction

1.1 Cell Cycle, chromosome segregation and human diseases associated with it

The cell division is a fundamental process of life through which a mother cell transmits genetic information to daughter cells. Depending on the requirement sensed mostly by the environmental cues cells undergo two types of cell division. The cell division that is associated with growth and repair is called mitosis. The other type of cell division associated with sexual reproduction is called meiosis. A cell, conducive to division, has to go through a cyclic series of processes known as cell cycle. The mitotic cell cycle is mainly divided into two phases: a) interphase (pre-mitotic) where duplication of genetic material takes place by DNA replication in S phase and b) mitotic phase where duplicated genome is distributed equally between the daughter cells by a process called chromosome segregation.

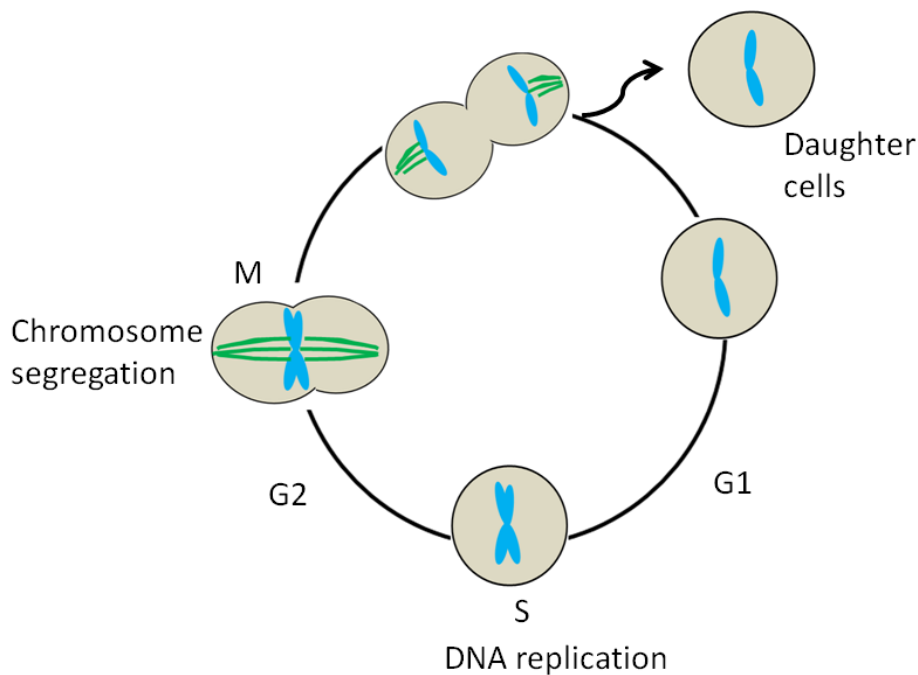


Figure 1. A schematic showing various stages of the cell cycle.

A cell spends time in gap phases G1 and G2 prior to DNA replication (S phase) and chromosome segregation (M phase), respectively, to prepare itself for these two events. The order and timing of cell cycle transitions (G1-S, G2-M and metaphase- anaphase) are

controlled by cell surveillance systems called checkpoints. Cell cycle checkpoints ensure that critical events such as DNA replication and chromosome segregation are completed correctly before allowing the cell to progress further through the cycle. The first checkpoint, the START (RESTRICTION in mammals), present at the end of G1, allows a cell to commit itself for the completion of cell cycle under favorable conditions. Cells with damaged DNA are arrested in G1 to prevent inheritance of wrong information during replication. Once the damage is repaired START allows G1/S transition. A cell enters into S- phase and duplicates its genome. The replication checkpoint ensures the fidelity of DNA replication. Arrest at G2/M transition allows DNA double-stranded breaks to be repaired before mitosis starts. The spindle assembly checkpoint ensures that chromosomes are correctly attached to spindle microtubules (MT) at kinetochores during mitosis before sister chromatids separate.

Faithful inheritance of duplicated genetic material into daughter cells during cell division relies on accurate chromosome segregation during mitosis where two sister chromatids are separated from each other with the help of spindle microtubule. Any error during chromosome segregation can lead to abnormalities such as genetic disorders, cancers and death. An altered chromosome number that results due to nondisjunction is the hallmark of most of these diseases. Nondisjunction occurs due to errors in capturing a chromosome by spindle MTs at the centromere. The centromere thus plays an indispensable role in the process of chromosome segregation.

1.2 Centromeres

According to the cytological definition the centromere is the primary constriction, usually present at the waist of a metaphase chromosome, that holds sister chromatids together and binds to mitotic spindle fibres to facilitate the movement of sister chromatids towards opposite poles during anaphase. Genetically a centromere is defined as the region of reduced recombination. Biochemists define a centromere as a transcriptionally inactive, gene poor and heterochromatic region. Cell biologically, a centromere is an essential, specialized chromosomal locus upon which a kinetochore (KT)— a macromolecular proteinaceous structure that links a centromere to spindle MTs— assembles and directs equal segregation of chromosomes during mitosis and meiosis.

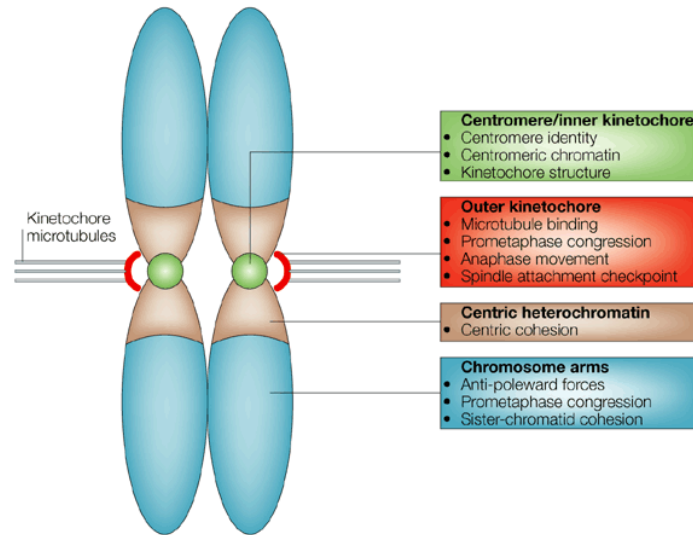


Figure 2. Sister chromatids attached to spindle MTs at KT's assembled on centromeres. (Sullivan B.A. 2001)

There has been a great contradiction on the relationship between centromere function and underlying DNA sequences. While centromeres discovered till date play an indispensable role in chromosome segregation, no two species exhibit discernable sequence conservation in centromeric DNA sequence. A functional centromere was first cloned and characterized from the budding yeast, *Saccharomyces cerevisiae* (Clarke & Carbon, 1980). Plasmids containing these centromeric (*CEN*) sequences are stably maintained in mitosis and meiosis.

1.3 Types of centromeres

Due to wide variations in length and sequence, it is difficult to classify centromeres into groups or classes. Thereby centromeres are broadly classified into four types based upon their size/organization, repetitive/non-repetitive and sequence dependent/independent nature: Point, regional, intermediate and diffused centromeres.

1.3.1 Point centromeres

Point centromeres (*CENs*) as the name suggests are short in size and bind to the KT proteins in a sequence-dependent manner. The point *CENs* of the budding yeast *S. cerevisiae* have three distinct *CEN* DNA elements, two of which act as sequence-specific binding sites of KT proteins (Clarke, 1990; Clarke & Carbon, 1980; Fitzgerald-Hayes et al,

1982). Soon after the discovery of point *CENs* in *S. cerevisiae*, it was speculated that similar analogous sequence elements might define *CENs* in other eukaryotes as well. Indeed several budding yeasts including *Candida maltosa*, *Candida glabrata*, *Yarrowia lipolytica* and *Kluyveromyces lactis* revealed presence of short point *CENs* with signature DNA sequence elements similar to *S. cerevisiae* (Fournier et al, 1993; Heus et al, 1993; Heus et al, 1994; Kitada et al, 1997; Ohkuma et al, 1995; Vernis et al, 1997; Vernis et al, 2001). *CENs* and autonomous replicating sequences (*ARSs*) are present together in *Y. lipolytica* and their functions are inseparable from each other (Fournier et al, 1993). Both *CEN* and *ARS* sequences are required to establish a replicative plasmid in *Y. lipolytica* (Vernis et al, 1997). Point *CENs* seem to be restricted to *S. cerevisiae* and closely related species. Identification of *CENs* in other eukaryotes over the years suggested that specific DNA sequences may not be the only determinant of *CEN* identity, instead it appeared that in many eukaryotes *CEN* function is a subject of epigenetic regulation.

1.3.2 Regional centromeres

Regional *CENs* are longer than point *CENs* and bind to KT proteins in a sequence independent manner. All the regional *CENs* discovered so far have a property in common which is their repetitive nature. Highly repetitive nature of regional *CENs* has made them difficult to analyze in most eukaryotes. The simplest and most extensively worked out regional *CENs* of fission yeast *Schizosaccharomyces pombe* are 40-110 kb long DNA sequences organized in a non-repetitive 4-7 kb central core region flanked on either side by pericentric repeats. Pericentric repeats are comprised of *CEN* specific innermost (*imr*) perfect inverted repeats surrounded by tandem array of outer repeats (*otr*) that vary in size and orientation (Fishel et al, 1988). The central core and *imr* repeats constitute CENP-A nucleosomes containing chromatin, which is involved in KT formation, whereas *otr* repeats, form heterochromatin, and are involved in the sister chromatid cohesion.

Similar to *S. pombe* *CENs*, many higher fungi carry highly repetitive regional *CENs*. *CENs* of *Aspergillus nidulans* are associated with a family of degenerate long terminal repeats (LTR) retrotransposons *Dane1* and *Dane2* (Degenerated *A. nidulans* element). These elements lost their capacity for transposition due to mutations suggesting that duplication occurred after the retroelement became inactive. Repeat induced mutations (RIP) are responsible for the

degenerate pattern of these elements. Bioinformatic analysis has predicted 40 to 100 kb long gene free regions that are rich in clustered blocks of transposable elements as sequence-independent regional *CENs* in *Cryptococcus neoformans*. During tetrad analysis *ADE2* and *URA5* exhibited a reduction in the proportion of tetra types (TT frequency) indicating that these markers are centromere-linked. Indeed *ADE2* and *URA5* are physically present close to putative *CENs*.

Neurospora crassa *CENs* are approximately 450-kb long highly repetitive A+T-rich recombination-deficient regions. These centromeric repeats are highly divergent due to operation of repeat induced point mutations (RIP) at the *CENs* (Cambareri et al, 1998; Centola & Carbon, 1994). Retrotransposon-like elements are features of *N. crassa* *CENs* as well. A Cluster of three new retrotransposon-like elements are associated with *N. crassa* *CENs*- 1) full length but nonmobile *copia*-like element *Tcen*, 2) portions of a *gypsy*-like element *Tgl1*, 3) *Tgl2* that shows similarity to the *Ty3* transposon of *S. cerevisiae* (Cambareri et al, 1998). Thus organization of *N. crassa* *CENs* appears to be intermediate between simple regional *CENs* of *S. pombe* and complex regional *CENs* of higher eukaryotes.

Regional *CEN* in *Drosophila melanogaster* consists of tandem repeats of AATAT and TTCTC sequences organized in a uniform “head-to-tail” orientation, with a few examples of “head-to-head” or “tail-to-tail” orientations (Sun et al, 1997). Molecular genetics of the *CEN* structure and its inheritance has been studied using the *Drosophila* minichromosome *Dp1187*. The AATAT and TTCTC satellite arrays are highly conserved and uniform. These simple repeats are interspersed with blocks of more complex transposable elements. These centromeric satellite repeats and the transposable elements are neither specific for nor universal to all *Drosophila* *CENs* (Sun et al, 1997).

Human and primates regional *CENs* consist of higher order structure of nucleosome length long 171 bp alpha satellite DNA units arranged in tandem head-to-tail orientation (Lee et al, 1997; Wayne et al, 1987; Willard, 1985; Willard, 1990). Each chromosome contains a chromosome-specific number of repeating units (Willard, 1985). Immunocytochemistry of human *CENs* has revealed that *CEN*-specific histone CENP-A binds only to a portion of entire higher order structure of alpha satellites. *CENs* of humans, mouse, ferrets, giant pandas, tree shrews and gerbils, contain so called CENP-B boxes that bind centromeric

protein CENP-B in a sequence-dependent manner. CENP-B shows high similarity to transposase proteins that bind to the transposable elements (Kipling & Warburton, 1997). Thus the origin of satellite repeats of *CEN* can be traced back to transposable elements and CENP-B might have coevolved with these repeats from the transposase protein.

Mouse *CENs* are present at a distance of 0.5-2.4 kb from telomere with the exception of the Y chromosome (Kipling et al, 1991). CENP-A binding regions consist of arrays of 120 bp minor satellites that range up to 1Mb in size. Minor satellites contain CENP-B boxes (CENP-B binding motifs) and are surrounded by arrays of 234 bp major satellite spanning over 2 Mb that lack CENP-B boxes. Major satellites constitute pericentric heterochromatin in mouse (Kalitsis et al, 2006; Kipling et al, 1991; Wong & Rattner, 1988; Zeng et al, 2004).

Plant *CENs* are highly repetitive AT-rich regions containing arrays of satellite DNA that carry no homology to human satellite repeats. However similar to humans the length of a satellite monomer is approximately equal to the length of one nucleosome: 155 bp CentO repeat of rice (Cheng et al, 2002), the 156 bp CentC repeat of maize (Ananiev et al, 1998; Zhong et al, 2002) and the 178 bp repeat of *Arabidopsis thaliana* (Round et al, 1997).

1.3.3 Intermediate centromeres

The third type of *CENs* termed intermediate *CENs* is present in human pathogenic budding yeast *Candida albicans*. They lack both sequence motifs which are characteristic of point *CEN* and repetitive DNA elements- the hallmark of regional *CENs*. *C. albicans* carries 3-5 kb long unique centromeric chromatin on each of its eight chromosomes (Sanyal et al, 2004). Naked centromeric DNA that is sufficient to confer *CEN* activity *in vivo* was shown to be unable to assemble functional centromeric chromatin and KTs *de novo* when reintroduced into cells suggesting epigenetic propagation of a *CEN* in *C. albicans* (Baum et al, 2006).

1.3.4 Diffused centromeres

Identification of *CENs* in nematodes including *Ceanorhabditis elegans* revealed that nematode chromosomes are holocentric with a clear absence of the primary constriction (Monen et al, 2005). KT proteins and spindle MTs bind along the entire length of the chromosome (Meraldi et al, 2006; Oegema et al, 2001). It has been speculated that all other

CENs are derived from the holocentric *CENs* with gradual inactivation of so called non-centromeric regions in other organisms.

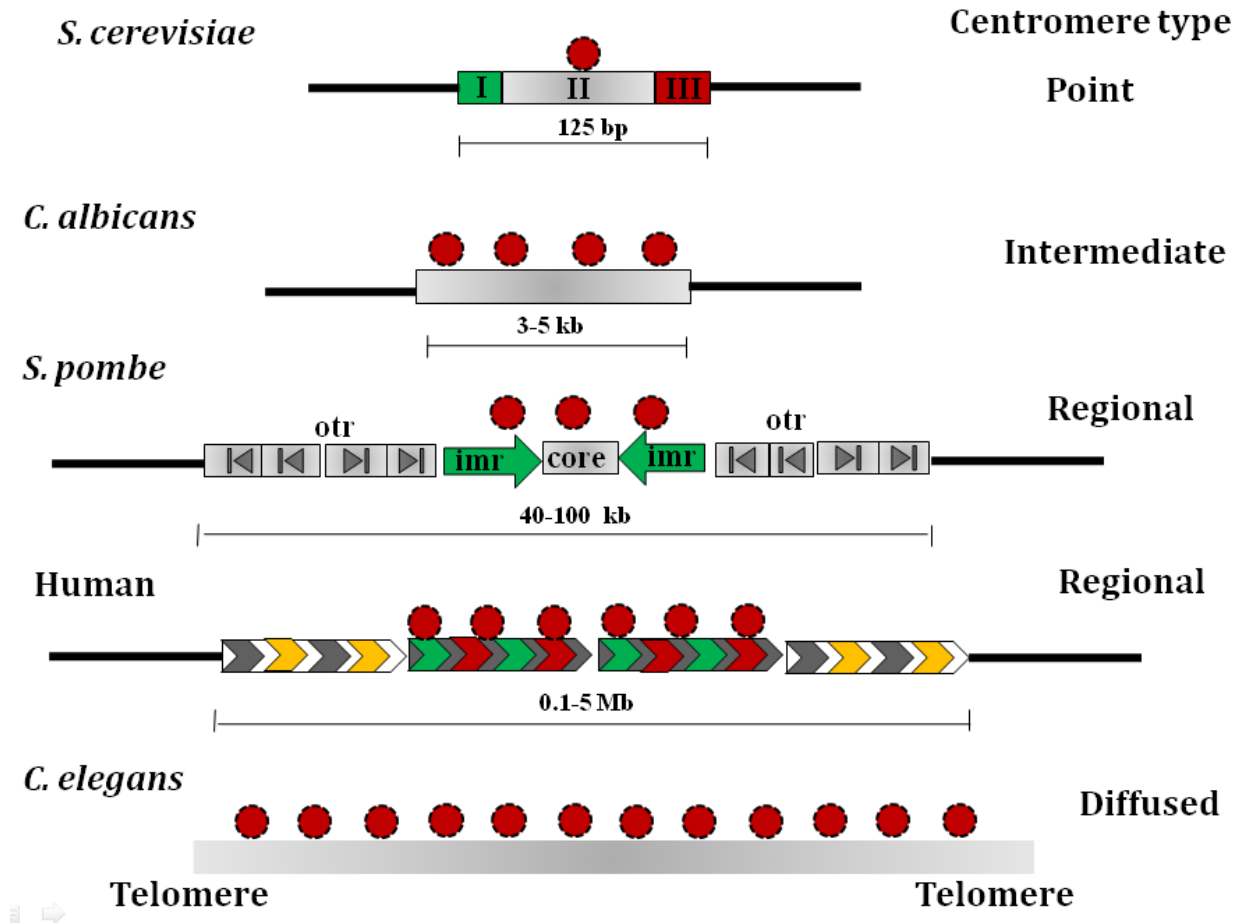


Figure 3. *CEN* organization in different organisms. Red sphere represents Centromeric histone.

1.4 Neocentromeres

Centromeric DNA sequences in human, *D. melanogaster*, *S. pombe* and *C. albicans* are not necessary for *CEN* establishment. This is evident from the formation of neocentromeres on non-centromeric DNA sequences in these organisms. The neocentromere is a site of KT formation on non centromeric DNA when native *CEN* is inactivated or deleted.

Neocentromeres were first identified in plants (Rhoades & Vilkomerson, 1942). These neocentromeres appear only at meiosis as heterochromatic knobs towards the distal arms

of the chromosome and were different from native *CENs* not only in the morphology but also in the mechanism by which they bind to spindles. Two key KT proteins CENH3 and CENP-C, do not localize to these neocentromeres (Dawe & Hiatt, 2004).

The first human neocentromere, mardel (10), was identified on a marker chromosome that lacked alpha satellite DNA (Voullaire et al, 1993). Ever since the discovery of the first human neocentromere, more than 100 neocentromeres have been reported and none of them share any sequence homology to the alpha satellites of the native *CENs* (Marshall et al, 2008). Neocentromere hotspots have been observed at the cytological level in humans, indicating that these loci are more prone to neocentromere formation (Amor & Choo, 2002). Interestingly, some of these neocentromere hotspots are sites for centromere repositioning during evolution (Ventura et al, 2004). Unlike classical plant neocentromeres human neocentromeres were found to bind all known KT proteins similar to alpha satellite containing native *CENs*. The establishment of neocentromeres is different from alpha satellite containing native *CENs*. An example is absence of CENP-B, a DNA binding protein from the neocentromeres. The CENP-B is required for the *de novo* establishment of *CEN* on alpha satellites in human artificial chromosome (Ohzeki et al, 2002).

The first report of neocentromere formation under experimental conditions appeared in *Drosophila X* chromosome. *Drosophila X* minichromosome (γ 238) released by radiation formed centromeric chromatin on subtelomeric fragment which was placed close to *CEN* due to rearrangement before release of minichromosome from X chromosome (Williams et al, 1998). A follow up study revealed that when the same subtelomeric fragment was released from a normal X chromosome from various *CEN* distal sites it failed to form a neocentromere. This suggested that proximity to the native *CEN* is a prerequisite for neocentromere formation in *Drosophila* (Maggert & Karpen, 2001). Generalization of this hypothesis however requires more experimental evidence such as to test the neocentromere activity of other chromosomal fragments (other than the subtelomeric fragment studied) when present at *CEN* proximal or *CEN* distal locations. Subsequently neocentromere formation has been experimentally induced in fission yeast *S. pombe* by removing a native *CEN* from a chromosome. Excision of *cen1* in *S. pombe* led to stabilization of chromosome either by chromosomal rearrangements or by neocentromere formation

(Ishii et al, 2008). Importantly upon *cen1* excision stabilization of acentric chromosome by neocentromere formation occurred at a lower frequency as compared to stabilization by telomere-telomere fusion. All the neocentromeres identified mapped to the subtelomeric regions suggesting that heterochromatic regions are preferred sites of neocentromere formation in *S. pombe*. RNAi has been shown to play an important role in *CEN* function in *S. pombe* (discussed later). Efficiency of neocentromere formation was further reduced when genes of RNAi pathway were inactivated suggesting that basic mechanism of formation of *CEN* and neocentromere is the same in *S. pombe*.

Recently budding yeast *C. albicans* has been shown to form neocentromeres at multiple loci (Ketel et al, 2009). Although genomic rearrangements occur frequently in *C. albicans* but upon deletion of a native *CEN*, rather than undergoing chromosomal rearrangements, *C. albicans* stabilizes the acentric chromosome efficiently by neocentromere formation. Neocentromeres provide an attractive system to reveal the secrets behind *CEN* formation by so called epigenetic memory.

1.5 Epigenetic behavior of centromeres in three different classes of centromeres

Epigenetics refers to a heritable phenotype that is not attributed to DNA sequence alone. A few examples of epigenetic behavior are transcriptional silencing of mating type locus in *S. cerevisiae*, position effect variegation in *Drosophila* telomeric regions and X chromosome inactivation. The best example of epigenetic regulation is *CEN* propagation. *S. cerevisiae*, *S. pombe* and *C. albicans* *CENs* have been reported to exhibit unique epigenetic behaviors.

S. cerevisiae centromeric sequence containing minichromosome when introduced into cells from outside is able to form centromeric chromatin on centromeric DNA sequences present in the minichromosome to assemble KT and thus helps in the equal segregation of centromeric plasmids in daughter cells. This segregation state of centromeric DNA in the plasmid introduced into a host cell via transformation has been shown to be epigenetically inheritable (Mythreye & Bloom, 2003). Chl4, a KT protein is required for the formation of a functional kinetochore. An established *CEN* can maintain itself in the absence of Chl4 but

naked *CEN* DNA fails to assemble centromeric chromatin in absence of Chl4, indicating a differential requirement for *de novo* and template-directed propagation of centromeric states. This suggests that Chl4 is required to mark a chromatin state to be heritably propagated. Furthermore, *CENs* with pre-existing assembled KTs were able to switch to an unstable form upon loss of Chl4, indicating epigenetic mechanism in *CEN* inheritance in *S. cerevisiae*.

Novel epigenetic effect acting at the plasmid centromeric sequences was demonstrated in *S. pombe* as well (Steiner & Clarke, 1994). Two phenotypic classes of transformants were obtained when *cen3* derived minichromosome containing *ura4* and *sup3e* (suppressor of *ade6.704* mutation) markers was transformed into *S. pombe* (*ade6.704 ura4.294*). *S. pombe ade-* strains form red colonies while *ade+* strains form white colonies when grown in media containing low levels of adenine. The first class carried a highly stable plasmid (white colonies or white colonies with red sectors phenotype) while the second class showed the presence of an unstable form of centromeric plasmid (red colonies phenotype). In vivo propagation of minichromosome containing transformants led to the switching from one phenotype to the other. The structure of plasmid DNA present in both the classes was indistinguishable ruling out the role of sequence alterations in such phenotypic switching. Thus two heritable states can co-exist within a population in the absence of any DNA structural rearrangement or chemical modification of the *S. pombe* minichromosome.

Intermediate *CENs* of *C. albicans* provide another example of epigenetic propagation of *CEN*. An 85 kb chromosome fragment generated in vivo by telomere mediated truncation retained an active *CEN* and was mitotically stable. But the same chromosome fragment when isolated to remove all the marks associated with chromatin and reintroduced into *C. albicans* cells as naked DNA was not sufficient for *de novo CEN* activation as it failed to assemble centromeric chromatin and was mitotically unstable (Baum et al, 2006). Thus *CEN* propagation in *C. albicans* relies on pre-existing epigenetic memory.

1.6 Factors controlling centromere formation

1.6 .1 Genetic

1.6 .1.1 DNA sequence motifs

Genetic factors play an important role in determining the identity of point *CENs*. Underlying DNA sequence elements are absolutely necessary and sufficient for *CEN* specification in point *CEN* containing organisms. *S. cerevisiae* *CENs* are 125 bp long which contain three functional *CEN* DNA elements CDEI, CDEII and CDEIII. The central AT-rich CDEII is 80 bp long and surrounded by two palindrome sequence elements CDEI (8 bp) and CDEIII (26 bp)(McAinsh et al, 2003). The CDEIII determines *CEN* identity as it serves as the binding site of a sequence-specific DNA binding KT protein CBF3. A single bp substitution in CCG of CDEIII leads to a complete disruption of *CEN* function. Binding of CBF3 to CDEIII helps recruiting Cse4, yeast centromeric histone to CDEII. Thus DNA sequence is self-sufficient in establishing *CEN* identity in *S. cerevisiae*. Point *CENs* of *C. glabrata*, *Y. lipolytica*, *C. maltosa* and *K. lactis* contain similar DNA sequence elements and are hence genetically determined.

Sequence-dependent binding of KT proteins on *CENs* is seen in epigenetically regulated regional centromeres as well. CENP-B boxes present in human centromeric region exhibit sequence-specific binding to the CENP-B. *CEN* formation is suppressed in cells expressing CENP-B when alpha-satellite DNA was integrated into a chromosomal site however *de novo* *CEN* assembly on human artificial chromosome carrying alpha satellite DNA is dependent on CENP-B. Thus it has been proposed that CENP-B plays a dual role, ensuring *de novo* *CEN* formation on DNA lacking a functional *CEN* but preventing the formation of excess *CENs* on chromosomes (Ohzeki et al, 2002; Okada et al, 2007).

1.6 .1.2 Centromere replication

In contrast to general belief that gene-poor and heterochromatic regions are late replicating, sequence-specific point *CENs* of *S. cerevisiae* were shown to replicate early during S phase. This finding also ruled out the possibility that a delay in the replication of *CENs* until mitosis is responsible for sister chromatid adherence and proper chromosome segregation at anaphase (McCarroll & Fangman, 1988). Recently sequence-independent intermediate *CENs* of *C. albicans* as well as neo*CENs* were shown to replicate early in the S

phase (Koren et al, 2010). Regional *CENs* of fission yeast *S. pombe* replicate very early in S phase (Kim et al, 2003). Active chromosomal origins of replication have been identified within centromeric DNA of *S. pombe* (Kim & Huberman, 2001). Even complex regional *CENs* of *Drosophila* are early replicating (Ahmad & Henikoff, 2002). Thus early replicating nature is independent of nature of *CENs*. Moreover, late replication, as thought before, does not seem to be an obligatory requirement for heterochromatic regions. Centromeric DNA in higher eukaryotes replicate in mid or late S phase. Mouse *CENs* replicate throughout S phase (Weidtkamp-Peters et al, 2006). The late replication timing of *CENs* in higher eukaryotes has been proposed to play a role in *CEN* function and transcriptional control (Csink & Henikoff, 1998; Gilbert, 2002).

Replication forks pause at different genomic sites such as the rDNA repeats (Ivessa et al, 2000). Replication forks stalling has also been reported at *S. cerevisiae* *CENs* (Greenfeder & Newlon, 1992). Replication fork pauses at the *CENs* due to hindrance provided by DNA protein interaction between *CEN* and KTs and not due to presence of distinct sequence elements at the *CENs*. Moreover the ability to cause replication forks to pause correlates with the ability of a *CEN* to form the nuclease-resistant core chromatin structure. Mutations that affect these DNA protein interactions and distinct chromatin structure at the *CEN* relieve replication fork pausing at the *CENs* (Greenfeder & Newlon, 1992).

1.6 .1.3 Recombination at centromeres

Recombination is required to bring about the mutations necessary to drive the evolution. However, it is intriguing to note that *CENs* which are among the most rapidly evolving regions in the genome are recombination-deficient in nature (Lambie & Roeder, 1986). During meiosis in wild-type strains of *S. cerevisiae* *CEN*-proximal crossovers are associated with the non-disjunction events that result from precocious separation of sister chromatids (Rockmill et al, 2006). Also recombination events too near to a *CEN* or too far from a *CEN* impart an increased risk for nondisjunction in humans (Lamb et al, 2005). It has been proposed that crossovers that are close to a *CEN* disrupt pericentric sister chromatid cohesion resulting in premature separation of sister chromatids and random segregation. Selective pressure that reduces crossing over near a *CEN* seems to be very strong (Talbert & Henikoff, 2010). Recombination-deficient nature of a *CEN* was earlier attributed to the heterochromatic nature of pericentric regions. This notion, however, turned wrong when

heterochromatic regions were shown to undergo recombination with frequency of recombination being dependent upon the distance from *CENs* (Mather, 1939). But subsequent work proved that heterochromatin has a tendency to block crossing over (Slatis, 1955). Studies based on analysis of meiotic events suggested that *CENs* were recombination-deficient; however, analysis of mitotic recombination later revealed that recombination tract can penetrate through centromeric region during mitosis. Mitotic recombination was found to be taking place at mammalian *CENs* at a very high rate (Jaco et al, 2008).

1.6 .1.4 Gene conversion

Gene conversion is a process which involves nonreciprocal copying of a stretch of DNA from one homolog onto the other. Gene conversion helps to repair a double-strand break (DSB) by recombination followed by copying of information from the homologous chromosome. Recombination is initiated by the formation of a DSB made by the Spo11 protein. Long 3' single-strand tails are generated from the DSB ends. Single-stranded DNA invades the homologous sequence on the other (uncut) chromosome. Three different pathways have been proposed to repair the breaks: 1) double-strand-break repair (DSBR), 2) dissolution of the double Holliday junctions and 3) synthesis-dependent strand-annealing (SDSA) (Pâques & Haber, 1999). The resulting intermediates have two possible outcomes based upon repair process used: crossovers and non-crossovers (Figure 4) and formation of heteroduplex DNA is a common event used by all the pathways.

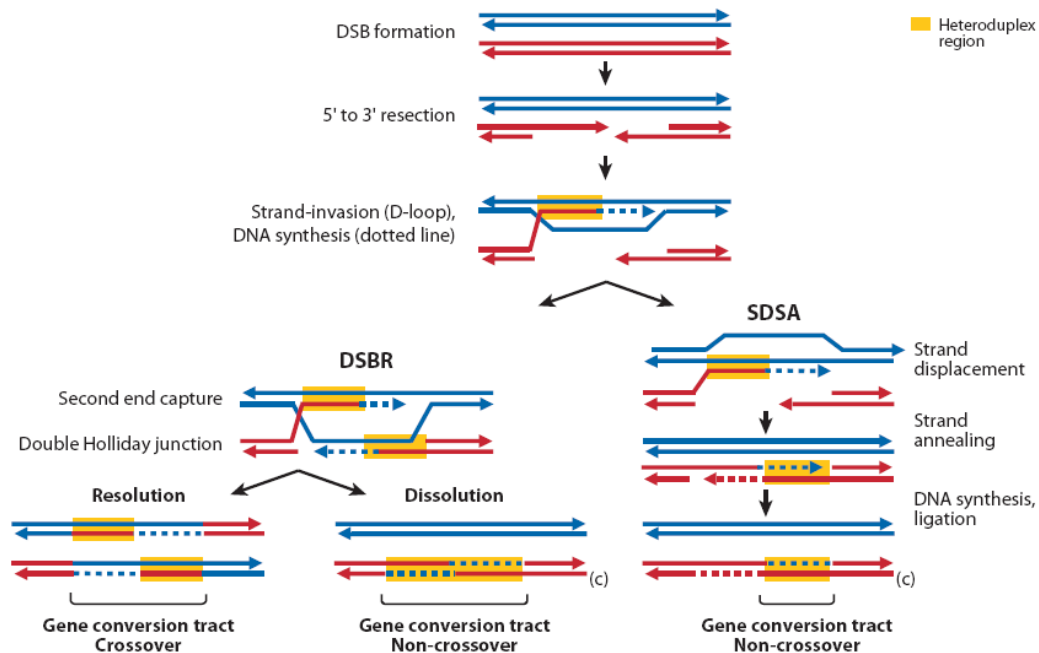


Figure 4. Mechanisms of gene conversion(Duret & Galtier, 2009) .

In meiosis, gene conversion tracts range from 1 to 2 kb (Borts & Haber, 1989; Detloff & Petes, 1992; Malone et al, 1992) while in mitosis, some gene conversion tracts range up to 4.2 kb while others extend for hundreds of kilobases (Judd & Petes, 1988).

Replication fork stalling creates DSBs. If replication forks happen to stall at *CENs*, the resulting DSBs could be repaired by gene conversion. Indeed gene conversion has been reported to occur at the *CENs*. Meiotic gene conversion events were found to occur within the *CEN* of *S. cerevisiae* at rates similar to other genomic sequences (Symington & Petes, 1988). It is difficult to detect gene conversion at the *CENs* of higher eukaryotes due to highly repetitive DNA sequence and the localized nature of gene conversion. To overcome this hurdle recently a novel and sophisticated CenH3 ChIP display method was developed to map KT footprints over transposon-rich areas of maize *CEN* cores. Centromeric chromatin was immunoprecipitated with an anti-CenH3 antibody and a total of 238 within-*CEN* markers were assessed in two parental lines and in 94 recombinant inbred lines derived from their progeny. Presence of single marker from one parent in a *CEN* with all markers of the other parent, indicated gene conversion event at maize *CENs*. Further studies in 53 highly diverse inbred lines revealed a wide spread gene conversion at maize

CEN (Shi et al, 2010). Gene conversion is now speculated to be a general feature of *CENs* of multicellular eukaryotes. It has been proposed that unequal exchange between sisters is the cause of large expansions and contractions of alpha satellite repeat arrays while gene conversion is responsible for periodic homogenization of the satellite repeats (Talbert & Henikoff, 2010).

1.6 .2 Epigenetic

1.6 .2 .1 CENP-A

Despite wide variations in centromeric sequences and organization, all the *CENs* as well as neo*CENs* share a common property, presence of a specialized chromatin where canonical histone H3 is replaced partially or fully by its variant CENP-A in human, Cse4 in *S. cerevisiae*, Cnp1 in *S. pombe* and CID in *D. melanogaster*. Despite the presence of excess amount of histone H3 in the cell, CENP-A replaces histone H3 to make specialized nucleosomes at centromeric chromatin by a mechanism that remains largely unknown.

CENP-A is structurally comprised of a highly variable N-terminal region and a conserved histone-fold domain (HFD). CENP-A and histone H3 differ significantly from each other at the N terminal domain. In addition, N-terminal domain of CENP-A is highly variable among closely related species. Divergence of the N-terminal domain of CENP-A has been attributed to the divergence in the underlying centromeric DNA sequences that are undergoing rapid evolution in different species (Malik et al, 2002). Although CENP-A differs from canonical histone H3 at the N-terminal, a CENP-A targeting domain (CATD) is present in the globular histone-fold (Sullivan et al, 1994). The HFD is comprised of alpha helices (α N, α 1, α 2 and α 3) separated by two loop structures (L1 and L2). Structural differences in the L1 loop and the α 2-helix are necessary and sufficient to target CENP-A to the centromeric DNA (Black et al, 2004). Three distinct properties of the CATD are responsible for CENP-A deposition at the *CEN*: 1) CENP-A – CENP-A interface that shows substantial rotation as compared to H3-H3 interface 2) a longer protruding loop L1 of opposite charge as that of H3 3) strong hydrophobic contacts between CENP-A and H4 (Sekulic et al, 2010). When HFD of CENP-A is swapped into the histone H3, the resulting hybrid histone H3 is incorporated into the *CEN* (Black et al, 2004). In spite of the variability in the amino acid sequences Cse4

orthologs of closely related species *Kluyveromyces marxianus*, *C. glabrata* and *S. servazzii* can complement *S. cerevisiae* Cse4 function. However Cse4 orthologs of *S. pombe*, *Pichia farinosa*, and *Pichia angusta* fail to complement *S. cerevisiae* Cse4 function. The complementation ability of CENP-A correlates with the evolutionary distance among the species. Unexpectedly, *S. cerevisiae* Cse4 is specifically incorporated into *CEN* nucleosomes and is able to complement RNAi-depleted CENP-A induced cell cycle arrest in human cells (Wieland et al, 2004).

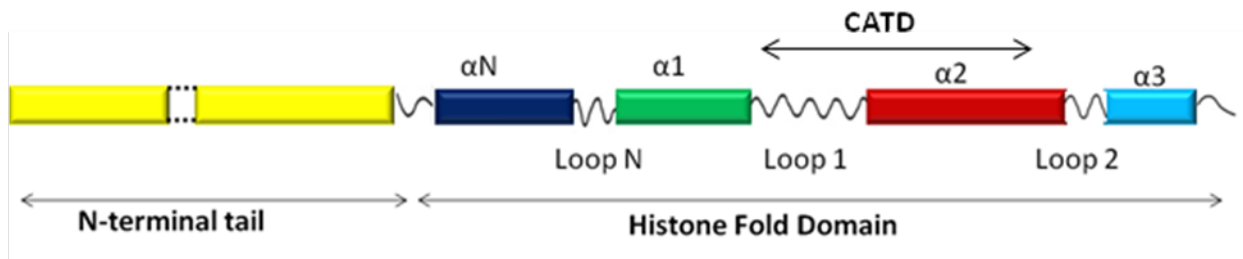


Figure 5. Schematic showing structural domains of CenH3.

The CENP-A is believed to be the initiator of the process of KT formation and hence considered as the epigenetic mark of a functional *CEN* in all eukaryotes studied till date. The CENP-A deposition on *CEN* DNA occurs in a sequence-dependent manner in point *CENs* but its deposition in regional *CENs* is not strictly sequence-dependent (such as in cases of neo*CENs*). Localization of most KT proteins is also shown to be regulated by CENP-A confirming that CENP-A initiates KT formation. However, a very few proteins have been shown to be acting upstream of CENP-A loading pathway. Mis6 and a cell cycle regulated GATA factor, Ams2 has been shown to be a component of CENP-A localization pathway in fission yeast *S. pombe* (Chen et al, 2003; Takahashi et al, 2000). Recently it has been shown that, unlike most other organisms an essential middle KT protein Mis12/Mtw1 is required for inner KT assembly including localization of CENP-A and CENP-C in a pathogenic yeast *C. albicans* (Roy et al, 2011). The reason for such dependency on KT localization is unknown.

1.6 .2 .1 .1 CENP-A loading

CENP-A loading to the *CENs* is cell cycle-regulated and takes place at different stages of the cell cycle in different organisms. Chaperones involved in the recruitment of CENP-A on

CENs are different from chromatin assembly factors involved in loading of canonical histone H3. In *S. cerevisiae* Cse4 loading occurs during S- phase when old Cse4 is evicted out and newly synthesized Cse4 is recruited at the replicated *CENs* with the help of Scm3, a member of the newly discovered family of chaperones (Pearson et al, 2004). In all other organisms CENP-A deposition takes place in replication independent manner outside the S phase. CENP-A loading in *S. pombe* takes place in two distinct phases during the cell cycle: the S phase and the late-G2 phase (Takahashi et al, 2005). Replication-coupled loading of CENP-A during S-phase is facilitated by Ams2, a cell cycle regulated GATA factor. The G2 loading pathway of CENP-A requires a different factor, Mis6, a constitutive *CEN*-binding protein (Takahashi et al, 2005). In *Drosophila* embryos where G1 and G2 phases are not observed, CID deposition takes place at anaphase stage (Schuh et al, 2007). Human CENP-A is loaded on the *CEN* during late mitosis and early G1 stages of cell cycle with the help of HJURP which is Scm3 homolog in humans (Camahort et al, 2007; Foltz et al, 2009; Sanchez-Pulido et al, 2009; Williams et al, 2009). Levels of nonchromosomal CENP-A and HJURP are at their lowest in S phase and early G2 phase but rise together to peak levels in mitosis and early G1 phase (Foltz et al, 2009). In *Arabidopsis*, loading of CENP-A occurs mainly in G2 phase (Lermontova et al, 2006).

Temporal separation of CENP-A recruitment from DNA replication leads to diluting of CENP-A molecules at centromeric chromatin from the time DNA is replicated till its recruitment which means that centromeric chromatin acquires different states of organization before and after CENP-A deposition. Existence of three possible forms of centromeric chromatin have been speculated: 1) nucleosome free gaps are created and maintained at the *CENs* till new CENP-A is recruited 2), nucleosome free gaps left due to halved number of CENP-A molecules are filled by canonical H3, 3) centromeric nucleosomes acquire tetrameric organization till new CENP-A is recruited (Black & Cleveland, 2011; Dalal et al, 2007; Mehta et al, 2010).

1.6 .2 .1 .2 Organization of CENP-A nucleosomes

Propagation of centromeric chromatin remains unclear partly due to uncertainty in composition of CENP-A containing nucleosome. In various models octameric -with two copies of each histone, H2A, H2B, H4, and CENP-A in place of H3, (Camahort et al, 2009;

Conde e Silva et al, 2007; Dimitriadis et al, 2010; Foltz et al, 2006; Palmer et al, 1987; Sekulic et al, 2010; Shelby et al, 1997), hexameric -H2A:H2B dimers are replaced by recruitment of two molecules of Scm3 (Mizuguchi et al, 2007), tetrameric -with two copies of CENP-A and H4 but lacking H2A:H2B dimers (Williams et al, 2009), and trimeric (Cse4, H4, and Scm3 (Furuyama & Henikoff, 2009), organization of CENP-A containing nucleosome have been proposed.

1.6 .2 .1 .3 CENP-A Overexpression

With the notable exception of holocentric chromosomes of *C. elegans*, lepidopterns and aphids where KTs are formed across the entire length of chromosome, only one KT is formed per chromosome in all other organisms studied till date. A KT is assembled on the neocentromere only when a native *CEN* is deleted or inactivated. Thus a mechanism to prevent KT formation on non-native locations exists in the presence of an already existing functional KT on the native *CEN*. Indeed, studies in several organisms suggested that CENP-A is always associated with functional KTs whether they are formed on native *CEN* DNA or non-centromeric DNA (neocentromeres). There must be a mechanism to prevent forming centromeric chromatin on neocentromeric loci when the native *CEN* is functional. Overexpression of CENP-A (CID) in *D. melanogaster* leads to its mislocalization throughout the chromosomes (Moreno-Moreno et al, 2006). CENP-A molecules that are not associated with the *CEN*, are evicted out and eventually targeted to degradation by the proteasome-mediated pathway in this organism. In contrast, CENP-A (Cse4) overexpression in *S. cerevisiae* does not lead to its mislocalization rather unbound Cse4 is degraded inside the cells (Collins et al, 2004, Hewawasam et al 2010, Ranjitkar et al 2010). Overexpression of human centromeric histone CENP-A results in its mislocalization to euchromatin and is associated with colorectal cancer (Tomonaga et al, 2003). Thus a species-specific active mechanism is present to prevent ectopic CENP-A-dependent *CEN* formation as well as stabilization of CENP-A at the functional KT in various organisms. Although studies discussed above suggest that ectopic CENP-A is destabilized to prevent multiple KT formation, the exact cellular signal that distinguishes CENP-A molecules present at the native *CEN* from those ectopically localized could not be determined.

1.6 .2 .2 RNA interference

RNAi plays an important role in *CEN* activity in *S. pombe*. Proper functioning of a *S. pombe CEN* relies upon RNAi machinery as inactivation of genes involved in RNAi pathway leads to defective chromosome segregation. Establishment of pericentromeric heterochromatin is of fundamental importance to proper functioning of *S. pombe CENs*. RNAi establishes heterochromatin by recruiting histone modifying enzymes at the pericentric region (Grewal, 2010; Kloc & Martienssen, 2008; Martienssen et al, 2005). The RNA-dependent RNA polymerase complex (RDRC) transcribes pericentric repeats to generate dsRNAs (Motamedi et al, 2004). Transcription from heterochromatin is an oxymoron because heterochromatic regions are generally transcriptionally inactive. Subsequently detailed analysis of the status of transcription from centromeric chromatin throughout the cell cycle solved the enigma. These transcripts are produced during a brief period in S phase when heterochromatin is displaced away from the pericentric region (Chen et al, 2008; Kloc et al, 2008). Subsequently Dicer (Dcr1) converts dsRNAs into siRNAs which then are incorporated into Argonaute (Ago1) containing RNA induced silencing complex (RISC) complex (Colmenares et al, 2007; Motamedi et al, 2004). Both Ago1 and siRNA, become part of another complex: the RNA-induced transcriptional silencing complex (RITS). Other components of RITS complex are Chp1, Tas3 (Motamedi et al, 2004; Verdell et al, 2004). RITS targets siRNA that are made at the pericentric loci and establishes a self-circulatory loop by again recruiting RDRC to amplify the RNAi response (Sugiyama et al, 2005). RITS recruits Clr4 (a member of the conserved chromo- and SET-domain family of proteins that modify the N-terminal tail of histone H3 by methylation) containing CLRC complex (Clr4-containing complex) that catalyzes the H3K9 methylation (Hong et al, 2005; Horn et al, 2005; Jia et al, 2005). The Swi6 (HP1-like protein) binds to H3K9me2 resulting in heterochromatin formation (Motamedi et al, 2004). Further spreading of heterochromatin occurs through recruitment of SHREC (Snf2/HDAC-containing Repressor Complex) complex by Swi6 (Sugiyama et al, 2007).

RNAi machinery is completely absent in the budding yeast *S. cerevisiae*. However homologs of Argonaute genes as well as existence of small RNAs have been reported in *Saccharomyces castellii*, *Kluyveromyces polysporus* and *C. albicans* (Drinnenberg et al, 2009). None of the small RNAs were found to map to centromeric regions of *C. albicans CENs* of *S.*

castellii and *K. polysporus* are to be identified yet and it is of paramount interest to examine centromeric origin of small RNAs in these two budding yeast which are closely related to *S. cerevisiae*.

There has been evidence for presence of small RNA species produced from the *CENs* in *N. crassa* (Lee et al, 2010). RNAi appears to be dispensable for heterochromatin formation and DNA methylation (Freitag et al, 2004b) both of which are involved in centromeric function in *N. crassa*. Thus RNAi might not be directly involved in *CEN* function in *N. crassa*.

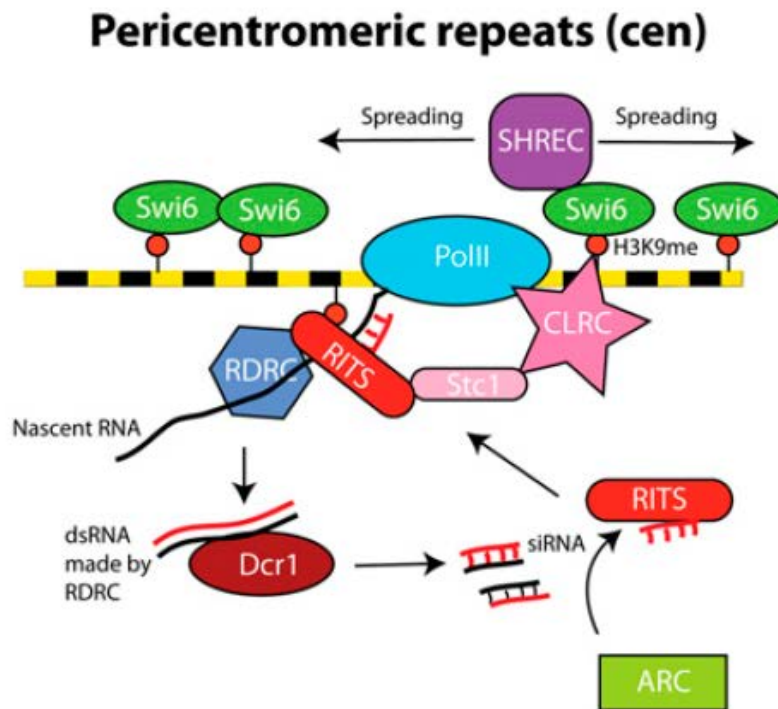


Figure 6. Mechanism of pericentric heterochromatin formation by RNAi
(Kamminga & Ketting, 2011).

1.6 .2 .3 Chromatin organization

A KT selectively assembles onto centromeric chromatin that is different from the rest of the genome in both point and regional *CENs*. Centromeric chromatin in *S. cerevisiae* consists of a single Cse4-containing nucleosome and has a distinct organization; a small ~200 bp nuclease-resistant core flanked by DNase I hypersensitive sites and an array of positioned nucleosomes (Bloom & Carbon, 1982). *S. pombe* centromeric chromatin assembles on the central core rich in Cnp1 (SpCENP-A) containing nucleosomes along with canonical H3-

containing nucleosomes. The central core of *S. pombe* when treated with micrococcal nuclease yields a smeary pattern rather than the characteristic ladder pattern of outer repeats and euchromatic chromosomal arms, suggesting a complete lack of a regular periodic nucleosomal array at the *CENs* (Polizzi & Clarke, 1991). *S. pombe cen2* central core was cloned in *S. cerevisiae* minichromosome, a system where *S. pombe cen2* is nonfunctional and also away from their functional context and protein environment. Micrococcal nuclease digestion revealed a pattern for *cen2* central core fragments that was indistinguishable from *S. cerevisiae* bulk chromatin indicating DNA sequences of the central core region in themselves do not avoid regular nucleosome formation. The 3-5 kb long intermediate *CENs* are bound to four CENP-A containing nucleosomes. Similar to *S. pombe*, centromeric chromatin in *C. albicans* yields smeary pattern upon micrococcal nuclease digestion (Baum et al, 2006). Such unusual chromatin organization of the core region forms the basis of a higher order structure that distinguishes the *CEN* from the chromosome arms. A growing body of evidence points to the altered micrococcal nuclease nucleosomal repeat pattern having a crucial role in CENP-A incorporation (Takahashi et al, 2000).

1.6 .2 .4 Transcriptional silencing

A marker gene *ura4* placed at a *S. pombe CEN* exhibits strong and reversible silencing when placed at the central core or at the outer repeats. Silencing at the central core is mediated by KT integrity (Pidoux et al, 2003). Mutations in KT proteins including Cnp1, Sim4 remove silencing in the central core, and affect centromeric chromatin, while silencing at the outer repeats results due to action of RNAi components, Clr4 histone H3K9 methyltransferase and Swi6 (homologue of HP1). Transcriptional silencing, thus, is correlated with the assembly of centromeric chromatin. ChIP assays with *SpCENP-A* (Cnp1) revealed that Cnp1 was associated with the *ura4* inserted at the *CENs*. The centromeric regions of most eukaryotes are inert and lack genes with the exception of rice *CENs* which have been shown to contain active genes (Nagaki et al 2004).

1.6 .2 .5 Chromatin modifications

Centromeric heterochromatin of certain regional *CENs* contains blocks of CENP-A containing nucleosomes interspersed with blocks of H3 containing nucleosomes. Canonical

H3 present at the *CENs* exhibits a distinct pattern of post-translational modifications which provides a distinguishable mark to centromeric chromatin as compared to rest of the chromatin. Centromeric chromatin is generally hypoacetylated due to the activity of histone deacetylases. Hypoacetylation is required for *CEN* function and treatment with the histone deacetylase inhibitor trichostatin A (TSA) that causes increase in histone acetylation of centromeric chromatin, leads to concomitant defect in chromosome segregation (Ekwall, 2007).

TSA-induced acetylated *CENs* display lagging chromosomes in anaphase cells of *S. pombe* (Ekwall et al, 1997). Perturbation of cohesin Rad21 function gives rise to similar lagging chromosome phenotype in *S. pombe* (Bernard et al, 2001). Thus, it has been speculated that underacetylation of centromeric outer domain in *S. pombe* is a prerequisite for the centromeric cohesion function. Hypoacetylation has been shown to be important for CENP-A assembly on neocentromeres as well. TSA-induced partial histone hyperacetylation causes a unidirectional shift in the position of a previously defined binding domain for the CENP-A at a human neocentromere (Craig et al, 2003). Moreover one of the *CENs* in a dicentric chromosome has been shown to get inactivated upon TSA treatment (Higgins et al, 2005).

Heterochromatin generally undergoes H3K9Me2/H3K9Me3 modifications but both these modifications are absent from centromeric chromatin. Studies from fission yeast, *Drosophila* and human revealed that histone H3 present at the *CENs* is dimethylated at lysine 4 (H3K4Me2) a modification which is generally associated with open but transcriptionally inactive chromatin. Hence centromeric chromatin appears to be of intermediate nature between heterochromatin and euchromatin (Sullivan & Karpen, 2004). It has been proposed that H3K4me2 is present at the *CEN* because centromeric repeats need to be transcribed in order to generate RNA that serves both structural and silencing roles (Cam et al, 2005; Du et al, 2010). Loss of H3K4me2 results in lack of transcription of satellite sequences and lower efficiency of HJURP-directed targeting of CenH3 to the *CEN* of an artificial human chromosome (Bergmann et al, 2011). Maize centromeric chromatin is different from the centromeric chromatin of other regional *CEN* containing organisms as it lacks H3K4Me2 and possesses H3K9Me2 characteristics of canonical constitutive

heterochromatin (Jin et al, 2008). Similar to maize *N. crassa* centromeric chromatin undergoes H3K9Me2 modification (Freitag et al, 2004a). Centromeric regions are gene-free and transcriptionally inactive in nature with the exception of *CENs* of rice and neocentromeres that contains some active genes (Nagaki et al, 2004; Yan et al, 2006).

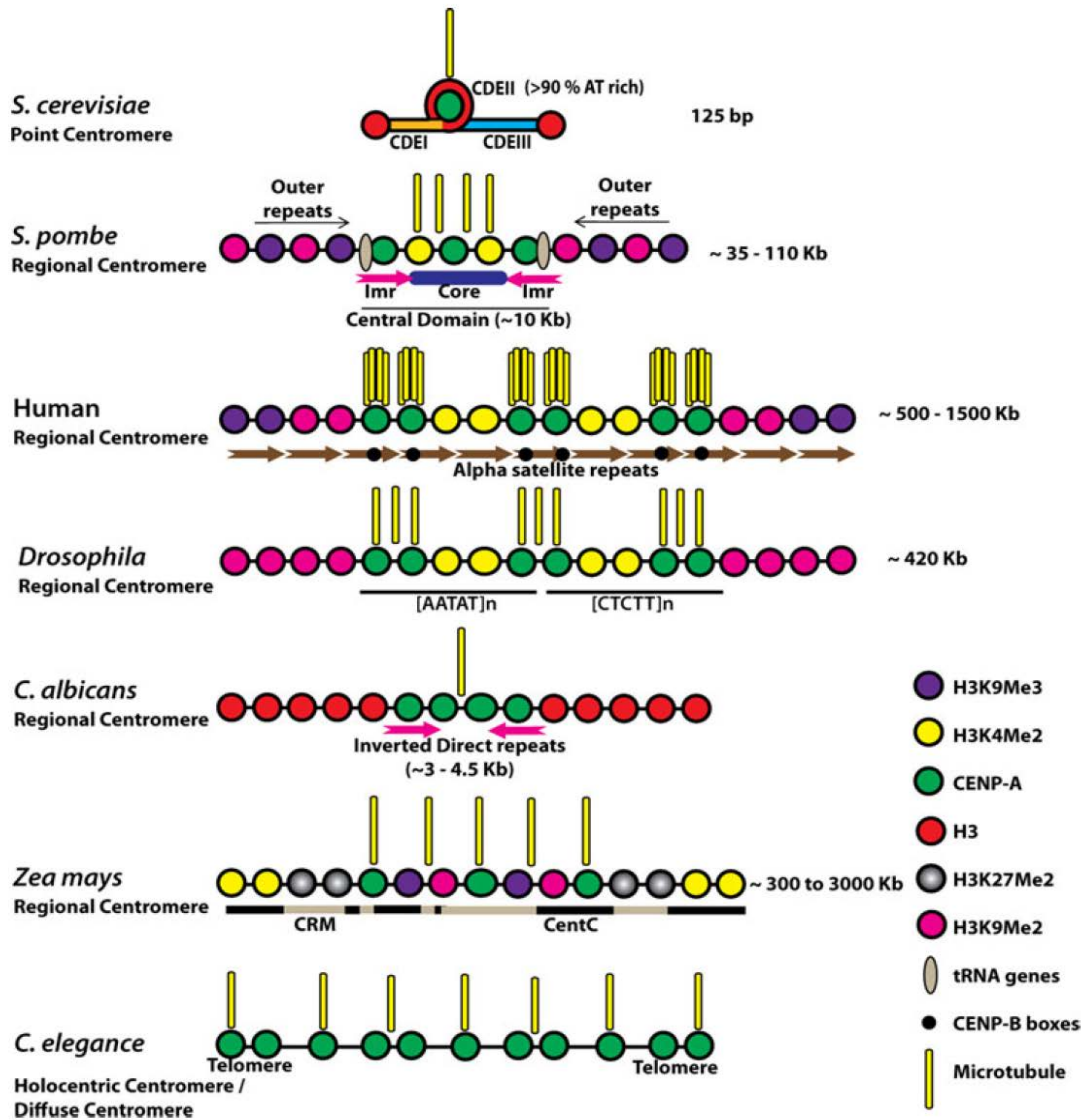


Figure 7. Histone modifications present at the centromeric and pericentromeric DNA of various organisms (Mehta et al, 2010).

1.6 .2 .6 DNA methylation

DNA methylation, an indicator of transcriptionally inactive chromatin, plays an important role in epigenetic demarcation of centromeric chromatin. Human *CENs* and neo*CENs* are

hypermethylated but this hypermethylation is not uniform as hypermethylated *CEN* DNA is interspersed with pockets of hypomethylated DNA that allows active transcription without compromising overall heterochromatic nature of centromere (Wong et al, 2006). DNA methylation at the human neocentromere does not show any strand bias. In human cells, CENP-C recruits the *de novo* DNA methyltransferase DNMT3B, which results in hypermethylation of *CEN* core sequences (Gopalakrishnan et al, 2009). Unlike human *CEN*s Arabidopsis 178-bp centromeric repeats are hypomethylated as compared to the same repeats located in the flanking pericentromeric regions. Hypomethylation of the DNA in centromeric chromatin was correlated with a reduced level of H3K9me2 in *A. thaliana*. Similar hypomethylation of centromeric DNA was also revealed in maize (Zhang et al, 2008). DNA methylation at *A. thaliana* centromeric DNA shows strand bias which has been proposed to be generated due to interference provided by *CEN* binding proteins.

An interesting difference exists in the pattern of centromeric DNA methylation between somatic and germ cells of mouse. While major and minor satellite repeats in all adult mouse tissues are hypermethylated those in sperm and metaphase II-arrested eggs are hypomethylated indicating that *CEN* DNA methylation is established later in somatic cells (Yamagata et al, 2007). Variable methylation pattern of major and minor repeats in germ cells and somatic cells may provide differential regulation to the KT attachment during meiosis and mitosis.

In addition DNA methyltransferases suppress recombination at centromeric heterochromatin (Jaco et al, 2008). This strongly suggests that the epigenetic state of *CEN*s controls recombination at these regions.

1.7 Centromere Evolution

As discussed before, *CEN*s in various organisms vary both in DNA sequence as well as in organization suggesting *CEN*s evolve rapidly (Henikoff et al, 2001). It is interesting to note that the *CEN*s which are under strong selective pressure to achieve chromosome segregation evolve even faster than the DNA elements such as transposable elements which are not under any selective pressure. For example *Oryza sativa* satellite CentO repeats have been replaced with another satellite sequences, called as CentO-F repeats in

closely related species *O. brachyantha* (diverged by ~ 7–9 million years) (Lee et al, 2005). Similarly, two other closely related rice species *O. officinalis* and *O. rhizomatis* show diversity in centromeric repeats (Bao et al, 2006). *Mus caroli* *CENs* have no similarities to minor satellites present in other mouse species instead they carry a completely unique sequence at the *CENs* that contains CENP-B box, a property similar to minor satellite (Kipling et al, 1995). Similar to DNA sequences a rapid evolution has been seen in *CEN* organization. Length of cent-O arrays in rice *CEN* vary from 65 kb to 2 Mb on different chromosomes (Cheng et al, 2002). Humans and great apes *CENs* contain 171 bp alpha satellites that are arranged in highly homogenous chromosome specific higher order repeat arrays flanked by monomeric repeats (Schueler et al, 2001; Schueler & Sullivan, 2006; Waye et al, 1987). On the other hand *CENs* of lower primates consist of only monomeric alpha satellites insinuating that complex higher order organization of alpha satellites present in humans has evolved from the simple monomeric alpha satellites (Schueler et al, 2001; Schueler & Sullivan, 2006). The possible reason for such variations in centromeric sequence and organization remains unknown. Asymmetric female meiosis has been proposed to be the drive for rapid centromeric evolution (Henikoff et al, 2001). ‘Selfish’ *CENs* gain a transmission advantage in a meiosis that is asymmetric with respect to the fate of the meiotic products. Evolution of point *CENs* of closely related lineages of the *S. paradoxus* with symmetric meiosis has been attributed to high mutation rate through a process of “centromere drift” not drive (Bensasson et al, 2008).

1.8 Evolution of CENH3

Centromeric histone, similar to *CEN* DNA, undergoes rapid evolution (Malik & Henikoff, 2001). Canonical histone H3 is highly conserved because of constant pressure to interact with entire genome. On the other hand highly variable CenH3 interacts with a comparatively smaller region which itself is undergoing a rapid change in sequence. A two-step model has been proposed to explain the rapid evolution of *CENs* and CenH3. Asymmetric meiosis in female contributes only one of the four meiotic products to form the egg. It has been shown that asymmetry of the meiotic tetrads provides an opportunity for the chromosome to compete for entry into oocyte nucleus by achieving preferential

orientation (NOVITSKI, 1955; Zwick et al, 1999). In the first step, any centromeric DNA variant which is capable of attracting more centromeric nucleosomes succeeds to sweep through the population. *CENs* achieve this by expansion of the satellite repeats. *CENs* with expanded repeats create more number of microtubule binding sites and make them stronger in terms of microtubule binding. Inequality of *CEN* strength in a heterozygote leads to nondisjunction during chromosome segregation. In the presence of such variations in *CEN* DNA, CenH3 has to recognize centromeric variants with equal efficiency to avoid nondisjunction. In the second step, CenH3 is subjected to positive selection to keep pace with rapidly evolving centromeric DNA. Any allele of CenH3 that suppresses inequality in the strength of *CEN* is selected for and fixed during evolution. Both N-terminal tail as well as loop-1 from HFD of CenH3 are subjected to the adaptive evolution (Malik & Henikoff, 2001) with the exception of budding yeasts. Loop-1 of the CenH3 is present at the interface of *CEN*-CenH3 interaction and thus presence of mutations in loop-1 supports the hypothesis that *CEN* and CenH3 are co-evolving.

Centromere drive model.

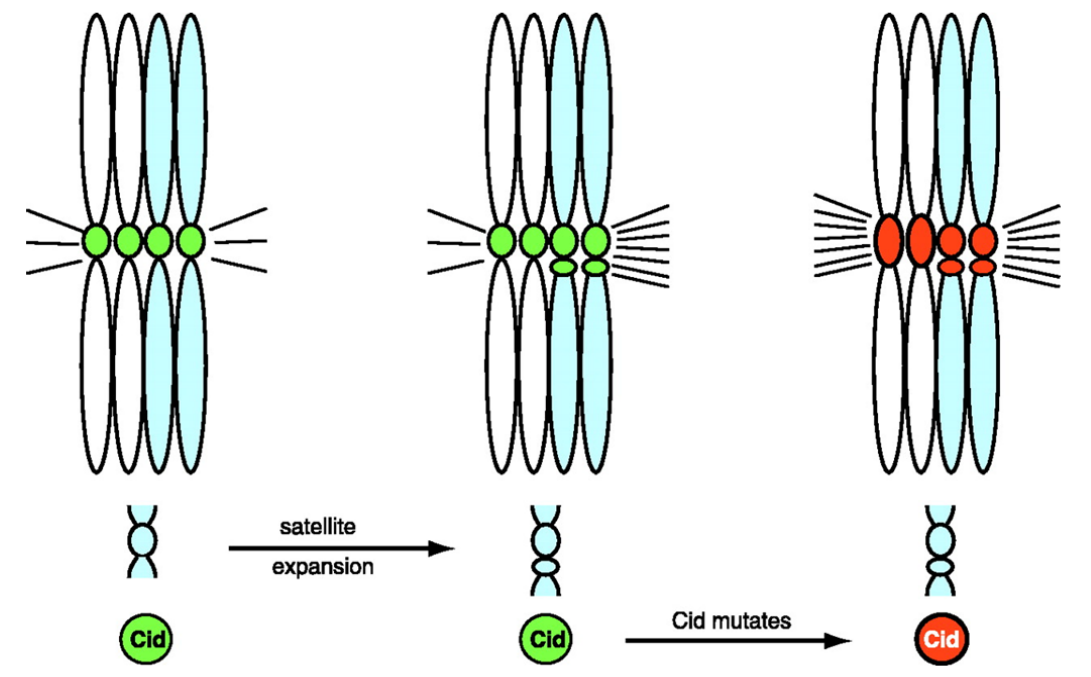


Figure 8. A model proposed by Henikoff and colleagues to explain co-evolution of *CENs* and CenH3.(Henikoff et al, 2001)

1.9.1 Kinetochores

The kinetochore (KT), a complex macromolecular structure, bridges mitotic spindle to the *CEN* to ensure faithful chromosome segregation during mitosis and meiosis. *CEN* DNA shows a wide range of diversity in length, sequence and composition across the species but KT proteins that bind to the *CEN* sequences show a higher degree of homology across the species (Allshire & Karpen, 2008; Cleveland et al, 2003). The inner layer of a KT interacts with *CEN* DNA while proteins present at outer layer interact with the spindle MTs. Several proteins in the middle layer link the inner and the outer layers to form the trilaminar KT structure. The simplest KT of budding yeast *S. cerevisiae* contains more than 80 proteins (Cheeseman & Desai, 2008) while that of humans contains more than 100 proteins (Fukagawa, 2004). Although the layers of the KTs are not visible in yeasts, based on similarity of specific domains in protein sequence along with biochemical evidence, KT proteins in yeasts have been classified into different layers. The KT proteins exist as sub-complexes that assemble on *CEN* DNA to form the KT (Cheeseman & Desai, 2008; De Wulf et al, 2003; Lechner & Carbon, 1991).

1.9.1.1 Inner kinetochore

In humans, inner CCAN complex (constitutive *CEN* associated network comprised of CENP-A, -B, -C, -H and -I) (Hori et al, 2008) is associated constitutively with *CEN* DNA throughout the cell cycle (McAinsh et al, 2003). The CENP-A (Cse4 in yeast) and the CENP-C (Mif2 in yeast) are evolutionarily conserved inner KT proteins and present in almost all the organisms where KTs have been studied. CENP-C depletion leads to severe defects emphasizing its importance in chromosome segregation, mitotic checkpoint function, and KT assembly (Heeger et al, 2005; Kwon et al, 2007). A DNA binding inner KT 4-protein CBF3 complex is point *CEN*-specific that is absent in regional *CEN* containing organisms. CENP-B, a DNA-binding protein helps in preventing *de novo* *CEN* formation in chromosomes with active *CENs* by ensuring that chromatin in the active *CEN* can be distinguished from other heterochromatin (Ohzeki et al, 2002; Okada et al, 2007).

1.9. 1.2 Middle Kinetochores

Middle KT complexes (the Spc105 complex, the Mis12 complex, the MIND complex and the COMA complex) similar to inner KT proteins are associated with *CENs* throughout the cell cycle. Spc105 appears to serve as a scaffold to which other KT components bind. In *C. elegans*, Spc105 is called KNL1 (kinetochores-null phenotype) as Spc105 depletion leads to a complete loss of the KT structure (Cheeseman et al, 2004). Depletion of Mis12 complex components leads to defects in chromosome alignment, orientation, segregation and integrity of the whole KT structure (Cheeseman et al, 2004; Goshima et al, 2003; Kline et al, 2006).

1.9. 1.3 Outer kinetochores

The outer KT proteins (such as the Ndc80 complex and the Ska1 complex) that help in KT-MT interaction are generally localized to KTs only during mitosis (Bharadwaj et al, 2004; Welburn et al, 2009). Because the NDC80 complex is located in the outer part of the structural KT core, its depletion usually does not disrupt the inner KT. Lack of the Ndc80 complex consistently results in severe spindle attachment defects (Ciferri et al, 2007). The Ndc80 complex is required to bind spindle assembly checkpoint proteins Mad1, Mad2, Mps1 kinase (Martin-Lluesma et al, 2002) and MTs *in vivo*. Motor proteins such as CENP-E, mitotic kinesin, dynein, chromosome passenger proteins, including INCENP, Aurora, and Survivin and spindle checkpoint proteins such as Mad, Bub, and ZW10 are part of the outer KT (De Wulf et al, 2003; Fukagawa, 2004; Maiato et al, 2004). Because outer KT proteins are present at the interface of KTs and kinetochores MTs, often these proteins are found to be associated with the mitotic spindle as well. In contrast to humans where outer KT proteins are assembled on KTs only during mitosis, the fungal specific Dam1 complex (the Ska1 complex is believed to be the functional homolog of the Dam1 complex in humans), an outer KT protein complex in budding yeast *S. cerevisiae*, remains associated with the KT throughout the cell cycle (Cheeseman et al, 2001a; Enquist-Newman et al, 2001; Janke et al, 2002).

Proteins from KNL-1/Spc105, the Mis12 and the Ndc80 complexes form a supercomplex called KMN network. The KMN network provides a link to connect *CENs* to the MTs. The KMN network permits the polymerization-depolymerization of the plus ends of MTs and responds efficiently to the regulatory mechanisms that enable chromosomes to align at the

metaphase plate prior to anaphase. The KMN also serves as the binding site for checkpoint proteins (Martin-Lluesma et al, 2002) .

KT components are separately recruited in space and time in a manner that reflects their physical separation. Although several proteins which constitute KT have been identified, not much is known about the assembly process of a KT.

1.9.2 Kinetochores assembly

Formation of mitotic spindles and establishment of KT-MT interaction occur during late S-phase in *S. cerevisiae* (De Souza & Osmani, 2007). KT-MT attachment is retained throughout the cell cycle. *CENs* replicate early in S-phase which results in detachment of chromosomes from the spindle. KT-MT interaction is re-established immediately after *CEN* DNA is replicated (Tanaka, 2010). KT assembly on point *CENs* of *S. cerevisiae* is considered to be a step-wise process that initiates with binding of inner KT proteins on specific *CEN* DNA sequence motifs. Unlike most eukaryotes, proteins present at the trilaminar KT are fully assembled early in the cell cycle and all the KTs remain clustered throughout the cell cycle in budding yeast *S. cerevisiae*.

The process of KT assembly has been shown to be species-specific as KT localization dependencies of various proteins vary from species to species. CENP-A is required for the localization of many KT proteins (Blower & Karpen, 2001; Goshima et al, 2003; Oegema et al, 2001). In *S. cerevisiae*, the inner and middle KT proteins Ndc10, Mif2, Mtw1, and Okp1 showed 50% decrease in occupancy at the active conditional *CEN* (*cCEN*) in the absence of Cse4, whereas the middle KT protein Ctf19 and many outer proteins (Ndc80, Dam1, Ask1, and Stu2) completely failed to localize (Collins et al, 2005). This suggests that Cse4 is the initiator for KT assembly in *S. cerevisiae*. However, several KT proteins do not require CENP-A for localization, suggesting that CENP-A-independent assembly pathways also exist in certain organisms (Goshima et al, 2003; Hayashi et al, 2004; Régnier et al, 2005). CENP-A localization has been shown to influence Mis12 localization in *S. cerevisiae*, *Drosophila* and humans but not in *S. pombe* (Liu et al, 2006; Przewloka et al, 2007; Takahashi et al, 2000; Westermann et al, 2003). On the other hand, Mis12 does not influence localization of CENP-A in most organisms except in *C. albicans* where CENP-A and Mis12 localization is interdependent (Goshima et al, 2003; Liu et al, 2006; Przewloka et al, 2007; Roy et al, 2011;

Takahashi et al, 2000). The localization dependencies of two inner KT proteins - CENP-A and CENP-C, in various organisms also showed species-specific differences. Depletion of CENP-A affects CENP-C localization in *S. cerevisiae*, *C. elegans* and humans but CENP-C has no effect on CENP-A localization in these organisms (Desai et al, 2003; Oegema et al, 2001). In contrast, CENP-A and CENP-C recruitment is interdependent in *Drosophila* (Erhardt et al, 2008), a dependency observed in our present study in *C. albicans*.

1.9.3 Kinetochores clustering

In mammalian cells KTs of thread like interphase chromosome are distributed throughout the nucleus while KTs of condensed mitotic chromosomes are arranged in a linear fashion on the metaphase plate. In budding yeasts *S. cerevisiae* due to small size, individual chromosomes are not visible and metaphase plate formation does not take place (Straight et al, 1997). All the KTs are clustered together throughout the cell cycle (Jin et al, 2000). Both assembly of KTs on *CEN* DNA during interphase and separation of sister KTs (hence separation of sister chromatids) by mitotic spindles during mitosis occur as a single unit in the clustered form probably to economize the protein segregation machinery in this unicellular organism. The KT clustering has been shown to be important for *CEN* function in *S. cerevisiae* as KTs are found to be unclustered in *ndc10*, *ame2* and *nuf2* mutants (Anderson et al, 2009; Jin et al, 2000). Interestingly, in *S. pombe* KTs are clustered only during interphase.

1.10 Chromosome segregation

Sister chromatids are glued together by cohesions till anaphase onset to avoid premature chromosome separation. Spindle MTs from the opposite poles provide poleward pulling forces to the chromosomes. Thus at the metaphase stage inward cohesive force due to sister chromatid cohesion is balanced by equal and opposite poleward forces generated by the spindles. At the onset of anaphase, cohesions are cleaved by an enzyme called separase and sister chromatids are set free to separate from each other under the action of net outward force generated by spindle MTs. Till the onset of anaphase, separase is kept inactive by its inhibitor securin to avoid premature separation of sister chromatids.

Anaphase promoting complex (APC), which in turn is activated by Cdc20, cleaves securin to activate separase to initiate anaphase A.

1.10 .1 Types of mitosis

The process of chromosome segregation has been extensively studied in various organisms including *S. cerevisiae*, *S. pombe* and humans. While the major sequence of events during sister chromatid separation remains the same, a few species-specific differences in mitotic cell division exist. Metazoan cells undergo open mitosis (Güttinger et al, 2009; Sazer, 2005) where the MTs, originating from microtubule organizing centers (MTOCs), gain access to the KT only when the nuclear envelope breaks down during mitosis. In these cells chromosomes are arranged in a metaphase plate at the equator of a mitotic spindle before sister chromatid segregation. On the contrary, the MTOCs in budding yeasts, called spindle pole bodies (SPBs), are embedded in the nuclear envelope and assemble an intra-nuclear mitotic spindle (Byers & Goetsch, 1975). Interaction of spindle MTs with KTs, which does not require nuclear envelope breakdown in closed mitosis in budding yeasts, starts early in the cell cycle (De Souza & Osmani, 2007; Heath, 1980). Although fission yeast *S. pombe* undergoes closed mitosis (Heath, 1980), SPBs remain outside the nuclear envelope during interphase (Kniola et al, 2001) and spindle MTs are only nucleated when the duplicated SPBs enter the nuclear membrane following mitotic initiation (Ding et al, 1997). Thus the process of chromosome segregation in *S. pombe* is somewhat intermediate between *S. cerevisiae* and humans. Finally, the number of MTs that bind to a single chromosome differs in these organisms: in *S. cerevisiae* only one (Winey et al, 1995), in *S. pombe* 2-3 (Ding et al, 1993) and in metazoans multiple MTs (20-25 in human) (McDonald et al, 1992) bind per KT. Thus, clear differences exist among budding yeast, fission and metazoans in the timing of onset of KT-MT interaction, the number of MTs associated with each KT and the pattern of nuclear breakdown.

1.10 .2 Spindle length regulation

Unlike fission yeast and metazoans, KT-MT interaction starts at a pre-mitotic phase in *S. cerevisiae* (Byers & Goetsch, 1975). Several lines of evidence suggest that the mitotic spindle in *S. cerevisiae* is kept short till anaphase onset to facilitate proper KT-MT

attachment and to avoid premature chromosome segregation (Bachant et al, 2005; Li et al, 2002; Liu et al, 2008). Hydroxyurea (HU), a DNA synthesis inhibitor, arrests cells in S-phase with a short spindle in the presence of S-phase checkpoint (Krishnan et al, 2004). *ask1-3*, a temperature-sensitive KT mutant in *S. cerevisiae* exhibits elongated spindles and abnormal KT localization in presence of HU (Liu et al, 2008) suggesting that a proper KT-MT interaction is important for spindle length maintenance even in the pre-mitotic phases of budding yeast cell cycle.

In contrast to fission yeast in which a long G2 phase separates S and M phases, budding yeast S phase overlaps with M phase (Nasmyth, 2001). Before sister chromatid separation takes place in mitosis, all chromosomes need to be bioriented (Tanaka, 2010). Improper KT-MT interaction (unattached KTs or improper tension) activates the spindle assembly checkpoint (SAC) system (Mad1p, Mad2p, Mad3p, Bub1p, Bub2p, Bub3p, and Mps1p are part of the SAC in yeast) that prevents metaphase-anaphase transition (Musacchio & Salmon, 2007). Eventually inactivation of SAC by proper KT-MT interaction allows sister chromatid separation. The process of chromosome segregation involves three types of MTs that originate from SPBs: i) KT MTs (kMTs) that connect SPBs to KTs, generate poleward pulling forces for sister chromatid separation during anaphase A. The Dam1 complex (described below) in *S. cerevisiae* has been shown to be a coupler that transduces MT depolymerization activity into poleward pulling forces, ii) non-KT/interpolar MTs (IPMTs), which interdigitate at spindle midzone with the help of plus-end MT binding proteins (Brinkley & Cartwright, 1971; Mastronarde et al, 1993), elongate to generate outward pushing forces to further separate sister chromatids during anaphase B and iii) astral/cytoplasmic MTs that protrude towards cytoplasm (Palmer et al, 1992) regulate spindle length and alignment (Goshima & Scholey, 2010). Interaction of astral MTs with cell cortex generates backward force that acts on spindle poles and keep them at a specific distance apart from each other (Carminati & Stearns, 1997; McCollum, 2002; Oliferenko & Balasubramanian, 2002; Palmer et al, 1992; Theesfeld et al, 1999).

1.10 .3 Spindle assembly checkpoint

Improper KT microtubule attachment (unattached KTs or improper tension) is capable of activating the SAC system that prevents metaphase-anaphase transition (Musacchio &

Salmon, 2007). SAC is not essential for viability in *S. cerevisiae* probably due to natural high fidelity of chromosome segregation imparted by almost constitutive KT-MT interactions during cell cycle. In other eukaryotes on the other hand owing to a more complex architecture of chromosomes, KT-MT interface and the timing of KT-MT interaction the probability of errors to occur during chromosome segregation is relatively high. To avoid frequent errors which might lead to nondisjunction events, SAC has been fixed as an essential surveillance system in metazoans. Majority of the mutations in variety of cancers are found in genes involved in SAC (Table 1).

Saccharomyces cerevisiae protein	Function/domain	Human protein (localization)	Homology	Conservation
CBF3 complex				
Ndc10	CBF3 component	-	-	-
Cep3	CBF3 component, zinc-finger domain	-	-	-
Ctf13	CBF3 component, F-box protein	-	-	-
Skp1	CBF3 component, Ctf13 activation, SCF component	p19/SKP1 (centrosome)	3.3e-52	C, RN
CBF3 regulator				
Sgt1	Ctf13 activation, SCF component	SGT1	1e-21	R
Ipl1	Ndc10 kinase	IAK1 (mouse) (spindle pole)	3e-73	S (mouse)*
Glc7	Ndc10 phosphatase?	PP1 (PPP1cc)	1e-162	ND
Other inner kinetochore				
Cse4	Centromeric histone H3	CENPA (centromere)	5e-16	F, CN
Cbf1	CDE1-binding protein, MET-gene regulation	TFE3?	3e-05	ND
Outer kinetochore and others				
Mif2	Inner/outer kinetochore?	CENPC (centromere)	0.31	ND
Ctf19	Outer kinetochore	-	-	-
Mcm21	Outer kinetochore	-	-	-
Okp1	Outer kinetochore	CENPF? (centromere)	0.94	ND
Slk19	Outer kinetochore?	CENPF? (centromere)	3.5e-07	ND
Mtw1	Outer kinetochore?	-	-	-
Plc1	Phospholipase C	PLC- δ 1	5.2e-57	R (soybean)
Ndc80	Outer kinetochore?	HEC1 (centromere)	2e-16	R
Nuf2	SPB?/Outer kinetochore?	HNUF2R	2.4	ND
Spc24	SPB?/Outer kinetochore?	-	-	-
Spc25	SPB?/Outer kinetochore?	-	-	-
Spc19	SPB?/Outer kinetochore?	-	-	-
Spc34	SPB?/Outer kinetochore?	-	-	-
Dam1	Microtubule-binding protein	-	-	-
Stu2	Microtubule-binding protein	Ch-TOG	2.6e-27	ND
Bik1	Microtubule-binding protein	CLIP170 (centromere)	1.5e-11	ND
Cin8	Kinesin-related protein	HKSP	1e-85	ND
Spindle checkpoint				
Bub1	Ser/Thr protein kinase	BUB1 (centromere)	1e-42	F
Bub3	WD-repeat protein	BUB3 (centromere)	4e-30	F
Mad1	Coiled-coil domain	MAD1 (centromere/centrosome?)	0.0081	F
Mad2		MAD2L1 [†] (centromere/centrosome)	6e-39	F, C (<i>Caenorhabditis elegans</i>) CN (<i>Xenopus laevis</i>)
Mad3	Similar to Bub1, but not to kinase domain	BUBR1 (centromere) [§]	4e-21	F
Mps1	Ser/Thr protein kinase	PYT/TTK1 (centromere)	9.5e-62	F

Table1. Budding yeast kinetochore and spindle- checkpoint components (Kitagawa & Hieter, 2001).

SAC is often referred to as the KT checkpoint as it is activated by unattached KTs. Unequal tension at the KTs is also capable of activating SAC through generation of unattached KTs. Mad2, a component of SAC is accumulated at the unattached KTs. Mad2 inhibits APC by inhibiting its activator Cdc20. In the absence of active APC, securin keeps separase inactive

and cells are arrested at metaphase-anaphase transition. A proper KT-MT interaction inactivates SAC, activates APC which in turn activates separase by cleaving securin and cells proceed towards anaphase as cohesin between sister chromatids is cleaved.

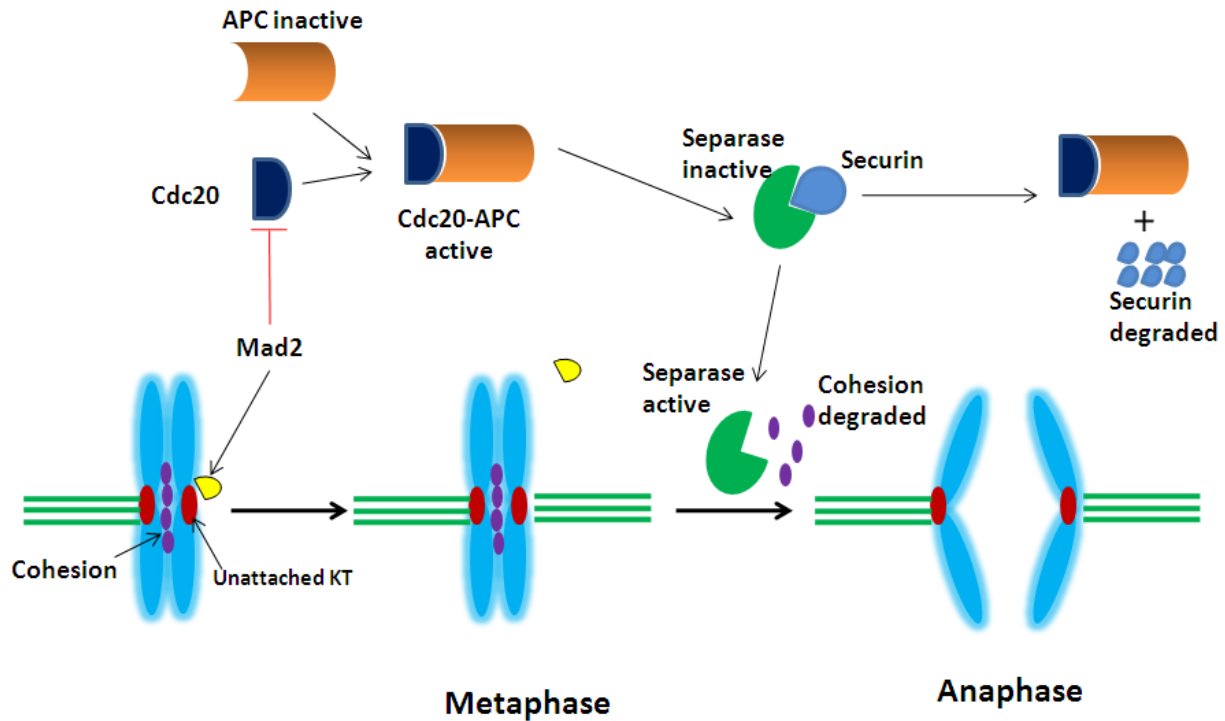


Figure 9. Schematic showing regulation of metaphase-anaphase transition.

1.10 .4 Dam1 complex

A fungal-specific 10-protein outer KT complex, namely the Dam1 complex, has been shown to be involved in KT-MT interaction in *S. cerevisiae* (Asbury et al, 2006; Franck et al, 2007; Kiermaier et al, 2009; Nogales & Ramey, 2009; Westermann et al, 2006). In this organism, mitotic spindles are highly compromised in various mutants of the Dam1 complex (Cheeseman et al, 2001a; Cheeseman et al, 2001b; Enquist-Newman et al, 2001; Hofmann et al, 1998). Each of the 10 proteins of the Dam1 complex is essential for viability, localized at the KT throughout the cell cycle and help in chromosome segregation by forming rings around the MTs in *S. cerevisiae* (Westermann et al, 2005).

In vitro reconstitution of the 10-protein Dam1 complex in *S. cerevisiae* facilitated electron microscopy studies of the complex bound to MTs, which revealed an array of rings and

spirals interacting in a novel manner with the underlying tubulin (Miranda et al, 2005; Westermann et al, 2005). End-on views suggested that 13-protofilament MTs are surrounded by 16 repeats of the Dam1 complex oligomerized into a ring (Westermann et al, 2006). Although rings are yet to be visualized *in vivo*, they are considered to be an ideal structure that allows coupling of the energy released during microtubule depolymerization, when GDP-tubulin relaxes into its low-energy state by protofilament peeling. Recent studies however have cast doubts on Dam1 ring structures *in vivo*, rather the separate Dam1 complex seem to work independently but in a co-ordinated fashion (Gao et al 2010). The Dam1 complex is one of the Ipl1 (Aurora B protein kinase) substrates. Ipl1-dependent phosphorylation of Dam1 is maximal during S phase and minimal during metaphase in *S. cerevisiae*. The phosphorylated/dephosphorylation pattern can be correlated with the cell cycle window. Chromosome bi-orientation occurs when KT and MT are under maximum tension. Interestingly, when tension was reduced at KTs through failure to establish sister chromatid cohesion, Dam1 phosphorylation persisted in metaphase arrested cells. Thus Ipl1-facilitated biorientation is stabilized in response to tension at KTs by dephosphorylation of Dam1 that results in termination of KT-MT attachment turnover (Keating et al, 2009).

In *S. pombe*, on the other hand, the Dam1 complex is localized at the KT only during mitosis and none of the proteins in this complex is essential for the viability but mutations in these proteins lead to increased chromosome mis-segregation. Non-essential Dam1 complex is required for the retrieval of unclustered KT in *S. pombe* at the depolymerising microtubule plus end. In the absence of Dam1 complex unclustered KTs are captured on the lateral surface of spindle microtubule bundles but KT fails to move towards poles. This was the first direct evidence to show that the Dam1 complex can couple the force generated by microtubule depolymerisation to direct chromosome movement *in vivo* (Franco et al, 2007).

Functional differences of the Dam1 complex in the conserved process of chromosome segregation raises an interesting question: can redundancy in essentiality of the Dam1 complex be correlated with the timing of KT-MT interaction (pre-mitotic or mitotic) as well as localization of this complex (constitutive or mitotic) at the KT or is it the type of a *CEN* (point or regional) that determines the essentiality of this complex?

1.11 *Candida albicans*

C. albicans is an asexual pathogenic budding yeast with eight chromosomes (named 1-7 and R) that constitutes a haploid genome size of 14,851 kilobases (kb), containing 6,419 open reading frames (ORFs) longer than 100 codons. *C. albicans* belongs to the CTG clade of subphylum Saccharomycotina of phylum Ascomycota and translates CTG as serine instead of leucine.

1.11 .1 Classification

Kingdom: Fungi

Phylum: Ascomycota

Subphylum: Saccharomycotina

Class: Saccharomycetes

Order: Saccharomycetales

Family: Saccharomycetaceae

Genus: *Candida*

Species: *C. albicans*

C. albicans is a polymorphic fungus which exists in budding yeast, hyphae, opaque cell with mating projections, chlamydospore and pseudohyphae forms. Switching between these forms (yeast to hyphae and white to opaque) involves interplay of a network of genes that encode well conserved polarity regulating proteins (Bachewich et al, 2005).

1.11 .2 Diseases

C. albicans is the most commonly isolated fungal pathogen, which causes candidiasis in immunocompromised patients that may lead to death up to 50% of patients (Eggimann et al, 2003; Gudlaugsson et al, 2003; Wey et al, 1988). Virulence factors involved are adhesions, integrin receptors, proteolytic enzymes, dimorphism and biofilm formation (de Groot et al, 2004; Klis et al, 2009; Kumamoto, 2002). Main reasons behind the success of *C. albicans* as an opportunistic pathogen is due to its capacity to live as a benign commensal in a variety of locations inside human body most notably the oral cavity, genitalia and gastrointestinal tract (Soll, 2002).

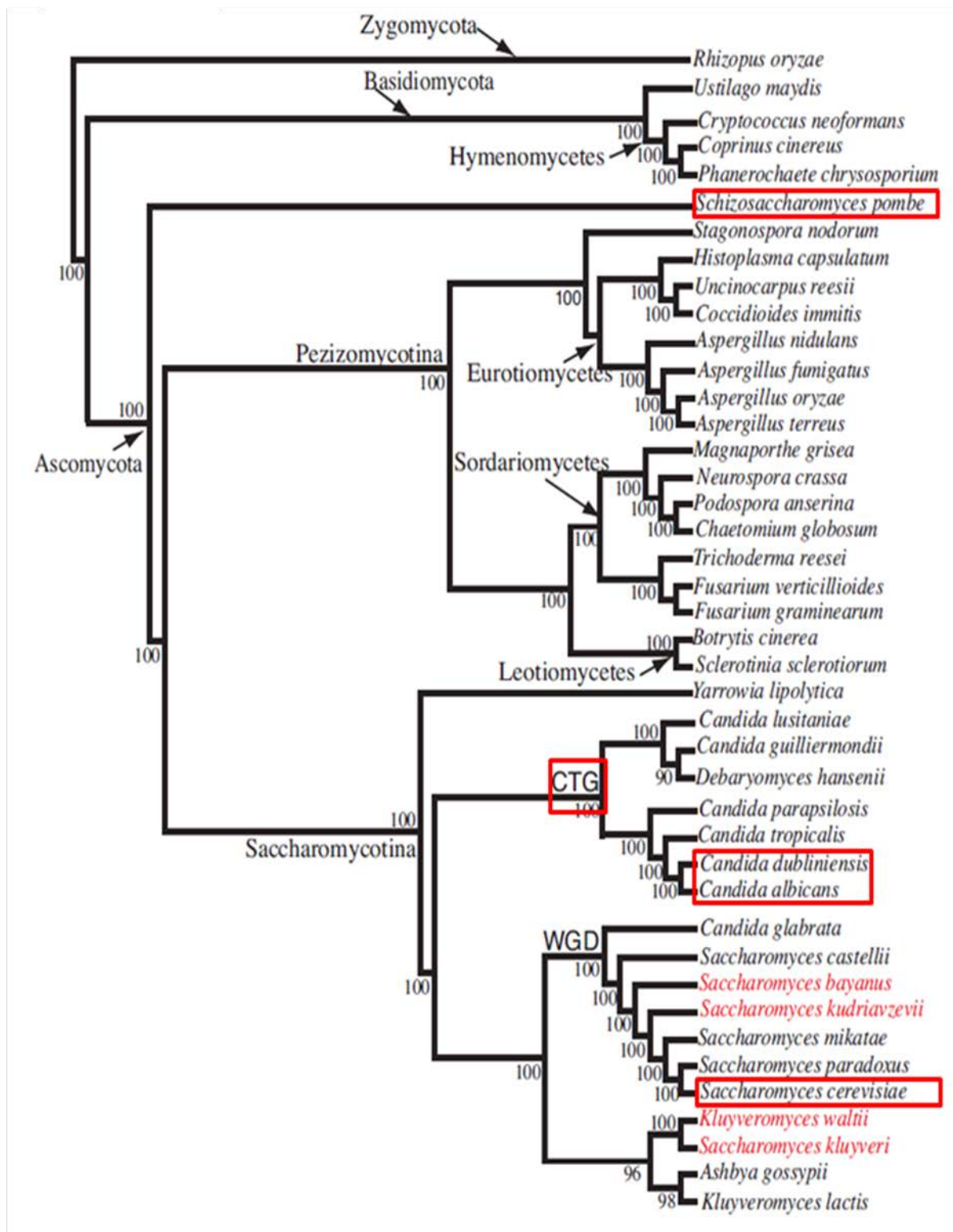


Figure10. Phylogenetic tree showing evolution of Ascomycetes including *S. cerevisiae*, *Candida* species and *S. pombe* (Fitzpatrick et al, 2006).

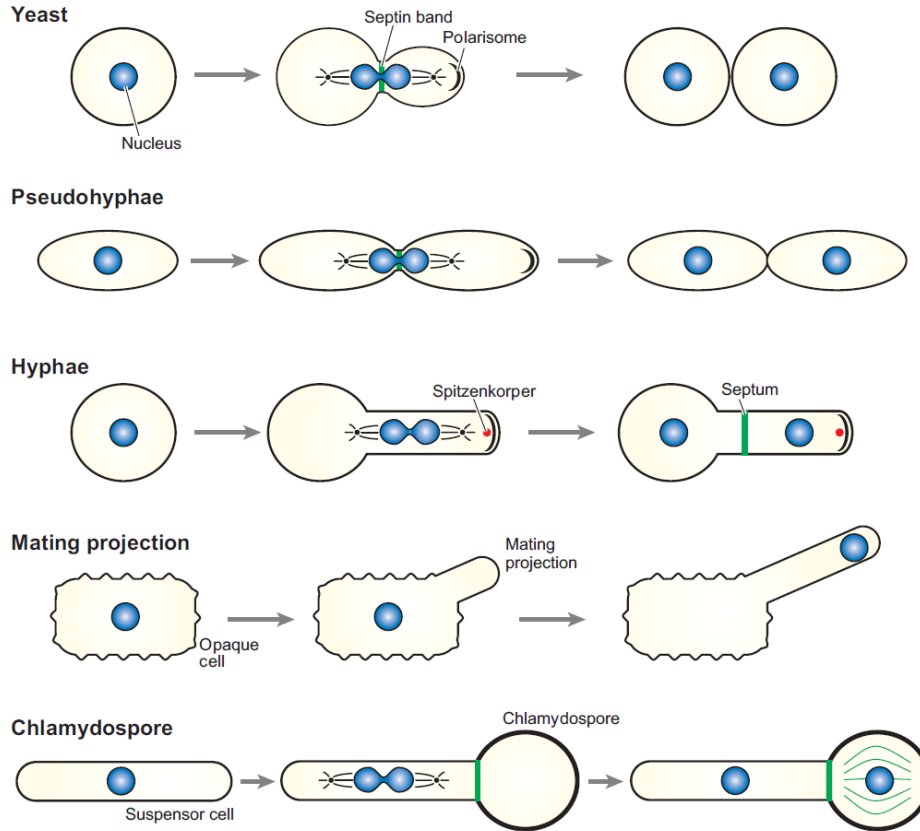


Figure 11. Various morphological forms of *C. albicans* (Bachewich et al, 2005).

1.11 .3 Ploidy, Aneuploidy and chromosomal rearrangements

Budding yeast *S. cerevisiae* and fission yeast *S. pombe* can propagate stably both in diploid as well as in haploid state. Both these yeasts, however, prefer a favorite ploidy state. *S. cerevisiae* is stably maintained as a diploid yeast while *S. pombe* prefers the haploid state. Pathogenic budding yeast *C. albicans* on the other hand propagate exclusively as a diploid yeast with no report of the existence of the haploid state either in nature or in laboratory. Despite absence of a discernable meiotic cycle *C. albicans* is capable of generating diversity in response to stress conditions either by undergoing parasexual cycle (Bennett & Johnson, 2003) or by mating with opposite or same mating type cells as demonstrated only in laboratory conditions (Alby et al, 2009). *C. albicans*, like other microbes, develops resistance against the antifungal drugs. Most commonly used antifungal drug for treating candidiasis is fluconazole. The appearance of azole-resistance in *Candida* poses a serious

problem after long-term treatment of recurrent candidiasis in HIV-infected patients. The evolution of drug resistance depends on phenotypic variability arising from the mutations that alter gene expression or protein activities (Cowen & Steinbach, 2008) or chromosomal rearrangements resulting in increased gene dosage (Selmecki et al, 2009). Drug resistant *Candida* strains isolated from patients or generated in laboratory conditions reveal high occurrence of aneuploidy and chromosomal rearrangements (Perepnikhatka et al, 1999; Poláková et al, 2009; Selmecki et al, 2006). Aneuploidy and chromosomal rearrangements are typical hallmarks of cancer cells. Thus *C. albicans* appears to be a suitable system to understand role of these events in cancer cells. Aneuploidy results due to non-disjunction of chromosomes during chromosome segregation and is monitored by cell surveillance system, the spindle assembly checkpoint. Could the occurrence of frequent chromosomal rearrangements and aneuploidy in *C. albicans* be due to inefficient surveillance during chromosome segregation? Thus studying both the process of chromosome segregation and the spindle assembly checkpoint is of fundamental importance to understand biology of *C. albicans* that might help in understanding and combating virulence of this deadly pathogen.

1.11 .4 Cell cycle, Chromosome segregation, Centromeres and Kinetochores

Major events of the cell cycle in *C. albicans* highly resemble those of *S. cerevisiae*. Both these budding yeasts undergo closed mitosis as nuclear envelope remains intact during mitosis. KT-MT interaction is established early during the cell cycle and persists throughout the cell cycle (Roy et al, 2011; Sanyal & Carbon, 2002). Similar to *S. cerevisiae* only one MT has been shown to bind to a single KT in *C. albicans* (Joglekar et al, 2008). To identify *CENs* the centromeric histone of *C. albicans* CaCse4 was first characterized. The CENP-A/CaCse4 the centromeric histone of CENP-A family in *C. albicans* was shown to be localized at the KTs, essential for viability and indispensable for chromosome segregation. The centromeric properties of pathogenic diploid budding yeast *C. albicans* turned out to be of an intermediate nature between 125 bp long point *CENs* (*CENs*) of *S. cerevisiae* and 40 -110 kb long repetitive regional *CENs* of *S. pombe*. CaCse4 binds to 3-5 kb *CEN* DNA sequences which are unique and different in *C. albicans*. These regions lack any conserved motifs or common repeats. These centromeric sequences have been shown to be insufficient to establish a functional *CEN* when placed at ectopic locations or when introduced

exogenously suggesting that *C. albicans* *CENs* are specified epigenetically (Baum et al, 2006; Sanyal et al, 2004). Replacement of native *CEN5* with *URA3* marker gene leads to neocentromere formation efficiently at multiple loci (Ketal et al 2009). Each *CEN* of *C. albicans* has been associated with a replication origin that is the first to fire on its respective chromosome (Koren et al 2010).

1.12 *Candida dubliniensis*

C. dubliniensis, another human fungal pathogen, is most closely related to *C. albicans*. *C. albicans* and *C. dubliniensis* diverged 20 million years ago from a common ancestor (Mishra et al, 2007). These two species differ significantly in virulence properties. *C. dubliniensis* is found mostly as an oral pathogen and only rarely in disseminated infections (Gilfillan et al, 1998). Two species can share more than 98% identity between orthologous genes and interspecific hybrids can be formed by mating (Pujol et al, 2004). However, *C. dubliniensis* can be distinguished from *C. albicans* on the basis of a few distinct biological properties (Coleman et al, 1998). *C. dubliniensis* is more sensitive to higher temperatures (Coleman et al, 1998), chlamydospores formation is more profuse under conditions where *C. albicans* does not make them (Staib & Morschhäuser, 1999). Decreased virulence of *C. dubliniensis* as compared to *C. albicans* has been attributed to its lower efficiency of hyphal formation and absence of many genes involved in the virulence in *C. albicans*.

1.13 Summary of present study

In this work we identified *CENs* of *C. dubliniensis* the most closely related sequenced species to *C. albicans*. We reasoned that *CEN* DNA sequence comparisons between related *Candida* species might uncover properties that were not evident from inter-chromosomal comparisons of *C. albicans* *CEN* sequences alone. A comparative genomic analysis of *CEN* DNA sequences of *C. albicans* and *C. dubliniensis* revealed no detectable conservation among CENP-A-associated *CEN* sequences. Most strikingly, a genome-wide analysis revealed that *CENs* are probably the most rapidly evolving genomic loci in *C. albicans* and *C. dubliniensis*. However, the lengths of CENP-A-enriched DNAs assembled as specialized centromeric chromatin and their relative locations in orthologous regions have been maintained for millions of years. We speculated that not the sequence but the relative

physical location of the *CENs* along the entire length of a chromosome defines the epigenetic memory for the establishment of a functional *CEN* in *Candida* species. Indeed, a noncentromeric DNA sequence (*URA3* marker) inserted at native *CEN7* could assemble centromeric chromatin on it. However it is difficult to rule out the contribution of *CEN7* sequences in the assembly of CENP-A containing centromeric chromatin at least when present in its natural context because *URA3* failed to recruit CENP-A on it when *CEN7* was deleted and replaced by *URA3*. Subsequently we show that neocentromere formation follows a pattern which supports our hypothesis of relative physical location to be one of the epigenetic determinants of neocentromere formation. We propose a model to explain how physical location of a *CEN* determines centromere/neocentromere identity in *C. albicans*. We also observed gene conversion at *C. albicans* *CEN*. Most strikingly we show that an already established neocentromere is inactivated in the presence of an active *CEN* acquired during gene conversion by *in vivo* recombination. We correlate this phenomenon to lateral inhibition a hypothesis which was proposed previously for *Drosophila* *CENs* (Maggert & Karpen, 2001).

Assembly of KTs on the CEN DNA is one of the epigenetic factors that determine identity of regional CENs. As discussed before KT assembly on point CENs of *S. cerevisiae* is considered to be a step-wise process that initiates with binding of inner KT proteins on specific CEN DNA sequence motifs. In this study, we investigated the process of KT assembly on regional CENs in *C. albicans*. To understand the process of KT assembly we sought to study localization interdependencies of KT proteins from three different layers of KTs in *C. albicans*. Proteins from inner (CENP-A and CENP-C) and middle KTs have been characterized in *C. albicans* (Sanyal et al, 2004; Sanyal & Carbon, 2002). In order to understand the process of entire assembly of KT, outer KT proteins needed to be studied in *C. albicans*. A fungal-specific outer KT complex, the Dam1 complex, is essential in *S. cerevisiae*, non-essential in fission yeast, and absent in metazoans. The reason for gradual decrease in the requirement of this complex from yeast to human remains unknown. We chose to characterize the Dam1 complex in *C. albicans* for three reasons 1) Dam1 complex subunits are good candidates for outer KT components to understand the process of KT assembly in *C. albicans* 2) Determining the essentiality of the Dam1 complex in *C. albicans*

would provide evolutionary insights into its function in organisms with three different types of *CENs* i.e. point *CENs* in *S. cerevisiae*, intermediate *CENs* in *C. albicans* and regional *CENs* in *S. pombe* 3) Fungal specific nature of the Dam1 complex makes it a potential target to develop drugs against candidiasis. Here, we show that the Dam1 complex is essential for viability and indispensable for proper mitotic chromosome segregation in *C. albicans*. KT localization of the Dam1 complex is independent of the KT-MT interaction but the function of this complex is monitored by spindle assembly checkpoint. Strikingly, the Dam1 complex is also required to prevent precocious spindle elongation in pre-mitotic phases. Thus, constitutive KT localization associated with one microtubule-one KT-type of interaction, but not the length of a *CEN*, is correlated with essentiality of the Dam1 complex.

Localization dependencies of various KT proteins studied by immunofluorescence using confocal microscopy and chromatin immunoprecipitation assays revealed that the three-layered KT assembly is a highly coordinated and interdependent event in *C. albicans*. Depletion of an essential KT protein from any of the three layers results in KT unclustering followed by a complete collapse of the KT architecture. We propose that these essential KT proteins help in inter-KT interaction to maintain the cluster of KTs - essential to keep integrity of an individual KT ensemble. Further, we show that each of inner, middle or outer layers of the KT is required to maintain integrity of centromeric chromatin formed by CENP-A/Cse4 molecules. Most strikingly, western blot analysis with anti-Cse4 antibodies revealed that depletion of any of these essential KT proteins results in complete degradation of CENP-A molecules. Taken together, we propose that a coordinated interdependent circuitry of many essential proteins from various layers of the KT maintains KT clustering, a phenomenon that ensures integrity of an individual KT formed on the foundation of CENP-A containing centromeric chromatin and protects CENP-A molecules from degradation.

Results

A. RAPID EVOLUTION OF CENP-A/CSE4P-RICH CENTROMERIC DNA SEQUENCES IN CLOSELY RELATED PATHOGENIC YEASTS, CANDIDA ALBICANS AND CANDIDA DUBLINIENSIS

With an aim of finding out conserved sequence motifs that might specify *CEN* identity in *Candida* species we identified *C. dubliniensis* *CENs* to perform a sequence comparison between *CENs* of *C. albicans* and *C. dubliniensis*. However, discovery of *C. dubliniensis* *CENs* revealed that unlike known point and regional *CENs* of other organisms, *CENs* in *C. albicans* and *C. dubliniensis* have no discernable common *CEN*-specific sequence motifs or repeats except some of the chromosome-specific pericentric repeats that are found to be similar between orthologous chromosomes of these two species.

A1. SYNTENY OF CENTROMERE-ADJACENT GENES IS MAINTAINED IN C. ALBICANS AND C. DUBLINIENSIS. Synteny (collinearity) of genes is maintained almost throughout the genome in these two species. To find out potential orthologous *CEN* regions in *C. dubliniensis* we identified homologs of *CEN* adjacent *C. albicans* ORFs in *C. dubliniensis* by BLAST analysis. *C. dubliniensis* genome database is available at http://www.sanger.ac.uk/cgi-bin/blast/submitblast/c_dubliniensis.

Table A1. Comparison of the amino acid (aa) sequence homology of the ORFs flanking the *CEN* regions in *C. albicans* and *C. dubliniensis*

Chr #	<i>C. albicans</i> ORF #	<i>C. dubliniensis</i> ORF #	<i>C. albicans</i>		<i>C. dubliniensis</i>		Orientation	aa homology (%)
			Coordinates	aa length	Coordinates	aa length		
1	4438	Cd36_06830	1580117-1581640	507	1611890-1613440	516	Direct	88
	4440	Cd36_06810	1559352-1561871	839	1591631-1594162	843	Direct	91
2	1601	Cd36_23540	1923194-1924363	389	1938439-1939608	389	Direct	99
	1604	Cd36_23560	1934775-1931570	916	1947203-1949623	806	Reverse	84

3	2812	Cd36_83930	828667-827105	503	871879-873366	495	Reverse	84
	6923	Cd36_83920	820347-821378	343	865253-866083	276	Direct	90
4	3818	Cd36_44310	1010148-1009312	278	1036396-1037226	276	Reverse	88
	3821	Cd36_44290	1000558-999371	395	1025948-1027126	392	Reverse	81
5	3160	Cd36_51930	467208-466702	168	493689-494072	127	Reverse	95
	4216	Cd36_51940	473741-474247	168	500592-500975	127	Direct	94
6	1096	Cd36_64780	965934-968573	879	934029-936683	884	Direct	84
	2124	Cd36_65100	982460-981390	353	1016599-1017672	357	Reverse	87
7	6522	Cd36_71800	431903-430173	586	439178-440899	573	Reverse	94
	6524	Cd36_71780	423631-422459	390	424821-425993	390	Reverse	99
R	597	Cd36_33630	1759087-1757405	560	1722610-1724292	560	Reverse	97
	600	Cd36_33620	1748818-1745649	1056	1710255-1713449	1064	Reverse	90

The coordinates of the *C. albicans* and *C.dubliniensis* chromosomes correspond to Assembly 20 of *C. albicans* Genome Database and *C. dubliniensis* Genome Database (version available on 16 May 2007).

The only chromosome that does not maintain gene synteny is Chr6 (Figure A1 and Figure A6). *C. albicans* CEN6 is flanked by Orf19.1097 (*C. dubliniensis* lacks Orf19.1097 homolog) and Orf19.2124. We identified the *C. dubliniensis* homolog of Orf19.1096 (next to Orf19.1097 in *C. albicans*) which is 80 kb away from homolog of Orf19.2124 as compared to 12.8 kb away in *C. albicans*. Detailed analysis of 80 kb region in *C. dubliniensis* revealed occurrence of intrachromosomal rearrangement explained in Figure. A1. Similarly due to absence of homolog of Orf19.3820 in Chr4 of *C. dubliniensis*, we considered adjacent Orf19.3818 for the sequence comparison.

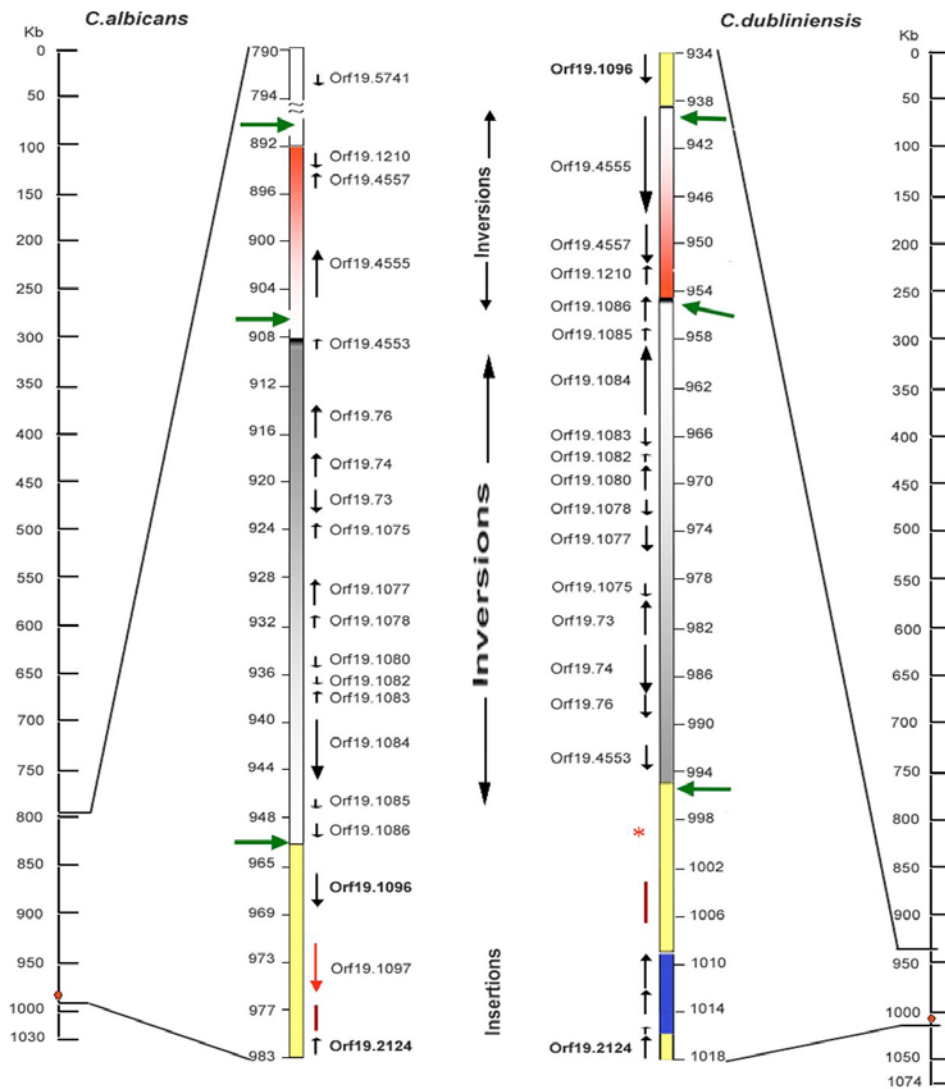


Figure A1. Comparative analysis of the orthologous regions spanning *CEN6* in *C. albicans* and *C. dubliniensis*. Chromosomal maps of Chr6 of *C. albicans* and *C. dubliniensis*. Red dots represent the *CEN* regions. Black arrows along with the ORF numbers show the gene arrangement and the direction of transcription. Two paracentric inversions in *C. dubliniensis* are marked in shaded red and gray boxes. Gradation of colors represents the inversions in *C. dubliniensis* when compared to *C. albicans*. The green arrows indicate breakpoints where the inversions have occurred. The blue region in *C. dubliniensis* shows the region of insertions of ORFs from other chromosomes. The yellow regions are unaltered. The orange star in the *C. dubliniensis* map shows a premature termination codon. Brown bar, Cse4p-binding region.

A2. THE CENTROMERIC HISTONE PROTEIN OF *C. DUBLINIENSIS* (CdCse4) IS LOCALIZED AT THE KINETOCHORE. Using CaCse4 as the query in BLAST analysis against the *C. dubliniensis* genome, we identified the centromeric histone of *C. dubliniensis*, CdCse4.

CdCse4 (212 aa-long) is highly similar (97% identity over 211 aa) to CaCse4 and the HFD of Cse4 in *C. albicans* and *C. dubliniensis* is identical (Figure A2A).

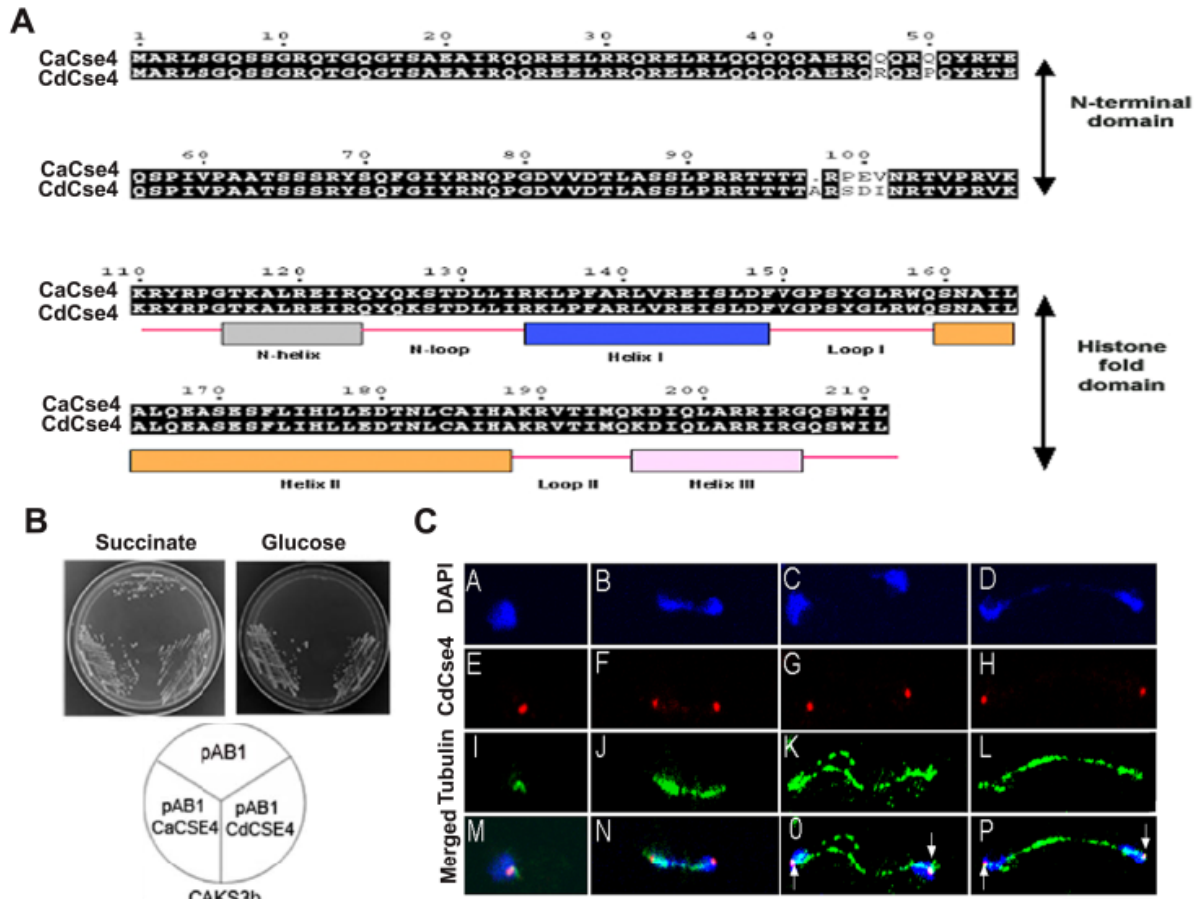


Figure A2. The centromeric histone in *C. dubliniensis*, CdCse4, is localized at the kinetochores throughout the cell cycle. (A) Pairwise comparison of Cse4p in *C. albicans* and *C. dubliniensis* showing homologies in the N-terminal region and the C-terminal histone-fold domain. (B) CAKS3b is transformed with pAB1, pAB1CaCSE4, and pAB1CdCSE4. These transformants were streaked on plates containing complete media lacking histidine with succinate or glucose as the carbon source. (C) *C. dubliniensis* strain Cd36 cells were fixed and stained with DAPI (a–d), anti-Ca/CdCse4 (e–h), and anti-tubulin (i–l) antibodies. The intense red dot-like CdCse4 signals were observed in unbudded (e) and at different stages of budded cells (f–h). Corresponding spindle structures are shown by coimmunostaining with anti-tubulin antibodies (i–l). Arrows indicate the position of spindle pole bodies in large-budded cells at anaphase. (Scale bar, 10 μ m)

To examine whether CdCse4 can functionally complement CaCse4, we expressed CdCSE4 from its native promoter (pAB1CdCSE4) in an *ARS2/HIS1* plasmid (pAB1) in a *C. albicans* strain (CAKS3b) carrying the only full-length copy of CaCSE4 under control of the *PCK1* promoter. The ability of the CAKS3b/pAB1CdCSE4 to grow as good as CAKS3b/pAB1CaCSE4 on glucose medium (where endogenous CaCSE4 expression is suppressed) suggests that CdCse4 can complement CaCse4 function and hence is bonafide centromeric histone in *C. dubliniensis* (Figure A2B). We further examined the subcellular localization of CdCse4 in *C. dubliniensis* strain Cd36 by indirect immunofluorescence (Sanyal & Carbon, 2002) using affinity-purified polyclonal anti-Ca/CdCse4 antibodies (against aa 1–18 of CaCse4/CdCse4) along with anti-tubulin antibodies. CdCse4 revealed bright dot-like signals that always colocalized with DAPI stained nuclei (Figure A2C). Each bright dot-like signal represents a cluster of 16 *CENs*. Unbudded G₁ cells exhibited one dot per cell and large-budded cells representing G₂/M stage of the cell cycle exhibited two dots that co segregated with the DAPI-stained nuclei in daughter cells (Figure A2C). The tubulin staining showed that CdCse4 signals are localized close to the spindle pole bodies, analogous to typical localization patterns of kinetochore proteins in *S. cerevisiae* and *C. albicans*. Together, these results strongly suggest that CdCse4 is the authentic centromeric histone of *C. dubliniensis*.

A3. CENTROMERIC CHROMATIN ON VARIOUS *C. DUBLINIENSIS* CHROMOSOMES IS RESTRICTED TO A 3- TO 5-KB REGION. Ca/CdCse4 chromatin immunoprecipitation (ChIP) assays were performed to examine enrichment of CdCse4 on putative *CEN* regions (orthologous to *C. albicans CENs*) in *C. dubliniensis* strain Cd36. PCR analysis on Cse4 ChIP DNA using a specific set of primers designed from the putative CdCEN (Table M4). Revealed that putative CdCEN regions identified by bioinformatic analysis are indeed associated with CdCse4 (Figure A3). CdCse4 binding regions were found to be restricted to 3- to 5-kb region on each chromosome. For CdCEN6 we first identified all of the intergenic regions ≥ 3 kb, in 80-kb region present between homologs of *C. albicans* Orf19.1096 and Orf19.2124 in *C. dubliniensis*. The ChIP–PCR analysis using specific primers from such regions delimited

Cse4 binding to a 3.6-kb region that is adjacent to the *C. albicans* Orf19.2124 homolog in *C. dubliniensis* (Figure A4).

Table A2. Sequence coordinates of the Cse4- binding and the pericentric regions in all the chromosomes of *C. albicans* and *C. dubliniensis*

Chr #	Regions	<i>C. albicans</i> coordinates	<i>C. dubliniensis</i> coordinates
R	Region from left ORF	1748819-1750873	1713450-1716138
	Cse4 binding region	1750874-1755348	1716139-1720954
	Region from right ORF	1755349-1757404	1720955-1722609
1	Region from left ORF	1561872-1564187	1594163-1596130
	Cse4 binding region	1564188-1567117	1596131-1600697
	Region from right ORF	1567118-1580116	1600698-1611889
2	Region from left ORF	1924364-1928514	1939609-1943699
	Cse4 binding region	1928515-1931474	1943700-1946867
	Region from right ORF	1931475-1931569	1946868-1947202
3	Region from left ORF	821379-823848	866084-867273
	Cse4 binding region	823849-826997	867274-870883
	Region from right ORF	826998-827104	870884-871878
4	Region from left ORF	1000559-1002628	1027127-1029834
	Cse4 binding region	1002629-1006266	1029835-1034637
	Region from right ORF	1006267-1009311	1034638-1036395
5	Region from left ORF	467209-469044	494073-495323
	Cse4 binding region	469045-472074	495324-499155
	Region from right ORF	472075-473740	499156-500591
6	Region from left ORF	975879-976872	993828-1003043
	Cse4 binding region	976873-980625	1003044-1006692
	Region from right ORF	980626-981389	1006693-1009568

7	Region from left ORF	423632-426037	425994-435239
	Cse4 binding region	426038-428938	435240-438230
	Region from right ORF	428939-430172	438231-439177

The DNA sequences present on either side of the *C. dubliniensis* Cse4-binding regions, orthologous to *C. albicans* CEN-containing ORF-free regions, are considered as pericentric regions. The region considered for pericentric sequence analysis in chromosome 6 in *C. dubliniensis* is the intergenic region between an ORF with no known *C. albicans* homolog and the homolog of Orf19.4553

A4. THE EVOLUTIONARILY CONSERVED KINETOCHORE PROTEIN CENP-C HOMOLOG IN C. DUBLINIENSIS, CdMIF2 BINDS PREFERENTIALLY TO CdCSE4-ASSOCIATED DNA. Proteins in the CENP-C family are shown to be associated with kinetochores in a large number of species (Copenhaver, 2004). Using CaMif2 as the query sequence, we identified the CENP-C homolog (CdMif2) in *C. dubliniensis*. CdMif2 shows 77% identity and 5% similarity in a 516-aa overlap. CdMif2 codes for a 520-aa-long predicted protein in which the CENP-C box (amino acid residues 275–297) is 100% identical in *C. albicans* and *C. dubliniensis* (Figure A4). The subcellular localization patterns using polyclonal anti-Protein A antibodies in the *C. dubliniensis* strain CDM1 (Prot-A tagged Mif2) at various stages of the cell cycle are very similar to those observed for CdCse4 (Figure A3). We analyzed binding of TAP-tagged CdMif2 in the strain CDM1 by standard ChIP assays using anti-Protein A antibodies (Figure A4). This experiment suggests that CdMif2 binds to the same 3-kb CdCse4-rich region of three different chromosomes (chromosomes 1, 3, and 7) in *C. dubliniensis* (Figure A3). Binding of two different evolutionarily conserved kinetochore proteins CdCse4 and CdMif2 at the same regions strongly implies that these regions are centromeric.

Thus we successfully identified CdCse4-rich CEN regions and determined the boundaries of centromeric chromatin in all eight chromosomes in *C. dubliniensis*. We also find that the relative distance of Cse4-rich centromeric chromatin from orthologous neighboring ORFs is similar in both species in most cases (Figure A3).

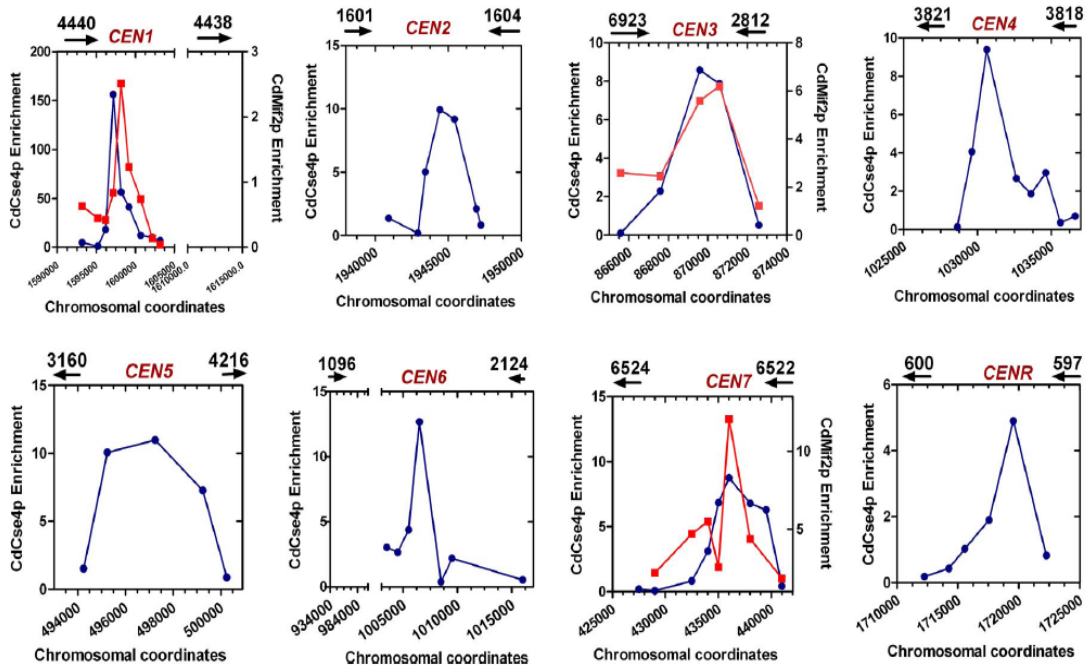


Figure A3. Two evolutionarily conserved key kinetochore proteins, CdCse4/CENP-A and CdMif2/CENP-C co localize on *CENs* of different *C. dubliniensis* chromosomes. Standard ChIP assays were performed on strains Cd36 and CDM1 (CdMif2-TAP-tagged strain) using anti-Ca/CdCse4 or anti-Protein A antibodies. Specific primers corresponding to putative *CEN* regions of *C. dubliniensis* located at specific intervals (Table M4) were used to PCR amplify DNA fragments (150–300 bp) from total, immunoprecipitated (+Ab), and beads-only control (-Ab) DNA fractions. Enrichment values are calculated by determining the intensities of (+Ab) minus (-Ab) signals divided by the total DNA signals and are normalized to a value of 1 for the values obtained for a noncentromeric locus (*CdLEU2*). The intensity of each band was determined by using Quantity One 1-D Analysis Software (Bio-Rad). Graphs show relative enrichment of CdCse4 (blue lines) and CdMif2 (red lines) that mark the boundaries of centromeric chromatin in various *C. dubliniensis* chromosomes. The chromosomal coordinates are marked along the x-axis while the enrichment values are marked along the y-axis. Black arrows show the location of ORFs and arrowheads indicate the direction of transcription.

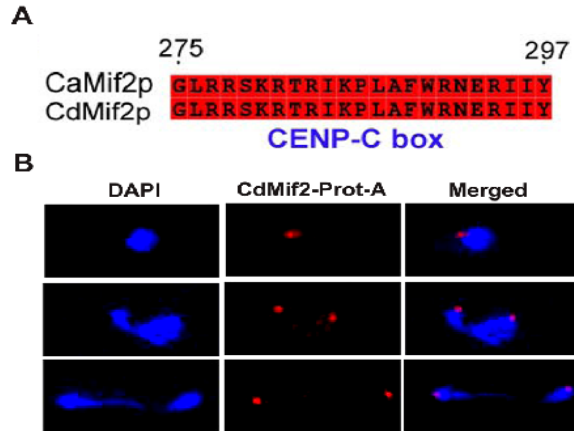


Figure A4. The CENP-C homolog in *C. dubliniensis* (CdMif2) is localized at the kinetochores throughout the cell cycle. (A) Sequence alignment of CaMif2 and CdMif2p showing the conserved CENP-C block (red box). (B) Localization of CdMif2 at various stages of the cell cycle in *C. dubliniensis*.

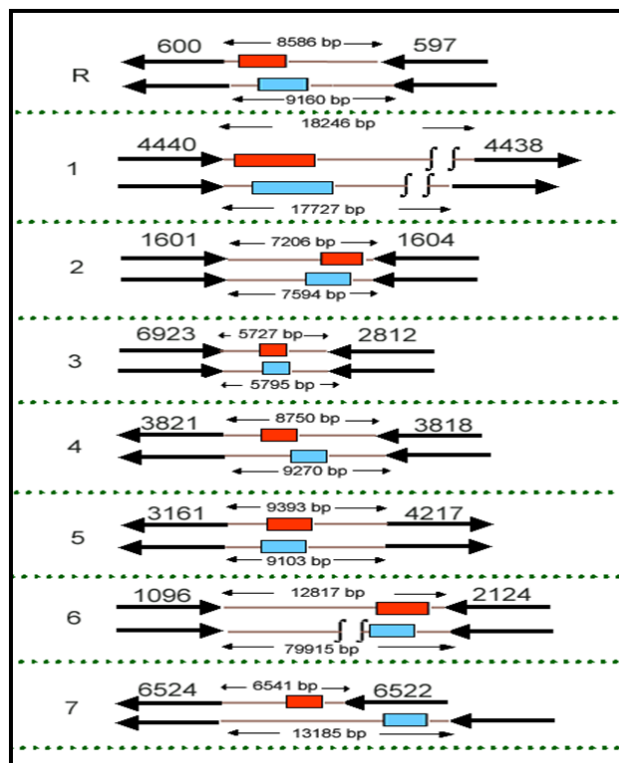


Figure A5. Orthologous Cse4p-rich CEN regions in *C. albicans* and *C. dubliniensis*. On the basis of BLAST analysis, the putative homologs of *C. albicans* CEN-adjacent ORFs in *C. dubliniensis* were identified. Chromosome numbers are shown on the left (R through 7).

The top line for each chromosome denotes *C. albicans* *CEN* regions and the bottom line corresponds to the orthologous regions in *C. dubliniensis*. The dotted and cross-hatched boxes correspond to Cse4p-binding regions in *C. albicans* (Mishra et al, 2007) and *C. dubliniensis*, respectively. Only one homolog is shown for each chromosome of *C. albicans* and *C. dubliniensis*. ORFs and the direction of transcription of corresponding ORFs are shown by open arrows. Only those ORFs that have homologs in both *C. albicans* and *C. dubliniensis* are shown. The number on the top of each arrow corresponds to the *C. albicans* assembly 19 ORF numbers (for example, orf19.600 is shown as 600). The lengths of *CEN*-containing intergenic regions of *C. albicans* and orthologous regions in *C. dubliniensis* are shown. This analysis was done on the basis of Assembly 20 of the *C. albicans* Genome Database and the present version (May 16, 2007) of the *C. dubliniensis* Genome Database.

A5. COMPARATIVE SEQUENCE ANALYSIS BETWEEN *C. ALBICANS* AND *C. DUBLINIENSIS* REVEALS THAT CSE4-RICH CENTROMERE REGIONS ARE THE MOST RAPIDLY EVOLVING LOCI OF THE CHROMOSOME.

Pairwise alignment of CdCse4-rich sequences on different chromosomes (Table A3) with one another reveals no homology. To compare orthologous *CEN* regions of *C. albicans* and *C. dubliniensis*, we performed pairwise alignments using Sigma (Siddharthan, 2006) and DIALIGN2 (Morgenstern, 1999). These programs assemble global alignments from significant gapless local alignments. Sigma detected no homology in Cse4-binding regions. DIALIGN2, with default parameters, reported a little homology; but when we compare known nonorthologous sequence (namely, *CEN* sequences from nonmatching chromosomes), it reports almost identical results (Table A3). In other words, it finds no homology beyond what it would with the “null hypothesis” of unrelated sequence. Similar results were obtained with other sequence alignment programs. We conclude there is no significant homology in the orthologous Cse4-containing *CEN* regions in *C. albicans* and *C. dubliniensis*. However, neighboring (pericentric) ORF-free regions, located between the Cse4-binding regions and *CEN*-adjacent ORFs, do exhibit a higher degree of homology compared to Cse4-rich regions. We count mutation rates only in aligned blocks (ignoring insertions and deletions); DIALIGN2 aligns 68% of these regions, with a mutation rate of 36%, while Sigma aligns 37% of the regions, with a mutation rate of 22% in aligned

regions. Much of the conservation occurs toward the outer ends of these regions, that is, near the bounding ORFs.

To estimate a “neutral” DNA mutation rate, we identified 2,653 putative gene orthologs of *C. albicans* in *C. dubliniensis*. We aligned these genes with T-Coffee (Notredame et al, 2000) and measured the synonymous mutation rates, using seven codons that are “fully degenerate” in the third position (the first 2 bases determine the coded amino acid). A naïve count of the third-position mutation rate yields 27%. Correcting for genome wide codon biases yields 42%, an upper-boundary estimate for the neutral rate of DNA mutation between these two yeasts. This rate corresponds to a pairwise conservation rate (“proximity”) $q = 0.58$ or a proximity to a common ancestor of 0.76. Tests on synthetic DNA sequence (Notredame et al, 2000) suggest that Sigma would easily align such sequence; therefore, it appears that CaCse4-binding sequences (but not pericentric regions) have diverged faster than expected from the neutral point-mutation rate in these yeasts.

Table A3. Comparison of mutation rates in Cse4-binding and other genomic non-coding regions in *C. albicans* and *C. dubliniensis*

	Cse4-binding	Cse4-binding (shuffled)	Pericentric	Intergenic
Total bases	26836	26836	40280	593782
Aligned (DIALIGN2)	12440	11650	27684	530847
Mutated (DIALIGN2)	7624 (61%)	7201 (62%)	10229 (33%)	154473 (25%)
Aligned (Sigma)	0	0	15015	334363
Mutated (Sigma)	0	0	3323 (22%)	57548 (17%)

The fraction of bases aligned by Sigma and DIALIGN2, and the mutation rates within the aligned regions, for Cse4-binding regions, pericentric regions, and intergenic regions. Also shown, as a null hypothesis, are numbers for “shuffled” Cse4p-binding regions, where regions from different non-orthologous chromosomes were aligned.

We also identified 309 homologous intergenic regions in these species that were between 1,000 and 5,000 bp long (comparable in length with the Cse4-binding regions). We aligned

these regions with Sigma and DIALIGN2 and measured mutation rates in aligned regions only (ignoring insertions and deletions). Sigma aligned 56% of the input intergenic sequence, with a mutation rate of 17%; DIALIGN2 aligned 89% of the input sequence, with a mutation rate of 29%. This rate is less than our estimated neutral mutation rate of 42%, suggesting constraints on the evolution of intergenic DNA sequences. Although pericentric regions evolve slower than the neutral rate determined above, they have a smaller fraction of conserved blocks and a greater mutation rate than intergenic sequences.

Interestingly, despite the rapid divergence of *CEN* DNA sequences, the relative position of the *CEN* on each chromosome is conserved in all cases (Figure B7). The relative location of the Cse4-rich centromeric chromatin in the ORF-free region is also similar in both species (Figure A5). Although we find no homology among Cse4-binding regions in matching chromosomes, some of the ORF-free pericentric regions have repeated segments, both within the same species and across the two species (Figure A6). These repeats are mostly singles and in some cases flank a core region; mostly these repeats are not conserved across chromosomes in *C. dubliniensis* but sometimes they are conserved across species (e.g., Chr5 repeats). However, these repeats are mostly chromosome specific and not restricted to only core centromeric or pericentric regions. These results strongly suggest that mechanisms other than the DNA sequence of Cse4-bound regions, such as specific chromatin architecture, determine *CEN* identity in these species. The role of pericentric regions in determining *CEN* identity remains unclear.

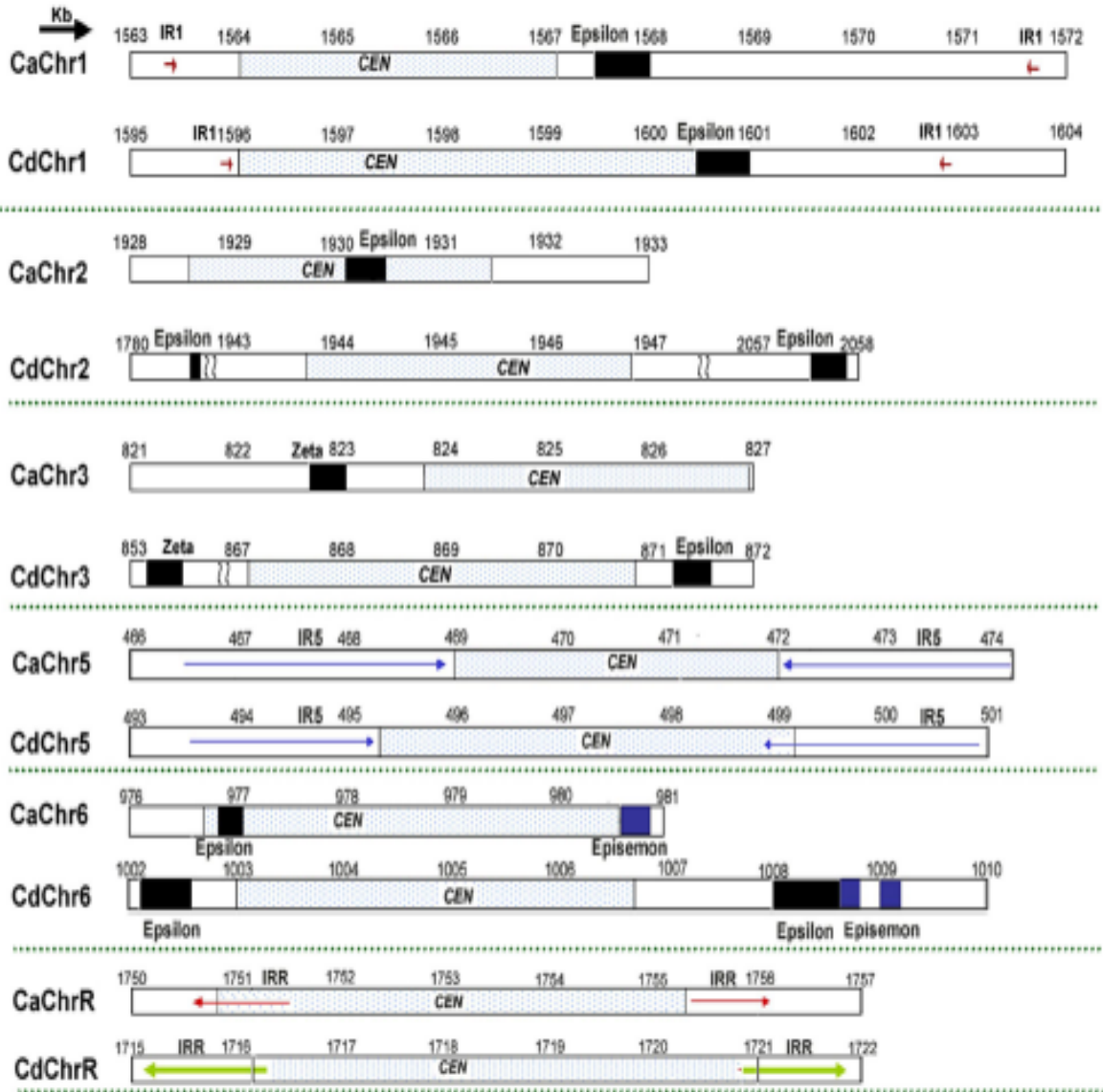


Figure A6. Conserved blocks in the pericentric regions of various chromosomes of *C. dubliniensis* and *C. albicans*. The cyan stippled blocks represent the Cse4p-binding regions. DNA sequence stretches of various chromosomes having significant similarities (ClustalW scores ≥ 80) are shown by colored arrows as indicated. The numbers on the chromosomes represent their coordinates in their respective genome database. The direction of the arrows represents the orientation of repeats. A BLAST search was done to identify the repeats flanking the *CEN* region against the *C. dubliniensis* genome database with *C. albicans* *CEN* flanking repeats as the query sequences (Mishra et al, 2007). The inverted repeats were observed in the chromosomes R, 1, and 5 of *C. albicans* and *C. dubliniensis*. The LTRs such as epsilon, zeta, episemon are also shown.

B. DYNAMICS OF CENTROMERE AND NEOCENTROMERE FORMATION IN C. ALBICANS.

It is interesting to note that although DNA sequence at *CENs* of *C. albicans* and *C. dubliniensis* changed rapidly during speciation, the relative chromosome location of the *CENs* is largely maintained in these species. This led us to speculate that the relative position of a *CEN* in a chromosome, rather than the DNA sequence *per se*, may determine *CEN* identity in *Candida* species. In order to prove this, we first placed a non-centromeric DNA sequence (*URA3* gene) at a functional centromeric region (*CEN7*) in *C. albicans* to see if centromeric chromatin can still assemble on a sequence entirely different from native *CEN* but placed at the same chromosomal location.

B1. CENTROMERIC CHROMATIN ASSEMBLES ON A MARKER GENE WHEN INTEGRATED AT *CEN7*. To test whether a non-*CEN* sequence placed at a *CEN* can become a part of centromeric chromatin, we integrated 1.4 kb *URA3* gene at the *CEN7* locus (coordinates Assembly 21 CaChr7, 427233) in *C. albicans* RM1000AH strain (Sanyal et.al 2004) to create RM1000AH/*CEN7::URA3* (Figure B1A). Karyotypic analysis was performed to eliminate RM1000AH/*CEN7::URA3* transformants that underwent chromosomal rearrangements. Genomic DNA plugs prepared from five *URA3* integrants, were separated on CHEF gels using conditions to separate all the chromosomes (see Materials and Methods), transferred to a membrane and probed with *URA3* and *CEN7* DNA. None of these integrants showed any observable chromosomal rearrangements (Figure B1B). All five RM1000AH/*CEN7::URA3* integrants were able to grow on 5-Fluorooritidic acid (FOA) containing plates. FOA is toxic for *URA* positive cells thus only the cells in which *URA3* is either absent or transcriptionally suppressed (silenced) grow on FOA containing media. FOA resistant *URA* minus colonies can also arise due to pop out of *URA3* from the site of integration or introduction of any missense point mutation in *URA3*. Our analysis suggested that FOA resistance in these transformants was due to reversible silencing of *URA3* as FOA resistant colonies were able to grow back on plates lacking uridine. Hence the marker gene placed at the *CEN7* region shows reversible silencing due to transcriptional suppression in *C. albicans*. To examine the nature of chromatin formed on *URA3* placed at *CEN7* Cse4/CENP-

A ChIP assays in two integrants were performed and analyzed by PCR using primers from *URA3*. The ChIP-PCR analysis revealed that CENP-A was recruited on *URA3* sequence (Figure B1C). Thus, we conclude that *CEN* or neocentromere (*NeoCEN*) formation took place on *URA3*. Whether transcriptional repression favors CENP-A deposition or CENP-A deposition leads to transcriptional repression is an open question. These results strongly suggest that centromeric chromatin can spread over non-centromeric DNA when placed at the native *CEN*, independent of the nature of the DNA sequence, in *C. albicans*. Thus we next sought to replace entire native *CEN7* with *URA3* to see if centromeric chromatin can still assemble on *URA3* sequence placed at the same location as native *CEN7*.

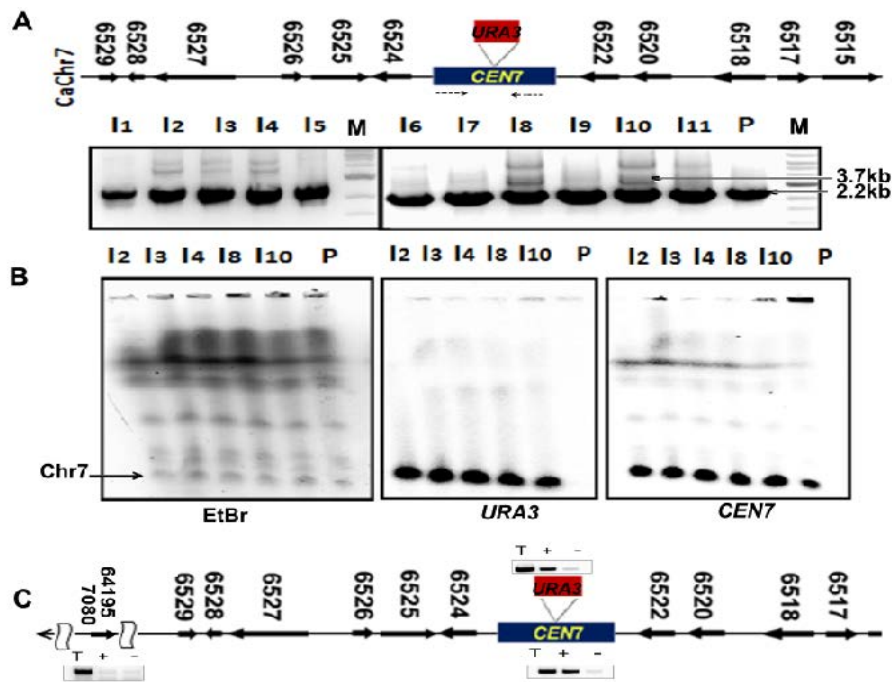


Figure B1. CENP-A chromatin assembles on the non-centromeric *URA3* sequence integrated at *CEN7* locus. (A) Schematic showing location of *URA3* insertion at *CEN7* in one homolog of Chr7 (upper panel). Solid arrows along with the ORF numbers show the gene location and the direction of transcription. Dashed arrows mark the location and orientation of the primers used for confirmatory PCR (bottom panel). (B) An inverted ethidium bromide (EtBr) stained CHEF gel image (left) showing no apparent alteration in the karyotype of RM1000AH/*CEN7*:: *URA3* integrants (lanes 1-5) as compared to the parent RM1000AH (lane 6, marked as P). The blot was probed with *CEN7* (middle) and *URA3* (right). (C) ChIP-PCR analysis showing recruitment of CENP-A on *URA3* of the altered homolog as well as on native *CEN7* of the unaltered homolog of Chr7.

B2. CENTROMERIC DNA SEQUENCES ARE NECESSARY (IF NOT SUFFICIENT) TO ASSEMBLE CENTROMERIC CHROMATIN ON *URA3* INTEGRATED AT *CEN7*.

To examine whether CENP-A containing centromeric chromatin can assemble on *URA3* in the absence of *CEN7*, we replaced the core 4.5 kb CENP-A-rich *CEN7* region (coordinates-Assembly 21 CaChr7,424438-428994) with the 1.4 kb *URA3* sequence in RM1000AH strain (Figure B2A). We performed 15 independent transformation experiments and only one correct transformant screened by Southern blot analysis (strategy described in materials and methods) was selected from each transformation experiment for subsequent analysis. The transformants with desired *CEN7* deletion were further analyzed by CHEF gel followed by Southern analysis as described above. One out of total 15 such transformants showed chromosomal rearrangement (Transformant # 6, lane 3, Figure B2B upper panel) and was excluded from further studies.

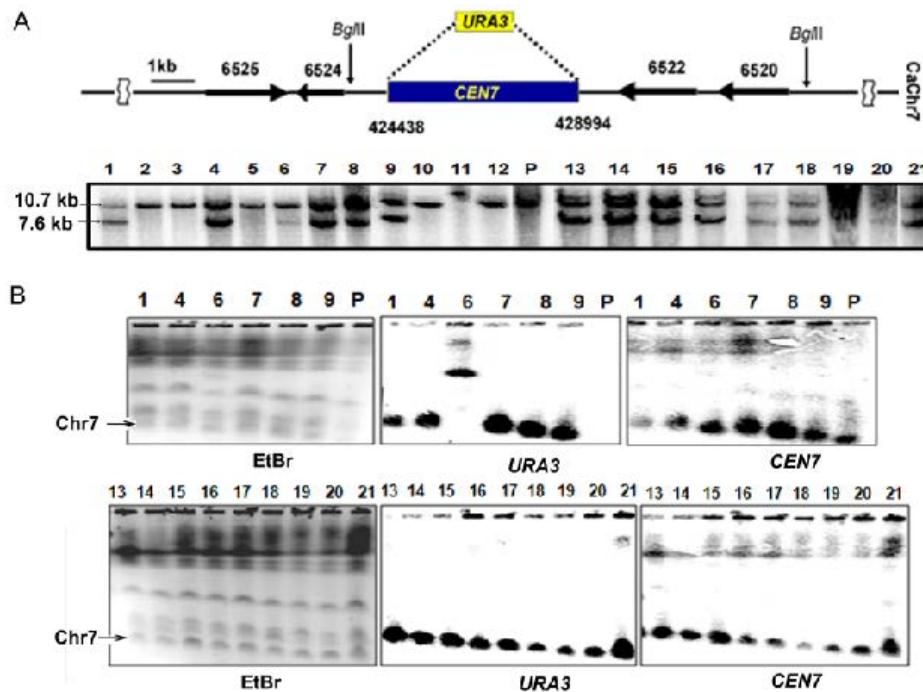


Figure B2. Replacement of CENP-A binding region on chromosome 7 with *URA3*.(A) Schematic showing replacement of 4.5 kb CENP-A/Cse4p rich centromeric region(Assembly21 Coordinates CaChr7,424438-428994) with *URA3* in one of the Chr7 homologs. Southern blot of *Bgl*III-digested (probe co-ordinates-Assembly21 CaChr7, 430002-431350) genomic DNA from parental strain RM1000AH (P) and RM1000AH/*CEN7* Δ transformants (bottom panel) (B) Inverted EtBr CHEF gels

(left) showing RM1000AH (P) and RM1000AH/*CEN7*Δ transformants. CHEF gels were probed with *URA3* (middle) and *CEN7* (right).

All genetic manipulations were performed in RM1000AH strain where each of the two homologs of Chr7 was marked with a unique marker *ARG4* or *HIS1* at the same location, unlinked to *CEN7* and present about 450 kb away from *CEN7* on Chr7 right arm. The chromosome loss assays were performed in RM1000AH/*CEN7*Δ transformants that did not show any chromosomal rearrangements. Chromosome loss was monitored by simultaneous loss of two markers-*ARG4* and *URA3* or *HIS1* and *URA3*. One out of 14 transformants showed high rate of loss of Chr7 (chromosome loss frequency-20%) and was excluded from further analysis. In all other transformants *CEN7*-deleted-Chr7 homolog was highly stable (*URA* loss < 1 in 5000 cells, Table B1) suggesting that neocentromere formation has taken place.

To find out whether or not centromeric chromatin assembled on *URA3* placed at the native centromeric location in the absence of *CEN* DNA, CENP-A/Cse4 ChIP assays were performed in 11 of the 14 stable RM1000AH/*CEN7*Δ transformants. PCR analysis using primers from *URA3* sequence revealed no CENP-A/Cse4 enrichment on *URA3* in any of the 11 transformants suggesting that neocentromere formation occurred elsewhere on the Chr7 when *CEN7* was replaced with *URA3*. Thus centromeric chromatin failed to assemble on *URA3* in the absence of the Cse4-rich *CEN7* sequence. This result strongly insinuates that *CEN* DNA sequence when present in native location, is necessary to favor CENP-A deposition on a non-centromeric sequence (*URA3* in present study) inserted at the *CEN* region. None of the neocentromere forming transformants showed loss of *URA3* – containing chromosome at a high rate revealing that neocentromeres form instantaneously, function efficiently and propagate stably through many generations in *C. albicans*.

B3. NEOCENTROMERE FORMATION IS PROGRAMMED AND NON-RANDOM IN *C. ALBICANS* - REPLACEMENT OF THE CORE CENP-A-RICH *CEN7* SEQUENCE WITH *URA3* REVEALED TWO PREFREED SITES OF NEOCENTROMERE FORMATION ON CHROMOSOME 7, ADJACENT TO THE NATIVE LOCUS.

Next, to find out where the neocentromeres were formed on Chr7 in RM1000AH/*CEN7*Δ transformants we first designed the primers covering an 80 kb region spanning *CEN7* with 1-3 kb gap between adjacent primers. Detailed PCR analysis of the CENP-A/Cse4 ChIP DNA from 11 RM1000AH/*CEN7*Δ transformants using these primers revealed two regions (Class I and Class II) where neocentromeres were formed in all the 11 transformants tested. Interestingly, both these regions mapped within 15 kb of deleted *CEN7* regions (Figure B4). The most prevalent (Class I, 9/11) site, considered as the hot-spot, is present 2-3 kb away from the *URA3* sequence towards right arm of Chr7 on Orf19.6520 and Orf19.6522. The second site (Class II, 2/11) is present 15 kb away from *CEN7* sequence towards left arm of Chr7 on Orf19.6528 and Orf19.6529 (Figure B4). In order to exclude the possibility of occurrence of non-specific CENP-A binding that might lead to spurious results we sought to examine the binding of another evolutionarily conserved KT protein CENP-C/Mif2 on both Class I and Class II neocentromeres. We integrated Myc-tagged Mif2/CENP-C in Class I and Class II neocentromere forming RM1000AH/*CEN7*Δ clones and performed Myc (Mif2) ChIP assays. PCR analysis of the Myc ChIP DNA revealed MycMif2/CENP-C enrichment on Class I and Class II neocentromere locations consistent with CENP-A/Cse4 binding (Figure B4). Together these results confirmed that the locations identified are bonafide neocentromeres that bind to two evolutionarily conserved KT proteins: CENP-A and CENP-C. Since we did not detect any neocentromere at any other sites on the chromosomal arms in a large number of transformants studied, we concluded that *CEN*-adjacent regions are the most preferred sites for the assembly of CENP-A containing centromeric chromatin in absence of the native core *CEN7* sequence.

B4. REPLACEMENT OF A 6.5 KB OR A 30 KB REGION SPANNING *CEN7* AGAIN LEADS TO FORMATION OF NEOCENTROMERES ADJACENT TO REPLACED REGIONS.

C. albicans lacks characteristic repeats associated with pericentric regions that are present in the regional *CENs* of *S. pombe*. An exclusive presence of neocentromere locations at *CEN7*-adjacent regions led us believe that potential pericentric regions might exist in *C. albicans* that are responsible for marking the adjacent region as the *CEN* /neocentromere. We speculated that the residual CENP-A present on *CEN7*-adjacent regions is responsible for seeding the assembly of CENP-A containing chromatin in nearby regions making them

neocentromeres in the absence of a native *CEN*. Thus pericentric regions could be potential candidates for determining CENP-A deposition at the relatively same chromosomal location in a sequence-independent manner in *C. albicans*. The length of non-ORF region spanning *CEN7* is 6.5 kb (Figure B3A). The hot-spot of neocentromere (9/11) (Class I) was mapped to a site next to the non-ORF region on right side of *CEN7* when 4.5 kb CENP-A-rich region was deleted in the previous experiment. Thus, we replaced the entire 6.5 kb non-ORF region including *CEN7* (coordinates- Assembly 21 CaChr7, 423450-429852) with the 1.4 kb *URA3* (Figure B3A). Five correct RM1000AH/*CEN7*-6.5 kb Δ transformants each obtained from an independent transformation experiment and identified by Southern analysis (strategy described in Materials and Methods) were subjected to CHEF gel analysis followed by probing with *CEN7* and *URA3* (Figure B3B). Chromosome loss assays were performed in RM1000AH/*CEN7*-6.5 kb Δ transformants showing no chromosomal rearrangements (Table B1).

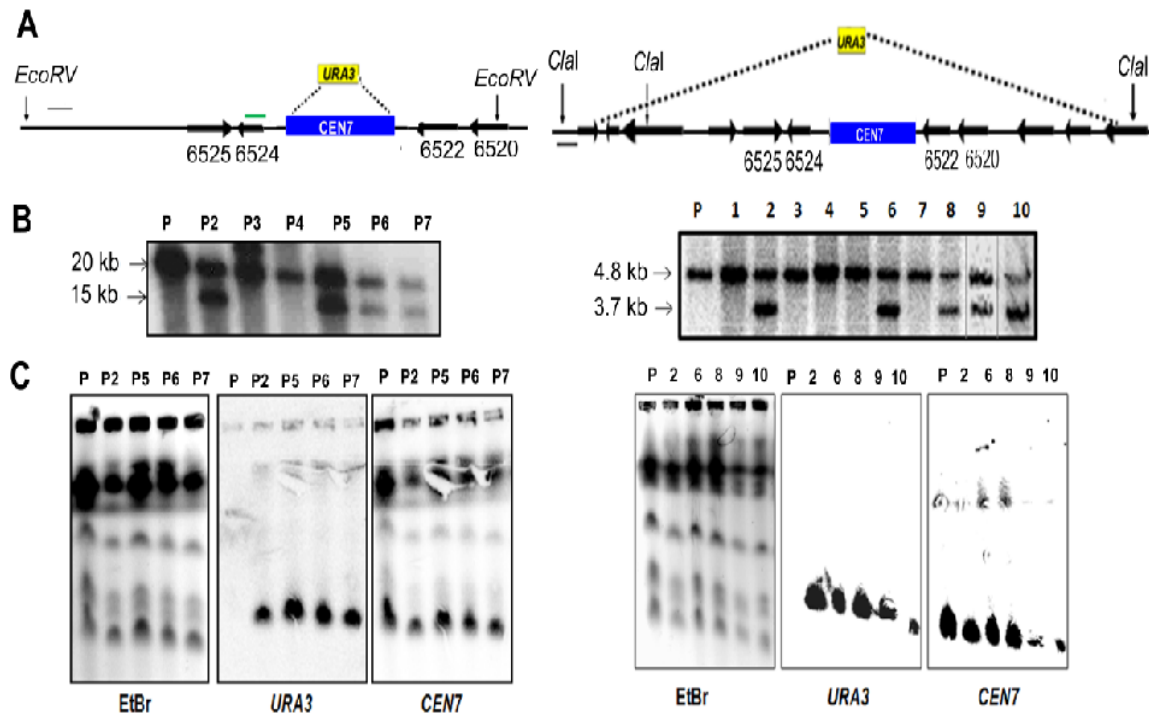


Figure B3. Replacement of pericentric regions spanning *CEN7* with *URA3*.(A) Schematic showing replacement of 6.5 kb non ORF (coordinates- Assembly 21 CaChr7, 423450-429852) or 30 kb(coordinates- Assembly 21 CaChr7, 411320-440780) region spanning *CEN7* with *URA3*. (B)

Southern blot of *EcoRV* (6.5 kb Δ , probe coordinates- Assembly 21 CaChr7, 422342-423450) or *ClaI* (30 kb Δ , probe coordinates- Assembly 21 CaChr7, 409600-410000)-digested genomic DNA from parental strain RM1000AH (marked as P) and RM1000AH/*CEN7*-6.5 kb Δ (left) or RM1000AH/*CEN7*-30 kb Δ transformants (right). (C) Karyotype analysis of transformants showing no rearrangements of Chr7 in RM1000AH/*CEN7*-6.5 kb Δ (left, P2-P7) or RM1000AH/*CEN7*-30 kb Δ (right, 2-10) transformants as compared to RM1000AH (P). CHEF gels were probed with *URA3* or *CEN7*.

CENP-A/Cse4 ChIP assays were performed in four RM1000AH/*CEN7*-6.5 kb Δ transformants with no chromosomal rearrangements to find out neocentromere locations. Strikingly, we found that the most prevalent site of neocentromere formation (3/4 transformants) mapped to the same hotspot identified in 4.5 kb *CEN7* deletion experiment (Class I). The other site (Class III, 1/4 transformants) was present 13 kb away from *CEN7* sequence towards right arm of chr7 (Class III) on ORF-free region (Assembly 21, CaChr7 Coordinates 442000-445000) (Figure B4). These neocentromere locations were further confirmed by showing CENP-C binding as described in previous experiment. Since *CENs* of *C. albicans* are 3-5 kb in length, pericentromeric module could be much bigger than just non-ORF region surrounding *CEN7*. To check this possibility we deleted a 30 kb region including *CEN7* (coordinates- Assembly 21 CaChr7, 411320-440780). We assumed that regions present within 30 kb region will cover the pericentric regions that are responsible for CENP-A deposition at the native *CEN* or neocentromere loci (*CEN* adjacent, class I, II, III) when a native *CEN* is deleted. We sought to identify neocentromere regions on Chr7 in two stable RM1000AH/*CEN7*-30 kb Δ transformants that apparently showed no rearrangement (Figure B3) or loss of the altered Chr7 homolog (Table B1). The Cse4/CENP-A ChIP followed by PCR analysis using primers from Chr7 revealed that neocentromere formation again took place at a site adjacent to the deleted region on Orf19.6531, Orf19.6532, Orf19.6533, Orf19.6534 (Class IV, 20 kb away from *CEN7* towards left arm of Chr7-next to *URA3*) in both the transformants. This Class IV neocentromere showed CENP-C binding that colocalized with the CENP-A-rich region. Together we conclude that neocentromeres always mapped to the *CEN* adjacent regions irrespective of the length of the deleted region spanning the centromere.

B5. NEOCENTROMERE FORMATION ON CHROMOSOME 1 ALSO TAKES PLACE AT *CEN* ADJACENT REGIONS.

In sharp contrast to our study where neocentromeres were always formed on *CEN*-adjacent regions, a previous study had shown that neocentromere formation in *C. albicans* takes place at multiple loci on chromosome 5 (Ketel et al, 2009). This difference could be explained if neocentromere formation occurs in chromosome specific manner in *C. albicans*. To see whether neocentromere behavior is chromosome-specific we studied neocentromere formation on Chr1. We replaced the 4.2 kb CENP-A/Cse4 binding region on Chr1 (coordinates- Assembly 21 CaChr1, 1562878-1567085) with the 1.4 kb *URA3* sequence. Chromosome loss assays in four RM1000AH/*CEN1* Δ transformants with correct integration obtained from independent transformation experiments exhibited high stability of the altered chromosome (*URA* loss < 1 in 2000 cells) suggesting neocentromere formation has taken place in these transformants. CENP-A/Cse4 ChIP assays were performed in two transformants to detect neocentromere locations. Again both the neocentromeres mapped to *CEN1* adjacent regions (coordinates-Assembly 21, CaChr1 1550000-1555000) ruling out the possibility of chromosome specific behavior of Chr7 in neocentromere formation in *C. albicans*.

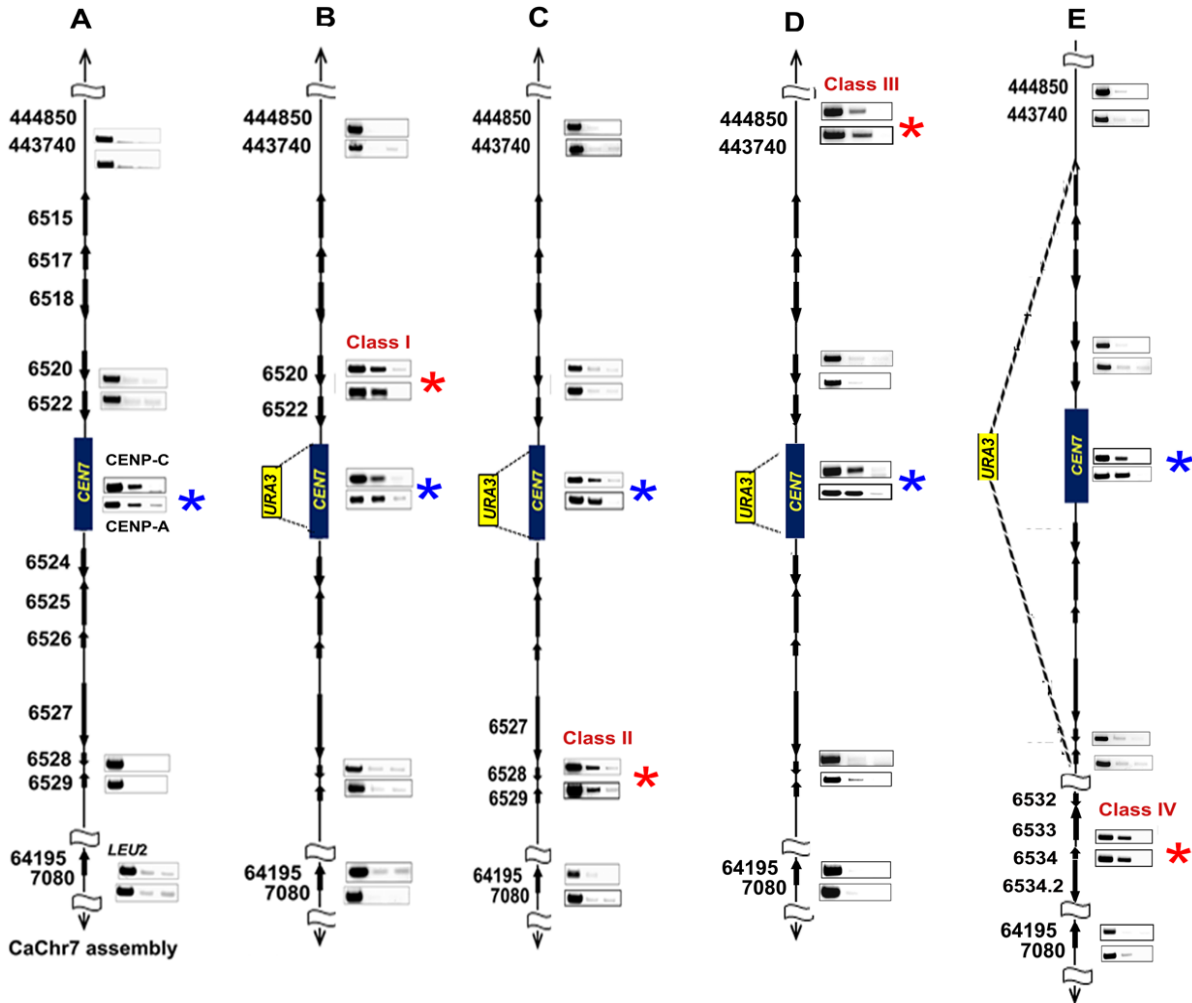


Figure B4. Neocentromere formation is programmed (non random) to *CEN* adjacent regions in *C. albicans*. PCR analysis using primers from *CEN7* (blue star), *CEN7* adjacent and Non*CEN* (*LEU2*) regions on CENP-A/Cse4 ChIP DNA from parent RM1000AH (A), RM1000AH/*CEN7* Δ , RM1000AH/*CEN7*-6.5 kb Δ or RM1000AH/*CEN7*-30 kb Δ transformants (B-E). Black arrows along with the ORF numbers show the gene arrangement and the direction of transcription. Strains expressing MycMif2/*CENP-C* in these transformants were constructed. PCR analysis using same primers on Myc ChIP DNA from resulting strains is also shown. Upper block at each location indicates MycMif2/*CENP-C* binding while bottom block indicates Cse4/*CENP-A* binding. All four neocentromere locations (Class I-IV, marked by red stars) identified mapped to a region within 20 kb upstream and 20 kb downstream of *CEN7*. One transformant from each class is shown in this figure. Class I Neocentromeres (9/11 RM1000AH/*CEN7* Δ transformants, 3/4 RM1000AH/*CEN7*-6.5 kb Δ transformants) formed on Orf19.6520 and Orf19.6522, Class II neocentromeres (2/11 RM1000AH/*CEN7* Δ transformants) mapped to Orf19.6528 and Orf19.6529, Class III neocentromere mapped on Orf free region-Assembly 21, *CaChr7* Coordinates 442000-445000 (1/4 RM1000AH/*CEN7*-6.5 kb Δ transformants) and class IV neocentromeres mapped on Orf19.6531, Orf19.6532, Orf19.6533, Orf19.6534 (RM1000AH/*CEN7*-30 kb Δ transformants).

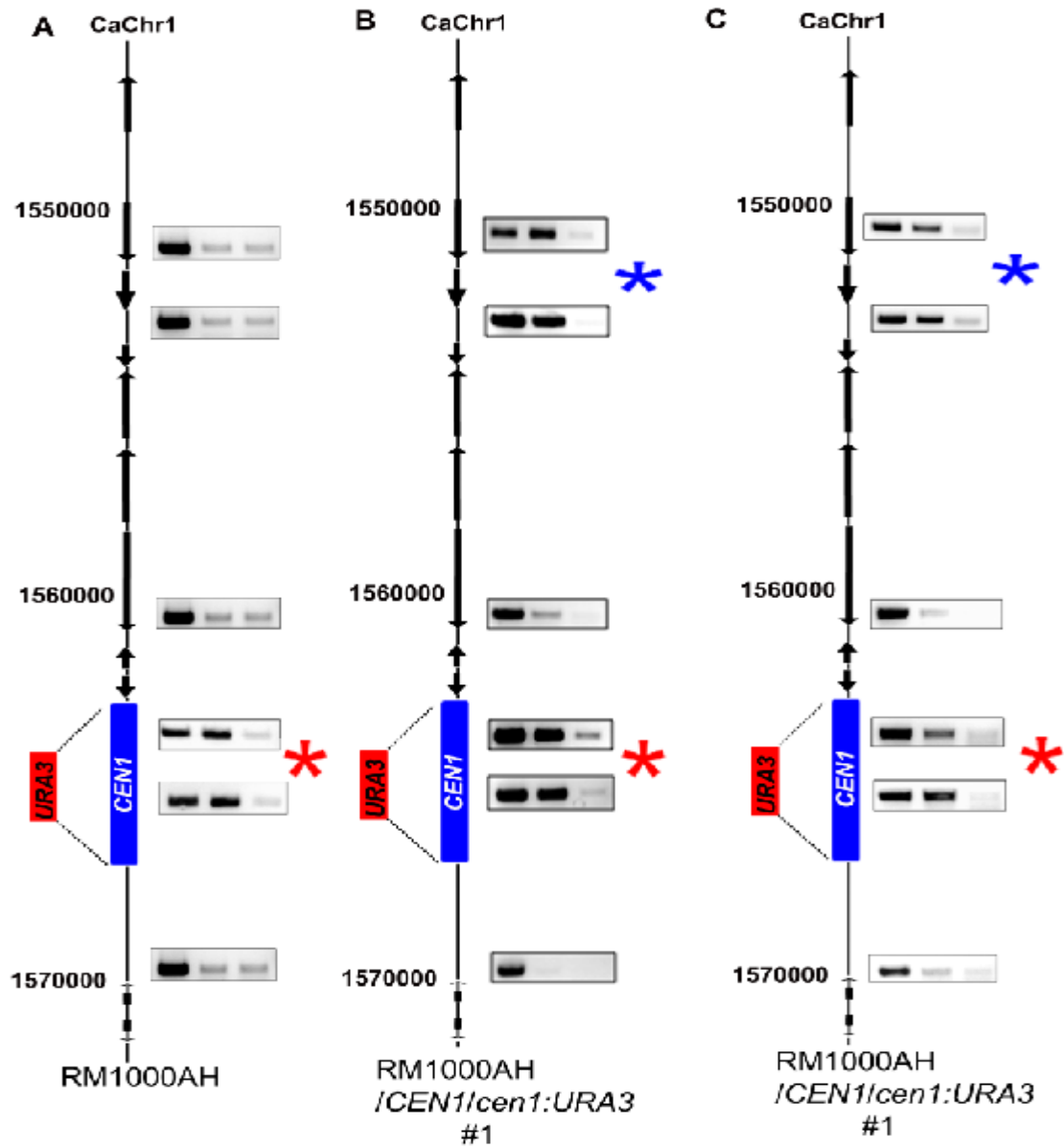


Figure B5. Neocentromere formation on chromosome1 takes place at *CEN1* adjacent region. PCR analysis using primers from *CEN1* (red star, coordinates: Assembly 21 *CaChr1*, 1562000-1567000) and *CEN1* adjacent regions (towards left arm-1550000- 1562000, towards right arm-1569000-1570000) on Cse4/CENP-A ChIP DNA from RM1000AH (A) or two independent RM1000AH/*CEN1* Δ clones (B&C). Arrows along with the ORF numbers show the gene location and the direction of transcription. Neocentromeres in both the clones mapped to *CEN1*-adjacent region towards the left arm (blue stars).

Clone no	Loss frequency (no growth)	Total no of colonies
RM1000AH/CEN7::URA3		
I2	ND	1900
I8	ND	900
I10	ND	771
I19	ND	1100
RM1000AH/cen7Δ-4.5kb		
F1	ND	5225
F5	ND	7040
F10	ND	8950
F11	ND	9436
F15	ND	7157
L1	ND	600
L2	ND	1150
L3	20%	1003
RM1000AH/cen7Δ-6.5kb		
P2	ND	2875
P5	0.56%	1410
P6	ND	2100
P7	0.64%	2340
P8	ND	2863
RM1000AH/cen7Δ-30kb		
30PX	ND	3600
30Pf	0.043%	2286
RM1000AH/cen1Δ-4.2kb		
C1-I	ND	1300
C1-II	ND	1000

Table B1. Chromosome loss frequency in RM1000AH/*CEN7*:: URA3, RM1000AH/*cen7Δ*-4.5kb, RM1000AH/*cen7Δ*-6.5kb, RM1000AH/*cen7Δ*-30kb, RM1000AH/*cen1Δ*-4.2kb transformants. ND - Not Detected

It is important to note that half of the *CEN5*-deleted transformants did form neocentromere at *CEN5* adjacent locations in previous report by Ketala et al, 2009, similar to our studies. However, absence of any far-*CEN* neocentromere among large number of transformants

screened from different deletion experiments in our study raises a significant difference between two studies which needs an explanation. We reasoned that results from previous study could be due to different behavior of Chr5 as compared to the rest of the *C. albicans* chromosomes. Indeed, centromeric organization of *CEN5* is significantly different from the rest of the *CENs* in *C. albicans*. *CEN5* is flanked by inverted repeats of considerable lengths on both sides (Coordinates- Assembly 21 CaChr5, 466702 –466861 (D) and 472089 – 474247 (R)) and shows a resemblance to the regional *CENs* of *S. pombe*. Detailed bioinformatic analysis to find out pericentric repeats in our study (Section A, Figure A6) revealed that pericentric regions surrounding all the *CENs* except *CEN5* lack proper repeats and contain only cryptic (or remnants of) transposable elements or inverted repeats that are too small to be considered as candidate pericentric repeats that control *CEN* function. Neocentromere formation in *S. pombe* has been shown to occur near the telomeric regions (far-*CEN*). It is thus tempting to correlate neocentromere locations (*CEN*-adjacent or far-*CEN*) with presence or absence of pericentric repeats.

B6. PROXIMITY TO A NATIVE CENTROMERE DEFINES NEOCENTROMERE FORMATION IN *C. ALBICANS*.

Results from our *CEN* deletion analysis described above led to a conclusion – neocentromere formation in *C. albicans* is not random and *CEN*-adjacent regions are the most potential sites of CENP-A deposition in the absence of a native *CEN*. Similar to budding yeast *S. cerevisiae*, *CENs* are always clustered towards the periphery of a nucleus throughout the cell cycle in *C. albicans* (3D reconstructed image in Figure B6). We propose that the all the native *CENs* together form a specific 3-dimensional scaffold near the periphery of a nucleus to create a zone of high CENP-A local concentration. Once the core centromeric region is removed, adjoining regions become part of this CENP-A-rich 3D scaffold and form neocentromeres. *S. cerevisiae* *CENs* have been shown to form a looped structure (Anderson et al, 2009). We speculate that each *CEN* in *C. albicans* probably forms a looped structure of certain fixed dimensions during the assembly of a KT on which a kinetochore microtubule (kMT) of the spindle apparatus binds and such a region in each chromosome is predisposed to become CENP-A-rich. Since the preferred sites for neocentromere formation are always at *CEN*-adjacent regions (Class I neocentromere is the most preferred one), it becomes difficult to completely rule out the role of underlying DNA

sequences. Underlying DNA sequences or chromatin structure might contain structural blueprints that help interchromosomal *CENs* to interact with each other in the 3D scaffold.

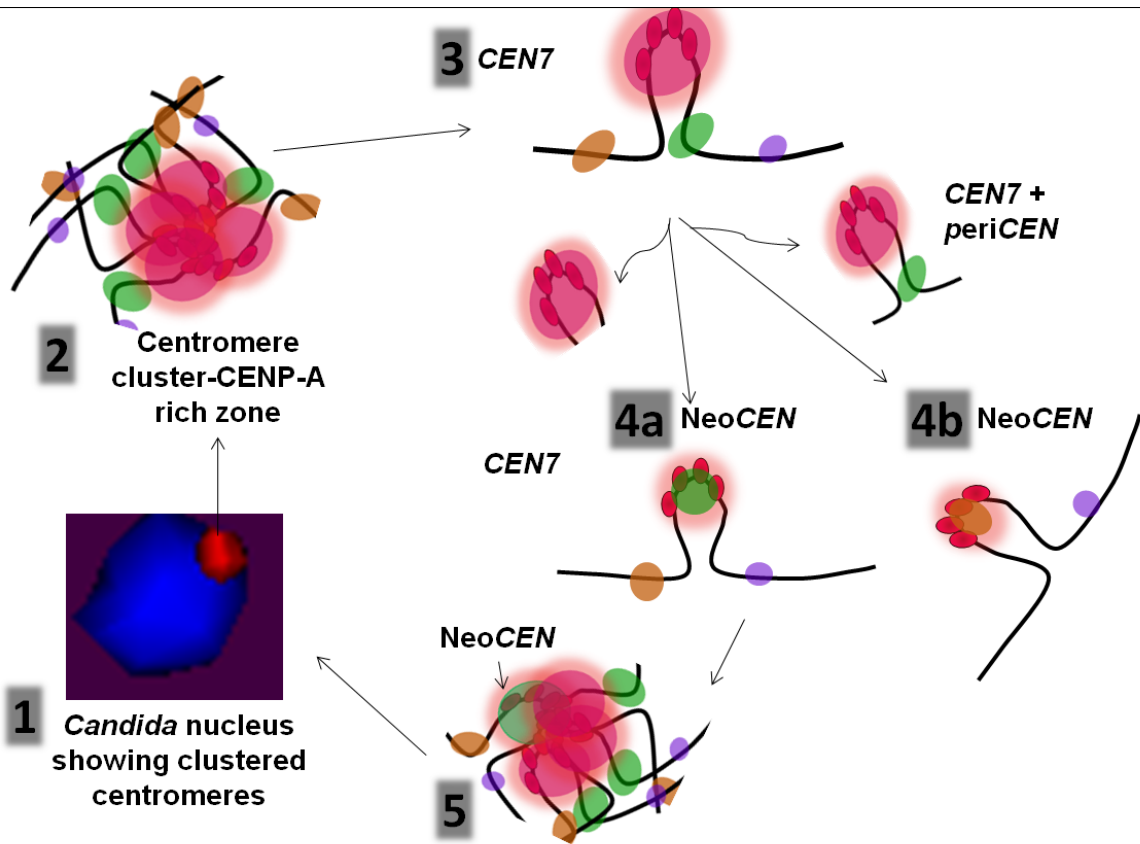


Figure B6. Proximity to a native *CEN* determines neocentromere formation in *C. albicans*. All the *CENs* are clustered in *C. albicans* towards nuclear periphery to create a zone of high CENP-A local concentration. Potential neocentromere sites exist at *CEN* adjacent region due to their close proximity to the CENP-A-rich zone. Under normal conditions the native *CEN* occupies a central position in the *CEN*-cluster and thus provides a lateral inhibition to form neocentromeres on sites lying next to the native *CEN*. Lateral inhibition occurs due to steric hindrance provided by the native *CEN* which keeps *CEN*-adjacent potential neocentromere sites away from the CENP-A rich zone. In the absence of the native *CEN*, *CEN* adjacent regions are brought in close proximity to the CENP-A-rich zone and neocentromere formation takes place on these regions.

B7. CHROMOSOMAL LOCATION DEFINES *CEN*/NEOCENTROMERE FORMATION IN CANDIDA SPECIES. Exclusive presence of potential neocentromere forming loci in *CEN*-adjacent region in *C. albicans* suggests that physical location of a *CEN* once determined for a chromosome becomes evolutionarily conserved in spite of massive changes in the underlying sequence.

The most convincing argument supporting this hypothesis is maintenance of relative locations of *C. albicans* and *C. dubliniensis* *CENs*. These two species have diverged ~ 20 million years ago and centromeric sequences of *C. albicans* and *C. dubliniensis* share no sequence homology due to rapid evolution of centromeric sequences in these two species as discussed in previous section. However relative locations of the *CENs* along the length of entire chromosome are maintained in these two species confirming that physical location on the chromosome is the epigenetic determinant for *CEN*/neocentromere formation in *Candida*.

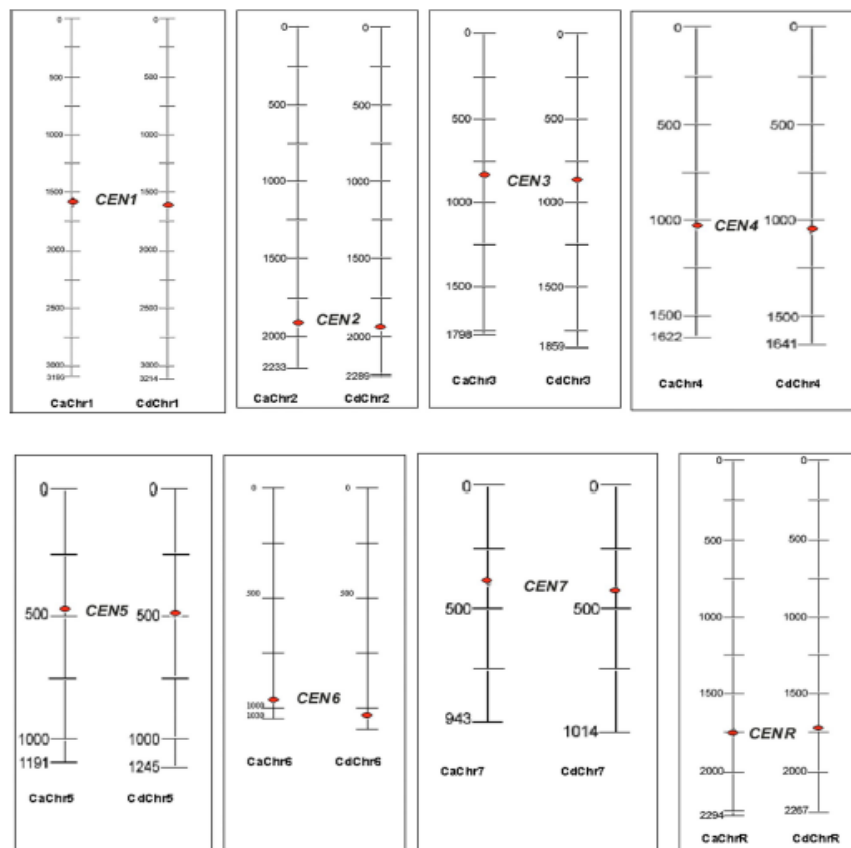


Fig. 55. Relative chromosomal positions of Cse4p-binding regions in *C. albicans* and *C. dubliniensis*. Red ovals, Cse4p-binding regions.

Figure B7. Relative chromosomal positions of CENP-A binding regions in *C. albicans* and *C. dubliniensis*. Red ovals, CENP-A binding regions.

B8. GENE CONVERSION AT *C. ALBICANS* CENTROMERES. In chromosome loss assays, 1 out of the 14 RM1000AH/4.5 kb *CEN7Δ* transformants exhibited a different behavior. We detected

URA minus derivatives that exhibited neither silencing of *URA3* (PCR analysis using various primers including internal primers from *URA3* sequence revealed total absence of *URA3* sequence from the genome) nor chromosome loss of the *CEN7*-deleted chromosome by *URA3* (presence of *HIS1* and *ARG4* revealed that both the homologs of Chr7 are present). Southern analysis of *Bgl*III digested genomic DNA from wild-type RM1000AH cells yields 10.7 kb band when probed with a fragment from *CEN7* adjacent region within *Bgl*III fragment (probe coordinates-Assembly21 CaChr7, 430002-431350). Replacement of the 4.5 kb *CEN7* with the 1.4 kb *URA3* (RM1000AH/4.5 kb *CEN7*Δ) generates an extra 7.6 kb band from *URA3* containing homolog. Above mentioned *URA* minus colonies revealed absence of *URA* containing 7.6 kb *Bgl*III fragment that was originally present in their parent RM1000AH/4.5 kb *CEN7*Δ (Figure B8B). Neither did we detect any *Bgl*III fragment smaller than 7.6 kb which clearly excludes the possibility of *URA3* pop out from such *URA* minus colonies. CHEF gel analysis in these *URA* minus colonies revealed no detectable genomic rearrangement as compare to wild-type RM1000AH and parent RM1000AH/4.5 kb *CEN7*Δ (Figure B6B). Presence of both the homologs of Chr7 and absence of *URA3* containing *Bgl*III fragment confirmed that *URA3* was replaced by native *CEN7* sequence copied from the other unaltered homolog of Chr7 through gene conversion. Gene conversion is a process by which DSBs are repaired by copying the sequence from the homologous chromosome. We detected similar gene conversion events in RM1000AH/6.5 kbΔ transformants as well (Figure B8, Right panel). Thus we conclude that gene conversion occurs at *C. albicans CEN*.

A recent study (Shi et al, 2010) has shown that *CEN* core regions in maize undergo widespread gene conversion. It has been shown that replication fork stalls at *CENs* and *CENs* are replicated by error prone replication. Demonstration of gene conversion at *C. albicans CENs* in this study suggests that stalling of replication fork may result DSBs at the *CENs*. Rapid evolution of centromeric regions (discussed in Section A) can be attributed to error prone replication. Accumulation of strand specific mutations during error prone replication with such a high rate can generate entirely different *CENs* in two homologs of the same chromosome. Such situation can pose serious problems in chromosome segregation during mitosis. We speculate that gene conversion is a mechanism to homogenize the mutations at the *CEN* region of two homologs. Moreover, DSBs have been

shown to recruit centromeric histone CENP-A (Zeitlin et al, 2009). Thus creation of DSBs at the *CEN* region during gene conversion might be one of the determinants for CENP-A deposition at the *CEN*s.

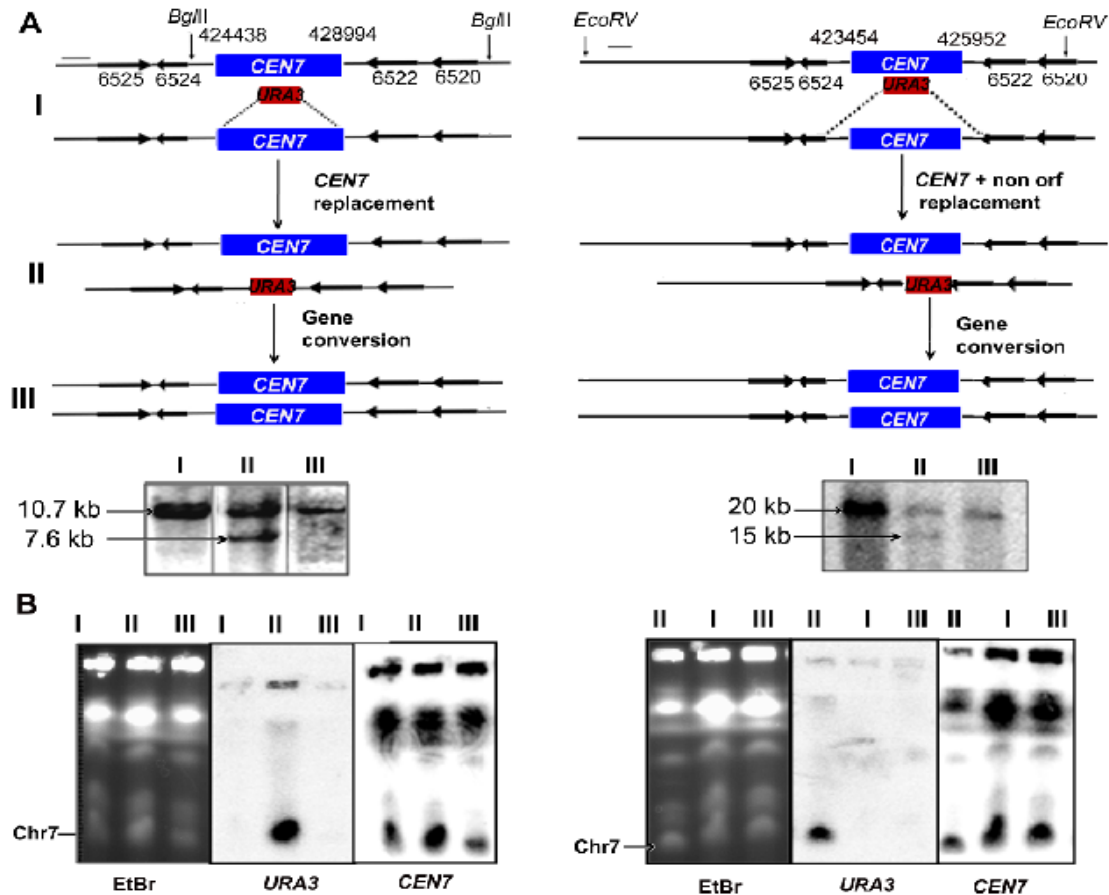


Figure B8. Gene conversion occurs at *C. albicans* *CEN*s. (A) Schematic showing the gene conversion in RM1000AH/4.5 kb *CEN7* Δ (left upper) and RM1000AH/6.5 kb Δ (right upper). Thick arrows along with the ORF numbers show the gene location and the direction of transcription. Genomic DNA from parent RM1000AH, RM1000AH/4.5 kb *CEN7* Δ or RM1000AH/6.5 kb Δ and *URA* minus derivative was digested with *Bgl*III (4.5 kb Δ) or *EcoRV* (6.5 kb Δ) and probed with DNA fragments that lies within *CEN7* containing *Bgl*III fragment (probe coordinates- Assembly 21 CaChr7, 430002-431350 for 4.5 kb) or *CEN7* containing *EcoRV* fragment (probe coordinate- Assembly 21 CaChr7, 422342-423450 for 6.5 kb). Absence of the smaller band (7.6 kb in 4.5 kb Δ and 15 kb in 6.5 kb Δ) in *URA* minus derivative confirmed gene conversion (Bottom panels). (B) Karyotypic analysis showed no rearrangement of Chr7 in gene-converted clones as compared to wild-type RM1000AH and RM1000AH/4.5 kb *CEN7* Δ or RM1000AH/6.5 kb Δ .

B9. INACTIVATION OF NEOCENTROMERE BY NATIVE *CEN7* ACQUIRED DURING GENE CONVERSION. A neocentromere may form on a chromosome only when a native *CEN* is either inactivated or deleted. One of the RM1000AH/4.5 kb *CEN7* Δ transformants with Class II neocentromere (~15 kb away from *CEN7* towards left arm of Chr7) and one RM1000AH/6.5 kb Δ transformant with Class III neocentromere (~13 kb away from *CEN7* towards right arm of Chr7) underwent gene conversion and acquired native *CEN7* on the homolog with a preexisting fully functional neocentromere. If both the acquired *CEN* and the pre-existing neocentromere in these two transformants are active on the same homolog, this chromosome will either become dicentric (and should become unstable) or may spread centromeric chromatin to fuse these two centromeric regions separated by 13-15 kb to one. However dicentric condition seems less likely to arise because *CEN* and neocentromere are present so close to each other (~15 kb) on approximately 1 Mb Chr7 and might not be recognized as two separate *CENs* by MTs coming from spindle poles. The third possibility is inactivation of one of the *CENs* – the native or the neocentromere. We performed CENP-A/Cse4 and CENP-C/Mif2 ChIP assays in gene converted derivatives and performed PCR on ChIP DNA using primers from already established neocentromere. We found no enrichment on the neocentromere location in both the transformants. We did not detect any spreading of centromeric chromatin between *CEN* and neocentromere in both the clones. Thus a native *CEN* once established suppresses all other potential *CEN* hot-spots (identified as neocentromeres in this case).

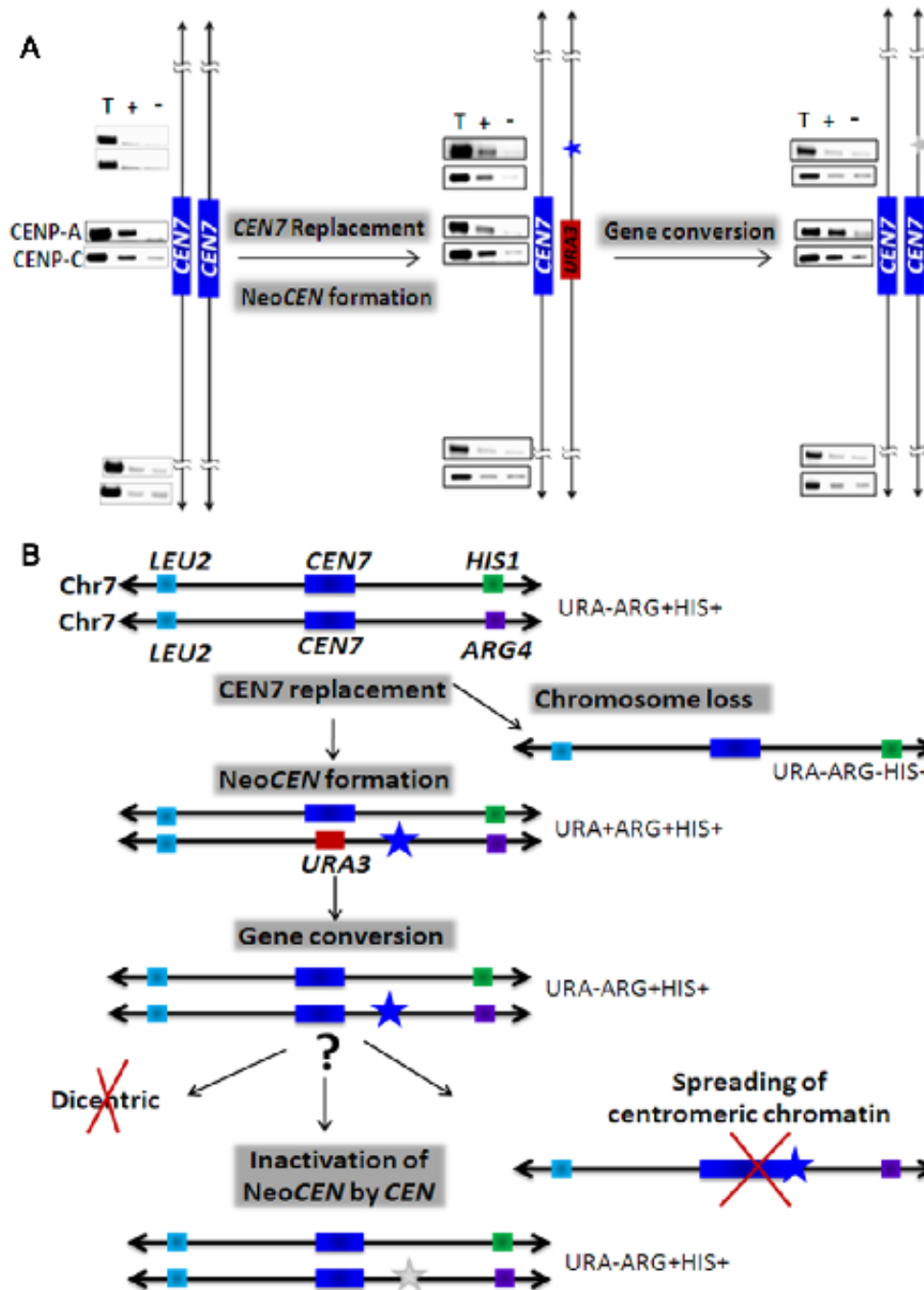


Figure B9. Established neocentromere is suppressed laterally in the presence of a native *CEN*.(A) PCR analysis of CENP-A/Cse4 ChIP DNA in wild-type RM1000AH (left), Class III neocentromere (~13 kb away from *CEN7* and marked by a blue star) forming RM1000AH/ 6.5 kbΔ transformant before (middle) and after (right) gene conversion. Absence of CENP-A binding at class III neocentromere after gene conversion confirms inactivation of the neocentromere. (B) Schematic summarizing details of events during neocentromere formation and gene conversion.

C. THE ESSENTIALITY OF THE FUNGAL SPECIFIC DAM1 COMPLEX IS CORRELATED WITH 1MT/1KT INTERACTION PRESENT THROUGHOUT THE CELL CYCLE, INDEPENDENT OF THE NATURE OF A CENTROMERE

A fungal-specific outer KT complex, the Dam1 complex, is essential in *S. cerevisiae*, non-essential in fission yeast, and absent in metazoans. The reason for reductive evolution of functionality of this complex remains unknown. Both *C. albicans* and *S. pombe* have regional *CENs* as opposed to short point *CENs* of *S. cerevisiae*. Interaction of one microtubule per KT is established both in *S. cerevisiae* and *C. albicans* early during cell cycle in contrast to multiple MTs that bind to a KT only during mitosis in *S. pombe*. Moreover, the Dam1 complex is associated with the KT throughout the cell cycle in *S. cerevisiae* and *C. albicans* but only during mitosis in *S. pombe*. In this section, we describe identification and characterization of the Dam1 complex in *C. albicans* and establish a possible link between essentiality of the Dam1 complex and the number of MTs associated with a KT.

C1. THE DAM1 COMPLEX IS LOCALIZED TO THE KINETOCHORE THROUGHOUT THE CELL CYCLE IN C. ALBICANS. Using polypeptide sequences of *S. cerevisiae* Dam1 complex components as queries in a BLAST analysis, we identified putative homologous open reading frames (ORFs) of each of the ten proteins that form the Dam1 complex in *C. albicans*. Subcellular localization of Dam1 and Dad2 in *C. albicans* was performed by indirect immunofluorescence microscopy using anti-Protein A antibodies in strains J117 (*dam1/DAM1TAP*) and J118 (*dad2/DAD2TAP*), respectively. Western blot analysis confirmed expression of Protein A tagged Dam1 and Dad2 (Figure C1A, top panel). The localization patterns suggest (discussed in section A-Fig A2) that Dad2 and Dam1 are present at KTs throughout the cell cycle. Co-localization of Dad2 and a key KT component Mif2p (Myc tagged) in the strain CAMB1 (Sanyal et al, 2004) confirmed that Dad2 is KT localized (Figure C1B). In order to find out *in vivo* association of these two proteins with the centromeric DNA, we performed standard chromatin immunoprecipitation (ChIP) assays with anti-Protein A antibodies in strains J117 and J118. The immunoprecipitated (IP) DNA samples were analyzed by PCR using a specific set of primers designed from *CEN7*

sequences. *CEN7* regions in J117 and J118 were enriched in the IP DNA indicating that Dam1 and Dad2 (Figure C1C) were associated with *CENs*. Taken together, these results indicate that Dam1 and Dad2, components of the Dam1 complex, are KT localized throughout the cell cycle in *C. albicans*.

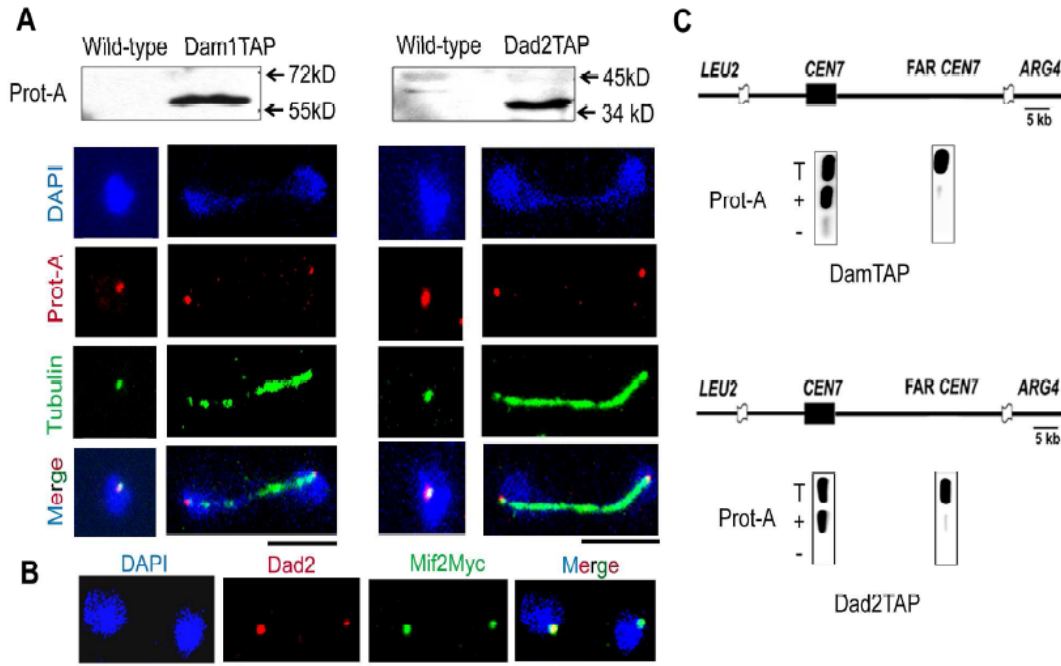


Figure C1. The Dam1 complex is localized to the KT throughout the cell cycle in *C. albicans*. (A) Western blot analysis using total cell lysates from BWP17 (wild-type) and J117 (Dam1-Prot A) or J118 (Dad2-Prot A) cells with anti-Protein A antibodies (top panel). DAPI stained cells of J117 (Dam1TAP) and J118 (Dad2TAP), at different stages of cell cycle, were immunostained with anti-protein A (red) and anti-tubulin (green) antibodies. (B) Indirect immunostaining with anti-Dad2 (red) and anti-myc (Mif2) (green) antibodies in *C. albicans* strain CAMB1 expressing a key KT component Myc-Mif2. (C) Anti-Protein A ChIP DNA from J117 or J118 cells was PCR analyzed with primers specific from *CEN7* (coordinates: Assembly 21- CaChr7, 427369 - 427560) or a region 17 kb away (coordinates: Assembly 21- CaChr7, 444584 - 444875) from it (FAR *CEN7*). T, total DNA; +, IP DNA with anti-Protein A antibodies; -, beads only control without antibodies.

C2. KINETOCHORE RECRUITMENT OF THE DAM1 COMPLEX IS INDEPENDENT OF PRESENCE OF MICROTUBULES. To examine the dependency of the Dam1 complex on spindle MTs for its KT recruitment, we observed KT localization of Dad2 in the presence of the spindle poison nocodazole (NOC). Indirect immunofluorescence was performed in untreated (DMSO only)

and nocodazole treated J118 (*dad2/DAD2TAP*) cells using anti-tubulin and anti-Protein A antibodies. Nocodazole treatment led to G2/M arrest followed by elongated bud phenotype with no visible tubulin staining (Figure C2A). Absence of tubulin staining in G2/M arrested NOC treated cells confirmed that mitotic spindle was disrupted. Untreated cells exhibited normal spindles (Figure C2A). However, the intensities of Dad2TAP signals in NOC treated cells were comparable to those in untreated cells suggesting that disruption of the spindle did not alter Dad2 localization to the KT (Figure C2A). To further confirm this result, we performed ChIP assays in untreated and NOC treated J118 cells using anti-Protein A antibodies. The immunoprecipitated (IP) DNA samples were analyzed by PCR using a specific set of primers designed from *CEN* regions of all the chromosomes. No significant difference in Dad2TAP binding at any of the *CENs* was observed (Figure C2B). Together these results confirm that Dad2 localization at the KTs is independent of KT-MT interaction.

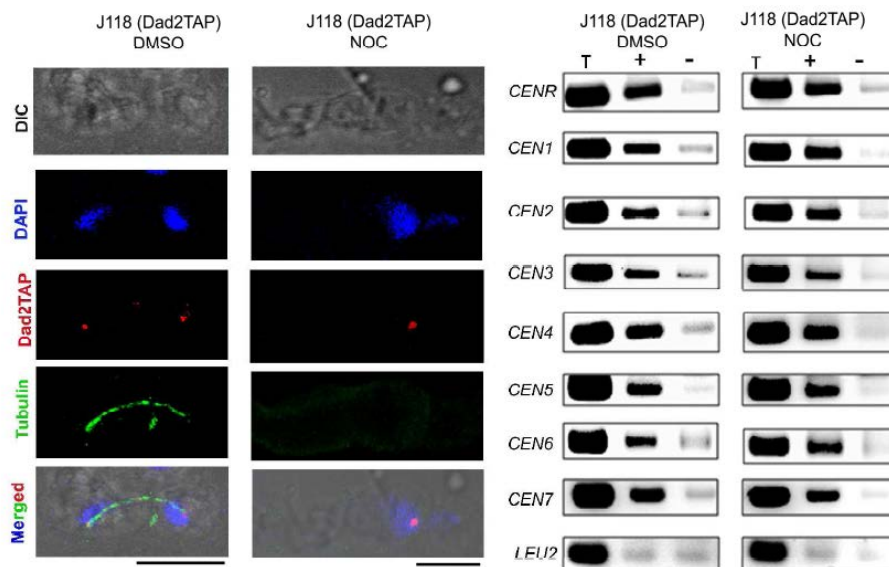


Figure C2. KT localization of Dad2 does not depend on the integrity of KT-microtubule interaction in *C. albicans*. (A) Nocodazole untreated (DMSO) or treated (NOC) J118 (*dad2/DAD2TAP*) cells were stained by DAPI, anti-Protein A and anti-tubulin antibodies. Lack of signals with anti-tubulin antibodies in NOC treated cells confirmed loss of spindle structure. However, Dad2 signals are comparable both in DMSO treated and NOC treated cells. (B) ChIP assays with anti-Protein A antibodies using DMSO treated and NOC treated J118 cells confirmed that Dad2 recruitment at the *CENs* is independent of KT-microtubule interaction. T, total DNA; +, IP with anti-Protein A antibodies; -, beads only control.

C3. THE DAM1 COMPLEX IS ESSENTIAL FOR VIABILITY AND REQUIRED FOR G2/M PROGRESSION AND COMPLETION OF MITOSIS IN C. ALBICANS. To construct the conditional mutants first copy of each of four genes *DAM1*, *ASK1*, *DAD2* and *SPC19* was replaced with *HIS1* marker and the remaining copy was placed under control of a regulable promoter (the *MET3* promoter for *DAM1*, *ASK1* and *SPC19*, and the *PCK1* promoter for *DAD2*). The *MET3* promoter is repressed in presence of cysteine (Cys) and methionine (Met)(Care et al, 1999) while the *PCK1* promoter is repressed when glucose is used as the carbon source (Leuker et al, 1997). Strains J102 (*dam1/MET3prDAM1*), J104 (*ask1/MET3prASK1*) and J106 (*spc19/MET3prSPC19*) failed to grow on 5 mM Cys and 5 mM Met containing plates (Figure C3). Similarly, the strain J108 (*dad2/PCK1prDAD2*), failed to grow when glucose was used as the carbon source. The parent strains J101 (*dam1/DAM1*), J103 (*ask1/ASK1*), J105 (*spc19/SPC19*) and J107 (*dad2/DAD2*) did not show any growth defects. Inability of the conditional mutants to grow under repressible conditions confirmed that each of these four genes is essential for viability.

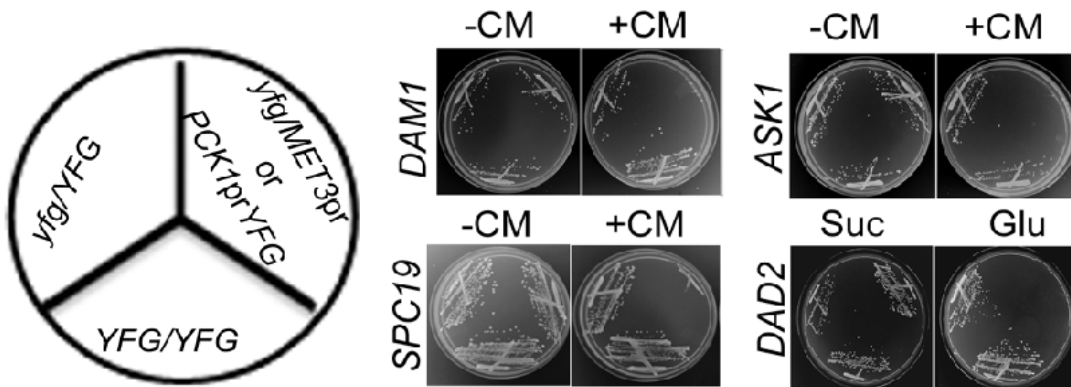


Figure C3. The Dam1 complex is essential for viability in *C. albicans*. *C. albicans* cells expressing both wild-type copies (*YFG/YFG*), one deleted copy and the remaining wild-type copy under control of either the native promoter (*yfg/YFG*) or the *MET3/PCK1* promoter (*yfg/MET3prYFG* or *yfg/PCK1prYFG*) of indicated genes (*DAM1*, *ASK1*, *SPC19* or *DAD2*) were streaked on plates containing inducible (-CM or Suc) or repressible (+CM or Glu) media. (CM, 5 mM Cysteine and 5 mM Methionine; Suc, succinate; glu, glucose). The *MET3* promoter, which is expressed in absence of CM (-CM) and repressed in presence of CM (+CM), was used for controlled expression of *DAM1*, *ASK1* or *SPC19*. The *PCK1* promoter, which is expressed in presence of succinate (Suc) and repressed in glucose (Glu) was used to control the expression of *DAD2*. Plate photographs were taken after 2-3 days of incubation at 30°C.

Conditional mutant strains of *DAM1* (J102), *ASK1* (J104), *SPC19* (J106) and *DAD2* (J108) showed accumulation of large budded cells followed by a transition from large bud to an elongated bud (pseudohyphal-like) phenotype in each case (Figure C4A). FACS analysis of these mutants confirmed that majority of the cells had 4N DNA content within 4h of protein depletion (Figure C4B). Almost all arrested cells with large bud (99%) that were depleted of either Dam1 or Ask1 had single undivided DNA mass (Figure C4C). On the other hand, depletion of either Spc19 or Dad2 resulted in large-budded cells containing either a single undivided nucleus (75 – 90%) or two unequally divided nuclei (10-25%). Nuclear mis-segregation increased drastically between 2-6h of growth under nonpermissive conditions in all cases with a concomitant loss in cell viability suggesting chromosome mis-segregation was the sole cause of loss in cell viability in these mutant cells (Figure C4C). The parent strains J101 (Dam1), J103 (Ask1), J105 (Spc19) and J107 (Dad2) grown under similar conditions exhibited normal cell cycle progression (with no obvious cell cycle arrest), proper nuclear segregation and unaltered cell viability throughout their growth under similar conditions (Figure C4). All these results strongly indicate that the Dam1 complex in *C. albicans* is essential for proper nuclear segregation, G2/M progression through cell cycle, and completion of mitosis.

C4. DEPLETION OF AN ESSENTIAL KINETOCHORE PROTEIN IN *C. ALBICANS* LEADS TO SEVERE SPINDLE DEFECTS. Most of the cells of Dam1 conditional mutants grown under nonpermissive conditions arrested at the large bud stage with unsegregated nucleus in each of the four cases. We examined and compared spindle morphology in known inner KT mutants of CENP-A (*Cse4*) and CENP-C (*Mif2*) with conditional mutant strains of the Dam1 complex - J102 (*Dam1*), J104 (*Ask1*), J106 (*Spc19*) and J108 (*Dad2*), grown under nonpermissive conditions for 4h (partial depletion) and 8h (near complete depletion). As opposed to wild-type (BWP17) (Figure C5), conditional mutant strains *CAKS3b* (*CSE4/PCK1PrCSE4*) and *CAMB2* (*mif2/PCK1PrMIF2*) when grown in nonpermissive conditions showed arrested cells at G2/M stage with either short (> 85%) or medium-long (<15%) spindles (Figure C5). Two of the four subunits of the Dam1 complex under study, Spc19- or Dad2-depleted cells, showed similar spindle defects (Figure C5). The spindle

defects exhibited due to depletion of the other two subunits, Dam1 and Ask1, were different from the rest of KT mutants of *C. albicans*.

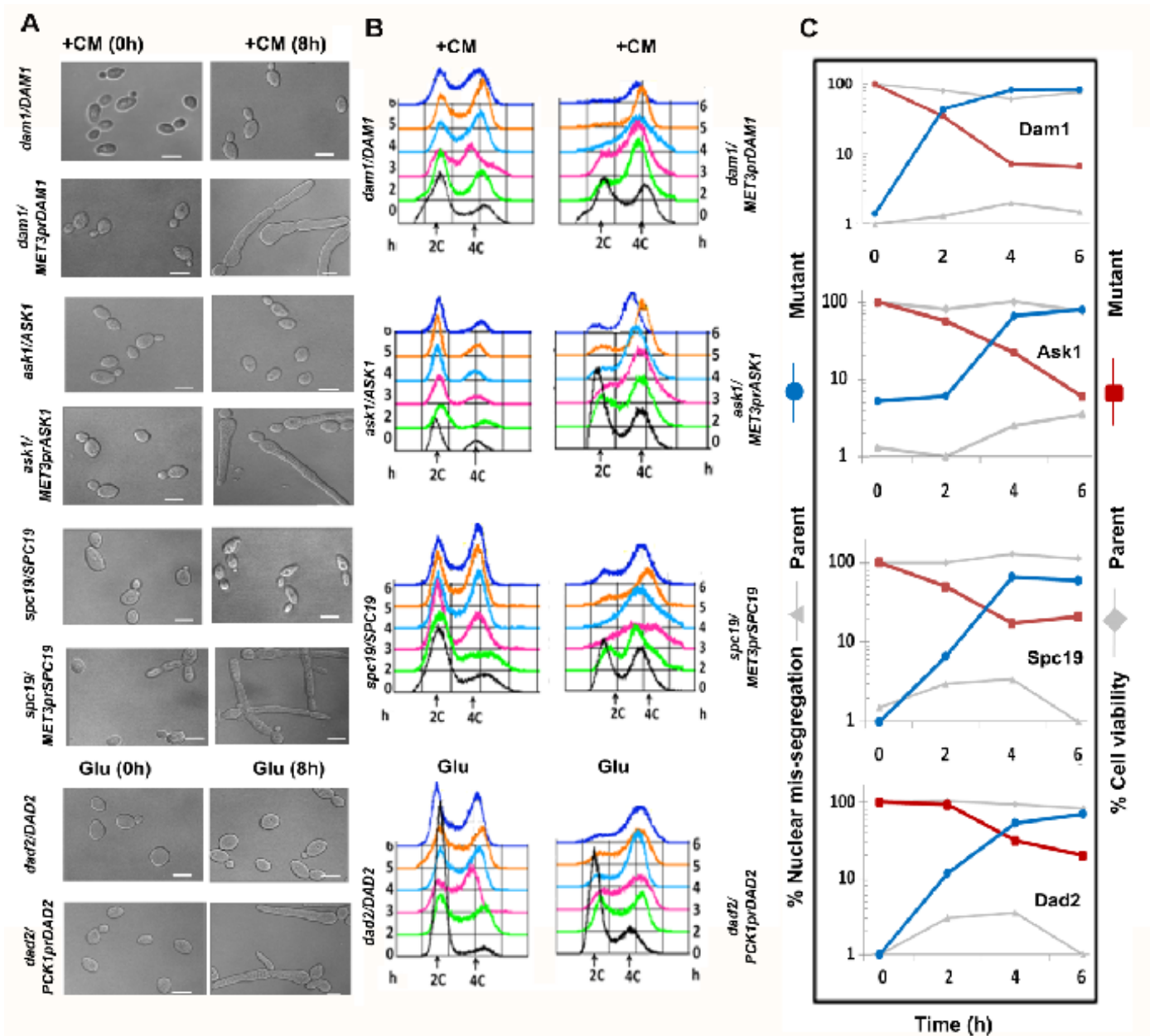


Figure C4. The Dam1 complex is required for G2/M progression through cell cycle and completion of mitosis. (A) DIC images showing phenotypes of indicated strains before (0h) and after (8h) growth in nonpermissive media. (B) The cellular DNA content of these strains were measured by flow cytometric analysis by collecting cells at different time from 0h to 6h of growth in nonpermissive conditions. (C) Graphs showing the proportion of cells exhibiting improper nuclear division of wild-type (grey triangles) or conditional mutant (blue circles) strains collected at various time points of growth in nonpermissive media. Cell viability of wild-type (grey diamonds) and mutant (red squares) strains at corresponding time points were also shown on the same graph. (+CM, in presence of cysteine and methionine; Glu, in presence of glucose). Bar, 5 μ m.

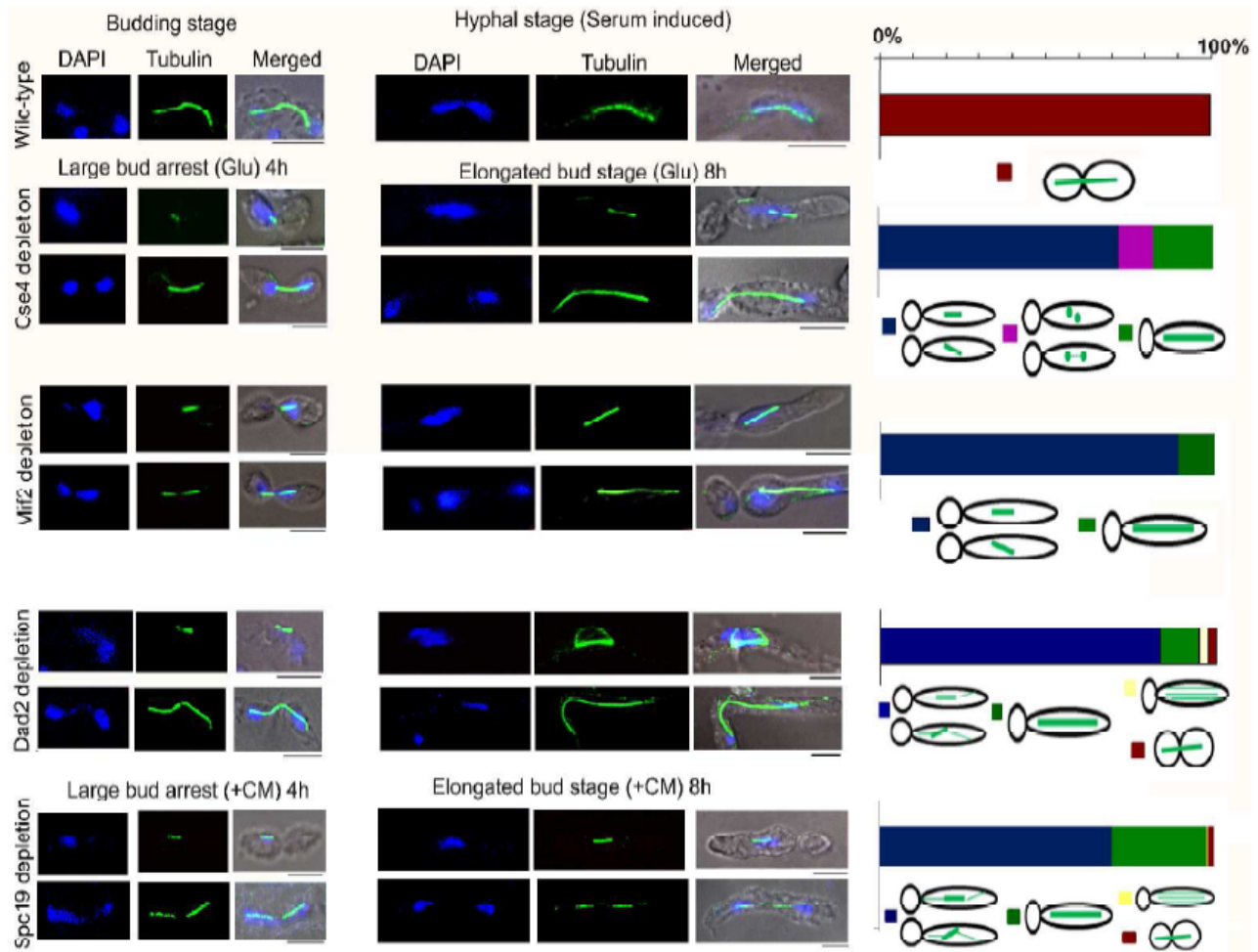


Figure C5. Depletion of an essential KT protein in *C. albicans* leads to severe spindle defects. Wild-type cells were grown in YPDU or YPDU + 10% serum, conditional mutants of inner KT proteins (CENP-A/Cse4 and CENP-C/Mif2) and two of the four tested outer KT proteins of the Dam1 complex (Dad2 and Spc19) were grown in nonpermissive media for 4h (left panels) or 8h (right panels), fixed and stained with DAPI and anti-tubulin antibodies. The percentage of cells with specific spindle phenotypes associated with each strain was calculated from cells at the elongated bud stage (right panel). Bar, 5 μ m.

C5. SUBUNITS OF THE DAM1 COMPLEX MAINTAIN DYNAMICS OF INTERPOLAR AND ASTRAL MTs.

Astral MTs are highly dynamic and their appearance is mostly undetectable in both wild-type budding and hyphal cells of *C. albicans* (Figure C6A-B). Dam1-depleted cells showed uniform short spindle phenotype but lacked astral MTs (Figure C7C-D, upper panels). More than 45% *dam1* mutant cells exhibited two SPB-like dots situated very close to each other with barely visible MTs between the two dots indicating an apparent absence of interpolar

MTs (Figure C6C-D, lower panels). Interestingly, Ask1-depleted cells showed uniform phenotype of short, often misaligned, spindles with brightly stained extensive network of cytoplasmic (astral) MTs (Figure C6E-F).

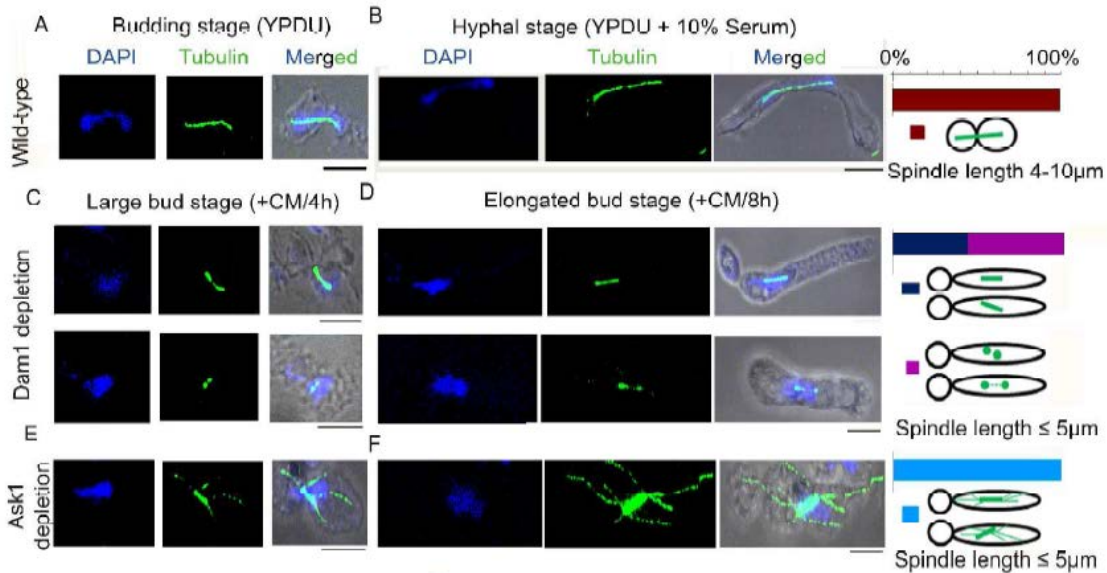


Figure C6. Dam1 and Ask1, two subunits of the Dam1 complex, maintain the polymerization/depolymerization dynamics of interpolar and astral MTs. Wild-type cells grown in YPD (A) or YPD + 10% serum (B), conditional mutants of Dam1 (*dam1prMET3DAM1/dam1*) and Ask1 (*ask1prMET3ASK1/ask1*) grown in nonpermissive media for 4h (C & E) or 8h (D & F) were fixed and stained with DAPI and anti-tubulin antibodies. More than 50% of short spindles resulting from Dam1 depletion showed no staining of IPMTs at the midzone and thus appeared as two dots (probably representing only SPBs) situated close to each other (C & D lower panels). Almost all the short spindles (>99%) caused by Ask1 depletion resulted in extensive growth of astral MTs towards cell cortex (E & F). The percentage of cells with specific spindle phenotypes associated with each strain was calculated from cells at the elongated bud stage (extreme right panels). Bar, 5 μ m.

C6. DAD2 IS LOCALIZED ALSO AT THE SPINDLE MIDZONE. Western blot analysis and immunostaining with Dad2 antibodies confirmed that J108 strain (*dad2/PCK1prDAD2*) expressed Dad2 in succinate media at a level higher than the wild-type level (BWP17) (Figure C7A-B). Overexpression of Dad2 did not alter chromosome segregation fidelity or cell viability as compared to the wild-type. Immunostaining with anti-Dad2 antibodies in J108 overexpressing Dad2 also revealed a bright dot-like signal in the midzone in addition to its KT localization (other two dot-like signals are at the KTs near the SPBs; Figure C7C). In extremely rare cases (<1% of total population), Dad2 signals were visible throughout the

spindle axis. However, midzone localization was rarely visible in wild-type BWP17 cells (*DAD2/DAD2*) (Figure C7C) probably due to low cellular levels of Dad2 present at the spindle midzone. Thus, in addition to its KT localization, Dad2 is probably localized to the plus end of the nuclear MTs. In either Dad2 or Spc19 depleted cells, albeit infrequently, we observed unbundled fibers of mitotic spindles connecting two nuclear masses (Figure C7D).

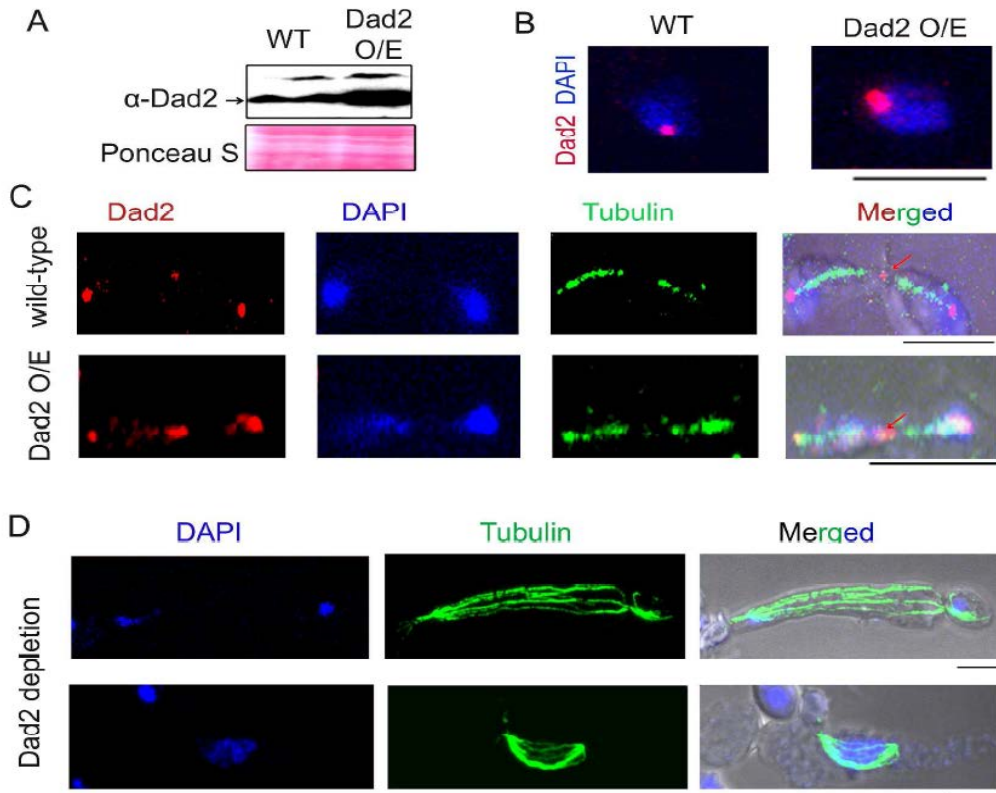


Figure C7. Dad2 is also localized at the spindle midzone. Dad2 was overexpressed under control of the *PCK1* promoter in succinate containing media. (A) Western blot analysis of cell lysates from wild-type (BWP17) and Dad2 overexpressing strain J108 (*dad2/PCK1prDAD2*) grown in succinate using anti-Dad2 or anti-PSTAIRE (loading control) antibodies. (B) BWP17 and J108 cells were grown in succinate, fixed and stained with DAPI and anti-Dad2 antibodies. (C) Succinate grown wild-type BWP17 and Dad2 overexpressing J108 (*dad2/PCK1prDAD2*) cells were fixed and stained with DAPI, anti-tubulin and anti-Dad2 antibodies. Apart from the usual KT localization (two spots each overlapping with a DAPI stained nuclear mass), an additional signal at the spindle midzone (shown by an arrow) was visible in anaphase cells. (D) Dad2 depleted cells (J108 grown in glucose) were fixed and stained with DAPI and anti-tubulin antibodies. Unbundling of spindle fibres was observed (although rarely) in both long and short spindles. Bar, 5µm

C7. THE SPINDLE ASSEMBLY CHECKPOINT (SAC) MONITORS KT-MT INTERACTION MEDIATED BY THE DAM1 COMPLEX. Several lines of evidence described above indicate that the subunits of the Dam1 complex in *C. albicans* are essential in the KT-MT-mediated process of chromosome segregation. In order to examine whether the large bud arrest in various Dam1 complex mutants was due to activation of the SAC, that senses improper KT-MT interaction, we deleted both copies of *MAD2*, an essential SAC component, in conditional mutant strains J102, J104 and J106 to construct conditional double mutant strains J112 (*mad2/mad2, dam1/MET3prDAM1*), J114 (*mad2/mad2, ask1/MET3prASK1*) and J116 (*mad2/mad2, spc19/MET3prSPC19*). Microscopic observation (DIC imaging) of J112 cells grown in nonpermissive conditions of the *MET3* promoter showed no large bud arrest phenotype (Figure C8A) even after prolonged growth (> 8h). Appearance of unbudded G1 cells with 2N DNA content determined by FACS analysis confirmed that G2/M arrest caused by Dam1 depletion was relieved in absence of Mad2-mediated checkpoint surveillance (Figure C8A). In spite of release from G2/M arrest, we observed no improvement in viability as well as growth rate of double mutants as compared to the conditional single Dam1 complex mutants. Viability of double mutants was marginally less than single mutants (Figure C8B). These results confirm that function of the Dam1 complex in mediating KT-MT interactions is under surveillance of Mad2-dependent spindle assembly checkpoint in *C. albicans*. Cells of J114 (*mad2/mad2, ask1/MET3prASK1*) and J116 (*mad2/mad2, spc19/MET3prSPC19*) conditional double mutants also showed similar results.

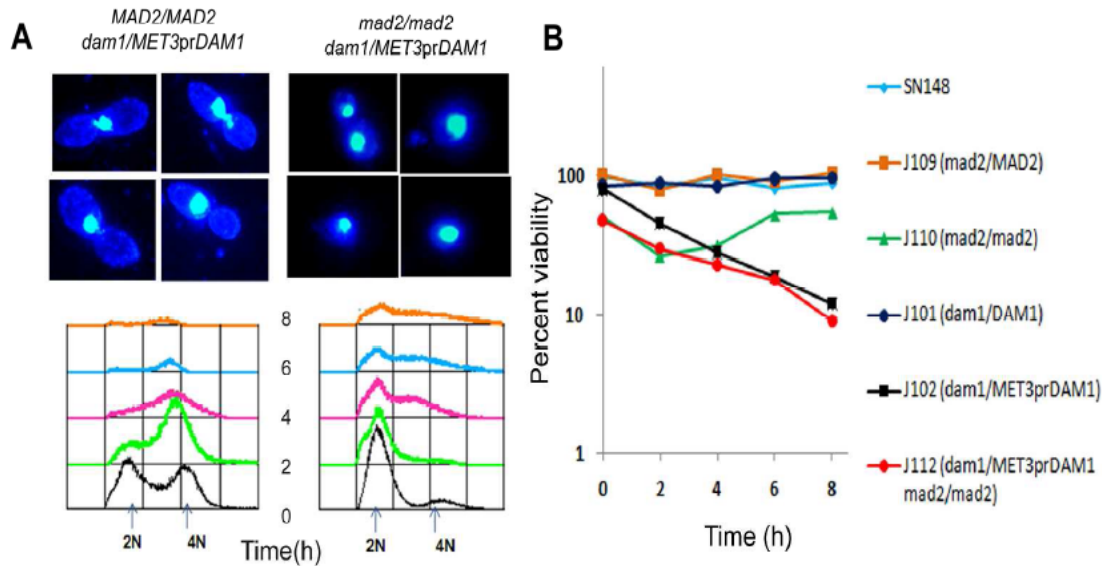


Figure C8. The function of the Dam1 complex is under the surveillance of Mad2-mediated spindle assembly checkpoint in *C. albicans*. (A) J102 (*dam1/MET3prDAM1*) and J112 (*dam1/MET3prDAM1, mad2/mad2*) cells were grown in nonpermissive media for 4h and stained with DAPI. J102 (*dam1* mutant) cells exhibited large bud arrest with unsegregated DNA mass, mostly at mother-bud neck when spindle assembly checkpoint was active. J112 (*dam1 mad2* double mutant) cells grown under similar conditions, on the other hand, exhibited cells at various stages of cell cycle including large budded cells with improperly segregated nuclear masses. FACS analysis in J102 and J112 cells at indicated time of growth in nonpermissive media (lower panel). (B) J116 (*spc19MET3/pr SPC19, mad2/mad2*) cells grown in nonpermissive media for 8h (depleted Spc19) were stained either with calcofluor white or DAPI. Spc19 depleted cells in the absence of Mad2 led to formation of cells with multiple buds and fragmented nuclear masses. Ask1 and Dam1 showed similar phenotypes.

C8. DAM1 COMPLEX-DEPENDENT KT-MT INTERACTION RESTRICTS SPINDLE LENGTH IN PRE-MITOTIC CELLS TO AVOID PREMATURE CHROMOSOME SEGREGATION. Tubulin staining in J112 (*mad2/mad2, dam1/MET3prDAM1*), J114 (*mad2/mad2, ask1/MET3prASK1*) and J116 (*mad2/mad2, spc19/MET3prSPC19*) strains grown in nonpermissive conditions exhibited long spindles (~ 5 μ m) in unbudded cells (Figure C9A). The control parent strain J110 (*mad2/mad2*) showed a single dot-like signal when stained with anti-tubulin antibodies, most probably representing the SPB, in unbudded cells (Figure C9A). This result eliminates the possibility of Mad2 in restricting the spindle length in pre-mitotic cells. Immunostaining with anti-Cse4 antibodies in these cells exhibited more than one Cse4 dot-

like signals associated with a single nuclear mass revealing the occurrence of unclustering of KT's (precocious separation of the chromosomes) that were either unattached or improperly attached to the MTs (Figure C9B). These results along with previous observations (spindle defects in metaphase) suggest that proper KT-MT interaction mediated by the Dam1 complex is required to restrict spindle elongation in premitotic cells. Figure C9C summarizes various roles of Dam1 complex components at different stages of cell cycle in *C. albicans*.

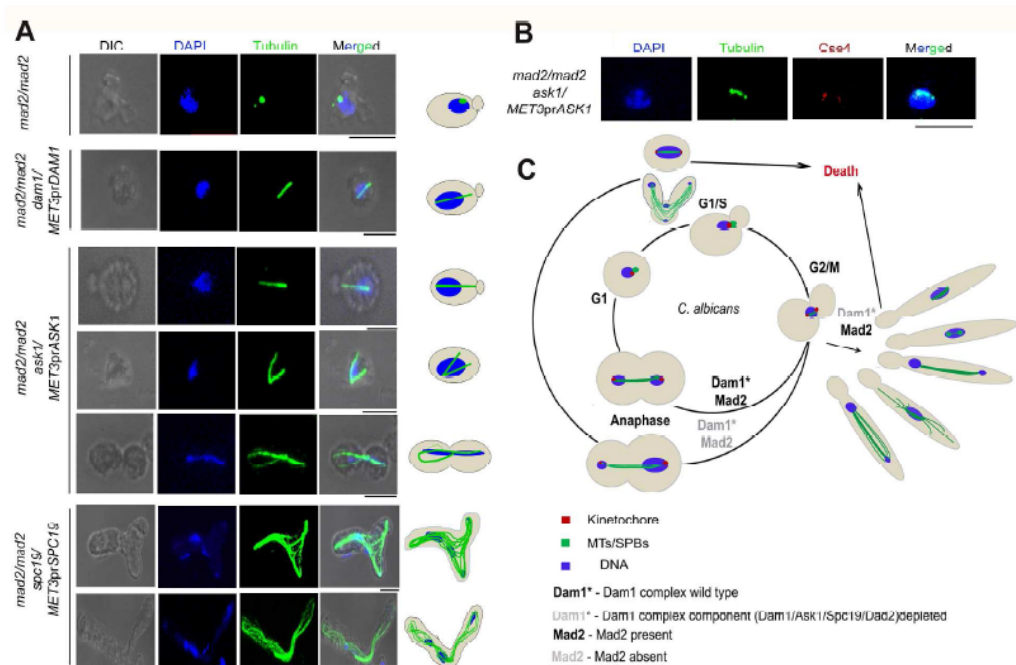


Figure C9. The Dam1 complex restricts spindle length in premitotic cells to avoid precocious chromosome separation. (A) Cells of indicated genotypes grown in nonpermissive media were fixed and stained with DAPI and anti-tubulin antibodies. Unbudded cells exhibited long spindle approaching metaphase length (2-5 μm) in Dam1 complex mutants when Mad2 was deleted. The *ask1 mad2* double mutant often showed branched spindle in unbudded cells. Unbudded or multiple-budded cells when formed elongated buds (due to stress response) often showed aberrantly segregated nuclear masses that were connected by the mitotic spindle. The *mad2* mutant cells depleted of Spc19 showed unbundled mitotic spindle fibers connecting aberrantly segregated nuclear masses. (B) Cells of indicated genotype grown in nonpermissive media were fixed and stained with DAPI, anti-Cse4 and anti-tubulin antibodies. Unbudded cells with long spindle exhibited two Cse4 dots associated with a single nuclear mass indicating precocious separation of chromosomes in premitotic cells. (C) A model highlighting the role of the Dam1 complex in maintenance of spindle length and its morphology throughout the cell cycle. Bar, 5 μm

D. A COORDINATED INTERDEPENDENT PROTEIN CIRCUITRY STABILIZES KINETOCHORE ENSEMBLE THAT PROTECTS CENP-A IN HUMAN PATHOGENIC YEAST CANDIDA ALBICANS

Unlike most eukaryotes, proteins present at the trilaminar KT are fully assembled early in the cell cycle and all the KTs remain clustered throughout the cell cycle in budding yeasts *S. cerevisiae* and *C. albicans*. Localization interdependencies of various proteins in different organisms indicate that the mechanism of KT assembly might be species-specific. KT assembly on point *CENs* of *S. cerevisiae* initiates with binding of inner KT proteins on specific *CEN* DNA sequence motifs. In contrary, KT formation in *C. albicans*, that carries regional *CENs* of 3-5 kb long, has been shown to be a sequence-independent but epigenetically regulated event. Although genetic, biochemical and microscopy studies on localization dependencies of several key evolutionarily conserved KT proteins suggest a possible hierarchical assembly of the 3-layered KT structure; it has also been proposed that KT may not be assembled in a single linear order. Bloom and colleagues also indicated *CEN* DNA bending caused by CBF3 complex in *S. cerevisiae* or by CENP-B binding in alpha-satellite DNA in mammalian *CENs* may provide proper geometry for KT formation, a process that may be evolutionarily conserved (Anderson et al, 2009). In this work, we chose to delineate the process of KT assembly in another budding yeast *C. albicans*. *C. albicans* lacks homologs of DNA binding centromeric proteins such as subunits of point *CEN*-specific CBF3 complex or regional *CEN*-specific CENP-B. Neocentromere formation does not take place in *S. cerevisiae* as *CEN* identity is strictly maintained in a sequence-dependent manner by DNA binding proteins. CENP-B is absent from the KT assembled on human neocentromeres unlike most of other KT proteins suggesting that the mechanism of KT assembly on a neocentromere might be different from that on the native one. . Interestingly, neocentromere formation is highly efficient in *C. albicans*. In absence of any known KT protein that binds to a specific sequence motif, *C. albicans* provides a unique system to study KT assembly. In this study, we investigated the process of KT assembly on regional *CENs* in *C. albicans*.

D1. THE KINETOCHORE SUPER-COMPLEX IS STABILIZED BY AN INTERDEPENDENT COORDINATED PROCESS.

In order to understand the process of KT assembly in *C. albicans*, we studied localization dependencies of various essential KT proteins. We depleted each of Dam1, Ask1, Spc19 and Dad2 - four subunits of an evolutionarily conserved outer KT protein complex, the Dam1 complex, to study localization dependencies of other KT proteins. Immunostaining with anti-Cse4 (CENP-A) antibodies in depleted levels of various subunits of the Dam1 complex such as Dam1 (J102), Ask1 (J104), Spc19 (J106) or Dad2 (J108), revealed that CENP-A localization at the KTs was dramatically reduced as compared to conditions when these proteins were present at wild-type levels (Fig D1A). This is the first example, to our knowledge, where an outer KT protein complex has been shown to influence localization of CENP-A. Next, to study KT localization patterns of another inner KT protein CENP-C/Mif2 in Dam1- or Ask1-depleted conditions, we expressed Myc-tagged CENP-C/Mif2 from the *PCK1* promoter in *dam1* (J123) or *ask1* (J124) conditional mutants. Similar to CENP-A, CENP-C/MycMif2 localization was dramatically reduced when levels of Dam1 or Ask1 were depleted by growing J123 or J124 for 8h under repressive conditions (+CM + Suc) of the *MET3* promoter (Figure D1B). These results revealed that recruitment of two key inner KT proteins, CENP-A and CENP-C, at the KT is dependent on the Dam1 complex. Recently, it was demonstrated that recruitment of these two proteins is dependent on the cellular levels of a middle KT protein, Mis12/ Mtw1 as well in *C. albicans* (Roy et al, 2011). Together, we conclude that assembly of the inner KT is dependent on the middle and outer KT in *C. albicans*.

These results prompted us to further investigate the role of an outer KT protein complex on the recruitment of a middle KT protein. In order to do this, we expressed Mtw1-GFP in *dam1* (J122) or *ask1* (J120) conditional mutant strains. While bright dot-like Mtw1-GFP signals representing clustered KTs were visible in all cells when Ask1 or Dam1 was expressed, Mtw1-GFP signals were not detectable in any cells depleted either of Dam1 or Ask1 (Figure D1C) indicating that integrity of the middle layer is also determined by outer KT proteins.

Having established localization dependencies of various layers on each other, we further examined how two inner KT proteins regulate each other for their KT localization. First, we examined localization of CENP-A under CENP-C/Mif2 depleted conditions. Cells of parent (CAMB1) or conditional mutant strain CAMB2 grown in repressive media (Glu) for 8h were fixed and stained with anti-Cse4 antibodies. No detectable CENP-A/Cse4 signals were observed in CENP-C/Mif2 depleted cells as opposed to bright dot-like signals in parent cells (Figure D1D) suggesting CENP-A localization is dependent on another inner KT protein (CENP-C). Together these results suggest that integrity of different layers of a KT is interdependent and assembly of all three layers of a KT is coordinated (Figure D1E).

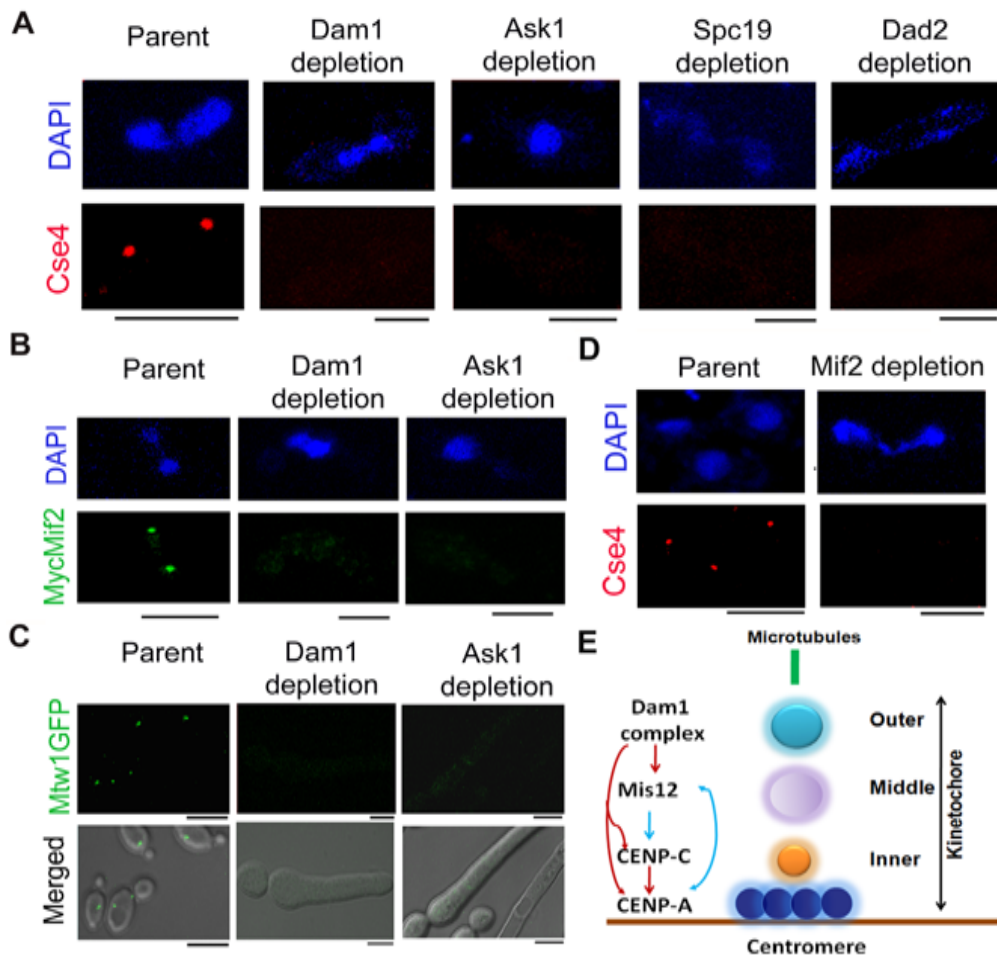


Figure D1. The process of KT assembly is interdependent and coordinated in *C. albicans*. (A) Parent BWP17 or conditional mutant strains J102 (*dam1/MET3prDAM1*), J104 (*ask1/MET3prASK1*), J106 (*spc19/MET3prSPC19*) and J108 (*dad2/PCK1prDAD2*) were grown for 8h

under nonpermissive conditions to deplete Dam1, Ask1, Spc19 and Dad2 respectively. These cells were fixed and stained with DAPI, anti-tubulin and anti-Cse4 antibodies. CENP-A/Cse4 signals, visible in parent cells, were undetected in Dam1, Ask1, Spc19 or Dad2 depleted cells. (B) Cells of the parent strain J125 (*MIF2/PCK1prMycMIF2*), conditional *dam1* mutant J123 (*dam1/MET3prDAM1 MIF2/PCK1prMycMIF2*), or conditional *ask1* mutant J124 (*ask1/MET3prASK1 MIF2/PCK1prMycMIF2*) were grown for 8h under nonpermissive (+CM + Suc) conditions of the *MET3* promoter, fixed and stained with DAPI, and anti-Myc antibodies. MycMif2 signals were undetected in Dam1- or Ask1-depleted cells. (C) Parent YJB10695 (*MTW1/MTW1GFP*), conditional *dam1* mutant J122 (*dam1/MET3prDAM1 MTW1/MTW1GFP*), or conditional *ask1* mutant J120 (*ask1/MET3prASK1 MTW1/MTW1GFP*) cells grown under nonpermissive conditions of the *MET3* promoter (+CM) for 8h were examined for GFP signals by confocal microscopy. Bright Mtw1-GFP dot-like signals were observed in wild-type cells while no Mtw1-GFP signals were detected in Dam1- or Ask-depleted cells. (D) Parent CAMB1(*MIF2/PCK1prMycMIF2*) and conditional *mif2* mutant CAMB2 (*mif2/PCK1prMycMIF2*) cells were grown for 8h under nonpermissive conditions (Glu) of the *PCK1* promoter, fixed and stained with DAPI, and anti-Cse4 antibodies. CENP-A/Cse4 signals were visible in the parent cells but undetected in Mif2-depleted cells. (E) A schematic showing localization dependencies of evolutionarily conserved KT proteins in *C. albicans*. Red lines, localization dependencies in this study; blue lines, localization dependencies reported previously (Roy et al, 2011). Bar, 5 μ m.

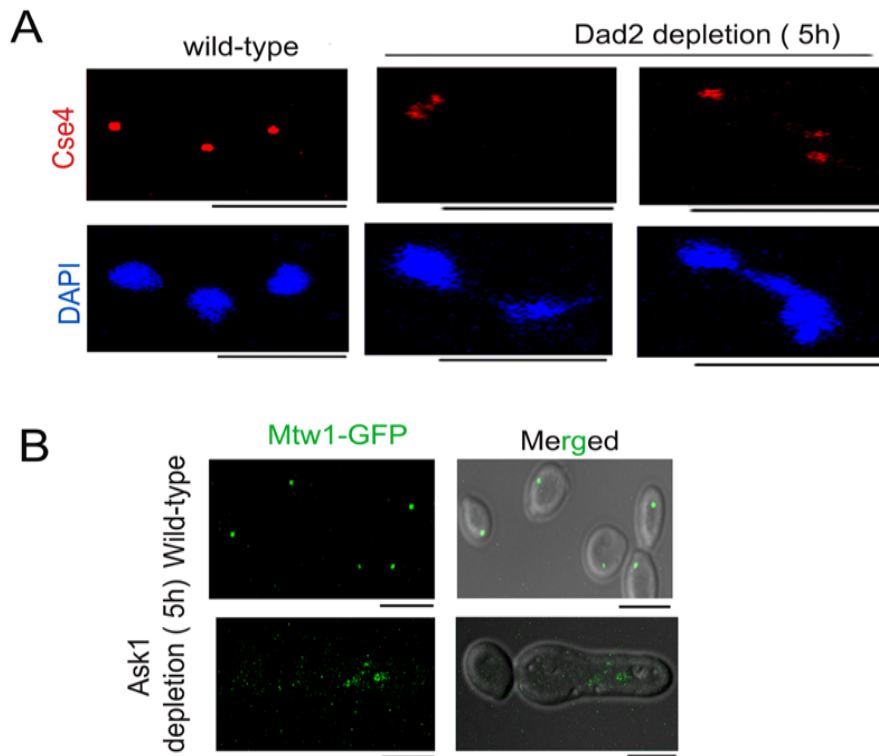


Figure D2. KTs are unclustered in the absence of an essential KT protein. (A) Dad2-depleted J108 (*dad2/PCK1prDAD2*) cells grown for 5h under nonpermissive conditions of the *PCK1* promoter

were fixed and stained with DAPI and anti-Cse4 antibodies. These Dad2-depleted cells exhibited 1-4 visible dot-like Cse4 signals per DAPI stained nuclear mass suggesting that *CENs* were unclustered. **(B)** Parent YJB10695 (*MTW1/MTW1GFP*) or *ask1* conditional mutant J120 (*ask1/MET3prASK1 MTW1/MTW1GFP*) cells grown under nonpermissive conditions of the *MET3* promoter (+CM) for 5h exhibited clustered or unclustered Mtw1GFP signals in presence or absence of Ask1. Bar, 5 μ m.

D2. INTEGRITY OF A KINETOCHORE IS INDEPENDENT OF KT-MT INTERACTION.

Unlike most organisms including fission yeast and humans, KTs are attached to spindle MTs throughout the cell cycle in *S. cerevisiae* except for a brief period of 2-3 minutes during *CEN* replication (Tanaka et al, 2010; Tanaka, 2010). A similar KT-MT interaction throughout the cell cycle is evident in *C. albicans* as well (Roy et al, 2011). Since the KT proteins discussed above have been shown to be essential in KT-MT-mediated process of chromosome segregation in *C. albicans* (Roy et al, 2011; Sanyal et al, 2004; Sanyal & Carbon, 2002; Thakur & Sanyal, 2011), we next examined whether or not reduced KT localization of the inner and middle KT proteins was due to improper KT-MT interaction caused by the depletion of these proteins. To test this possibility, we disrupted the mitotic spindle to impair KT-MT interaction by treating wild-type cells expressing GFP-tagged Cse4 (strain 10118) with a spindle depolymerizing drug nocodazole. Tubulin staining of these nocodazole treated cells exhibited loss in mitotic spindle structure as expected (Figure D3A). However, no significant change in the intensity of Cse4-GFP signals was observed between nocodazole treated and untreated cells of 10118 (Figure D3B). A similar experiment to measure Mtw1-GFP levels in nocodazole treated and untreated cells of YJB10695 exhibited no significant difference (Figure D3C). The localization of Dad2, a subunit Dam1 complex, is not altered as well in the presence or absence of nocodazole (Thakur & Sanyal, 2011). These results together suggest that KT-MT interaction is not required to maintain the integrity of a KT in *C. albicans*.

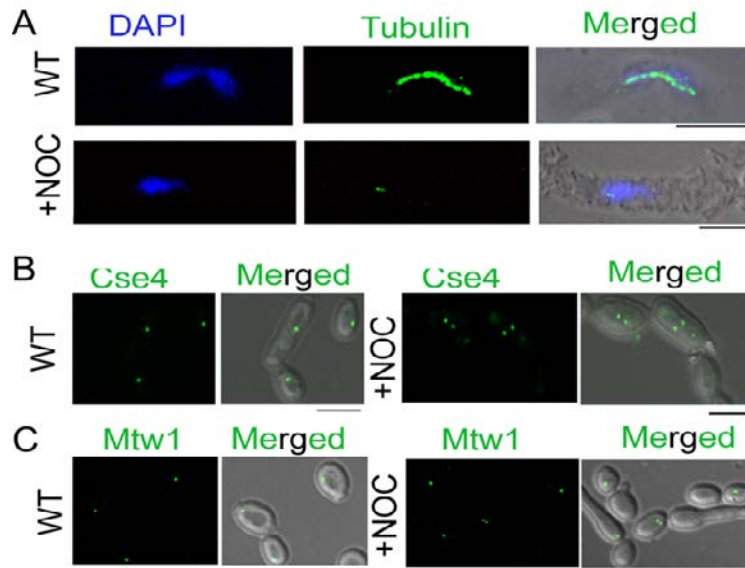


Figure D3. KT integrity is independent of KT-MT interaction. A) Wild-type BWP17 cells, untreated (WT) or treated with nocodazole (+NOC), were fixed and stained with DAPI, and anti-tubulin antibodies. As compared to WT (upper panel), NOC treated cells (lower panel) exhibited collapsed mitotic spindle. (B) CENP-A/Cse4-GFP signals were analyzed in absence (WT) or presence of NOC (+NOC) in 10118 (*cse4::dpl200-URA3/CSE4:GFP:CSE4*) cells. (C) Similarly, Mtw1-GFP signals were analyzed in the absence (WT) or presence of NOC (+NOC) in YJB10695 (*MTW1/MTW1GFP*) cells. No significant change in intensity of either Cse4-GFP or Mtw1-GFP signals in NOC treated cells as compared to untreated cells indicated that the role of an essential KT protein in maintaining KT integrity is independent of its function in KT-MT attachment. Bar, 5 μ m.

D3. KT CLUSTERING ENSURES INTEGRITY OF INDIVIDUAL KTs IN *C. ALBICANS*.

In order to find out how absence of a KT protein leads to collapse of an entire KT, we monitored the process of KT disassembly during the process of gradual depletion of KT proteins. To visualize KTs, we observed both CENP-A (Cse4) and CENP-C (MycMif2) signals in wild-type or gradually depleted levels of Dam1 (J123) or Ask1 (J124). Bright dot-like KT signals seen in wild-type cells (Figure D4, upper panels) showed a decrease in the intensities of both CENP-A and CENP-C after 4h of growth of Dam1 or Ask1 conditional mutants in conditions that repressed the *MET3* promoter. Interestingly, after 4-5h of Dam1 depletion we observed faint multiple dot-like signals of CENP-A (Cse4) and CENP-C (MycMif2) (Figure D4A, lower panels) indicating unclustering of KTs due to partial depletion of outer KT proteins. We also observed multiple CENP-A (Cse4) signals in Dad2

conditional mutant (J108) after 4-5h of growth under nonpermissive conditions (Figure D2A). After 8h of depletion of Dam1 or Ask1 (as discussed in previous section) no CENP-A (Cse4) and CENP-C (MycMif2) signals were visible. This unequivocally indicates that unclustering caused in the absence of Dam1 or Ask1 is an intermediate step before KT disassembly. To further confirm the unclustering of the KTs in cells depleted of the Dam1 complex, we examined another KT protein, Mtw1-GFP signals by depleting Dam1 (J122) or Ask1 (J120) for 5h. In both the cases of protein depletion, we observed multiple Mtw1-GFP signals per nucleus (Figure D2B). Thus we demonstrated KT unclustering by visualizing inner and middle KT proteins in reduced levels of Dam1 or Ask1.

To test whether KT unclustering occurs due to depletion of middle (Mis12/Mtw1) or inner (CENP-A/Cse4) KT proteins as well, we first depleted Mis12/Mtw1, and examined the status of KT clustering using anti-Cse4 antibodies in CAKS12. KT unclustering was clearly evident with multiple faint CENP-A signals co-localized with a single DAPI stained nucleus (Figure D4B). An inner KT protein such as CENP-A has already been shown to affect Mis12/Mtw1 in *C. albicans* (Roy et al, 2011). Here we monitored the process of Mis12/Mtw1 delocalization upon depletion of CENP-A. Strain YJB11483 expressing CENP-A/Cse4 under the *PCK1* promoter was grown either in permissive (+Suc) or nonpermissive (+Glu for 5h) conditions and Mtw1-GFP signals were examined (Figure D4C). We observed multiple Mtw1-GFP signals per cell confirming KT unclustering in these cells as well (as opposed to wild-type where KTs remained clustered). These results together suggest that unclustering is a common intermediate step of KT disassembly caused by depletion of an essential KT protein.

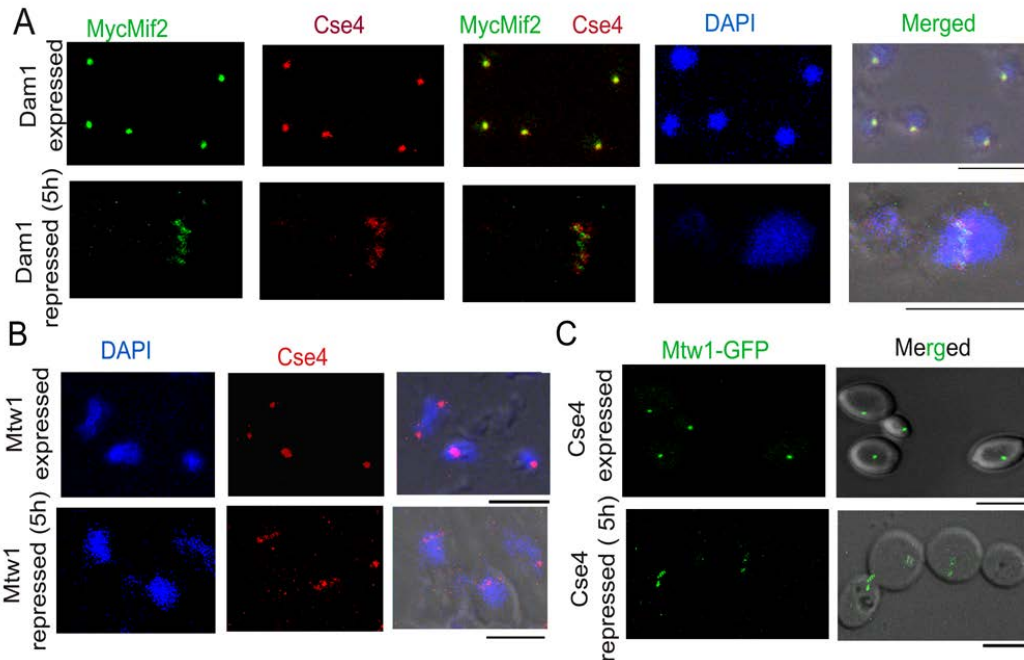


Figure D4. KT unclustering and KT disassembly are consequential events. (A) J123 (*dam1/MET3prDAM1 MIF2/PCK1prMycMIF2*) cells, expressing Dam1 from the *MET3* promoter were grown under conditions that expressed (-CM + Suc) or repressed (+CM + Suc for 5h) Dam1. Cells were fixed and stained with DAPI, anti-Cse4, and anti-Myc (Mif2) antibodies. Multiple faint Cse4 and MycMif2 dot-like signals that were often co-localized on a single DAPI-stained nuclear mass were observed indicating unclustering of KTs in Dam1-depleted cells. Cells expressing Dam1 showed one single cluster of KTs detected as colocalized CENP-A/Cse4 and CENP-C/Mif2 signals per DAPI stained nuclear mass confirming that the Dam1 is essential to maintain clustered KTs. (B) CAKS12 (*mtw1/PCK1prMTW1*) cells, expressing Mis12/Mtw1 from the *PCK1* promoter grown under conditions that expressed (Suc) or repressed (Glu for 5h) Mis12/Mtw1, were fixed and stained with DAPI and anti-Cse4 antibodies. Similar KT unclustering was visible in Mis12/Mtw1-depleted cells in contrast to clustered KTs visible in cells expressing this protein suggesting that depletion of a middle KT protein leads to KT unclustering. (C) Mis12/Mtw1-GFP signals were observed in YJB11483 (*cse4/PCK1prCSE4 MTW1/MTW1-GFP*) cells expressing CENP-A/Cse4 from the *PCK1* promoter grown under conditions that expressed (Suc) or repressed (Glu for 5h) CENP-A/Cse4. Multiple Mis12/Mtw1-GFP dots per cell were observed when CENP-A/Cse4 was repressed indicating that depletion of an inner KT protein also results in KT unclustering. Bar, 5 μ m.

D4. NUCLEAR PERIPHERAL LOCALIZATION IS MAINTAINED IN UNCLUSTERED KINETOCHORES.

All KTs are clustered and such clusters are localized towards the nuclear periphery (Figure D5, top panel) suggesting KTs occupy a fixed nuclear territory in wild-type *C. albicans* cells (Thakur & Sanyal, 2011). Reconstruction of 3D images revealed unclustered KT signals

resulting due to Dad2 depletion in conditional mutant strain J108 grown under nonpermissive conditions were also localized at the nuclear periphery. These signals were although scattered but not randomly localized (Figure D5, bottom panels). Since nuclear territory of unclustered KT is maintained, we propose that factors involved in nuclear peripheral localization of the KT must be different from those determining KT clustering.

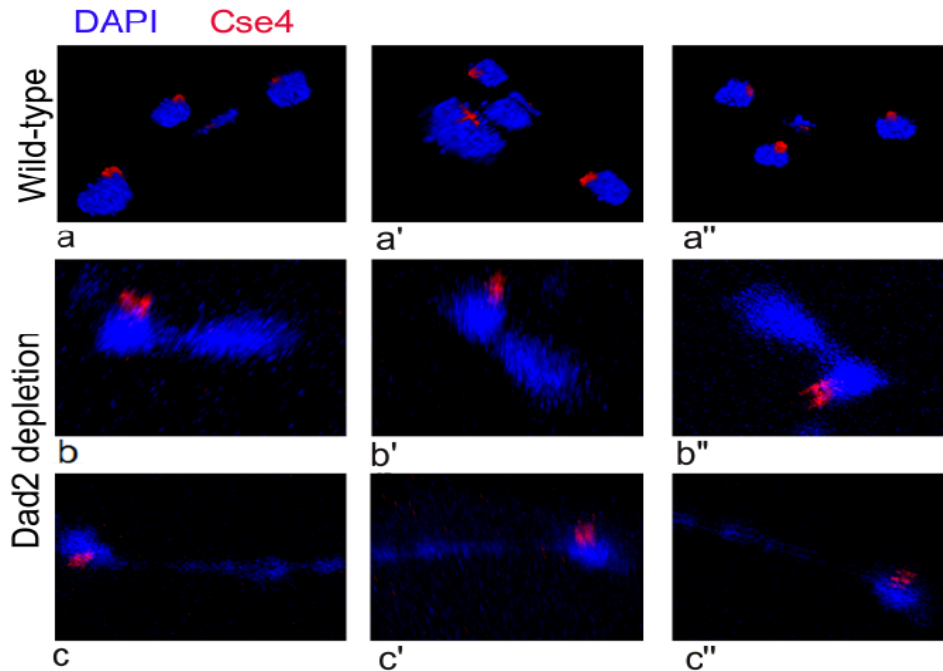


Figure D5. Nuclear peripheral localization is maintained in unclustered KTs. J108 (*dad2/PCK1prDAD2*) cells grown for 5h under nonpermissive conditions of the *PCK1* promoter were fixed and stained with DAPI and anti-Cse4 antibodies. Images were captured using confocal microscopy and 3D images were reconstructed using AxioVision 4.8 (Carl Zeiss, Germany). Three different images showing frames (a-c) from different rotational angles are shown in each case. Wild-type cells exhibited a single bright dot-like signal per DAPI-stained nuclear mass localized at the nuclear periphery (upper panel). Dad2-depleted cells exhibited multiple visible dot-like Cse4 signals per DAPI stained nuclear mass suggesting that *CENs* were unclustered. Similar to clustered KTs in wild-type, multiple unclustered KT signals were localized at the nuclear periphery (lower panels).

D5. KINETOCHORE ENSEMBLE MAINTAINS CENTROMERIC CHROMATIN.

To examine the status of centromeric chromatin when KT integrity is lost, chromatin immunoprecipitation assays (ChIP) with anti-Cse4 antibodies were performed in wild-type (BWP17, (Wilson et al, 1999)) and *dam1* (J102) or *dad2* (J108) conditional mutants grown

in repressive media for 8h. These experiments revealed a drastic decrease in CENP-A binding to *CENs* in Dam1- or Dad2-depleted cells as compared to wild-type confirming that integrity of CENP-A-bound centromeric chromatin is highly affected in these mutants (Figure D6A). Nocodazole treated G2/M arrested cells, however, showed no change in CENP-A binding to *CENs* confirming that integrity of centromeric chromatin is largely unaffected even in absence of KT-MT interaction. Thus, we conclude that individual KT proteins independent of their role in mediating KT-MT attachment, are essential to maintain integrity of centromeric chromatin. Since, the localization of CENP-C, another inner KT protein, was also affected when Dam1, a component of the Dam1 complex was depleted, we tested CENP-C recruitment at various *CENs* in wild-type (J125) or depleted levels of Dam1 (J123) by ChIP assays with anti-MycMif2 antibodies (Figure D6B.). The ChIP-PCR analysis confirmed that CENP-C recruitment to the *CENs* was also dramatically reduced in Dam1-depleted cells. Together these results confirmed that Dam1 is required for KT integrity formed on the foundation of centromeric chromatin in *C. albicans*. We have recently shown that, Mtw1/Mis12 is required for inner KT assembly including localization of CENP-A and CENP-C. Thus we propose that maintenance of centromeric chromatin is orchestrated with KT assembly.

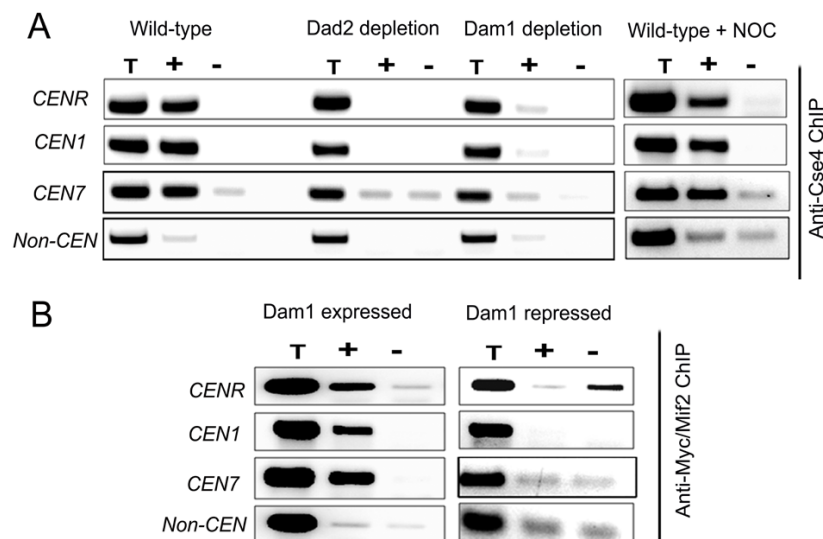


Figure D6. KT ensemble maintains centromeric chromatin. (A) Cse4 ChIP-PCR analysis with DNA obtained from wild-type (BWP17), Dam1-depleted J102 (*dam1/MET3prDAM1*) or Dad2-

depleted J108 (*dad2/PCK1prDAD2*) cells grown for 8h in nonpermissive conditions. Primers from *CENR* (CaChrR: 1747812-1748023), *CEN1* (CaChr1: 1565723-1565967), *CEN7* (CaChr7: 427369 - 427560) or 17 kb away from *CEN7* (CaChr7: 444584 -444875) (non-*CEN*) were used for PCR analysis. T, total DNA; +, IP DNA with anti-Cse4 antibodies and -, beads only control without antibodies. CENP-A/Cse4 recruitment was found to be highly reduced at *CENs* in Dam1- or Dad2-depleted cells as compared to WT. (B) MycMif2 ChIP-PCR analysis with DNA obtained from J123 (*dam1/MET3prDAM1 MIF2/PCK1prMycMIF2*) either expressing Dam1 (WT) or depleted of it. Primers from *CENR* (CaChrR: 1747812-1748023), *CEN1* (CaChr1: 1565723-1565967), *CEN7* (CaChr7: 427369 - 427560) or non-centromeric region *LEU2* (non *CEN*) were used for PCR analysis. T, total DNA; +, IP DNA with anti-Myc antibodies and -, beads only control without antibodies. Mif2 recruitment at *CENs* was found to be reduced in Dam1 depleted conditions as compared to when Dam1 was present.

D6. STABILIZATION OF CENTROMERIC CHROMATIN BY KINETOCHORE ENSEMBLE PROTECTS CENP-A

The results described above strongly implicate that proteins from each of three different layers of the KT is essential for maintaining KT assembly that is built on the foundation of CENP-A containing centromeric chromatin. To find out the fate of unbound CENP-A, we examined the status of CENP-A protein levels in these mutants. We prepared protein lysates from J108 expressing Dad2 under the *PCK1* promoter grown overnight in succinate (expressed condition) or various time intervals after transferring in glucose (repressed condition) and performed western blot analysis to measure the levels of both Dad2 and CENP-A. A decrease in Dad2 protein levels in cells grown at increasing time in glucose confirmed repression of Dad2 expression by the *PCK1* promoter (Figure D7A, left panel). Strikingly, a concomitant reduction in CENP-A protein levels (determined by anti-Cse4 antibodies) with decreasing levels of Dad2 was also observed (Figure D7A, right panel). These results strongly indicated that reduction in CENP-A localization at the KT in Dad2-depleted cells resulted in CENP-A degradation. To examine the fate of CENP-A in reduced levels of other subunits of the Dam1 complex, total cell lysates were prepared from strains where Dam1 (J102), Ask1 (J104), or Spc19 (J106) was either expressed or repressed for 8h. As observed in Dad2-depleted cells, CENP-A levels in the total cell lysates were found to be highly reduced in absence of each of these proteins (Figure D7B). To examine whether

CENP-A stability is only determined by the integrity of the outer KT alone or KT as a whole, we next examined CENP-A stability in depleted conditions of Mis12/Mtw1 (present at the middle KT) or CENP-C/Mif2 (present at the inner KT). Strain CAKS12 or CAMB2 expressing Mis12/Mtw1 or CENP-C/Mif2 respectively under the *PCK1* promoter were grown in succinate (expressed) or glucose (repressed) for 8h and total cell lysates were prepared. Western blot analysis of these cell lysates with anti-Cse4 antibodies confirmed a decrease in CENP-A levels when either Mis12 or CENP-C was depleted. Thus, CENP-A protein stability is dependent on integrity of centromeric chromatin which is maintained by the integrity of a functional KT.

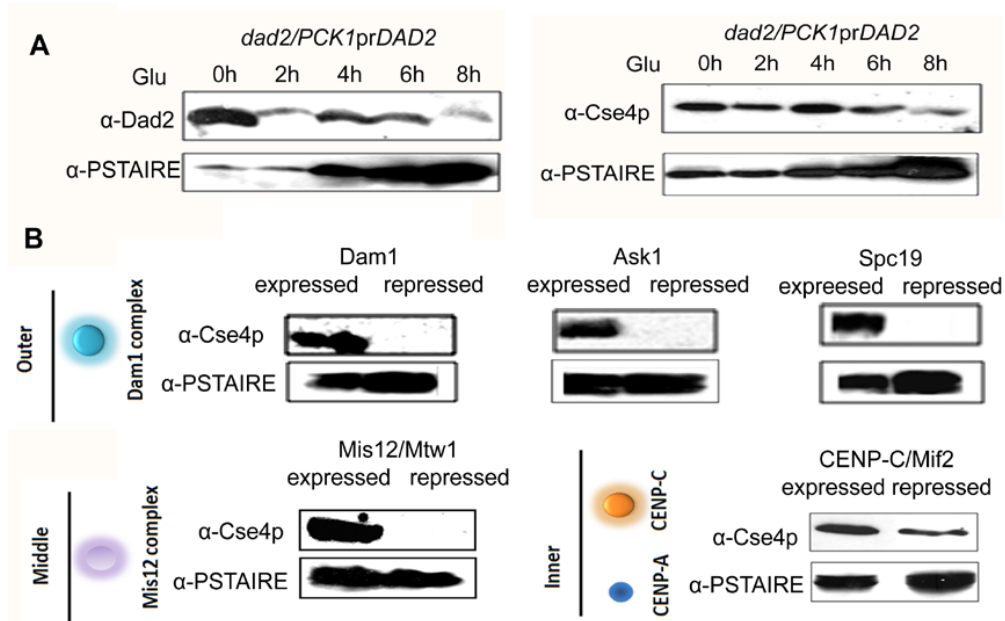


Figure D7. CENP-A is protected by KT ensemble. (A) J108 (*dad2/PCK1prDAD2*) expressing Dad2 under the *PCK1* promoter was grown overnight in succinate (when the *PCK1* promoter was expressed), transferred to media containing glucose (when the *PCK1* promoter is repressed) and collected cells at specific time intervals as shown. Western blot analysis was performed using anti-Dad2, anti-Cse4 and anti-PSTAIRE antibodies with cell lysates prepared from these cells. Both Dad2 (left panels) and CENP-A/Cse4 (right panels) protein levels showed a gradual decrease as time of repression of Dad2 prolonged. PSTAIRE was used as loading control. Increasing amount of protein was loaded to visualize the reduced Dad2 or CENP-A/Cse4 protein signals in these western blots. (B) Western blot analysis using anti-Cse4 and anti-PSTAIRE antibodies with cell lysates prepared from conditional mutant strains of indicated KT proteins after 0h and 8h of growth in nonpermissive media. CENP-A/Cse4 levels decreased drastically when each of Dam1, Ask1, Spc19, Mis12 /Mtw1 or CENP-C/Mif2 was depleted.

Discussion

3.1 Rapid evolution of centromeric DNA sequences in closely related pathogenic yeasts, *Candida albicans* and *Candida dubliniensis*

In the absence of any obvious sequence motifs and repetitive elements, the nature of epigenetic factors that regulate *CEN* identity of *C. albicans* remains an enigma. In the present study, we identified *CENs* of closely related species *C. dubliniensis* using two evolutionarily conserved KT proteins, CdCse4p and CdMif2p. We predicted that identification of *CENs* of *C. dubliniensis* and their comparison with *CENs* of *C. albicans* might reveal the factors responsible for determining *CEN* identity in these two closely related species. Each of *C. dubliniensis* *CENs* is unique and has different DNA sequence composition without any strong sequence motifs or *CEN*-specific repeats that are common to all of the eight *CENs* and has A-T content similar to that of the overall genome. All these properties match those of *C. albicans* *CENs* (Mishra et al, 2007; Sanyal et al, 2004). The sequence comparison between *C. dubliniensis* and *C. albicans* *CEN* revealed that *CENs* have diverged faster than other intergenic sequences of similar length and even faster than our best estimated neutral mutation rate for ORFs. Due to highly repetitive nature, *CENs*, in general, are subject to several events such as mutation, recombination, deletion, and translocation that may contribute to rapid change observed in *CEN* sequence across the species. Such accelerated evolution is particularly striking in the absence of such repetitive sequences at *CEN* regions of *C. albicans* and *C. dubliniensis*. A recent report based on comparison of chromosome III of three closely related species of *S. paradoxus* suggests that the *CEN* seems to be the fastest evolving part in the chromosome (Bensasson et al, 2008). Rapid evolution of centromeric DNA and associated proteins (discussed in the Introduction) may act as a driving force for speciation (Henikoff et al, 2001; Malik & Henikoff, 2002). Rapid change in *CEN* sequences we observed in these two closely related *Candida* species may generate functional incompatibility of *CENs* to facilitate speciation. Interestingly, despite sequence divergence, the location of the Cse4p-rich regions in orthologous regions of *C. albicans* and *C. dubliniensis* has been maintained for millions of years.

3.2 Physical location determines centromere/neocentromere formation in *Candida* sp.

The work described above led us to speculate a new paradigm in which we propose that the relative position of a *CEN*, rather than the DNA sequence alone, may determine *CEN* identity in *Candida* species. Indeed, centromeric chromatin assembled on the non-centromeric sequence (1.4 kb *URA3*) inserted at the *CEN7* locus as determined by enrichment of CENP-A on *URA3*. Integration of a non-centromeric sequence *URA3* at the *CEN7* does not destabilize the chromosome suggesting that the function of the native *CEN* remains unaltered as *URA3* becomes an integral part of centromeric chromatin. This experiment strongly implicated that the redundancy of DNA sequence requirement associated with site selection for *CEN* formation. In absence of any boundary element (such as tRNA genes in *S. pombe*), H3K9 methylation (found in *S. pombe* outer centromeric repeats) or common repeat elements, it was not easy to assign pericentric region in *C. albicans*. Thus, in absence of existence of a specified pericentric region or differences in the chromatin modification status at core CENP-A chromatin and surrounding chromatin, it is difficult to speculate how CENP-A deposition takes place on *URA3* inserted at *CEN7*. Therefore, we sought to replace the region that forms CENP-A chromatin with a non-centromeric DNA. When the entire 4.5 kb CENP-A binding *CEN7* region was replaced with 1.4 kb *URA3*, CENP-A recruitment (neocentromeres formation) occurred elsewhere suggesting that centromeric DNA sequences when present at the native context do play a role in recruiting the CENP-A on a non-centromeric DNA (*URA3* in this case) inserted into a *CEN*. Detailed analysis of neocentromeres revealed that neocentromere formation always occurred at *CEN* adjacent regions. Exclusive presence of neocentromeres close to the deleted region provided us with a clue about the determinant of *CEN*/neocentromere formation in *C. albicans*. As discussed previously, orthologous pericentric regions contain several short stretches of DNA sequences that are common in pericentric regions of some, but not all, *C. albicans* and *C. dubliniensis* chromosomes. Presence of neocentromeres at *CEN* adjacent locations made us hypothesize that in the absence of specific sequence motifs or repeats, it is possible that more conserved pericentric regions might be responsible for recruiting the CENP-A at *CEN* adjacent regions in the absence of a functional native *CEN* to facilitate the formation of a specialized 3D common structural scaffold that favors *CEN*

formation in *Candida* species. Deletion of pericentric regions of various lengths (4.5 kb – 30 kb) along with centromeric sequences with *URA3* revealed that neocentromeres are always formed at the sites next to deleted regions ruling out the possibility of contribution of pericentric region in neocentromere formation. These results together with conservation of relative centromeric location in *C. albicans* and *C. dubliniensis* on orthologous chromosomes, implicate that relative location of a *CEN* across the entire length of a chromosome is one of the epigenetic factors determining centromere/neocentromere formation in *C. albicans*. As mentioned in the Results section all the *CENs* are clustered together in *C. albicans* and occupies a specific position towards the nuclear periphery. We reason that the native *CEN* is the candidate for *CEN* formation but other potential sites (Class I-IV neocentromeres) are present at *CEN* adjacent regions due to their similar relative location as that of the native *CEN* along the length of chromosome when it is altered. This raises an important question of mechanism of suppression of neocentromere formation in the native context.

3.3 Native centromere suppresses other potential neocentromeres

As proposed before that CENP-A may get deposited to multiple locations in a replication-coupled or replication independent manner but an unknown mechanism can evict out CENP-A from DNA except at the unique *CEN* DNA. It is thus possible that CENP-A deposited at the *CEN* is further stabilized by fully functional kinetochores due to their attachment to the spindle microtubules. While our results suggest that a fully functional kinetochore stabilizes CENP-A at the *CEN* but a proper KT-MT attachment seem to have no role to play in CENP-A stabilization (see below). Alternatively, based on CENP-A overexpression studies from various organisms, it seems to be apparent that retention of CENP-A exclusively at the *CEN* may be species-specific. Nonetheless, in absence of DNA sequences cues, the mechanism by which CENP-A is deposited on a single site, especially when there are other potential CENP-A binding sites, needs further insight of factors regulate *CEN* formation.

As proposed above, the native *CEN* is the most preferred site of CENP-A deposition across the length of entire chromosome and secondary sites including a hotspot are present at *CEN* adjacent regions (neocentromeres) due to their proximity to the looped structure where local concentration of CENP-A is high due to clustering of all the *CENs* (CENP-A-rich 3D scaffold). Since the native *CEN* occupies the central position in looped structure all other secondary hotspots which lie nearby are suppressed. The absence of a native *CEN* pulls one of these secondary sites towards CENP-A rich 3D scaffold and places it at the centre of looped structure making it the neocentromere. This hypothesis can be tested if a chromosome that carries an established neocentromere acquires a native *CEN* sequence, a situation that does not exist in a natural context because neocentromere is formed only when native *CEN* is deleted or inactivated. Fortunately, we obtained derivative clones from *CEN7* deleted transformants where native *CEN7* sequence from the other unaltered Chr7 homolog was copied *in vivo* into neocentromere containing homolog by a non-reciprocal exchange mechanism, popularly known as gene conversion. This event resulted in a chromosome that now carried a functional native *CEN* in the presence of an already established neocentromere about 12 kb away from the native *CEN*. If our hypothesis of lateral inhibition is correct, one of these two *CENs* (regained native *CEN* and pre-established neocentromere) should be inactivated depending upon the relative occupancy of the CENP-A rich 3D scaffold. Gene conversion has been reported in *S. cerevisiae* and maize *CENs*. The *CENs* of *C. albicans* lack repeats and thus we could easily detect such gene conversion events. Lack of enrichment of CENP-A and CENP-C on neocentromere sequence in such clones clearly suggests that neocentromere has been inactivated in the presence of a functional native *CEN* through *CEN* repositioning. It is interesting to note that a human chromosome with two *CEN* sequences does not get destabilized by creating a dicentric chromosome instead one of the *CENs* gets inactivated by a not yet understood mechanism.

3.4 The Dam1 complex is essential for 1MT-1KT interaction

The KT is one of the epigenetic determinants of centromeric identity. Presence of two *CEN* sequences on a point *CEN* containing chromosomes of *S. cerevisiae* leads to formation of a dicentric chromosome. Because KT assembly is sequence-dependent both these *CENs* are capable of assembling KT on them. The resulting dicentric chromosome is prone to

breakage due to unequal forces from opposite spindle poles. On the contrary presence of two centromeric sequences on a regional *CEN* containing chromosome in human does not result in dicentric condition as kinetochore is formed only on one of these two *CENs*. Thus regulation of KT formation is more stringent over the presence of centromeric sequences on a chromosome. Understanding the process of KT assembly on *CEN* DNA therefore is of fundamental importance to gain further insights into *CEN* behavior as well as mechanism that ensures that KT is formed only once per chromosome. In this study we sought to study the process of KT assembly on *C. albicans* *CENs*. KT proteins studied so far in *C. albicans* include evolutionary conserved inner (Cse4/CENPA, Mif2/CENPC) and middle (Mis12/Mtw1) KT proteins (Roy et al, 2011; Sanyal et al, 2004; Sanyal & Carbon, 2002). In this work, we characterized the Dam1 complex, an evolutionarily conserved fungal-specific protein complex present at the outer KT *C. albicans*. Despite its indispensable role in chromosome segregation in *S. cerevisiae*, the Dam1 complex is nonessential in fission yeast and, even absent in metazoans indicating that there is reductive evolution of this complex and adaptive evolution of an alternative mechanism that governs KT-MT interaction. Such a dramatic but a gradual change in requirement of the Dam1 complex in chromosome segregation across species can be correlated with evolution of complexity of the mechanism of chromosome segregation. In *S. cerevisiae* and *C. albicans*, one MT binds per KT and this KT-MT interaction is established early during cell cycle in contrast to 2-3 MTs per KTs in *S. pombe* where KT-MT interaction is established only during mitosis. We found that the Dam1 complex is essential for viability in *C. albicans*. Hence essentiality of the Dam1 complex is correlated with maintaining proper one MT-one KT interaction which is established during interphase. Interestingly, the Dam1 complex has been shown to be localized at the KTs while they are associated with the spindle (i.e. throughout the cell cycle in *S. cerevisiae* and *C. albicans* but only during mitosis in *S. pombe*). Figure E1 summarizes a comparative analysis of the Dam1 complex from different organisms.

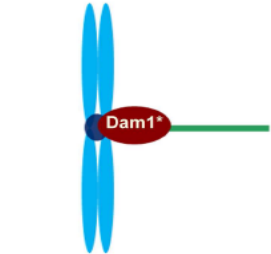
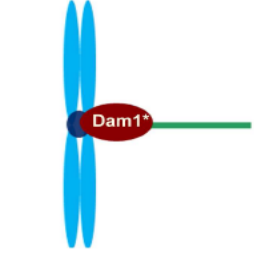
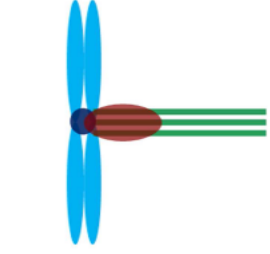
	<i>S. cerevisiae</i>	<i>C. albicans</i>	<i>S. pombe</i>
			
Centromere type/CENP-A rich region	Point/125bp	Regional/3-5 kb	Regional/4-7 kb
Onset of KT-MT interactions	Interphase	Interphase	Mitosis
MT(s)/KT	1	1	Multiple (2-4)
Kinetochores clustering	Throughout cell cycle	Throughout cell cycle	Only interphase
Dam1 complex	Essential	Essential*	Non-essential

Figure E1. Reductive evolution of the Dam1 complex.

Although KT localization of the Dam1 complex is independent of the KT-MT interaction, the cell cycle arrest at G2/M stage is under the surveillance of the Mad2-dependent spindle assembly checkpoint confirming the evolutionarily conserved role of the Dam1 complex in KT-MT interaction shown previously in *S. cerevisiae* and *S. pombe*.

KT localization of *S. cerevisiae* Dam1 has been shown to be compromised in the absence of spindle MTs (Enquist-Newman et al, 2001; Li et al, 2002). However, results from immunofluorescence and ChIP assays in the present study unequivocally prove that KT recruitment of the Dam1 complex is not dependent upon spindle MTs in *C. albicans*. This suggests that there might be functional differences in the Dam1 complex of *S. cerevisiae* and *C. albicans* in terms of their mechanistic roles in KT-MT interaction. Indeed we found that spindle defects associated with Dam1 and Ask1, two subunits of the Dam1 complex in *C. albicans* are unique (discussed below) and have not been observed in *S. cerevisiae*. Besides short and long spindles, all four components showed mutant specific defects in spindle morphology in *C. albicans*. Most of the short spindles in Dam1 mutant were found to have very weak or no staining at the midzone probably due to a faster

depolymerisation/destabilization of interpolar MTs. Abnormal growth of astral MTs in absence of Ask1 might be due to stabilization of these MTs by inhibiting their rate of depolymerization. We anticipate that these abnormally elongated astral MTs interact with the cell cortex and generate a backward force on SPBs. This may prevent cell cycle stage-specific spindle elongation and alignment resulting in short and misaligned spindles.

Since the Dam1 complex in *C. albicans* is localized throughout the cell cycle we studied the role of this complex in pre-mitotic interphase cells in conditional mutants in absence of SAC (Mad2 null mutant). Presence of long metaphase-like spindles (3-5 μ m) in these unbudded cells revealed premature spindle elongation in pre-mitotic cells. This led us to propose that the Dam1 complex restricts interphase spindle length elongation.

3.5 Localization dependency of proteins at the KT is species-specific

Subsequently towards understanding the process of kinetochore assembly in *C. albicans* we studied localization interdependencies of proteins from three layers of a KT. Recently it has been shown that Mis12/Mtw1, a middle KT protein, influences assembly of two inner KT proteins CENP-A and CENP-C in *C. albicans* (Roy et al, 2011). Conversely, Mis12 localization has also been shown to be CENP-A-dependent. In the present study, we extended this observation to examine the dependencies of various proteins on each other for their KT localization. Intriguingly, KT localization of proteins present at inner (CENP-A and CENP-C) or at middle KT (Mis12) was dramatically reduced due to depletion of each of 4 subunits tested of the outer KT protein complex – the Dam1 complex. Together these results strongly indicate that proteins of all three layers act in an interdependent and coordinated manner to stabilize the KT architecture. Absence of one of the several essential KT proteins, irrespective of the layer of the KT it belongs to, leads to delocalization of most proteins that results in complete collapse of the KT architecture. Localization of CENP-A or Mis12 was found to be unaffected in presence of a MT-depolymerizing drug nocodazole. In addition as discussed in previous section localization of Dad2, a subunit of the Dam1 complex is independent of KT-MT interactions in *C. albicans*. Thus each of these KT proteins maintains KT integrity that is independent of its role in KT-MT interaction.

This unprecedented observation of the collapse of an entire KT architecture in absence of an essential protein from any of three different layers of the KT in *C. albicans* raises an important question. How does an individual protein from any of the 3 layers of the KT determine integrity of an entire KT? It is important to note that unlike most organisms where outer KT proteins assemble only during mitosis, all the 3 layers of a KT are fully assembled throughout the cell cycle in budding yeasts as evident by constitutive localization of inner, middle and outer KT proteins in *S. cerevisiae* and *C. albicans*. Although genetic, biochemical and microscopy studies on localization dependencies of several key evolutionarily conserved KT proteins suggest a possible hierarchical assembly of the 3-layered KT structure, it has also been proposed that the KT may not be assembled in a single linear order. Bloom and colleagues also indicated *CEN* DNA bending caused by the CBF3 complex in *S. cerevisiae* or by CENP-B binding in alpha-satellite *CEN* DNA in mammalian *CENs* may provide proper geometry for KT formation, a process that may be evolutionarily conserved (Anderson et al, 2009). A complete collapse of the KT due to depletion of outer KT proteins suggests that localization of middle and inner KT proteins is dependent on outer KT proteins in *C. albicans*. Thus, we propose that KT assembly is probably not a step-wise process in *C. albicans*.

3.6 Clustered KTs stabilize integrity of an individual KT in *C. albicans*

Like *S. cerevisiae*, all KTs are clustered together throughout the cell cycle in *C. albicans*. In absence of a metaphase plate in budding yeasts, clustered KTs may provide a platform for MT attachment and synchronous separation of sister chromatids during anaphase. It has been shown that the middle layer, not the inner layer, is required for such KT clustering in *S. cerevisiae* (Anderson et al, 2009). It has also been proposed that such clustered KTs in *S. cerevisiae* are analogous to multiple MT attachment sites of a single KT in organisms with regional *CENs*. We extensively studied KT clustering status upon gradual depletion of several key KT proteins from each of the three layers of the KT. Our results clearly indicate that KT unclustering is a common intermediate step before the complete collapse of the KT upon depletion of an essential KT protein. Thus each of the three layers – inner, middle and outer – is required to keep all the KTs clustered. This is in sharp contrast to *S. cerevisiae* where only the middle/linker layer has been shown to be required for KT clustering. Based

on these results, we propose a model (Figure E2) to show a possible pathway of KT destabilization due to depletion of an essential KT protein. Signals of the unclustered KTs, resulted due to depletion of a KT protein, maintain nuclear peripheral localization indicating that memory for the peripheral localization of KTs/*CENs* is still active. Based on our results we propose that KT proteins are required to keep KTs clustered together in one unit to facilitate KT- MT interaction and to ensure integrity of an individual KT ensemble in budding yeast *C. albicans*.

3.7 An intact KT maintains centromeric chromatin and protects CENP-A from degradation

Very few proteins have been shown to affect CENP-A localization. Importantly, both in *S. cerevisiae* and humans, CENP-A has been shown to influence localization of most KT proteins. This study along with our previous observation (Roy et.al, 2011) proves that centromeric chromatin is disintegrated in the absence of a key KT protein. We predicted that depletion of KT proteins that leads to unclustering and disintegration of centromeric chromatin may expose free CENP-A molecules for cellular degradation. Indeed, western blot analysis confirmed that cellular CENP-A protein levels were drastically reduced in mutant tested together with the results from ChIP assays and immunolocalization studies. Thus we conclude that an individual KT protein is not only required to maintain overall KT integrity but also it is essential to stabilize specialized centromeric chromatin to protect CENP-A molecules. This could be an active mechanism to prevent multiple KT formation on a single chromosome especially in *C. albicans* where neocentromere formation can take place efficiently.

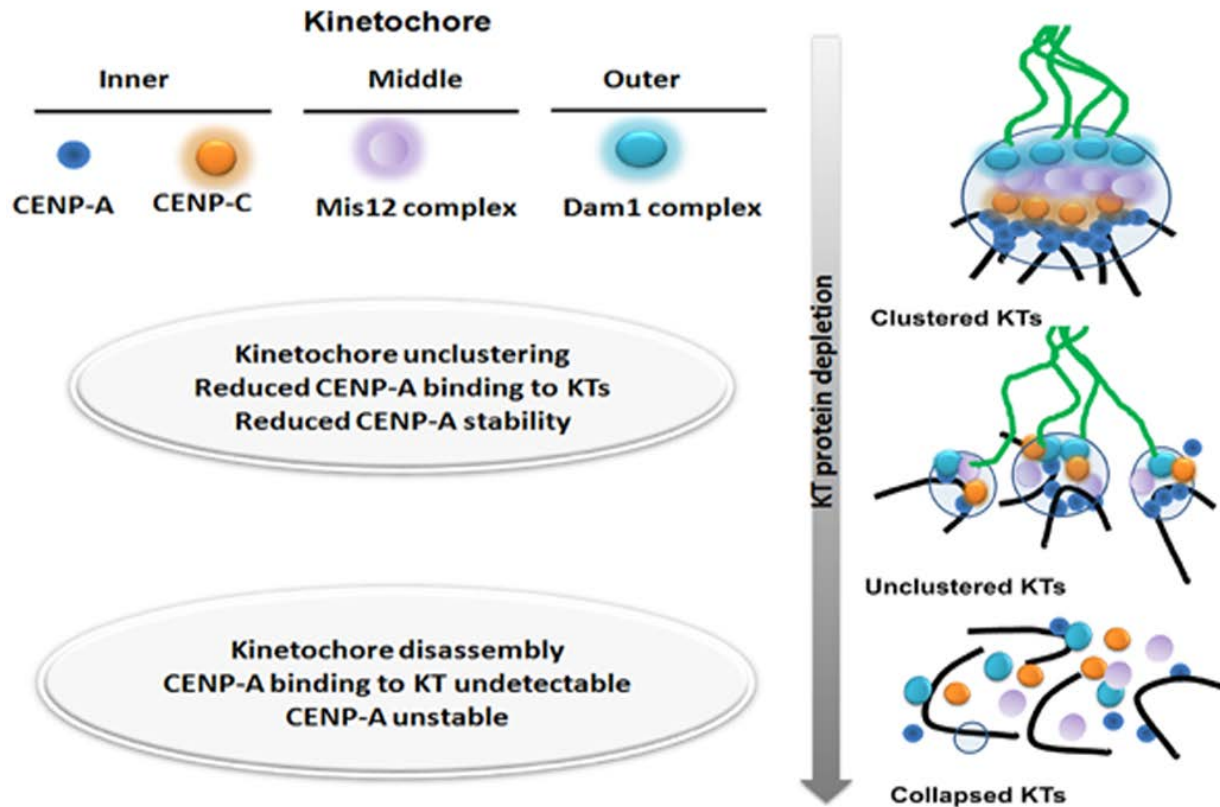


Figure E2. A coordinated interdependent protein circuitry maintains KT ensemble that protects CENP-A in a functional KT. Cellular levels of an essential KT protein maintain KT clustering and integrity of a KT formed on the foundation of CENP-A containing centromeric chromatin. A cluster of KTs resulting from KT-KT interactions maintains centromeric chromatin to protect CENP-A from degradation. A gradual depletion of any of the proteins from the inner, middle or outer KT first inhibits inter-KT interaction that leads to unclustering of KTs. This unclustering finally destabilizes integrity of KT ensemble. Disassembled KT fails to protect centromeric chromatin. CENP-A molecules that are no longer present as centromeric chromatin eventually get degraded. Hence a coordinated interdependent sequence of events governs KT assembly.

Material and Methods

4.1 Sequence analysis

4.1.1 Identification of orthologous ORF. We performed a BLAST search for the ORFs flanking the *CENs* of *C. albicans* against the *C. dubliniensis* database (http://www.sanger.ac.uk/cgi-bin/blast/submitblast/c_dubliniensis). Pair wise sequence alignment was performed using ClustalW (Thompson et al, 1994) to analyze amino acid (aa) sequence homology between the ORFs of *C. albicans* and their homologs in *C. dubliniensis*. The synteny of genes for a distance of 20 kb on either side of the ORFs flanking the *CEN* regions was determined by BLAST search. The synteny of the ORFs is maintained on both sides of the *CEN* regions in all chromosomes of *C. albicans* and *C. dubliniensis* except chr6. Putative ORFs in *C. dubliniensis* genome were identified by sequence analysis software Vector NTI (Invitrogen) where the minimum ORF length was set as 100 aa. The *C. dubliniensis* CdCse4p was identified by BLAST search CaCse4p as the query sequence against the *C. dubliniensis* genome sequence database (http://www.sanger.ac.uk/cgi-bin/blast/submitblast/c_dubliniensis).

4.1.2 Identification of CdCse4p and CdMif2p. The *C. dubliniensis* Cse4p was identified by a BLAST search (http://www.sanger.ac.uk/cgi-bin/blast/submitblast/c_dubliniensis) with *C. albicans* Cse4p (CaCse4p) as the query sequence against the *C. dubliniensis* genome sequence database. The CdCSE4 gene encodes a putative 212-aa-long protein with 100% identity in the C-terminal histone-fold domain of CaCse4p. A pair wise comparison of the CaCse4p and CdCse4p sequences revealed that they share 97% identity over a 212-aa overlap (Figure A2A). Using CaMif2p as the query sequence in the BLAST search against the *C. dubliniensis* genome database, we retrieved a single hit that was identified as the CENP-C homolog (Cd36_63360) in *C. dubliniensis*, showing 77% identity in a 516-aa overlap with CaMif2p. The CdMIF2 gene codes for a putative 520-aa-long protein with a conserved CENP-C box required for *CEN* targeting (Hull & Johnson, 1999; Sanyal et al, 2004) that is identical in *C. albicans* and *C. dubliniensis*.

4.1.3 Homology Detection and Mutation Rate Measurement. Sigma (version 1.1.3) and DIALIGN 2 (version 2.2.1) were used to align ORF-free DNA sequences. Default parameters

were used for both programs, but Sigma was given an auxiliary file of intergenic sequences from which to estimate a background model. Orthologous genes were aligned (at the aa level) with T-Coffee. We examined instances of the following seven codons where the first two positions were conserved in both species: GTn (valine), TCn (serine), CCn (proline), ACn (threonine), GCn (alanine), CGn (arginine), and GGn (glycine) (n, any nucleotide). Third-position mutations here do not change the amino acid. (Leucine was ignored because of a variant codon in these species.)

For protein-coding sequence, we ran WU-BLAST 2.0 (tblastn) querying each annotated coding region of *C. albicans* against the chromosome sequences of *C. dubliniensis*. Parameters used were “filter=seg matrix=blosum62 hspsepQmax=1000 hspsepSmax=2000”. Hits with a summed P-value of $1e-30$ or less were identified as potential orthologs. Criteria for ortholog assignment were sequence similarity and synteny (requiring at least two common syntenous immediate neighbors out of four). This led to 2653 high-confidence predictions.

A naïve count of mutation rates in the third position yields 0.27. Taking into consideration genome wide bias for each codon an upper-bound mutation rate of 0.42 was obtained. To further improve this we considered the genome-wide bias for each codon, as follows: let the third-position conservation probability be q . Then if a third position nucleotide in *C. albicans* is b , in *C. dubliniensis* it stays b with probability q , and mutates with probability $(1-q)$. If it mutates, we assume that the probability of the new nucleotide is drawn from the known codon bias. For each amino acid A , we measure the individual mutation rates $P(b_2/b_1, A)$ for third-position codon changing from b_1 in *C. albicans* to b_2 in *C. dubliniensis* (the results are mathematically identical for evolution from a common ancestor), and solve for q ; we then take the weighted average of q for all amino acids and all pairs of observed third-position nucleotides b_1 and b_2 . This works out to $q=0.58$, giving a mutation rate of 0.42. (Technically, this mutation rate is a slight overestimate, because we draw a mutated b_2 from a distribution that includes b_1 ; but it is a credible upper bound.)

4.1.4 Data Availability. The coordinates of the ORFs of *C. dubliniensis* mentioned in Table A1 and Table A2 are obtained by the BLAST analysis from the *C. dubliniensis* genome

database (www.sanger.ac.uk/cgi-bin/blast/submitblast/c_dublinsiensis) as of May 16, 2007, and the coordinates apply to the 031907 release of the contigs. Subsequent to this work, an independent annotation and new nomenclature of ORFs in the *C. dubliniensis* genome have been made available from the GeneDB database (www.genedb.org/genedb/). The CdCse4p-rich *CEN* sequences of *C. dubliniensis* can be obtained from www.jncasr.ac.in/sanyal/Cdsequences.txt.

4.2 Strain construction.

4.2.1 Construction of CAKS3b. To examine whether CdCse4p can complement CaCse4p function, we constructed a *C. albicans* strain where the first allele of *CaCSE4* was disrupted using a *URA*- blaster cassette followed by recycling of the *URA3* marker, and the second allele was placed under control of the *PCK1* promoter (Leuker et al, 1997). To disrupt the first *CaCSE4* allele, a 4.9-kb *URA*-blaster-based *CaCSE4* deletion cassette was released from pDC3 (Sanyal et al, 2004) as a *SalI*-*SacI* fragment and transformed BWP17, selecting for uridine prototrophy. The correct integrant (CAKS1b) was selected by Southern analysis. Thereafter, a *URA* minus strain, obtained by intrachromosomal recombination between *hisG* repeats resulting in the loss of *URA3* marker, was selected on medium containing 5-fluoroorotic acid (5-FOA). The correct revertant (CAKS2b) was identified by PCR analysis. To place the wild-type *CSE4* allele under regulation of the *PCK1* promoter in CAKS2b we linearized p*PCK1*-*CSE4* by *EcoRV* and used it to transform the strain CAKS2b, selecting transformants for uridine prototrophy. The desired integrant (CAKS3b) carrying the only full-length copy of *CSE4* under control of the *PCK1* promoter was identified by PCR analysis. CAKS3b can grow on succinate medium (where the *PCK1* promoter is induced) but is unable to grow on glucose medium (where *PCK1* promoter is repressed). To test whether CdCse4p can complement CaCse4p function, we cloned both Cd*CSE4* and Ca*CSE4* genes in an *ARS2/HIS1* plasmid, pAB1. A 2.14-kb fragment carrying Cd*CSE4* (CdChr3 coordinates 170,543–172,683) and a 2.13-kb fragment carrying Ca*CSE4* (CaChr3 coordinates 172,252–174,384) genes along with their respective promoters and terminators were amplified using FCd*CSE4*/RCd*CSE4* and FCa*CSE4*/RCa*CSE4* primer pairs (see Table M4 for primer sequences), respectively. These amplified Cd*CSE4* and Ca*CSE4* sequences were digested

with *SacI*/*HindIII* and *SacI*/*XbaI*, respectively, and cloned into corresponding sites of pAB1 to get pAB1Cd*CSE4* and pAB1Ca*CSE4*. Subsequently CAKS3b was transformed with pAB1, pAB1Ca*CSE4*, or pAB1Cd*CSE4* and transformants were selected for histidine prototrophy on succinate medium followed by streaking on succinate and glucose-containing media.

4.2.2 Construction of CDM1 Carrying C-Terminally TAP-Tagged CdMIF2. Cd*MIF2* downstream sequence was PCR amplified with primer pair CDM3 and CDM4 thereby introducing *KpnI* and *SacI* restriction sites (underlined). The resulting PCR amplified fragment was digested with *KpnI* and *SacI* and cloned into corresponding sites of pUC19 to generate pCDM1. The TAP cassette along with the Ca*URA3* gene was released from plasmid pPK335 (Corvey et al, 2005)) as a *BamHI-KpnI* fragment and cloned into corresponding sites of pCDM1 to generate pCDM2. Subsequently the Cd*MIF2* ORF sequence was PCR amplified using primer pair CDM1 and CDM2 and cloned into pCDM2 as an *NcoI-SalI* fragment to get pCDM3. Finally, a 2-kb amplicon was PCR amplified by the primer pair CdM1 and CdM4 using pCDM3 as the template. This PCR fragment was used to transform the CdUM4B strain (Staib & Morschhäuser, 1999). The correct Ura⁺ transformant (CDM1) was identified by PCR analysis.

4.2.3 Construction of centromeric deletion strains

The cassette for 4.5 kb *CEN7* deletion was released from pBSCR7Δ as described before (Sanyal 2004). Cassettes for the deletion of all the *CEN7* spanning fragments were constructed as follows –Ca*URA3* was cloned in pBluescript as *NotI* and *PstI* fragment to generate plasmid pBSURA3. Sequences upstream and downstream to the region to be deleted were cloned in *SacI/NotI* and *PstI/XhoI* sites of pBSURA3. Co-ordinates of the deleted region, sequences upstream and downstream to the region to be deleted that were used for the homologous recombination are given in the Table M1. Names of the primers used to amplify sequences upstream and downstream to the region to be deleted are also given. Primer sequences are given in the Table M4.

Table M1. Details of construction of cassettes for the deletion of centromeric and pericentric regions.

Co-ordinates of the deleted region	coordinate- Assembly 21 CaChr7-upstream and downstream	Primer names-upstream &downstream
URA3 integration-NA	426596-427269 &427269-427927	CEN7URA3int1/CEN7URA3int2& CEN7URA3int3/CEN7URA3int4
Cen7-6.5 kb-423452-429853	422342-423452& 429853-430960	Pericen1/Pericen2& Pericen3/Pericen4
Cen7-30 kb-411320 -440758	410123-411320 &440758-441772	30Pericen1/30Pericen2& 30Pericen3/30Pericen4
Cen1-4.2 kb-1562977 &1566061	1562038-1562977 &1566061-1566956	Cen1del1/Cen1del2& Cen1del3/Cen1del4

Cassettes were released as *SacI/XhoI* fragments and transformed into strain RM1000AH. Correct integrants were confirmed by southern analysis (details for Southern analysis strategy is given in Table M2).

Table M2. Table summarizing the details of Southern strategies used for the confirmation of deletions of centromeric regions.

Deletion	Restriction enzyme	Probe (coordinate- Assembly 21 CaChr7)	Size of the bands Wild type/Transformant
4.5 kb	<i>BglII</i>	430002-431350	10.7/7.6 kb
6.5 kb	<i>EcoRI</i>	422342-423450	20/15 kb
30 kb	<i>ClaI</i>	409600-410000	4.8/3.7 kb

4.2.4 Expression of MycMif2 in neocentromere containing clones. To examine the binding of CENP-C/Mif2 at various neocentromeres (Class I-IV) we expressed MycMif2 in RM1000AH, RM1000AH/*CEN7::URA3*, RM1000AH/*cen7-4.5 kbΔ*, RM1000AH/*cen7-6.5 kbΔ*, RM1000AH/*cen7-30 kb Δ*, RM1000AH/*cen1-4.2kbΔ* clones. A cassette containing *PCK1MycMIF2* was constructed in pSF2A vector that contained the NAT marker. Resulting plasmid was linearized using *HpaI* and introduced into neocentromere containing clones. Correct integration was confirmed using primers MycpckMif2pstF and Mif69248. Expression and localization of Myc tagged CENP-C/Mif2 was checked by indirect immunofluorescence using anti-Myc antibodies. Clones that exhibited localization pattern similar to CENP-A/Cse4 were selected for further analysis

4.2.5 Construction of conditional mutants of *DAM1*, *ASK1*, *SPC19* and *DAD2*. The first copy of each of *DAM1*, *ASK1* or *SPC19* was replaced by *HIS1* in the strain SN148. 5' sequences of long primers (Table M4) that were homologous to sequences upstream and downstream of each gene, and 3' ends that were homologous to *HIS1* gene were used to construct deletion cassettes by PCR using the plasmid *HIS1GFP* (Gerami-Nejad et al, 2001) as the template. Each deletion construct carries 90 – 110 bp of upstream and downstream homology regions flanked by *HIS1* gene. Transformants were selected on complete media lacking histidine (CM-His medium). In resulting strains J101, J103 or J105 remaining wild-type allele of *DAM1*, *ASK1* or *SPC19* was placed under control of the *MET3* promoter respectively. We cloned part of the ORF including the start codon of each gene (that carries a unique restriction site) as *BamHI* (*DAM1* and *ASK1*) or *BamHI/PstI* (*SPC19*) fragments into the corresponding site(s) of pCaDis (Care et al, 1999). Each of these resulting plasmids was linearized with *Clal* (for *DAM1* and *ASK1*) or *SwaI* (for *SPC19*) and transformed into J101, J103 or J105 to give rise to J102, J104 or J106 respectively (see Table M3 for genotypes of strains used).

To delete the first copy of *DAD2*, we cloned *HIS1* gene into pBluescript KS II (-) as *EcoRI* /*BamHI* fragment to generate pDad2-1. Subsequently, we cloned *DAD2* upstream (523 bp) and downstream (583bp) sequences into the sites flanking *HIS1* in pDad2Δ1 as *BamHI* /*SacI* and *HindIII* /*KpnI* fragments respectively. The resulting plasmid pDad2-3 was digested with *SacI* and *KpnI* and transformed into BWP17 to give rise to J107. To place the

remaining allele of *DAD2* under control of the *PCK1* promoter, *URA3* sequence was cloned as a *HindIII* fragment into the same site of pBluescript to give rise to pDad2-4. Subsequently, pDad2-5 was generated by cloning the *DAD2* upstream sequence (459 bp) as *KpnI* and *XhoI* fragment into pDad2pck1a. The *PCK1* promoter was released from pCA01 (Leuker et al, 1997) as *BamHI*-*BglIII* fragment and cloned into *BamHI* site of pDad2-5 to get pDad2-6. Finally, pDad2-7 was constructed by cloning the *DAD2* ORF into pDad2-6 as *BamHI*-*NotI* fragment. A 3.6 kb *KpnI*-*NotI* fragment was released from pDad2-7 and used to transform J107 to give rise to J108.

4.2.6 Construction of the *mad2* null mutant and conditional double mutants of the Dam1 complex proteins in the *mad2* null mutant background.

To delete both copies of *MAD2*, two deletion cassettes were constructed. *MAD2* upstream and downstream sequences were PCR amplified (see Table M4) and cloned into *BamHI* /*SmaI* and *Sall* / *XhoI* sites of pBluescript to generate pMad2-1. The construct for deletion of first copy of *MAD2* was generated by cloning *C. maltosa LEU2* (Noble & Johnson, 2005) (PCR amplified from the vector pSN42, a gift from Suzanne M. Noble) into *EcoRI* and *Sall* sites of pMad2-1. The resulting plasmid pMad2-2 was digested with *SacII* and *XhoI* and used to transform *C. albicans* SN148, J102, J104 or J106 to give rise to J109, J111, J113 or J115 respectively. To delete remaining copy of *MAD2* we constructed pMad2-3 by cloning *C. albicans ARG4* into *SmaI* and *Sall* sites of pMad2-1. The resulting plasmid pMad2-3 was digested with *BamHI* and *XhoI* and transformed into J109, J111, J113 or J115 to give rise to J110, J112, J114 and J116 respectively.

4.2.7 Construction of Protein A tagged strains.

A TAP-tag cassette was chromosomally fused to the C-terminus of *DAM1* or *DAD2* gene. A calmodulin binding domain (CBD) and a Protein A domain are the two epitopes present in the TAP tag. The CaURA3-TAP cassette was amplified from the vector pPK335 (Corvey et al, 2005) using long primer pairs (Table M4) homologous to the gene locus (Dam1 or Dad2) at the 5' end and CaURA3-TAP cassette at the 3' end. These TAP-tagging cassettes were transformed into *C. albicans* J101 or J107 where the first allele of each gene was deleted

using *CaHIS1* to give rise to J117 or J118. All strains were analyzed for correct integration by confirmatory PCRs using primers listed in the Table M4.

4.2.8 Construction of Dam1 and Ask1 conditional mutants expressing Mtw1 GFP. To visualize Mtw1 signals under Ask1- or Dam1-depleted conditions, we constructed Dam1 and Ask1 conditional mutant strains in YJB10695 (*MTW1/MTW1GFP*) background. The first copy of each of *DAM1* or *ASK1* was replaced by *HIS1* in the strain YJB10695. 5' sequences of long primers (Table M4) that were homologous to sequences upstream and downstream of each gene, and 3' ends that were homologous to *HIS1* gene were used to construct deletion cassettes by PCR using the plasmid *HIS1GFP* (Gerami-Nejad et al, 2001) as the template. Each deletion construct carries 90 – 110 bp of upstream and downstream homology regions flanked by *HIS1* gene. Transformants were selected on complete media lacking histidine (CM-His). In resulting strains J119 or J121 wild-type allele of *DAM1* or *ASK1* was placed under control of the *MET3* promoter respectively. In the plasmids pAskMET3 or pDam1MET3 (Thakur & Sanyal, 2011) that contained part of the ORF including the start codon of *ASK1* or *DAM1* respectively next to the *MET3* promoter (Care et al, 1999) and *C. albicans URA3* (*CaURA3*), we replaced *CaURA3* with *C. dubliniensis ARG4*. Each of these resulting plasmids was linearized with *ClaI* (for *DAM1* and *ASK1*), transformed into J119 or J121 and selected on media lacking arginine (CM-Arg). Resulting conditional Ask1 and Dam1 mutant strains in Mtw1-GFP background were named J120 or J122 respectively.

4.2.9 Construction of Dam1 and Ask1 conditional mutants expressing Mtw1 GFP. To visualize CENP-C/Mif2 signals in Ask1- or Dam1-depleted conditions we constructed the strains expressing Myc tagged Mif2 in Dam1 and Ask1 conditional mutant strains. A cassette containing *PCK1MycMIF2* was introduced into J102 (Dam1 conditional mutant) and J104 (Ask1 conditional mutant) strains to give rise to J123 (*dam1/MET3DAM1, MIF2/PCK1prMycMIF2*) and J124 (*ask1/MET3ASK1, MIF2/PCK1prMycMIF2*).

All strains were analyzed for correct integration by confirmatory PCRs using primers listed in the Table M4.

4.3 Media and growth conditions.

Conditional mutant strains J102, J104 and J106 carrying *DAM1*, *ASK1* and *SPC19* respectively under control of the *MET3* promoter were grown in YPDU (1% Yeast Extract, 2% Peptone, 3% Glucose and 0.01% Uridine) as permissive media and YPDU + 5 mM Cysteine + 5 mM Methionine as nonpermissive media. Conditional mutant strains J108 carrying *DAD2* under control of the *PCK1* promoter was grown in YPSU (1% Yeast Extract, 2% Peptone, 2% Succinate and 0.01% Uridine) as permissive media and YPDU as nonpermissive media. All *C. albicans* strains were grown at 30°C.

4.4 Viability assays.

Conditional mutants of *DAM1*, *ASK1*, *SPC19* or *DAD2*, were grown overnight in inducing media (YPU- succinate for the *PCK1* promoter driven expression or CM -Met-Cys for the *MET3* promoter driven expression). Overnight grown cells were pelleted down, washed with water, transferred into repressive media (YPU + 3% glucose *PCK1* promoter repression and YPDU +5 mM Met + 5mM Cys for *MET3* promoter repression) and grown at 30°C. Cells were collected at different time points, counted and then plated on plates containing inducing media. The number of viable cells that formed colonies was counted after 2 days of incubation at 30° C. Percent viability was plotted at different time points (Figure C4).

4.5 DAPI staining, calcoflour staining and FACS analysis.

Various *C. albicans* strains were grown overnight in inducing media. These overnight grown cells were pelleted down, washed with water, transferred into repressible media and grown at 30°C. Cells were finally harvested at various time points after growth in repressible media and were fixed with 70% alcohol for 10 minutes. Cells were then pelleted down, suspended in water and incubated in DAPI solution (50ng/ml) for 10 minutes. For calcoflour staining cells were incubated in calcoflour solution (Sigma Cat # 18909) for 5 min and subsequently washed with 10% potassium hydroxide solution. For

FACS analysis cells collected from various time point were fixed and subsequent steps were followed as described previously (Sanyal & Carbon, 2002). Images were captured by using LSM 510 META software using a laser confocal microscope (Carl Zeiss, Germany).

4.6 Nocodazole treatment.

For nocodazole treatment, J118 (*dad2/DAD2TAP*) cells were grown overnight in YPDU and reinoculated in YPDU with an initial OD₆₀₀ = 0.2. Nocodazole (Sigma, Cat # M1404) was added at a concentration of 20 µg/ml when OD₆₀₀ = 0.4 (1 generation) was achieved. Cells were grown for additional 4h before harvesting for immunolocalization and ChIP assays.

4.7 Subcellular immunolocalization and image analysis

Asynchronous and exponentially growing culture was fixed using 1ml 37% formaldehyde per 10 ml culture for one hour. Fixed cells were washed and resuspended in 0.1 M Phosphate buffer (pH 6.4). Next, 70-80% spheroplasting was achieved using lyticase (Sigma) and β-mercaptoethanol. Spheroplasts were pelleted and resuspended in PBS. Teflon coated slide was incubated with polylysine (1 mg/ml) for 5 min, washed with water and dried. Next 15 µl of fixed cells were placed onto each well and incubated for 5 min. Cells attached to the slides were fixed in ice cold methanol (-20°C) for 6 minutes and ice-cold acetone (-20°C) for 30 seconds. Blocking was performed with 2% skim milk in PBS for 30 min. Subsequently cells were incubated with primary antibodies for 1 hour and washed with PBS four times. Next secondary antibodies were added onto each well and incubated for 1 hour in a dark humid chamber. Secondary antibodies solution was removed and slide was washed four times with PBS. DAPI solution (50 ng/ml in 70% glycerol) was added on to each well and coverslip and slide were sealed together. Co-immunolocalization experiments were performed using the same protocol.

4.8 Microscopy, image capture and image processing.

All microscopic images were taken by LSM 510 META software using a laser confocal microscope (Carl Zeiss, Germany) with following lasers for specific fluorophores: Ar laser (bandpass 500 – 550 nm) for Alexa fluor 488, He/Ne laser (bandpass 565-615 nm) for Alexa fluor 568 and a 2-photon laser near IR (bandpass~ 780 nm) for DAPI. Palette adjustment was performed to get optimal intensity for each image. Z-stacks were collected at 0.4-0.5 μm intervals and stacked projection images were further processed in Adobe Photoshop. 3D images were generated using AxioVision 4.8 Carl Zeiss, Germany.

4.9 Chromatin Immunoprecipitation assay.

An exponentially growing culture of *C. albicans* strain was fixed with 1% formaldehyde for 15 min. The reaction was quenched for 5 min at room temperature using glycine to a final concentration of 125 mM. Cells were washed and suspended in resuspension buffer (0.2 mM Tris-HCl pH, 9.4, 10mM DTT). Resuspended cells were incubated at 30°C for 15 min on a shaker at 180 rpm. Cells were washed and resuspended in spheroplasting buffer (1.2M Sorbitol, 20mM Na-HEPES, pH 7.5). Spheroplasting (95%) was performed using lyticase (Sigma, Cat # L2524) at 30°C at low speed. Spheroplasting was stopped by adding ice-cold postspheroplasting buffer (1.2 M Sorbitol, 1 mM MgCl_2 , 20 mM Na-PIPES, pH 6.8). Spheroplasts were subsequently washed with ice-cold 1X PBS, Buffer I (0.25% TritonX-100, 10 mM EDTA, 0.5 mM EGTA, 10 mM Na-HEPES, pH 6.5), Buffer II (200 mM NaCl, 1 mM EDTA, 0.5 mM EGTA, 10 mM Na-HEPES) and finally resuspended in extraction buffer (140 mM NaCl, 1 mM EDTA, 50 mM K-HEPES, 0.1% sodium deoxycholate, 1% Triton X-100, pH 7.5) with protease inhibitor cocktail (Sigma) at a concentration of 100 μl /100ml starting culture. Next, sonication was performed to get sheared chromatin fragments of an average size of 300–700 bp by SONICS Vibra cell sonicator. Sonication conditions were as follows: pulse on 10 sec, pulse off 50 sec, total time-2 min (12 times pulse on), and amplitude 30%. The soluble fraction of sheared chromatin was obtained by centrifuging the sonicated solution at 13000 rpm for 15 min at 4°C.

Total DNA (T). About 1/10th of total soluble chromatin was processed separately as total DNA (whole cell lysate). Equal volume of elution buffer I (50 mM Tris·HCl, pH 8/10 mM EDTA/1% SDS) was added to the chromatin solution separated for Total DNA, and incubated at 65°C overnight to reverse crosslinking. TE (10 mM Tris·HCl, pH 8, 1 mM EDTA,) was added to the starting material to make final SDS concentration 0.5%. Sample was treated with RNase A (Sigma # R4875) and Proteinase K (NEB Cat # P8102). The DNA was extracted with an equal volume of phenol/chloroform/isoamyl alcohol (25:24:1) in the presence of 0.4 M LiCl and precipitated with ethanol for 15 min at room temperature. It was spun at 16,000 × *g* for 20 min at room temperature. The DNA pellet was washed with 70% ethanol and resuspended in TE.

Immunoprecipitated material (IP)

Rest of soluble chromatin solution was diluted 5.7-fold with IP dilution buffer (167 mM NaCl, 1.1 mM EDTA, 1.1% Triton X-100, 167 mM Tris-HCl, pH 8.0) and divided equally in two tubes. Rabbit anti-CaCse4p antibody was added to a final concentration of 4 µg/ml in one tube (+Ab) and no antibody (-Ab) was added to the other. The tubes were slowly rotated overnight at 4°C. A slurry of Protein A-Sepharose beads (50 µl per ml of 50% slurry in TE) (Sigma) was added and the tube was again rotated overnight at 4°C. Next beads were sequentially washed twice in 12 ml of extraction buffer, and once each in 12 ml of extraction buffer + 500 mM NaCl, LiCl wash buffer (10 mM Tris-HCl, pH 8, 250 mM LiCl, 1 mM Igepal CA-630, 0.5% sodium deoxycholate/1 mM EDTA), and TE. Beads were subjected to elution of IP complexes in elution buffer I (1/10 volume of IP dilution buffer) at 65°C for 15 min, and then centrifuged at 4000 rpm for 5 min. Supernatant was collected and beads were washed a second time with elution buffer II (10 mM Tris-HCl, pH 8/1 mM EDTA/0.67% SDS) for 5 min at 65°C and the supernatant was collected as above. Pooled eluates were incubated overnight at 65°C to reverse crosslinking. To purify DNA, the SDS concentration was diluted to 0.5% with TE, and the reaction was treated with RNase A, followed by Proteinase K. The 4 M LiCl was added to a final concentration of 0.4 M and the DNA was extracted with an equal volume of phenol/chloroform/isoamyl alcohol (25:24:1). Aqueous layer was precipitated with 100% ethanol overnight at -20°C. DNA was recovered

by centrifugation at $16,000 \times g$ for 45min at 4°C, washed with 70% ethanol, spun for 15 min, and the DNA pellet was dried for 30 min. The recovered DNA was resuspended in TE.

ChIP assays with anti-Myc antibodies in J123 (MycMIF2) strain were performed using the same protocol except for the following modification: J123 cells were crosslinked with 1 % formaldehyde for 45 min. The protein enrichment on a specific DNA sequence was determined by specific PCR primers (Table M4).

PCR amplification of ChIP-enriched DNA fragments. The IP material was subjected to PCR amplification using primers from centromeric and non centromeric regions. PCR with total DNA (1:10 dilution) and \pm antibody ChIP DNA fractions were performed using 1/10th of the template. The boundaries of the *CEN* regions on each chromosome of *C. dubliniensis* were mapped using semi-quantitative ChIP-PCR in strain Cd36. Sequence-specific PCR primers were designed at approximately 1 kb sequence intervals that spans the putative *CEN* region of each chromosome of *C. dubliniensis* (Table M4). *CdLEU2* (for *C. dubliniensis*) and *CaLEU2* (for *C. albicans*) PCR primers were used as an internal control in all PCR reactions. PCR amplification was performed and the PCR products were resolved on 1.5% agarose gels and band intensities were quantified using Quantity One 1-D Analysis Software (BioRad). Enrichment values were calculated by determining the intensities of (+Ab) minus (-Ab) signals divided by the total DNA signal and were normalized to a value of 1 for *LEU2*. The PCR primers used in this study are listed in Table M4.

I) **Cse4 ChIP assays.** ChIP assays with anti-CENP-A antibodies were performed as described above.

II) **Protein-A ChIP assays** ChIP assays with anti Protein A antibodies in J117 (Dam1-Prot A) and J118 (Dad2-Prot A) strains were performed using the same protocol except for the following modifications:

a) J117 (Dam1TAP) cells were crosslinked with 1 % formaldehyde for 90 min while J118 (Dad2TAP) cells were cross linked for 120 min. b) Sonication conditions were as follows: pulse on 10 sec, pulse off 50 sec, total time-2 min 25 sec (15 times pulse on), and amplitude 30%. c) Rabbit anti-protein A antibody (Sigma, cat #P3775) was used for ChIP at a final

concentration of 75 ug/ml d) The DNA recovered after reversing the cross-linking was precipitated using herring sperm DNA and ethanol.

III) **MycMif2 ChIP assays.** ChIP assays with anti-Myc antibodies (Calbiochem, Cat # OP10L) in J123 (MycMIF2) strain were performed using the same protocol except for the following modification: J123 cells were crosslinked with 1 % formaldehyde for 45 min.

4.10 Pulsed field gel electrophoresis

C. albicans cells were grown in appropriate media (YPDU for RM1000AH and Complete-Uridine for RM1000AH/CEN7Δ) till OD₆₀₀= 1.0. Exponentially grown cells were pelleted down and washed with ice chilled 50mM EDTA. The plugs were made according to the instruction manual protocol (BioRad Kit, Cat No #170-3593) with clean cut agarose (0.6%) and lyticase enzyme provided in the kit. Plugs were introduced into agarose gels in 0.5X TBE buffer (0.1 M Tris, 0.09M boric acid, 0.01 M EDTA, pH 8), and electrophoresis was performed with a Bio-Rad CHEF-DRIII system. The gels were run in 0.5x TBE buffer and maintained at 14°C throughout the procedure. Electrophoresis settings were as follows:

All chromosomes: 0.6% BIORAD Pulsed Field Certified Agarose, in 0.5X TBE buffer (50 mM Tris, 50 mM boric acid, 1 mM EDTA, pH8.3) 60–300 s switch ramp, 24 h, 4.5 V/cm 120°; 720–900 s ramp, 12 h, 2.0 V/cm.

Lower chromosomes: 0.9% agarose, 60–120 s ramp 24 h, 6.0 V/cm; 120–360 s ramp, 15h, 4.5 V/cm, 120°.

SfiI digests: 1.0% Bio-Rad Pulsed Field certified agarose, 7–100 s ramp, 20 h, 4.5 V/cm; 80–400 s ramp, 20 h, 3.5 V/cm, 120°.

The gel was stained with EtBr and analyzed by using Quantity one software (Bio-Rad).

4.11 Generation of polyclonal antibodies against Dad2 in rabbits.

We cloned and expressed CaDad2 as a C-terminally HIS6-tagged protein in *E. coli*. Bacterially expressed Dad2 was purified from soluble fraction using Ni-NTA based affinity chromatography. Purified Dad2 was injected into rabbits. Antiserum obtained from rabbits after 3rd booster (1:250 dilutions) was used for Western blot analysis to detect Dad2 in *C. albicans* cell lysate. The anti-serum was subjected to affinity purification using CNBr-activated sepharose beads. Purified anti-Dad2 antibodies were used for immunostaining experiments.

4.12 Western blot analysis.

For the confirmation of expression of TAP- tagged proteins, untagged BWP17 or TAP tagged J117 (*dam1/DAM1TAP*) and J118 (*dad2/DAD2TAP*) strains were grown in YPDU. To check the over expression of Dad2 wild-type BWP17 and J108 (*dad2/PCK1prDAD2*) strains were grown under inducing conditions (YPSU) for 8h.

Wild-type or conditional mutant strains were grown under inducing and repressed conditions for 8h. Protein extracts were made by disrupting the cells in RIPA buffer (300 mM NaCl, 50 mM Tris-HCl pH 8.0, 5 mM EDTA pH 8.0, 0.5% Triton-X) using glass beads (Sigma cat # G8772). The lysates were subjected to electrophoresis using 12% SDS PAGE. The proteins were transferred to nitrocellulose membrane for 1h at 20V by semi-dry method. Proper transfer was checked by Ponceau staining. Membranes were blocked with 5% skim milk for 1h followed by incubation with primary antibodies in 5% skim milk overnight at 4^oC. Membranes were washed five times with PBS + 0.05% Tween and incubated with secondary antibodies in 5% skim milk for 2h. Membranes were washed five times with 1X PBS + 0.05% Tween and exposed to X-ray films.

4.13 Antibodies

Primary antibodies used for immunolocalization studies were as follows- affinity purified rabbit anti-Dad2 antibodies-1:50 dilution, , rabbit anti-protein A antibodies (Sigma, cat #P3775) - 1:1000, affinity purified rabbit anti-CENP-A antibodies (Sanyal & Carbon, 2002) - 1:500, mouse anti Myc -1:50 (Calbiochem, Cat # OP10L), rat anti tubulin (Invitrogen, Cat#

YOL1/34) - 1:100. The fluorescent secondary antibodies were obtained from Invitrogen and used at dilution 1:500 for Alexa Fluor goat anti rabbit IgG 568 (Cat #A11011) , 1:100 for Alexa Fluor goat anti rat IgG 488 (Cat # A11006) and 1:500 for Alexa Fluor anti mouse 488(Cat # A11001).

Primary antibodies used for western blot analysis were rabbit anti-CENP-A (1:500), mouse anti-PSTAIRE (1:2000, Sigma Cat # P7962) and rabbit anti-Dad2 (1:500, unpurified sera) antibodies. Secondary antibodies used were anti-rabbit HRP conjugated (1:2000, Bangalore Genei Cat # 105499), anti-mouse HRP conjugated (1:2000, Bangalore Genei Cat # HP06).

Table M3. *C. albicans* and *C. dubliniensis* strains used in present study

Strain name	Genotype	Reference
Cd36	<i>C. dubliniensis</i> Clinical isolate	Sullivan <i>et al.</i> , 1995
CdUM4B	<i>C. dubliniensis</i> (<i>ura3D1::FRT/ ura3D2::FRT</i>)	Staib <i>et al.</i> , 2001
BWP17	$\Delta ura3::imm434/ \Delta ura3::imm434 \Delta his1::hisG/ \Delta his1::hisG$ $\Delta arg4::hisG/ \Delta arg4::hisG$	Wilson <i>et al.</i> , 1999
SN148	$ura3\Delta-iro1\Delta::imm434/ ura3\Delta-iro1\Delta::imm434, his1\Delta/his1\Delta,$ $arg4\Delta/arg4\Delta, leu2\Delta/leu2\Delta$	Noble & Johnson, 2005
CAMB1	$\Delta ura3::imm434/ \Delta ura3::imm434 \Delta his1::hisG/ \Delta his1::hisG$ $\Delta arg4::hisG/ \Delta arg4::hisG$ MIF2/ mif2::PCK1pr12XMycMIF2 (URA3)	Baum <i>et al.</i> , 2004
CAMB2	$\Delta ura3::imm434/ \Delta ura3::imm434 \Delta his1::hisG/ \Delta his1::hisG$ $\Delta arg4::hisG/ \Delta arg4::hisG$ mif2::HIS1/ mif2::PCK1pr12XMycMIF2 (URA3)	Baum <i>et al.</i> , 2004
CAKS3b	$\Delta ura3::imm434/ \Delta ura3::imm434 \Delta his1::hisG/ \Delta his1::hisG$ $\Delta arg4::hisG/ \Delta arg4::hisG$ CSE4::PCK1prCSE4/ cse4::hisG:URA:hisG	Padamanabhan <i>et al.</i> , 2008
10118	$ura3\Delta-iro1\Delta::imm434/ ura3\Delta-iro1\Delta::imm434, his1\Delta/his1\Delta,$	Joglekar <i>et al.</i> ,

	<i>arg4Δ/arg4Δ, cse4::dpl200-URA3/CSE4:GFP:CSE4</i>	2010
J101	<i>ura3Δ-iro1Δ::imm434/ ura3Δ-iro1Δ::imm434, his1Δ/his1Δ, arg4Δ/arg4Δ, leu2Δ/leu2Δ leu2Δ/leu2Δ</i> DAM1/dam1::HIS1	Present study
J102	<i>ura3Δ-iro1Δ::imm434/ ura3Δ-iro1Δ::imm434, his1Δ/his1Δ, arg4Δ/arg4Δ, leu2Δ/leu2Δ dam1</i> MET3prDAM1(URA3)/dam1::HIS1	Present study
J103	<i>ura3Δ-iro1Δ::imm434/ ura3Δ-iro1Δ::imm434, his1Δ/his1Δ, arg4Δ/arg4Δ, leu2Δ/leu2Δ ASK1/ask1::HIS1</i>	Present study
J104	<i>ura3Δ-iro1Δ::imm434/ ura3Δ-iro1Δ::imm434, his1Δ/his1Δ, arg4Δ/arg4Δ, leu2Δ/leu2Δ</i> ask1MET3prASK1(URA3)/ask1::HIS1	Present study
J105	<i>ura3Δ-iro1Δ::imm434/ ura3Δ-iro1Δ::imm434, his1Δ/his1Δ, arg4Δ/arg4Δ, leu2Δ/leu2Δ SPC19/spc19::HIS1</i>	Present study
J106	<i>ura3Δ-iro1Δ::imm434/ ura3Δ-iro1Δ::imm434, his1Δ/his1Δ, arg4Δ/arg4Δ, leu2Δ/leu2Δ</i> spc19MET3prASK1(URA3)/spc19::HIS1	Present study
J107	<i>Δura3::imm434/ Δura3::imm434 Δhis1::hisG/ Δhis1::hisG</i> <i>Δarg4::hisG/ Δarg4::hisG DAD2/dad2::HIS1</i>	Present study
J108	<i>Δura3::imm434/ Δura3::imm434 Δhis1::hisG/ Δhis1::hisG</i> <i>Δarg4::hisG/ Δarg4::hisG dad2::HIS1/PCK1prDAD2(URA3)</i>	Present study
J109	<i>ura3Δ-iro1Δ::imm434/ ura3Δ-iro1Δ::imm434, his1Δ/his1Δ, arg4Δ/arg4Δ, leu2Δ/leu2Δ MAD2/mad2::LEU2</i>	Present study
J110	<i>ura3Δ-iro1Δ::imm434/ ura3Δ-iro1Δ::imm434, his1Δ/his1Δ, arg4Δ/arg4Δ, leu2Δ/leu2Δ mad2::ARG4/mad2::LEU2</i>	Present study
J111	<i>ura3Δ-iro1Δ::imm434/ ura3Δ-iro1Δ::imm434, his1Δ/his1Δ, arg4Δ/arg4Δ, leu2Δ/leu2Δ dam1</i> MET3prDAM1(URA3)/dam1::HIS1 MAD2/mad2::LEU2	Present study
J112	<i>ura3Δ-iro1Δ::imm434/ ura3Δ-iro1Δ::imm434, his1Δ/his1Δ, arg4Δ/arg4Δ, leu2Δ/leu2Δ</i> dam1MET3prDAM1(URA3)/dam1::HIS1 mad2::ARG4/mad2::LEU2	Present study
J113	<i>ura3Δ-iro1Δ::imm434/ ura3Δ-iro1Δ::imm434, his1Δ/his1Δ, arg4Δ/arg4Δ, leu2Δ/leu2Δ</i> ask1MET3prASK1(URA3)/ask1::HIS1 mad2::LEU2	Present study

J114	<i>ura3Δ-iro1Δ::imm434/ ura3Δ-iro1Δ::imm434, his1Δ/his1Δ, arg4Δ/arg4Δ, leu2Δ/leu2Δ</i> <i>ask1MET3prASK1(URA3)/ask1::HIS1</i> <i>mad2::ARG4/mad2::LEU2</i>	Present study
J115	<i>ura3Δ-iro1Δ::imm434/ ura3Δ-iro1Δ::imm434, his1Δ/his1Δ, arg4Δ/arg4Δ, leu2Δ/leu2Δ</i> <i>spc19MET3prASK1(URA3)/spc19::HIS1</i> <i>MAD2/mad2::LEU2</i>	Present study
J116	<i>ura3Δ-iro1Δ::imm434/ ura3Δ-iro1Δ::imm434, his1Δ/his1Δ, arg4Δ/arg4Δ, leu2Δ/leu2Δ</i> <i>spc19MET3prASK1(URA3)/spc19::HIS1</i> <i>mad2::ARG4/mad2::LEU2</i>	Present study
J117	<i>ura3Δ-iro1Δ::imm434/ ura3Δ-iro1Δ::imm434, his1Δ/his1Δ, arg4Δ/arg4Δ, leu2Δ/leu2Δ</i> <i>DAM1-TAP-URA3/dam1::HIS1</i>	Present study
J118	<i>Δura3::imm434/ Δura3::imm434 Δhis1::hisG/ Δhis1::hisG</i> <i>Δarg4::hisG/ Δarg4::hisG</i> <i>DAD2-TAP-URA3/dad2::HIS1</i>	Present study
10118	<i>ura3Δ-iro1Δ::imm434/ ura3Δ-iro1Δ::imm434, his1Δ/his1Δ, arg4Δ/arg4Δ, cse4::dpl200-URA3/CSE4:GFP:CSE4</i>	Present study
J119	<i>ura3Δ-iro1Δ::imm434/ ura3Δ-iro1Δ::imm434, his1Δ/his1Δ, arg4Δ/arg4Δ, leu2Δ/leu2Δ</i> <i>ASK1/ask1::HIS1</i> <i>MTW1/MTW1GFP</i>	This study
J120	<i>ura3Δ-iro1Δ::imm434/ ura3Δ-iro1Δ::imm434, his1Δ/his1Δ, arg4Δ/arg4Δ, leu2Δ/leu2Δ</i> <i>ask1prMET3ASK1(CdARG4)/ask1::HIS1</i> <i>MTW1/MTW1GFP</i>	This study
J121	<i>ura3Δ-iro1Δ::imm434/ ura3Δ-iro1Δ::imm434, his1Δ/his1Δ, arg4Δ/arg4Δ, leu2Δ/leu2Δ</i> <i>DAM1/dam1::HIS1</i> <i>MTW1/MTW1GFP</i>	This study
J122	<i>ura3Δ-iro1Δ::imm434/ ura3Δ-iro1Δ::imm434, his1Δ/his1Δ, arg4Δ/arg4Δ, leu2Δ/leu2Δ</i> <i>dam1prMET3DAM1(CdARG4)/dam1::HIS1</i> <i>MTW1/MTW1GFP</i>	This study
J123	<i>ura3Δ-iro1Δ::imm434/ ura3Δ-iro1Δ::imm434, his1Δ/his1Δ, arg4Δ/arg4Δ, leu2Δ/leu2Δ</i> <i>dam1prMET3DAM1(URA3)/dam1::HIS1</i>	This study

	<i>MIF2/mif2PCK1pr12XMYCMIF2(NAT)</i>	
J124	<i>ura3Δ-iro1Δ::imm434/ ura3Δ-iro1Δ::imm434, his1Δ/his1Δ, arg4Δ/arg4Δ, leu2Δ/leu2Δ</i> <i>ask1prMET3ASK1(URA3)/ask1::HIS1</i> <i>MIF2/mif2PCK1pr12XMYCMIF2(NAT)</i>	This study
J125	<i>Δura3::imm434/ Δura3::imm434 Δhis1::hisG/ Δhis1::hisG</i> <i>Δarg4::hisG/ Δarg4::hisG</i> <i>MIF2/</i> <i>mif2::PCK1pr12XMYCMIF2 (NAT)</i>	This study
RM1000AH	<i>Δura3::imm434/ Δura3::imm434 Δhis1::hisG/ Δhis1::hisG</i> <i>arg4::HIS1/ARG4</i>	Sanyal K <i>et al</i> , 2004
RMI2	<i>Δura3::imm434/ Δura3::imm434 Δhis1::hisG/ Δhis1::hisG</i> <i>arg4::HIS1/ARG4 CEN7::URA3/CEN7</i>	This study
RMI4	<i>Δura3::imm434/ Δura3::imm434 Δhis1::hisG/ Δhis1::hisG</i> <i>arg4::HIS1/ARG4 CEN7::URA3/CEN7</i>	This study
RMI8	<i>Δura3::imm434/ Δura3::imm434 Δhis1::hisG/ Δhis1::hisG</i> <i>arg4::HIS1/ARG4 CEN7::URA3/CEN7</i>	This study
RMI10	<i>Δura3::imm434/ Δura3::imm434 Δhis1::hisG/ Δhis1::hisG</i> <i>arg4::HIS1/ARG4 CEN7::URA3/CEN7</i>	This study
RMI16	<i>Δura3::imm434/ Δura3::imm434 Δhis1::hisG/ Δhis1::hisG</i> <i>arg4::HIS1/ARG4 CEN7::URA3/CEN7</i>	This study
RMI19	<i>Δura3::imm434/ Δura3::imm434 Δhis1::hisG/ Δhis1::hisG</i> <i>arg4::HIS1/ARG4 CEN7::URA3/CEN7</i>	This study
RMF1	<i>Δura3::imm434/ Δura3::imm434 Δhis1::hisG/ Δhis1::hisG</i> <i>arg4::HIS1/ARG4 Δcen7::URA3/ CEN7</i>	This study
RMF5	<i>Δura3::imm434/ Δura3::imm434 Δhis1::hisG/ Δhis1::hisG</i> <i>arg4::HIS1/ARG4 Δcen7::URA3/ CEN7</i>	This study
RMF10	<i>Δura3::imm434/ Δura3::imm434 Δhis1::hisG/ Δhis1::hisG</i> <i>arg4::HIS1/ARG4 Δcen7::URA3/ CEN7</i>	This study
RMF11	<i>Δura3::imm434/ Δura3::imm434 Δhis1::hisG/ Δhis1::hisG</i> <i>arg4::HIS1/ARG4 Δcen7::URA3/ CEN7</i>	This study

RMF15	<i>Δura3::imm434/ Δura3::imm434 Δhis1::hisG/ Δhis1::hisG arg4::HIS1/ARG4 Δcen7::URA3/ CEN7</i>	This study
RML25	<i>Δura3::imm434/ Δura3::imm434 Δhis1::hisG/ Δhis1::hisG arg4::HIS1/ARG4 Δcen7::URA3/ CEN7</i>	This study
RMCR7Δ1	<i>Δura3::imm434/ Δura3::imm434 Δhis1::hisG/ Δhis1::hisG arg4::HIS1/ARG4 Δcen7::URA3/ CEN7</i>	This study
RMCR7Δ2	<i>Δura3::imm434/ Δura3::imm434 Δhis1::hisG/ Δhis1::hisG arg4::HIS1/ARG4 Δcen7::URA3/ CEN7</i>	This study
RMCR7Δ3	<i>Δura3::imm434/ Δura3::imm434 Δhis1::hisG/ Δhis1::hisG arg4::HIS1/ARG4 Δcen7::URA3/ CEN7</i>	This study
RMCR7Δ5	<i>Δura3::imm434/ Δura3::imm434 Δhis1::hisG/ Δhis1::hisG arg4::HIS1/ARG4 Δcen7::URA3/ CEN7</i>	This study
RMP2	<i>Δura3::imm434/ Δura3::imm434 Δhis1::hisG/ Δhis1::hisG arg4::HIS1/ARG4 Δcen7-6.5 kb7::URA3/ CEN7</i>	This study
RMP5	<i>Δura3::imm434/ Δura3::imm434 Δhis1::hisG/ Δhis1::hisG arg4::HIS1/ARG4 Δcen7-6.5 kb7::URA3/ CEN7</i>	This study
RMP6	<i>Δura3::imm434/ Δura3::imm434 Δhis1::hisG/ Δhis1::hisG arg4::HIS1/ARG4 Δcen7-6.5 kb7::URA3/ CEN7</i>	This study
RMP7	<i>Δura3::imm434/ Δura3::imm434 Δhis1::hisG/ Δhis1::hisG arg4::HIS1/ARG4 Δcen7-6.5 kb7::URA3/ CEN7</i>	This study
RMP8	<i>Δura3::imm434/ Δura3::imm434 Δhis1::hisG/ Δhis1::hisG arg4::HIS1/ARG4 Δcen7-6.5 kb7::URA3/ CEN7</i>	This study
RM30P2	<i>Δura3::imm434/ Δura3::imm434 Δhis1::hisG/ Δhis1::hisG arg4::HIS1/ARG4 Δcen7-30 kb7::URA3/ CEN7</i>	This study
RM30P6	<i>Δura3::imm434/ Δura3::imm434 Δhis1::hisG/ Δhis1::hisG arg4::HIS1/ARG4 Δcen7-30 kb7::URA3/ CEN7</i>	This study
RM30P8	<i>Δura3::imm434/ Δura3::imm434 Δhis1::hisG/ Δhis1::hisG arg4::HIS1/ARG4 Δcen7-30 kb7::URA3/ CEN7</i>	This study
RM30PX	<i>Δura3::imm434/ Δura3::imm434 Δhis1::hisG/ Δhis1::hisG arg4::HIS1/ARG4 Δcen7-30 kb7::URA3/ CEN7</i>	This study

RM30Pa	<i>Δura3::imm434/ Δura3::imm434 Δhis1::hisG/ Δhis1::hisG arg4::HIS1/ARG4 Δcen7-30 kb7::URA3/ CEN7</i>	This study
RM30Pc	<i>Δura3::imm434/ Δura3::imm434 Δhis1::hisG/ Δhis1::hisG arg4::HIS1/ARG4 Δcen7-30 kb7::URA3/ CEN7</i>	This study
RM30Pd	<i>Δura3::imm434/ Δura3::imm434 Δhis1::hisG/ Δhis1::hisG arg4::HIS1/ARG4 Δcen7-30 kb7::URA3/ CEN7</i>	This study
RM30Pf	<i>Δura3::imm434/ Δura3::imm434 Δhis1::hisG/ Δhis1::hisG arg4::HIS1/ARG4 Δcen7-30 kb7::URA3/ CEN7</i>	This study
RM30Pj	<i>Δura3::imm434/ Δura3::imm434 Δhis1::hisG/ Δhis1::hisG arg4::HIS1/ARG4 Δcen7-30 kb7::URA3/ CEN7</i>	This study
RM30Pi	<i>Δura3::imm434/ Δura3::imm434 Δhis1::hisG/ Δhis1::hisG arg4::HIS1/ARG4 Δcen7-30 kb7::URA3/ CEN7</i>	This study
RMJTF1 (J125)	<i>Δura3::imm434/ Δura3::imm434 Δhis1::hisG/ Δhis1::hisG arg4::HIS1/ARG4 MIF2/ mif2::PCK1_{pr}12XMycMIF2 (NAT1) Δcen7::URA3/ CEN7</i>	This study
RMJTF1	<i>Δura3::imm434/ Δura3::imm434 Δhis1::hisG/ Δhis1::hisG arg4::HIS1/ARG4 MIF2/ mif2::PCK1_{pr}12XMycMIF2 (NAT1) Δcen7::URA3/ CEN7</i>	This study
RMJTF10	<i>Δura3::imm434/ Δura3::imm434 Δhis1::hisG/ Δhis1::hisG arg4::HIS1/ARG4 MIF2/ mif2::PCK1_{pr}12XMycMIF2 (NAT1) Δcen7::URA3/ CEN7</i>	This study
RMJTF11	<i>Δura3::imm434/ Δura3::imm434 Δhis1::hisG/ Δhis1::hisG arg4::HIS1/ARG4 MIF2/ mif2::PCK1_{pr}12XMycMIF2 (NAT1) Δcen7::URA3/ CEN7</i>	This study
RMJTP2	<i>Δura3::imm434/ Δura3::imm434 Δhis1::hisG/ Δhis1::hisG arg4::HIS1/ARG4 MIF2/ mif2::PCK1_{pr}12XMycMIF2 (NAT1) Δcen7-6.5 kb7::URA3/ CEN7</i>	This study
RMJT30PX	<i>Δura3::imm434/ Δura3::imm434 Δhis1::hisG/ Δhis1::hisG arg4::HIS1/ARG4 MIF2/ mif2::PCK1_{pr}12XMycMIF2 (NAT1) Δcen7-6.5 kb7::URA3/ CEN7</i>	This study

Table M4. Primers used in present study.

Primer name	Sequence	Description
CDM1	ACG CGT CGA CCC CCC ACT GAT TAC GAT TAT GAA TCT GAT CC	TAP tagging of CdMif2
CDM2	CAT GCC ATG GCC CAA TTC GTA TCG ATT TCT TCT GGT TTC	TAP tagging of CdMif2
CDM3	CGG GGT ACC GAT TGC AAG AAG TAC TAC ATA AGA GAG	TAP tagging of CdMif2
CDM4	GCC CGA GCT CGC AGG TAA AAT TGT TCT TGA GGA GCC G	TAP tagging of CdMif2
FCaCse4	CCCGAGCTCCAATTAACAAATATTAATTACAAATG	Cse4 Complementation
RCaCse4	TGCTCTAGACCAAAATCCCTCTTTCTGTATTTG	Cse4 Complementation
FCdCse4	CCCGAGCTCCAAGTGTATTTTCATCTTTGGTAG	Cse4 Complementation
RCdCse4	CCCAAGCTTCTATTTTGCCACCAAAACCCATCTT	Cse4 Complementation
ChIP primers for <i>CdCEN1</i>		Co-ordinates
CdCEN1-1(F)	AAGCCCTTTGGATGTTGACTACGC	1593208-1593231
CdCEN1-2(R)	CCATCGACAGGGCCCATGTG	1593417-1593398
CdCEN1-3(F)	TATGATTATACCCCAATCCA	1595086-1595105
CdCEN1-4(R)	AGGATCAGTTACCAATGTTG	1595287-1595268
CdCEN1-3_(F)	CAACAATCAACAATTTCTGCTCCTCATG	1596131-1596158
CdCEN1-4_(R)	AAGTGGGTATCACCTTATTCGCAAATGA	1596368-1596341
CdCEN1-5(F)	CCTTTTAAACGTGACACGCTCAA	1597063-1597087
CdCEN1-6(R)	GGAAAAGTTGCGTGAGGAAATGGA	1597302-1597279
CdCEN1-5_(F)	CGGGTGCATCTAAGAAGGGTTTTA	1598062-1598085
CdCEN1-6_(R)	CAATATAACCTTGCACCCGTCAAATACG	1598347-1598320
CdCEN1-7(F)	GTTGCAGTGCATTGTACGAGTAAGCTC	1599081-1599108
CdCEN1-8_(R)	TGCAACTGATCCGAGACAACCTCAAAC	1599271-1599245
CdCEN1-7_(F)	GATCGCAAGCGAAGCAGCAAATGAC	1600481-1600505
CdCEN1-8_(R)	CAATGTCTGTTGACCACCATTCCC	1600721-1600697

CdCEN1-9(F)	AGAGCGAGCACCTGGTATTCCAAG	1601290 - 1601314
CdCEN1-10(R)	CACCCAAAGCCCAGCTTAAATTCC	1601509-1601486
CdCEN1-9_(F)	TTTCAATTTAGCTGACTCCTTACCCTGG	1602167-1602194
CdCEN1-10_(R)	TTTTCGGTGATTTTGCCAAGAAGTTC	1602410 - 1602385
CdCEN1-11(F)	CAGCATTTCATCCGGGTAAAGTGTTG	1603320-1603344
CdCEN1-12(R)	CAACGGATCCAAGGTCACCACATAG	1603543-1603519
CdLeu2-1(F)	AACTATCACAGTCTTGCCTGGTGA	119386-119409
CdLeu2-2(R)	ACAGACCAGTGCCCCATTT	119618-119637
ChIP primers for <i>CdCEN2</i>		
CdCEN2-1(F)	CGCGGTCCAAGAAGATAATC	1940515-1940534
CdCEN2-2(R)	CATCATGGGATGTAATTGCT	1940649-1940668
CdCEN2-3(F)	AGTGTAAAGTCTTCGGGATAC	1942509-1942528
CdCEN2-4(R)	GTGAGCGAATAGAATAATTG	1942685-1942704
CdCEN2-5(F)	AGCTACATCTATTTTCAATGCACTC	1944606-1944630
CdCEN2-6(R)	AATTGCTCTGAAACAGCCAG	1944877-1944896
CdCEN2-7(F)	TATACCCCGAATTAACAAGTGCGC	1943700-1943724
CdCEN2-8(R)	CAGTGCAGGTGCTTTCGTTTACCAG	1943847-1943871
CdCEN2-9(F)	CATCAGTTCAATTGATGGGGTTGTTCTG	1945542-1945569
CdCEN2-10(R)	AAACTGGCATAGCTTTTGCATTATGCC	1945736-1945764
CdCEN2-11(F)	ATTTTCGAGAGGACTTGGTTTCGTGC	1946646-1946669
CdCEN2-12(R)	CCGTACCCAAATAAACTCCCAGC	1946844-1946867
CdCEN2-15(F)	TACAAAGCGGGTGATAAGGA	1947305-1947054
CdCEN2-16(R)	GGCGAAAAGGAAATAGC	1947234-1947217
ChIP primers for <i>CdCEN3</i>		
CdCEN3-1(F)	ACACTGTCTTGTCTTGTGTCTGAAGTCG	865133-865160
CdCEN3-2(R)	TTCTGTGTGTGGGCCCTCAGTAC	865293-865317
CdCEN3-3(F)	TCATCCATCATATCACAATCCTACTG	867274-867300

CdCEN3-4(R)	GTTATTTTGAAAGTTGGGGAGAGGG	867456-867480
CdCEN3-5(F)	CCTACGACATGAACACATCAAACACTCTC	869090-869117
CdCEN3-6(R)	TGCTTTTGTGAAAACCTGCGAAAC	869243-869267
CdCEN3-7(F)	AGGCTAGTCGGTGGTTAACGGTTGTGTG	870638-870665
CdCEN3-8(R)	GACTCGGAATAAACACCATCGCCGATGC	870856-870883
CdCEN3-9(F)	GGTCCAATTAGAATCGGGTCGTTCCATG	872528-872555
CdCEN3-10(R)	CGTCATCCCTTCTATCTCTAACGTG	872683-872707
ChIP primers for <i>CdCEN4</i>		
CdCEN4-1(F)	ATCATATCATGCAGCCAACTCCG	1028245-1028268
CdCEN4-2(R)	CGGACGTAGTGAAACGATTGTTGG	1028410-1028433
CdCEN4-3(F)	ACAATTTCCAGTAAACCATTATAAAAAG	1029835-1029861
CdCEN4-4(R)	CATTATAATCTGATTTGTAGGCTC	1029965-1029989
CdCEN4-3_(F)	TGCTAAACGACCCCTCAAAA	1030554-1030574
CdCEN4-4_(R)	GTACGACGATCATCAGCAACCAA	1030776-1030798
CdCEN4-5(F)	AATTAATTCGATAGTTGGGGGAGACCG	1032446-1032473
CdCEN4-6(R)	ATTGAGCTGCTCACTTCACTGCCAC	1032619-1032643
CdCEN4-5_(F)	GCAGCGTTCTTGTGACCGTGAG	1033199-1033220
CdCEN4-6_(R)	TTGAATTGGACAGGGGCTTAGG	1033477-1033498
CdCEN4-7(F)	TGTGGTGGAGGGTCATCCATTTGTTGGTTG	1034406-1034435
CdCEN4-8(R)	GGCGACCCTCATGCACCCTACCAAATAAA	1034609-1034637
CdCEN4-7_(F)	AAGTACGGATGGTTGTTA	1035010 - 1035028
CdCEN4-8_(R)	TAGTCATTCTGCCATCTCTTAT	1035231-1035252
CdCEN4-9(F)	CCATGAACAAAAGGTTAGGTGGTGCTCC	1036158-1036185
CdCEN4-10(R)	GGGGAGTTGAATGGTGTGGTGTAC	1036367-1036391
ChIP primers for <i>CdCEN5</i>		
CdCEN5-7(F)	TCCAGCGTCAGACATTTTCCAGT	494058-494081
CdCEN5-8(R)	TGCCCCGCGGTTGACAGT	494213-494230
CdCEN5-1(F)	TGGCTCTCCCTTACAAAATTTGCC	495324-495349

CdCEN5-2(R)	GGGAGATGAGGGGTGATTGAGGTAATAG	495504-495531
CdCEN5-3(F)	GCTCCAGTACCAACGAAAACGACTTC	496907-496932
CdCEN5-4(R)	GCATTTGAAAAGTCCAATGTAGTC	497035-497059
CdCEN5-5(F)	GCTGGGATAGTTTAGAGGCAGACTGTG	498944-498971
CdCEN5-6(R)	CCTCAATCACCCCTCATCTCCCTAC	499130-499155
CdCEN5-9(F)	AAGGGCAAGGAACAAGTCACAAGT	500673-500696
CdCEN5-10(R)	TATCAGCGCCGGTTTTAGCAC	500941-500961
ChIP primers for CdCEN6		
CdCEN6-15(F)	GTGCCAACTTCTCCTGAT	1002806-1002824
CdCEN6-16(R)	AGCGATTATTAAGTCTATGTGG	1002985-1002964
CdCEN6-13(F)	GAAGCAGCGACCCAACAGATAA	1003044-1003065
CdCEN6-14(R)	TTGAGCGAAATTGGGTAGAGTC	1003262-1003283
CdCEN6-5(F)	TGTCCATTCCCCAAACTTCATACGGACCAC	1004039-1004068
CdCEN6-6(R)	GAATGCTGGAAGGACTTGAGAAATG	1004175-1004199
CdCEN6-5_(F)	GAAACCAATAACAAGGAAAGAGTA	1005046-1005069
CdCEN6-6_(R)	CAATGGGAAAAAGAAATCAGTAG	1005313-1005335
CdCEN6-7(F)	GACGAGAGCATGTACTCAACTACGTGTC	1006472-1006499
CdCEN6-8(R)	GAATCTTGATTGAAATGCGAGGAAC	1006668-1006692
CdCEN6-9(F)	CATCCAATAACATTGATTTACTACTTTTAG	1008985-1009014
CdCEN6-10(R)	TTTTTTTTTCTCAAAGATTTAGCAG	1009115-1009139
CdCEN6-9_(F)	TGTACGATCAACCCAGAGTGC	1009504-1009524
CdCEN6-10_(R)	ACATGCCATTACCAACAACAGTC	1009749-1009771
CdCEN6-3(F)	TAGCTGTATTAATAAATTCTGGCCGCATA	1015917-1015945
CdCEN6-4(R)	TCTGACAAAAAACCTCGTATGACCC	1016066-1016042
ChIP primers for CdCEN7		
CdCEN7-1(F)	CTAGAGCTATGTTGTGACAGTCCACC	427615-427640
CdCEN7-2(R)	CTTCTGGAATTGAGCCAATCCCTAG	427777-427801
CdCEN7-3(F)	CTAGCTATTCAAGCATCCGTAGGCAGTC	429103-429130

CdCEN7-4(R)	CCCATACCCGGGTGGTGTAGTATAA	429228-429252
CdCEN7-5(F)	GTAGGCGCTACATATGAACTTCGTGC	436328-436354
CdCEN7-6(R)	AGATAATGTCTGAATGTCATTCCGGG	436479-436504
CdCEN7-9_(F)	TCCAATGGGTGCTAAGATGAA	434047-434068
CdCEN7-10_(R)	TCCCGCCTGATTTTGTAA	434292-434310
CdCEN7-7(F)	TTATTTGATAGCCTAATTTACCTGATG	438005-438031
CdCEN7-8(R)	ATTAAGTACTTTGAACCAGCAATG	438205-438230
CdCEN7-9(F)	AACGGTCACCTGATGAATAGAGTGGC	432732-432758
CdCEN7-10(R)	GACTGAAGCGTCCATACTTGGGATC	432956-432981
CdCEN7-11(F)	CCCAGAAGTATCCACTAGGGAAGTGG	435240-435268
CdCEN7-12(R)	TTGTTCTGGTCAATGGTACAGCAAC	435365-435390
CdCEN7-13(F)	CACGCAACTAGAATGGCATGAATATATG	439500-439527
CdCEN7-14(R)	AGATCCGGTGTCTGTCTTATTGCTC	439630-439654
CdCEN7-15(F)	CCTGCGTTGTAATCATTGTTGTC	440443-440466
CdCEN7-16(R)	TTACTCCGCCTTTGATCCCTATTT	440640-440617
ChIP primers for <i>CdCENR</i>		
CdCENR-1(R)	ATTAAGGAGCTTCGTGAGGCTGTGC	1723671-1723647
CdCENR-2(F)	CATTTCCCTCAAAGGCACCGGGATG	1723429-1723453
CdCENR-3(R)	ACGTTGCTTACTGGTGGCTATGCGG	1721710-1721686
CdCENR-4(F)	AAGCTTTTATTGCGGTGAACTGGGG	1721461-1721485
CdCENR-5(R)	ACATATAATAGCCTACCACACGCCTTGC	1719373-1719346
CdCENR-6(F)	TGACATTGTGAAAAGTTAATCGCGG	1719202-1719226
CdCENR-7(R)	TGAAATTGGAGACTAAGTGTTCATTTCG	1717531-1717504
CdCENR-8(F)	ACAGTTTCCACACAAGTCAAGACA	1717330-1717356
CdCENR-9(R)	TTTGCCGGGATAAGCTTTTATTGCG	1715642-1715618
CdCENR-10(F)	TTTCAGGACACCAGAAGATGGCCAC	1715409-1715433
CdCENR-9_(F)	CCCCCGCGTGAAAAACA	1713200-1713217
CdCENR-10_(R)	CTACAAACGCCACACCCGAAACT	1713426-1713404

CdCENR-11(R)	ACCTCAACATCGACACAGTCGCACC	1712709-1712185
CdCENR-12(F)	AGCAGAAACCTCGATGTTTGAGCCG	1712487-1712511
DamdelHis1	GAG ATC TCT TAT TAT TTG ATT TCT TTT TCT GCA AAT TAA CAA CCT TTC AGG AGA ATG TCC TCA TCT AAA CCA GTT ACC CCT AGG AAT TCC GGG GAT CCT GGA GGA TGA GGA G	Forward long primer for the replacement of first allele of <i>DAM1</i> with <i>HIS1</i>
DamdelHis2	CAA AAC AAG TCT GTT GAA CAA GTG AAA TAC GAA TTA AAA CTA AAA CTC ATA TAC GGG GGA TAA GTA TAT ATA TAT ATA TAT AAC GAA TTC CGG AAT ATT TAT GAG AAA CTA TCA C	Reverse long primer for the replacement of first allele of <i>DAM1</i> with <i>HIS1</i>
DamdelHis3	CAA ACA AAA TAG TAA AAA TTA TTG AGA TCT CTT ATT ATT TG	Forward short primer to amplify cassette cloned in pBluescript using Damdel His1 and DamdelHis2 for the replacement of first allele of <i>DAM1</i> with <i>HIS1</i>
DamdelHis4	CTT TTA ATG ATT GCC TCC CAA CAA AAC AAG TCT GTT GAA CAA G	Reverse short primer to amplify cassette cloned in pBluescript using Damdel His1 and DamdelHis2 for the replacement of first allele of <i>DAM1</i> with <i>HIS1</i>
Dam1probe5'	CAA AGA CCT GTT GAT AGA TTG TTG ACT AC	Forward primer for the confirmation of the replacement of deletion of <i>DAM1</i> with <i>HIS1</i>
Ask1His1	CAC GCA AAA AAG AAA AAC CAC AAC AAA TCA GAA AAC AAC AAC AAC ATC ATC ATA TCA ACA TTA ACC AAC TTT CTG CTG CAT CAA ATG AAT TCC GGG GAT CCT GGA GGA TGA GGA G	Forward long primer for the replacement of first allele of <i>ASK1</i> with <i>HIS1</i>
Ask1His2	CTA CGA TGA TTT CAT TAC TAA TAT TAT ATT TTT ACA TTA CTA CCA ACT GTT GAT GTC TAT TGA CTA CGT AGT TAT GTT TTC CTC CGA ATT CCG GAA TAT TTA TGA GAA ACT ATC AC	Reverse long primer for the replacement of first allele of <i>ASK1</i> with <i>HIS1</i>
Ask1His3	GCA CTA GTC GCA CAC ACA CCT ACA CGC AAA AAA GAA AAA C	Forward short primer to amplify cassette cloned in pBluescript using Ask1His1 and Ask1His2 for the replacement of first allele of <i>ASK1</i> with <i>HIS1</i>
Ask1His4	GGG AAG CTT CTT ACT TGA AAA ACT ACG ATG	Reverse short primer to amplify cassette cloned in pBluescript using Ask1His1 and Ask1His2 for the replacement of first allele of <i>ASK1</i> with <i>HIS1</i>
Ask1HisProbe	CTC TGT GTA CCA TTT ATT AAA ACA ATC ATC	Forward primer for the confirmation of the replacement of deletion of <i>ASK1</i> with <i>HIS1</i>
Spc19His1	CTT ATT ATT ATT CCA TCT ACT TAG ACC TTT TTC AAT TAA TAC ATA TAT TGT CAA CCC TTA AGA TAC ACA TAA ATA TAC ACT ACT AAC GAA TTC CGG GGA TCC TGG AGG ATG AGG AG	Forward long primer for the replacement of first allele of <i>SPC19</i> with <i>HIS1</i>
Spc19His2	CCA AAG CTC AAC TTC AAG TAC ATG CTA ATA ACT TCC CCC AAC AAT CCT ATG TAC TTG TAT CAT ACA CTT TAT TAA CTT CTT	Reverse long primer for the replacement of

	GGT GGA ATT CCG GAA TAT TTA TGA GAA ACT ATC AC	first allele of <i>SPC19</i> with <i>HIS1</i>
Spc19His3	GCA CTA GTC ACA ATA TCA TCT TAT TAT TAT TCC ATC	Forward short primer to amplify cassette cloned in pBluescript using Spc19His1 and Spc19His2 for the replacement of first allele of <i>SPC19</i> with <i>HIS1</i>
Spc19His4	CCC AAG CTT GTA TGT TCA TAT TCC AAA GCT CAA CTT C	Reverse short primer to amplify cassette cloned in pBluescript using Spc19His1 and Spc19His2 for the replacement of first allele of <i>SPC19</i> with <i>HIS1</i>
Spc19His1probe	GCT ATT ATG TTG GTT GGA AAG ATG TAG	Forward primer for the confirmation of the replacement of deletion of <i>SPC19</i> with <i>HIS1</i>
Damet1	CGG GAT CCG ATG TCC TCA TCT AAA CCA GTT AC	Forward primer with <i>BamHI</i> site at 5' for placing <i>DAM1</i> under control of the <i>MET3</i> promoter
Damet2	CGG GAT CCG ATC GTG GCT GTT GTT TAA TCT G	Reverse primer with <i>BamHI</i> site at 5' for placing <i>DAM1</i> under control of the <i>MET3</i> promoter
AskMet1	CGG GAT CCG ATG AAG AGA TAT TCA ATT GC	Forward primer with <i>BamHI</i> site at 5' for placing <i>ASK1</i> under control of the <i>MET3</i> promoter
AskMet2	CGGGATCCCTAGATTGTAGTCGTTGATGTTG	Reverse primer with <i>BamHI</i> site at 5' for placing <i>ASK1</i> under control of the <i>MET3</i> promoter
Spc19Met1	CGG GAT CCG ATG GCA CAG CAA GAC CTA CCA CAG AAC C	Forward primer with <i>NotI</i> site at 5' for placing <i>SPC19</i> under control of the <i>MET3</i> promoter
Spc19Met2/Spc1 9pck2	GCC TGC AGC CAT TAC TAT TAA AAT TTT TCC CTC CTT CTT C	Reverse primer with <i>PstI</i> site at 5' for placing <i>SPC19</i> under control of the <i>MET3</i> promoter
URA3-1	G GTC TTA GTG TTG ACT GTC	Reverse primer for the confirmation of integration of <i>MET3</i> containing Cassettes at <i>DAM1</i> , <i>ASK1</i> and <i>SPC19</i> loci
Dad2-16	CGA GCT CGT TGA CAT TAG TCA TCA	Forward primer with <i>SacI</i> site at 5' for the amplification of <i>DAD2</i> upstream fragment to construct a cassette for replacing <i>DAD2</i> with <i>HIS1</i>
Dad2-17	CGC GGA TCC TTG AAA GGT TTT GTG	Reverse primer with <i>BamHI</i> site at 5' for the amplification of <i>DAD2</i> upstream fragment to construct a cassette for replacing <i>DAD2</i> with <i>HIS1</i>

Dad2-18	CCC AAG CTT AGT ATA TTG CTA CAT	Forward primer with <i>Hind</i> III site at 5' for the amplification of <i>DAD2</i> downstream fragment to construct a cassette for replacing <i>DAD2</i> with <i>HIS1</i>
Dad2-19	GGG GTA CCC CAA CAT TTA CAA AG	Reverse primer with <i>Kpn</i> I site at 5' for the amplification of <i>DAD2</i> downstream fragment to construct a cassette for replacing <i>DAD2</i> with <i>HIS1</i>
Dad2-20	GGG GTA CCC TAG TAT TCT CCA AGT TAG	Forward primer with <i>Kpn</i> I site at 5' for the amplification of <i>DAD2</i> upstream fragment to construct a cassette for placing <i>DAD2</i> under control of <i>PCK1</i> promoter
Dad2-21	CCG CTC GAG TTG AAA GGT TTT TGT	Reverse primer with <i>Xho</i> I site at 5' for the amplification of <i>DAD2</i> upstream fragment construct a cassette for placing <i>DAD2</i> under control of the <i>PCK1</i> promoter
Dad2-8	CGC GGATCC GCA TGC TGA AAA CAA ATA CTG C	Forward primer with <i>Bam</i> HI site at 5' for the amplification of <i>DAD2</i> ORF to construct a cassette for placing <i>DAD2</i> under control of <i>PCK1</i> promoter
Dad2-22	ATA AGA ATG CGG CCG CCC GTG GAT TCT TC	Reverse primer with <i>Not</i> I site at 5' for the amplification of <i>DAD2</i> ORF fragment to construct a cassette for placing <i>DAD2</i> under control of <i>PCK1</i> promoter
Dad2-TAP1	CAA GAC GAA GAA GAA GCA GAT GAA GAA GAA GGT GTT AGA GAT AGT GAA GAA GTT GAA GAA TCC ACG GAA GGA GGA TCC ATG GAA AAG AGA AGA TGG AAA AAG	Forward primer for the amplification of Dad2TAP tag cassette from pPK335
Dad2TAP-2	CAA CTT GGA AAT GCT AAA TTC AAG TCC TGG GTT GAA GCA GTG AAA GAA CAA GCT AGA ATT TAG AGT TAT TAT ATG GCG CGC GTA ATA CGA CTC ACT ATA GGG CG	Reverse primer for the amplification of Dad2TAP tag cassette from pPK335
DamTAP-1	CTA ATT ATA GTC GAA TCA AAA AAC CTA TCC ATA ACC GAT CAG TAA ATA ATT TGC AAA ATA GAC CAC CCT TTA GAG GAG GAT CCA TGG AAA AGA GAA GAT GGA AAA AG	Forward primer for the amplification of Dad2TAP tag cassette from pPK335
DamTAP-2	CGA AGA CAA TTA ATT ATG AAC TCA ATG GAG AAT ATG GAT TAT CTT TTA ATG ATT GCC TCC CAA CAA AAC AAG TCT GCG CGC GTA ATA CGA CTC ACT ATA GGG CG	Reverse primer for the amplification of Dad2TAP tag cassette from pPK335
Mad2UPS-1	GCG GAT CCG TGT AGT ATC ATT TTT ACA TTC TAA TTC C	Forward primer with <i>Bam</i> HI site at 5' for the amplification of <i>MAD2</i> upstream fragment
Mad2UPS-2	GAC CCG GGG ATA AGG GGG GAA GGG ATA GAT AGG GTT G	Reverse primer with <i>Sma</i> I site at 5' for the amplification of <i>MAD2</i> upstream fragment

Mad2DS-1	GCG TCG ACC TAT GGT TAT TAT TTT TCT AAT TC	Forward primer with <i>SalI</i> site at 5' for the amplification of <i>MAD2</i> downstream fragment
Mad2DS-2	GCC TCG AGG AAT CTA GTG GAT TAT CAT ATA TTG	Reverse primer with <i>XhoI</i> site at 5' for the amplification of <i>MAD2</i> downstream fragment
Leu2-ECORI	CGG AAT TCG GAT CCA ATC ATC ACT GGT GGG GGT CAA G	Forward primer with <i>ECORI</i> site at 5' for the amplification of <i>C. maltosa LEU2</i>
Leu2-Sal1	GCG TCG ACC CTA CCC ATG TCT AGA AAG AGC CAA TC	Reverse primer with <i>ECORI</i> site at 5' for the amplification of <i>C. maltosa LEU2</i>
ARG4SalI	GCG TCG ACC GCA AAT CTA AGA GTA GAG GCT ACA GG	Reverse primer with <i>SalI</i> site at 5' for the amplification of <i>C. albicans ARG4</i>
Dam1 Probe2	GCA TCG ATC TTG TTA AAG TAT AAA CAA ACA AAA TAG	Forward primers from Dam1 upstream sequence for the confirmation of MET3-Dam1-URA cassette integration
CEN7URA3int1	TAC GGA GCT CCA ACG TAA ATC TTT TAA GC	Integration of <i>URA3</i> at <i>CEN7</i>
CEN7URA3int2	TAC AGC GGC CGC TAG TCA GCT TCT TCT TTG	Integration of <i>URA3</i> at <i>CEN7</i>
CEN7URA3int3	TAC GCT GCA GAC TCT ATC ATT TCC TAC	Integration of <i>URA3</i> at <i>CEN7</i>
CEN7URA3int4	GAA GTG ATG GTT GAT GAA GG	Integration of <i>URA3</i> at <i>CEN7</i>
PeriCEN7del1	CGG AGC TCC CCA AAC CCA AAC GAG ATG TAT TCT TG	Deletion of CEN7-6.5 kb region
PeriCEN7del2	GAG CGG CCG CGC TTC CAG CTT ATT TAT TTT CAA GAA GC	Deletion of CEN7-6.5 kb region
PeriCEN7del3	CGC TGC AGC TAT ATA GGT TAT TTA ATT TGC ATA AGT AC	Deletion of CEN7-6.5 kb region
PeriCEN7del3	CGC TCG AGG TTG CCA GTT AGA TTA TCC TGG TTT TGG	Deletion of CEN7-6.5 kb region
30PeriCEN7del1	CGG AGC TCC AAA GAA ATA CCG TTG AAT CTT TGA CTA CTG C	Deletion of CEN7-30 kb region
30PeriCEN7del2	GAG CGG CCG CCA TCA CGA TAA ACA TTT GGA TGA TAT AAT G	Deletion of CEN7-30 kb region
30PeriCEN7del3	CGC TGC AGC TTT CTC CAA GAA CAT CAA ATT GGG TAT T	Deletion of CEN7-30 kb region
30PeriCEN7del4	CGC TCG AGG TGT GTT TTT GGT CCT CTA CTA CAA AAC TG	Deletion of CEN7-30 kb region
30PeriCEN probe-1	CAG AAT GAC ACA CTT AGC AGC ATC	Probe primers for the deletion of CEN7-30 kb region
30PeriCEN probe-2	CTC ATC AAA GTT AAA TAT TTG TTC TTA TTT GG	Probe primers for the deletion of CEN7-30 kb region

CEN1del1	CGG AGC TCC TGC TCG CCA TGC GGA AAA GAT TG	Deletion of <i>CEN1</i>
CEN1del2	GAG CGG CCG CCA TTA TTG CTT TGA GTT GTT TTA TC	Deletion of <i>CEN1</i>
CEN1del3	CGCTGCAGGGTTTTGGAATCTAAATTCTAATAG	Deletion of <i>CEN1</i>
CEN1del4	CGC TCG AGC TTC TTG TCC TGC TGA ATA ATC	Deletion of <i>CEN1</i>
Mif2pckMycPst1 F	AGA ACT GAC ACT GCA GGG ATC CAC TGT ATT CCA ATT TAA CAG AG	MycMif2 integration
Mif2 pck1SacII R	GAG CCG CGG CTG TAA CTG GTG GTT TAA ATC CAT CC	MycMif2 integration
Mif69248	GGTGACTAACTACGAGTAGGTGG	Confirmatory PCR for MycMif2 integration
ChIP primers		
p20057-3	GTCTTCGATTGCAGTGGCTCCTCAAT	Co-ordinates- Assembly 21 CaChrR-1745148- 1745172
p20057-4	GCAACCACACAAACATGTGTCTCG	Co-ordinates- Assembly 21 CaChrR-1745145- 1745168
p2488-1	CACTCTGACCAAATTCTCGTTTCC	Co-ordinates- Assembly 21 CaChr1-1567094 - 1567117
p2488-2	GCAACATCCGAGTAAGGTTTGTGG	Co-ordinates- Assembly 21 CaChr1-1566850 - 1566873
CACH2F	ACTGCTGGGCTTGTGAAGTT	Co-ordinates- Assembly 21 CaChr2-1929703 - 1929723
CACH2R	GAGTCACAGCCAAACACGAA	Co-ordinates- Assembly 21 CaChr2-1929971 - 1929951
CACH3F	AGATATGACGGCGCTGTTG	Co-ordinates- Assembly 21 CaChr3-823849 - 823861
CACH3R	CAAACATCAACCTCCCAAT	Co-ordinates- Assembly 21 CaChr3-824148 - 814128
CACH4R	CTCTAATAACGCTAATCAAGAGA	Co-ordinates- Assembly 21 CaChr4-1004002 - 1003979
CACH4F	GCTCTTACAAAAGCCAATCCA	Co-ordinates- Assembly 21 CaChr4-1003913 - 1003934
CEN5-168F	TAATACCTAATGCTCATTCTTCCG	Co-ordinates- Assembly 21 CaChr5-470830- 470853
CEN5-168R	ATTTTCATGGAAGAGGGGTTTCAT	Co-ordinates- Assembly 21 CaChr5-470686- 470709

p1873-1	GTAGGTGAGCGTTCAGAAGTCTGC	Co-ordinates- Assembly 21 CaChr6-979483 - 979506
p1873-2	CCGGAACAACATGGGTCTTGAC	Co-ordinates- Assembly 21 CaChr6-979722 - 979745
2498-21	CTG GTG CAA GAC CCT CAT AGA AGC	Co-ordinates- Assembly 21 CaChr7 - 427537 - 427560
2498-22	CCT GAC ACT GTC GTT TCC CAT AGC	Co-ordinates -Assembly 21 CaChr7 - 427369 - 427392
2498-11	CGT ACA GTT GCG CAC TCA TTC AGA TG	Co-ordinates- Assembly 21 CaChr7 - 444850 - 444875
2498-12	CAG TCT GCC AAG TGT AAA ACT GAG G	Co-ordinates -Assembly 21 CaChr7 - 444584 - 444608
CaLeu2-1	GTGACCATGTCGGTACCGAAATTGTC	Co-ordinates- Assembly 21 CaChr7 -64195 - 64220
CaLeu2-2	CTTGTCAGGACGAACAGTGCCAGTA	Co-ordinates- Assembly 21 CaChr7 -64415 - 64440
Cachr7F1	CCATACTGGTAGGTAATCTCTCTTG	ChIP primers for neocentromere mapping
Cachr7R1	ATGCTTGGCCTTCTATGTTG	ChIP primers for neocentromere mapping
Cachr7F2	ATCCTGTTGACGACAATCTTCTC	ChIP primers for neocentromere mapping
Cachr7R2	TGCAAATTGGTACCTCATTGTTAG	ChIP primers for neocentromere mapping
Cachr7F3	ACAGCCACAGTAGTTCCAAT	ChIP primers for neocentromere mapping
Cachr7R3	TGAAATCCAGAATGCCGTAAG	ChIP primers for neocentromere mapping
Cachr7F4	TCTACCACGTACTTTTGTGG	ChIP primers for neocentromere mapping
Cachr7R4	AATGACGTTTTGATGCATATTGC	ChIP primers for neocentromere mapping
CaChr7F5	GTA AGT TCA CTG TTA CTT TGG ATG	ChIP primers for neocentromere mapping
CaChr7R5	GGT CTT CTT TTC TTT CTT TTC GTC	ChIP primers for neocentromere mapping
CaChr7F6	GAC TCA ATT GAA GGA ATT TGA AGA C	ChIP primers for neocentromere mapping
CaChr7R6	GAA GAT GGA GAA ATT TCA AAG GTC	ChIP primers for neocentromere mapping
CaChr7F7	CTA ACC TAC CAG CTA GCC AGC	ChIP primers for neocentromere mapping
CaChr7R7	GTT GAT TAC TCC TCA AAA ATT TTC AG	ChIP primers for neocentromere mapping
CaChr7F8	CTT TCT TCA CCA CCA TGG CAC G	ChIP primers for neocentromere mapping

CaChr7R8	GCT GGC GTT GAT ACT GCT AG	ChIP primers for neocentromere mapping
CaChr7F9	CTT CGA AGT TAG TTT GGT TTG	ChIP primers for neocentromere mapping
CaChr7R9	GTA GAT ATG AGG GAA GAA AAT AGC	ChIP primers for neocentromere mapping
CaChr7F10	GAT AGT CAT TAT GCA CAG TAG	ChIP primers for neocentromere mapping
CaChr7R10	GAA TGC ACT CCA CAT TTA CTC	ChIP primers for neocentromere mapping
CaChr7F11	CAC ACT TTG GAA GTT CAT CAC	ChIP primers for neocentromere mapping
CaChr7R11	GAC TAA AGC ACA ACT AAA AGA CTG	ChIP primers for neocentromere mapping
CaChr7F12	AGGAAGTCAAGTGAAGTCAAGTTACAG	ChIP primers for neocentromere mapping
CaChr7R12	GCGTCATGTCGATTCGAAAT	ChIP primers for neocentromere mapping
CaChr7F13	TTAGATGTACTTCGACAAGGACGTT	ChIP primers for neocentromere mapping
CaChr7R13	CAATGCTCGTCGAAGAAAAATC	ChIP primers for neocentromere mapping
CaChr7S5	GGACGGTAAATAGGTTAATGGAG	ChIP primers for neocentromere mapping
CaChr7AS5	CCCTAAAAAAGAAACATCTC	ChIP primers for neocentromere mapping
CaChr7S6	TTTCCATATTGCACCAAGGG	ChIP primers for neocentromere mapping
CaChr7AS6	CGAGTTGTTATAGTTTGAATAAGCG	ChIP primers for neocentromere mapping
CaChr7S7	CACTAAATACATATCAAGACATCGTT	ChIP primers for neocentromere mapping
CaChr7AS7	CCCACCTCAATCAAGTCTATTTCG	ChIP primers for neocentromere mapping
CaChr7S8	TCTCCTTCTCGTCAATGGC	ChIP primers for neocentromere mapping
CaChr7AS8	TCATTGCTCGAGGAATTGGA	ChIP primers for neocentromere mapping
CaChr7S9	TTGTTTTGGCGGTGCAATG	ChIP primers for neocentromere mapping
CaChr7AS9	AGTCAAAGTCCAACCAGCA	ChIP primers for neocentromere mapping
CaChr7S10	TTGTTAGCATTGTGTTGTTGTTGT	ChIP primers for neocentromere mapping
CaChr7AS10	GCTAGAAACATAAACTTTCAAAC	ChIP primers for neocentromere mapping
CaChr7S11	GTAATTTACCTTCATTTGATTCC	ChIP primers for neocentromere mapping
CaChr7AS11	CGGTATTTCTGAGTGAATTAAGG	ChIP primers for neocentromere mapping
CaChr7S12	TAATGCATACCTTTTCATCTAAGCAACAG	ChIP primers for neocentromere mapping

CaChr7AS12	CCAACACTTCCTCTTGTACCA	ChIP primers for neocentromere mapping
CaChr7S13	TCCACCTCCACCTCCACCT	ChIP primers for neocentromere mapping
CaChr7AS13	TCAGCGATTGTATTAAATAGAGTAAC	ChIP primers for neocentromere mapping
CaChr7S14	GGACTCAACAATTCCCTCAA	ChIP primers for neocentromere mapping
CaChr7AS14	ACCTCGACATCGACTTGATTGA	ChIP primers for neocentromere mapping
CaChr7F14	TTGGAATTGGAGTTGGCAGTAG	ChIP primers for neocentromere mapping
CaChr7R14	TCTCAGTAGTAGTCTTCCACTGGTGT	ChIP primers for neocentromere mapping
CaChr7F15	GCTTTGTGTAGCTGCCTATTCTT	ChIP primers for neocentromere mapping
CaChr7R15	TGGTGGTGGTGTGTAGGTTAGATT	ChIP primers for neocentromere mapping
CaChr7F16	AAAGGGCAAGCAAGGAAA	ChIP primers for neocentromere mapping
CaChr7R16	GATGTACATACTTTGTGTGTTCTACCA	ChIP primers for neocentromere mapping
CaChr7F17	AACAACACTTAAACAATAAGATTGA	ChIP primers for neocentromere mapping
CaChr7R17	GCAAGAGAAAAAAACCACGC	ChIP primers for neocentromere mapping
CaChr7F18	GCTGAGTAGCAATTGTTGTCATG	ChIP primers for neocentromere mapping
CaChr7R18	TGATTCATTGCCACTGTCTCT	ChIP primers for neocentromere mapping
CaChr7F19	CTAACCTCTGTAAATAGTTCAATCCA	ChIP primers for neocentromere mapping
CaChr7R19	GAAATATTCCAATAGTGAAAGTG	ChIP primers for neocentromere mapping
CaChr7F20	CAACTAGCACATTATTTATATGAAAAC	ChIP primers for neocentromere mapping
CaChr7R20	AAAAAAGCAATCCCCGTCAG	ChIP primers for neocentromere mapping
CaChr7F21	AGAATCATAATTGATGATTTGGTGC	ChIP primers for neocentromere mapping
CaChr7R21	CCTTTGCCTAAAGCTTGACAAG	ChIP primers for neocentromere mapping
CaChr7F22	GGTGTTAGTGGCTTTATAGTGTGTA	ChIP primers for neocentromere mapping
CaChr7R22	GTTGTCGTTGTTGTCTTGTCTTG	ChIP primers for neocentromere mapping
CaChr7F23	GGGTGAAGCTGATTTATGGAGA	ChIP primers for neocentromere mapping
CaChr7R23	CCAAAAATTTTTACACTTGCAAGG	ChIP primers for neocentromere mapping
CaChr7F24	CAAGAAAGATTGGTTTTATATGGACC	ChIP primers for neocentromere mapping

CaChr7R24	GGCAATAAGATTTTATGATTAAGTGG	ChIP primers for neocentromere mapping
CaChr7F25	CGAATTGAGACAATCGCTATTAATGAG	ChIP primers for neocentromere mapping
CaChr7R25	GTCGTTTTCTTTTACCTCCTCCTC	ChIP primers for neocentromere mapping
CaChr7F26	GAATTGGGGTGAAGACATGGAA	ChIP primers for neocentromere mapping
CaChr7R26	CCTATAACTGTGAACAATGCGTCTAG	ChIP primers for neocentromere mapping
CaChr7F27	AAATATCACACGACCGCCAA	ChIP primers for neocentromere mapping
CaChr7R27	AACATTACCAATGATTAGATCAG	ChIP primers for neocentromere mapping
CaChr7F28	AAAACAAGGCGGCTTTGTCT	ChIP primers for neocentromere mapping
CaChr7R28	CAAATCTTTATTATAGTACTAGAGAGA	ChIP primers for neocentromere mapping
CaChr7S15	CGAAAACCTAGAAAACCCAGTTGTA	ChIP primers for neocentromere mapping
CaChr7AS15	AAAGTCTTATCGGGCCACAA	ChIP primers for neocentromere mapping
CaChr7S16	CTCTTTTCAATCTCAGACACTGAGTG	ChIP primers for neocentromere mapping
CaChr7AS16	GACACGTAATTTTTCACTTCCTGC	ChIP primers for neocentromere mapping
CaChr7S17	CGAGGTTTGAATTATTATAAATGCC	ChIP primers for neocentromere mapping
CaChr7AS17	TGCTCTCTAATGGTTTGCAAC	ChIP primers for neocentromere mapping
CaChr7S18	GGTGTTCAAATGTGGACTTTGATG	ChIP primers for neocentromere mapping
CaChr7AS18	CCATAAAACCAATTCTTGATGAAAG	ChIP primers for neocentromere mapping
CaChr7S19	CCCCCCCCTTCTATAACATTT	ChIP primers for neocentromere mapping
CaChr7AS19	GGGCATCGTTTTTATCCCAAG	ChIP primers for neocentromere mapping
CaChr7S20	GGCTTTTGATCATATCGCTAGAGG	ChIP primers for neocentromere mapping
CaChr7AS20	TTAACCATACATACATAAAACG	ChIP primers for neocentromere mapping
CaChr7S21	ACACACTTAGCAGCATCTTGAACC	ChIP primers for neocentromere mapping
CaChr7AS21	AATCTGCTGTCAAAGCGAAG	ChIP primers for neocentromere mapping
Cen1-1550-F	TTCATATTCATTGCAAATCCAAC	ChIP primers for neocentromere mapping
Cen1-1550-R	GGTATTTGATTTAGTTCCTGCACT	ChIP primers for neocentromere mapping
Cen1-1552-F	GTATGGGTCTTAGGAGAAAAAGG	ChIP primers for neocentromere mapping

Cen1-1552-R	AAGCAACTTTCCATTAGCAGGG	ChIP primers for neocentromere mapping
Cen1-1554-F	ATGGGTGTGCTTTGTTAGAGCA	ChIP primers for neocentromere mapping
Cen1-1554-R	CTATCCAAACTGTCTACAACCTGGT	ChIP primers for neocentromere mapping
Cen1-1556-F	AGTATTCCCATGTTTGCTTCCC	ChIP primers for neocentromere mapping
Cen1-1556-R	GAAAACATTCTTGTTTCTTCATCCA	ChIP primers for neocentromere mapping
Cen1-1557-F	TTGCATCTGCTATTATCTAGCTTTC	ChIP primers for neocentromere mapping
Cen1-1557-R	GGTTGCTGCCAACAACTCTAAA	ChIP primers for neocentromere mapping
Cen1-1558-F	CAAACCAACAAAACACGCTG	ChIP primers for neocentromere mapping
Cen1-1558-R	TGAAATTCACTTTTGGTAAAAGG	ChIP primers for neocentromere mapping
Cen1-1544-F	ACGGATGCAGATGAAAAGTTG	ChIP primers for neocentromere mapping
Cen1-1544-R	GACCGATGGATTATTTCTGATAGT	ChIP primers for neocentromere mapping
Cen1-1546-F	CCAGAGAATTGAAGACACATCCTA	ChIP primers for neocentromere mapping
Cen1-1546-R	AAACTGCAAAATGTTGCC	ChIP primers for neocentromere mapping
Cen1-1548-F	TTCCAGAACCAATAAGTGACCG	ChIP primers for neocentromere mapping
Cen1-1548-R	GATTGGTTTCATATGGGGCTATTC	ChIP primers for neocentromere mapping
Cen1-1549-F	AGCAACCTAGAAAAGAAAATGGG	ChIP primers for neocentromere mapping
Cen1-1549-R	TGTGTGGCGATTCTTCTTTG	ChIP primers for neocentromere mapping
Cen1-1581-F	GAGTCTTATTAGAAATGGTTTTGG	ChIP primers for neocentromere mapping
Cen1-1581-R	CGCAGAACAAAGAGAAGGAA	ChIP primers for neocentromere mapping
Cen1-1584-F	GGTCAAGATTCAAAAAGGAAGCGT	ChIP primers for neocentromere mapping
Cen1-1584-R	CATCCAATAATGTGTTACACCTTC	ChIP primers for neocentromere mapping
Cen1-1586-F	CTAAAGGATTGGAGATTACTCGTT	ChIP primers for neocentromere mapping
Cen1-1586-R	CGATGGTTTCAATGGTAATTTTAG	ChIP primers for neocentromere mapping
Cen1-1588-F	GTGATAGTGACTTGATAAGGAGGG	ChIP primers for neocentromere mapping
Cen1-1588-R	GCTGACTCATAAAAAGTCAGAACA	ChIP primers for neocentromere mapping
Cen1-1590-F	CCGTACAGAGTTTTAACTTTAC	ChIP primers for neocentromere mapping

Cen1-1590-R	CACGAAATGGTACCTTATCA	ChIP primers for neocentromere mapping
Cen1-1593-F	TGATTGGCAATATAGGACGTTATG	ChIP primers for neocentromere mapping
Cen1-1593-R	GAAAGAAGGTTGGAAGATCTAGCA	ChIP primers for neocentromere mapping
Cen1-1595-F	GTAACGATTAATTCAGGGGGG	ChIP primers for neocentromere mapping
Cen1-1595-R	TGTTTTGCTTGGCAAGAGAG	ChIP primers for neocentromere mapping

References

Ahmad K, Henikoff S (2002) Histone H3 variants specify modes of chromatin assembly. *Proc Natl Acad Sci U S A* **99 Suppl 4**: 16477-16484

Alby K, Schaefer D, Bennett RJ (2009) Homothallic and heterothallic mating in the opportunistic pathogen *Candida albicans*. *Nature* **460**: 890-893

Allshire RC, Karpen GH (2008) Epigenetic regulation of centromeric chromatin: old dogs, new tricks? *Nature Reviews Genetics* **9**: 923-937

Amor DJ, Choo KH (2002) Neocentromeres: role in human disease, evolution, and centromere study. *Am J Hum Genet* **71**: 695-714

Ananiev EV, Phillips RL, Rines HW (1998) Chromosome-specific molecular organization of maize (*Zea mays* L.) centromeric regions. *Proc Natl Acad Sci U S A* **95**: 13073-13078

Anderson M, Haase J, Yeh E, Bloom K (2009) Function and assembly of DNA looping, clustering, and microtubule attachment complexes within a eukaryotic kinetochore. *Mol Biol Cell* **20**: 4131-4139

Asbury CL, Gestaut DR, Powers AF, Franck AD, Davis TN (2006) The Dam1 kinetochore complex harnesses microtubule dynamics to produce force and movement. *Proceedings of the National Academy of Sciences of the United States of America* **103**: 9873-9878

Bachant J, Jessen SR, Kavanaugh SE, Fielding CS (2005) The yeast S phase checkpoint enables replicating chromosomes to bi-orient and restrain spindle extension during S phase distress. *J Cell Biol* **168**: 999-1012

Bachewich C, Nantel A, Whiteway M (2005) Cell cycle arrest during S or M phase generates polarized growth via distinct signals in *Candida albicans*. *Mol Microbiol* **57**: 942-959

Bao W, Zhang W, Yang Q, Zhang Y, Han B, Gu M, Xue Y, Cheng Z (2006) Diversity of centromeric repeats in two closely related wild rice species, *Oryza officinalis* and *Oryza rhizomatis*. *Mol Genet Genomics* **275**: 421-430

Baum M, Sanyal K, Mishra PK, Thaler N, Carbon J (2006) Formation of functional centromeric chromatin is specified epigenetically in *Candida albicans*. *Proc Natl Acad Sci U S A* **103**: 14877-14882

Bennett RJ, Johnson AD (2003) Completion of a parasexual cycle in *Candida albicans* by induced chromosome loss in tetraploid strains. *EMBO J* **22**: 2505-2515

Bensasson D, Zarowiecki M, Burt A, Koufopanou V (2008) Rapid evolution of yeast centromeres in the absence of drive. *Genetics* **178**: 2161-2167

Bergmann JH, Rodríguez MG, Martins NM, Kimura H, Kelly DA, Masumoto H, Larionov V, Jansen LE, Earnshaw WC (2011) Epigenetic engineering shows H3K4me2 is required for HJURP targeting and CENP-A assembly on a synthetic human kinetochore. *EMBO J* **30**: 328-340

Bernard P, Maure JF, Partridge JF, Genier S, Javerzat JP, Allshire RC (2001) Requirement of heterochromatin for cohesion at centromeres. *Science* **294**: 2539-2542

Bharadwaj R, Qi W, Yu H (2004) Identification of two novel components of the human NDC80 kinetochore complex. *J Biol Chem* **279**: 13076-13085

Black BE, Cleveland DW (2011) Epigenetic centromere propagation and the nature of CENP-a nucleosomes. *Cell* **144**: 471-479

Black BE, Foltz DR, Chakravarthy S, Luger K, Woods VL, Cleveland DW (2004) Structural determinants for generating centromeric chromatin. *Nature* **430**: 578-582

Bloom KS, Carbon J (1982) Yeast centromere DNA is in a unique and highly ordered structure in chromosomes and small circular minichromosomes. *Cell* **29**: 305-317

Blower MD, Karpen GH (2001) The role of *Drosophila* CID in kinetochore formation, cell-cycle progression and heterochromatin interactions. *Nat Cell Biol* **3**: 730-739

Borts RH, Haber JE (1989) Length and distribution of meiotic gene conversion tracts and crossovers in *Saccharomyces cerevisiae*. *Genetics* **123**: 69-80

Brinkley BR, Cartwright J (1971) Ultrastructural analysis of mitotic spindle elongation in mammalian cells in vitro. Direct microtubule counts. *J Cell Biol* **50**: 416-431

Byers B, Goetsch L (1975) Behavior of spindles and spindle plaques in the cell cycle and conjugation of *Saccharomyces cerevisiae*. *J Bacteriol* **124**: 511-523

Cam HP, Sugiyama T, Chen ES, Chen X, FitzGerald PC, Grewal SI (2005) Comprehensive analysis of heterochromatin- and RNAi-mediated epigenetic control of the fission yeast genome. *Nat Genet* **37**: 809-819

Camahort R, Li B, Florens L, Swanson SK, Washburn MP, Gerton JL (2007) Scm3 is essential to recruit the histone h3 variant cse4 to centromeres and to maintain a functional kinetochore. *Mol Cell* **26**: 853-865

Camahort R, Shivaraju M, Mattingly M, Li B, Nakanishi S, Zhu D, Shilatifard A, Workman JL, Gerton JL (2009) Cse4 is part of an octameric nucleosome in budding yeast. *Mol Cell* **35**: 794-805

Cambareri EB, Aisner R, Carbon J (1998) Structure of the chromosome VII centromere region in *Neurospora crassa*: degenerate transposons and simple repeats. *Mol Cell Biol* **18**: 5465-5477

Care RS, Trevethick J, Binley KM, Sudbery PE (1999) The MET3 promoter: a new tool for *Candida albicans* molecular genetics. *Mol Microbiol* **34**: 792-798

Carminati JL, Stearns T (1997) Microtubules orient the mitotic spindle in yeast through dynein-dependent interactions with the cell cortex. *J Cell Biol* **138**: 629-641

Centola M, Carbon J (1994) Cloning and characterization of centromeric DNA from *Neurospora crassa*. *Mol Cell Biol* **14**: 1510-1519

Cheeseman IM, Brew C, Wolyniak M, Desai A, Anderson S, Muster N, Yates JR, Huffaker TC, Drubin DG, Barnes G (2001a) Implication of a novel multiprotein Dam1p complex in outer kinetochore function. *J Cell Biol* **155**: 1137-1145

Cheeseman IM, Desai A (2008) Molecular architecture of the kinetochore-microtubule interface. *Nat Rev Mol Cell Biol* **9**: 33-46

Cheeseman IM, Enquist-Newman M, Müller-Reichert T, Drubin DG, Barnes G (2001b) Mitotic spindle integrity and kinetochore function linked by the Duo1p/Dam1p complex. *J Cell Biol* **152**: 197-212

Cheeseman IM, Niessen S, Anderson S, Hyndman F, Yates JR, Oegema K, Desai A (2004) A conserved protein network controls assembly of the outer kinetochore and its ability to sustain tension. *Genes Dev* **18**: 2255-2268

Chen ES, Saitoh S, Yanagida M, Takahashi K (2003) A cell cycle-regulated GATA factor promotes centromeric localization of CENP-A in fission yeast. *Mol Cell* **11**: 175-187

Chen ES, Zhang K, Nicolas E, Cam HP, Zofall M, Grewal SI (2008) Cell cycle control of centromeric repeat transcription and heterochromatin assembly. *Nature* **451**: 734-737

Cheng Z, Dong F, Langdon T, Ouyang S, Buell CR, Gu M, Blattner FR, Jiang J (2002) Functional rice centromeres are marked by a satellite repeat and a centromere-specific retrotransposon. *Plant Cell* **14**: 1691-1704

Ciferri C, Musacchio A, Petrovic A (2007) The Ndc80 complex: hub of kinetochore activity. *FEBS Lett* **581**: 2862-2869

Clarke L (1990) Centromeres of budding and fission yeasts. *Trends Genet* **6**: 150-154

Clarke L, Carbon J (1980) ISOLATION OF A YEAST CENTROMERE AND CONSTRUCTION OF FUNCTIONAL SMALL CIRCULAR CHROMOSOMES. *Nature* **287**: 504-509

Cleveland DW, Mao Y, Sullivan KF (2003) Centromeres and kinetochores: from epigenetics to mitotic checkpoint signaling. *Cell* **112**: 407-421

Coleman DC, Rinaldi MG, Haynes KA, Rex JH, Summerbell RC, Anaissie EJ, Li A, Sullivan DJ (1998) Importance of *Candida* species other than *Candida albicans* as opportunistic pathogens. *Med Mycol* **36 Suppl 1**: 156-165

Collins KA, Castillo AR, Tatsutani SY, Biggins S (2005) De novo kinetochore assembly requires the centromeric histone H3 variant. *Mol Biol Cell* **16**: 5649-5660

Collins KA, Furuyama S, Biggins S (2004) Proteolysis contributes to the exclusive centromere localization of the yeast Cse4/CENP-A histone H3 variant. *Curr Biol* **14**: 1968-1972

Colmenares SU, Buker SM, Buhler M, Dlakić M, Moazed D (2007) Coupling of double-stranded RNA synthesis and siRNA generation in fission yeast RNAi. *Mol Cell* **27**: 449-461

Conde e Silva N, Black BE, Sivolob A, Filipski J, Cleveland DW, Prunell A (2007) CENP-A-containing nucleosomes: easier disassembly versus exclusive centromeric localization. *J Mol Biol* **370**: 555-573

Copenhaver GP (2004) Who's driving the centromere? *J Biol* **3**: 17

Corvey C, Koetter P, Beckhaus T, Hack J, Hofmann S, Hampel M, Stein T, Karas M, Entian KD (2005) Carbon source-dependent assembly of the Snf1p kinase complex in *Candida albicans*. *Journal of Biological Chemistry* **280**: 25323-25330

Cowen LE, Steinbach WJ (2008) Stress, drugs, and evolution: the role of cellular signaling in fungal drug resistance. *Eukaryot Cell* **7**: 747-764

Craig JM, Wong LH, Lo AW, Earle E, Choo KH (2003) Centromeric chromatin pliability and memory at a human neocentromere. *EMBO J* **22**: 2495-2504

Csink AK, Henikoff S (1998) Something from nothing: the evolution and utility of satellite repeats. *Trends Genet* **14**: 200-204

Dalal Y, Furuyama T, Vermaak D, Henikoff S (2007) Structure, dynamics, and evolution of centromeric nucleosomes. *Proc Natl Acad Sci U S A* **104**: 15974-15981

Dawe RK, Hiatt EN (2004) Plant neocentromeres: fast, focused, and driven. *Chromosome Res* **12**: 655-669

de Groot PW, de Boer AD, Cunningham J, Dekker HL, de Jong L, Hellingwerf KJ, de Koster C, Klis FM (2004) Proteomic analysis of *Candida albicans* cell walls reveals covalently bound carbohydrate-active enzymes and adhesins. *Eukaryot Cell* **3**: 955-965

De Souza CP, Osmani SA (2007) Mitosis, not just open or closed. *Eukaryot Cell* **6**: 1521-1527

De Wulf P, McAinsh AD, Sorger PK (2003) Hierarchical assembly of the budding yeast kinetochore from multiple subcomplexes. *Genes Dev* **17**: 2902-2921

Desai A, Rybina S, Müller-Reichert T, Shevchenko A, Hyman A, Oegema K (2003) KNL-1 directs assembly of the microtubule-binding interface of the kinetochore in *C. elegans*. *Genes Dev* **17**: 2421-2435

Detloff P, Petes TD (1992) Measurements of excision repair tracts formed during meiotic recombination in *Saccharomyces cerevisiae*. *Mol Cell Biol* **12**: 1805-1814

Dimitriadis EK, Weber C, Gill RK, Diekmann S, Dalal Y (2010) Tetrameric organization of vertebrate centromeric nucleosomes. *Proc Natl Acad Sci U S A* **107**: 20317-20322

Ding R, McDonald KL, McIntosh JR (1993) Three-dimensional reconstruction and analysis of mitotic spindles from the yeast, *Schizosaccharomyces pombe*. *J Cell Biol* **120**: 141-151

Ding R, West RR, Morpew DM, Oakley BR, McIntosh JR (1997) The spindle pole body of *Schizosaccharomyces pombe* enters and leaves the nuclear envelope as the cell cycle proceeds. *Mol Biol Cell* **8**: 1461-1479

Drinnenberg IA, Weinberg DE, Xie KT, Mower JP, Wolfe KH, Fink GR, Bartel DP (2009) RNAi in budding yeast. *Science* **326**: 544-550

Du Y, Topp CN, Dawe RK (2010) DNA binding of centromere protein C (CENPC) is stabilized by single-stranded RNA. *PLoS Genet* **6**: e1000835

Duret L, Galtier N (2009) Biased gene conversion and the evolution of mammalian genomic landscapes. *Annu Rev Genomics Hum Genet* **10**: 285-311

Eggimann P, Garbino J, Pittet D (2003) Epidemiology of *Candida* species infections in critically ill non-immunosuppressed patients. *Lancet Infect Dis* **3**: 685-702

Ekwall K (2007) Epigenetic control of centromere behavior. *Annu Rev Genet* **41**: 63-81

Ekwall K, Olsson T, Turner BM, Cranston G, Allshire RC (1997) Transient inhibition of histone deacetylation alters the structural and functional imprint at fission yeast centromeres. *Cell* **91**: 1021-1032

Enquist-Newman M, Cheeseman IM, Van Goor D, Drubin DG, Meluh PB, Barnes G (2001) Dad1p, third component of the Duo1p/Dam1p complex involved in kinetochore function and mitotic spindle integrity. *Mol Biol Cell* **12**: 2601-2613

Erhardt S, Mellone BG, Betts CM, Zhang W, Karpen GH, Straight AF (2008) Genome-wide analysis reveals a cell cycle-dependent mechanism controlling centromere propagation. *J Cell Biol* **183**: 805-818

Fishel B, Amstutz H, Baum M, Carbon J, Clarke L (1988) Structural organization and functional analysis of centromeric DNA in the fission yeast *Schizosaccharomyces pombe*. *Mol Cell Biol* **8**: 754-763

Fitzgerald-Hayes M, Clarke L, Carbon J (1982) Nucleotide sequence comparisons and functional analysis of yeast centromere DNAs. *Cell* **29**: 235-244

Fitzpatrick DA, Logue ME, Stajich JE, Butler G (2006) A fungal phylogeny based on 42 complete genomes derived from supertree and combined gene analysis. *BMC Evol Biol* **6**: 99

Foltz DR, Jansen LE, Bailey AO, Yates JR, Bassett EA, Wood S, Black BE, Cleveland DW (2009) Centromere-specific assembly of CENP-a nucleosomes is mediated by HJURP. *Cell* **137**: 472-484

Foltz DR, Jansen LE, Black BE, Bailey AO, Yates JR, Cleveland DW (2006) The human CENP-A centromeric nucleosome-associated complex. *Nat Cell Biol* **8**: 458-469

Fournier P, Abbas A, Chasles M, Kudla B, Ogrydziak DM, Yaver D, Xuan JW, Peito A, Ribet AM, Feynerol C (1993) Colocalization of centromeric and replicative functions on autonomously replicating sequences isolated from the yeast *Yarrowia lipolytica*. *Proc Natl Acad Sci U S A* **90**: 4912-4916

Franck AD, Powers AF, Gestaut DR, Gonen T, Davis TN, Asbury CL (2007) Tension applied through the Dam1 complex promotes microtubule elongation providing a direct mechanism for length control in mitosis. *Nature Cell Biology* **9**: 832-U171

Franco A, Meadows JC, Millar JB (2007) The Dam1/DASH complex is required for the retrieval of unclustered kinetochores in fission yeast. *J Cell Sci* **120**: 3345-3351

Freitag M, Hickey PC, Khlafallah TK, Read ND, Selker EU (2004a) HP1 is essential for DNA methylation in neurospora. *Mol Cell* **13**: 427-434

Freitag M, Lee DW, Kothe GO, Pratt RJ, Aramayo R, Selker EU (2004b) DNA methylation is independent of RNA interference in Neurospora. *Science* **304**: 1939

Fukagawa T (2004) Centromere DNA, proteins and kinetochore assembly in vertebrate cells. *Chromosome Res* **12**: 557-567

Furuyama T, Henikoff S (2009) Centromeric nucleosomes induce positive DNA supercoils. *Cell* **138**: 104-113

Gerami-Nejad M, Berman J, Gale CA (2001) Cassettes for PCR-mediated construction of green, yellow, and cyan fluorescent protein fusions in *Candida albicans*. *Yeast* **18**: 859-864

Gilbert DM (2002) Replication timing and metazoan evolution. *Nat Genet* **32**: 336-337

Gilfillan GD, Sullivan DJ, Haynes K, Parkinson T, Coleman DC, Gow NA (1998) *Candida dubliniensis*: phylogeny and putative virulence factors. *Microbiology* **144** (Pt 4): 829-838

Gopalakrishnan S, Sullivan BA, Trazzi S, Della Valle G, Robertson KD (2009) DNMT3B interacts with constitutive centromere protein CENP-C to modulate DNA methylation and the histone code at centromeric regions. *Hum Mol Genet* **18**: 3178-3193

Goshima G, Kiyomitsu T, Yoda K, Yanagida M (2003) Human centromere chromatin protein hMis12, essential for equal segregation, is independent of CENP-A loading pathway. *J Cell Biol* **160**: 25-39

Goshima G, Scholey JM (2010) Control of mitotic spindle length. *Annu Rev Cell Dev Biol* **26**: 21-57

Greenfeder SA, Newlon CS (1992) Replication forks pause at yeast centromeres. *Mol Cell Biol* **12**: 4056-4066

Grewal SI (2010) RNAi-dependent formation of heterochromatin and its diverse functions. *Curr Opin Genet Dev* **20**: 134-141

Gudlaugsson O, Gillespie S, Lee K, Vande Berg J, Hu J, Messer S, Herwaldt L, Pfaller M, Diekema D (2003) Attributable mortality of nosocomial candidemia, revisited. *Clin Infect Dis* **37**: 1172-1177

Güttinger S, Laurell E, Kutay U (2009) Orchestrating nuclear envelope disassembly and reassembly during mitosis. *Nat Rev Mol Cell Biol* **10**: 178-191

Hayashi T, Fujita Y, Iwasaki O, Adachi Y, Takahashi K, Yanagida M (2004) Mis16 and Mis18 are required for CENP-A loading and histone deacetylation at centromeres. *Cell* **118**: 715-729

Heath IB (1980) Variant mitoses in lower eukaryotes: indicators of the evolution of mitosis. *Int Rev Cytol* **64**: 1-80

Heeger S, Leismann O, Schittenhelm R, Schraidt O, Heidmann S, Lehner CF (2005) Genetic interactions of separate regulatory subunits reveal the diverged *Drosophila* Cenp-C homolog. *Genes Dev* **19**: 2041-2053

Henikoff S, Ahmad K, Malik HS (2001) The centromere paradox: stable inheritance with rapidly evolving DNA. *Science* **293**: 1098-1102

Heus JJ, Zonneveld BJ, de Steensma HY, van den Berg JA (1993) The consensus sequence of *Kluyveromyces lactis* centromeres shows homology to functional centromeric DNA from *Saccharomyces cerevisiae*. *Mol Gen Genet* **236**: 355-362

Heus JJ, Zonneveld BJ, Steensma HY, Van den Berg JA (1994) Mutational analysis of centromeric DNA elements of *Kluyveromyces lactis* and their role in determining the species specificity of the highly homologous centromeres from *K. lactis* and *Saccharomyces cerevisiae*. *Mol Gen Genet* **243**: 325-333

Higgins AW, Gustashaw KM, Willard HF (2005) Engineered human dicentric chromosomes show centromere plasticity. *Chromosome Res* **13**: 745-762

Hofmann C, Cheeseman IM, Goode BL, McDonald KL, Barnes G, Drubin DG (1998) *Saccharomyces cerevisiae* Duo1p and Dam1p, novel proteins involved in mitotic spindle function. *J Cell Biol* **143**: 1029-1040

Hong EJ, Villén J, Gerace EL, Gygi SP, Moazed D (2005) A cullin E3 ubiquitin ligase complex associates with Rik1 and the Clr4 histone H3-K9 methyltransferase and is required for RNAi-mediated heterochromatin formation. *RNA Biol* **2**: 106-111

Hori T, Amano M, Suzuki A, Backer CB, Welburn JP, Dong Y, McEwen BF, Shang WH, Suzuki E, Okawa K, Cheeseman IM, Fukagawa T (2008) CCAN makes multiple contacts with centromeric DNA to provide distinct pathways to the outer kinetochore. *Cell* **135**: 1039-1052

Horn PJ, Bastie JN, Peterson CL (2005) A Rik1-associated, cullin-dependent E3 ubiquitin ligase is essential for heterochromatin formation. *Genes Dev* **19**: 1705-1714

Hull CM, Johnson AD (1999) Identification of a mating type-like locus in the asexual pathogenic yeast *Candida albicans*. *Science* **285**: 1271-1275

Ishii K, Ogiyama Y, Chikashige Y, Soejima S, Masuda F, Kakuma T, Hiraoka Y, Takahashi K (2008) Heterochromatin integrity affects chromosome reorganization after centromere dysfunction. *Science* **321**: 1088-1091

Ivessa AS, Zhou JQ, Zakian VA (2000) The *Saccharomyces* Pif1p DNA helicase and the highly related Rrm3p have opposite effects on replication fork progression in ribosomal DNA. *Cell* **100**: 479-489

Jaco I, Canela A, Vera E, Blasco MA (2008) Centromere mitotic recombination in mammalian cells. *J Cell Biol* **181**: 885-892

Janke C, Ortiz J, Tanaka TU, Lechner J, Schiebel E (2002) Four new subunits of the Dam1-Duo1 complex reveal novel functions in sister kinetochore biorientation. *Embo Journal* **21**: 181-193

Jia S, Kobayashi R, Grewal SI (2005) Ubiquitin ligase component Cul4 associates with Clr4 histone methyltransferase to assemble heterochromatin. *Nat Cell Biol* **7**: 1007-1013

Jin QW, Fuchs J, Loidl J (2000) Centromere clustering is a major determinant of yeast interphase nuclear organization. *J Cell Sci* **113 (Pt 11)**: 1903-1912

Jin W, Lamb JC, Zhang W, Kolano B, Birchler JA, Jiang J (2008) Histone modifications associated with both A and B chromosomes of maize. *Chromosome Res* **16**: 1203-1214

Joglekar AP, Bouck D, Finley K, Liu X, Wan Y, Berman J, He X, Salmon ED, Bloom KS (2008) Molecular architecture of the kinetochore-microtubule attachment site is conserved between point and regional centromeres. *J Cell Biol* **181**: 587-594

Judd SR, Petes TD (1988) Physical lengths of meiotic and mitotic gene conversion tracts in *Saccharomyces cerevisiae*. *Genetics* **118**: 401-410

Kalitsis P, Griffiths B, Choo KH (2006) Mouse telocentric sequences reveal a high rate of homogenization and possible role in Robertsonian translocation. *Proc Natl Acad Sci U S A* **103**: 8786-8791

Kammaing LM, Ketting RF (2011) RNAi genes pave their own way. *Genes Dev* **25**: 529-533

Keating P, Rachidi N, Tanaka TU, Stark MJ (2009) Ipl1-dependent phosphorylation of Dam1 is reduced by tension applied on kinetochores. *J Cell Sci* **122**: 4375-4382

Ketel C, Wang HS, McClellan M, Bouchonville K, Selmecki A, Lahav T, Gerami-Nejad M, Berman J (2009) Neocentromeres form efficiently at multiple possible loci in *Candida albicans*. *PLoS Genet* **5**: e1000400

Kiermaier E, Woehrer S, Peng Y, Mechtler K, Westermann S (2009) A Dam1-based artificial kinetochore is sufficient to promote chromosome segregation in budding yeast. *Nat Cell Biol* **11**: 1109-1115

Kim SM, Dubey DD, Huberman JA (2003) Early-replicating heterochromatin. *Genes Dev* **17**: 330-335

Kim SM, Huberman JA (2001) Regulation of replication timing in fission yeast. *EMBO J* **20**: 6115-6126

Kipling D, Ackford HE, Taylor BA, Cooke HJ (1991) Mouse minor satellite DNA genetically maps to the centromere and is physically linked to the proximal telomere. *Genomics* **11**: 235-241

Kipling D, Mitchell AR, Masumoto H, Wilson HE, Nicol L, Cooke HJ (1995) CENP-B binds a novel centromeric sequence in the Asian mouse *Mus caroli*. *Mol Cell Biol* **15**: 4009-4020

Kipling D, Warburton PE (1997) Centromeres, CENP-B and Tigger too. *Trends Genet* **13**: 141-145

Kitada K, Yamaguchi E, Hamada K, Arisawa M (1997) Structural analysis of a *Candida glabrata* centromere and its functional homology to the *Saccharomyces cerevisiae* centromere. *Curr Genet* **31**: 122-127

Kitagawa K, Hieter P (2001) Evolutionary conservation between budding yeast and human kinetochores. *Nat Rev Mol Cell Biol* **2**: 678-687

Kline SL, Cheeseman IM, Hori T, Fukagawa T, Desai A (2006) The human Mis12 complex is required for kinetochore assembly and proper chromosome segregation. *J Cell Biol* **173**: 9-17

Klis FM, Sosinska GJ, de Groot PW, Brul S (2009) Covalently linked cell wall proteins of *Candida albicans* and their role in fitness and virulence. *FEMS Yeast Res* **9**: 1013-1028

Kloc A, Martienssen R (2008) RNAi, heterochromatin and the cell cycle. *Trends Genet* **24**: 511-517

Kloc A, Zaratiegui M, Nora E, Martienssen R (2008) RNA interference guides histone modification during the S phase of chromosomal replication. *Curr Biol* **18**: 490-495

Kniola B, O'Toole E, McIntosh JR, Mellone B, Allshire R, Mengarelli S, Hultenby K, Ekwall K (2001) The domain structure of centromeres is conserved from fission yeast to humans. *Mol Biol Cell* **12**: 2767-2775

Koren A, Tsai HJ, Tirosh I, Burrack LS, Barkai N, Berman J (2010) Epigenetically-inherited centromere and neocentromere DNA replicates earliest in S-phase. *PLoS Genet* **6**: e1001068

Krishnan V, Nirantar S, Crasta K, Cheng AY, Surana U (2004) DNA replication checkpoint prevents precocious chromosome segregation by regulating spindle behavior. *Mol Cell* **16**: 687-700

Kumamoto CA (2002) *Candida* biofilms. *Curr Opin Microbiol* **5**: 608-611

Kwon MS, Hori T, Okada M, Fukagawa T (2007) CENP-C is involved in chromosome segregation, mitotic checkpoint function, and kinetochore assembly. *Mol Biol Cell* **18**: 2155-2168

Lamb NE, Sherman SL, Hassold TJ (2005) Effect of meiotic recombination on the production of aneuploid gametes in humans. *Cytogenet Genome Res* **111**: 250-255

Lambie EJ, Roeder GS (1986) Repression of meiotic crossing over by a centromere (CEN3) in *Saccharomyces cerevisiae*. *Genetics* **114**: 769-789

Lechner J, Carbon J (1991) A 240 kd multisubunit protein complex, CBF3, is a major component of the budding yeast centromere. *Cell* **64**: 717-725

Lee C, Wevrick R, Fisher RB, Ferguson-Smith MA, Lin CC (1997) Human centromeric DNAs. *Hum Genet* **100**: 291-304

Lee HC, Li L, Gu W, Xue Z, Crosthwaite SK, Pertsemlidis A, Lewis ZA, Freitag M, Selker EU, Mello CC, Liu Y (2010) Diverse pathways generate microRNA-like RNAs and Dicer-independent small interfering RNAs in fungi. *Mol Cell* **38**: 803-814

Lee HR, Zhang W, Langdon T, Jin W, Yan H, Cheng Z, Jiang J (2005) Chromatin immunoprecipitation cloning reveals rapid evolutionary patterns of centromeric DNA in *Oryza* species. *Proc Natl Acad Sci U S A* **102**: 11793-11798

Lermontova I, Schubert V, Fuchs J, Klatt S, Macas J, Schubert I (2006) Loading of Arabidopsis centromeric histone CENH3 occurs mainly during G2 and requires the presence of the histone fold domain. *Plant Cell* **18**: 2443-2451

Leuker CE, Sonneborn A, Delbrück S, Ernst JF (1997) Sequence and promoter regulation of the PCK1 gene encoding phosphoenolpyruvate carboxykinase of the fungal pathogen *Candida albicans*. *Gene* **192**: 235-240

Li Y, Bachant J, Alcasabas AA, Wang Y, Qin J, Elledge SJ (2002) The mitotic spindle is required for loading of the DASH complex onto the kinetochore. *Genes Dev* **16**: 183-197

Liu H, Liang F, Jin F, Wang Y (2008) The coordination of centromere replication, spindle formation, and kinetochore-microtubule interaction in budding yeast. *PLoS Genet* **4**: e1000262

Liu ST, Rattner JB, Jablonski SA, Yen TJ (2006) Mapping the assembly pathways that specify formation of the trilaminar kinetochore plates in human cells. *J Cell Biol* **175**: 41-53

Maggert KA, Karpen GH (2001) The activation of a neocentromere in *Drosophila* requires proximity to an endogenous centromere. *Genetics* **158**: 1615-1628

Maiato H, DeLuca J, Salmon ED, Earnshaw WC (2004) The dynamic kinetochore-microtubule interface. *J Cell Sci* **117**: 5461-5477

Malik HS, Henikoff S (2001) Adaptive evolution of Cid, a centromere-specific histone in *Drosophila*. *Genetics* **157**: 1293-1298

Malik HS, Henikoff S (2002) Conflict begets complexity: the evolution of centromeres. *Curr Opin Genet Dev* **12**: 711-718

Malik HS, Vermaak D, Henikoff S (2002) Recurrent evolution of DNA-binding motifs in the *Drosophila* centromeric histone. *Proc Natl Acad Sci U S A* **99**: 1449-1454

Malone RE, Bullard S, Lundquist S, Kim S, Tarkowski T (1992) A meiotic gene conversion gradient opposite to the direction of transcription. *Nature* **359**: 154-155

Marshall OJ, Chueh AC, Wong LH, Choo KH (2008) Neocentromeres: new insights into centromere structure, disease development, and karyotype evolution. *Am J Hum Genet* **82**: 261-282

Martienssen RA, Zaratiegui M, Goto DB (2005) RNA interference and heterochromatin in the fission yeast *Schizosaccharomyces pombe*. *Trends Genet* **21**: 450-456

Martin-Lluesma S, Stucke VM, Nigg EA (2002) Role of Hec1 in spindle checkpoint signaling and kinetochore recruitment of Mad1/Mad2. *Science* **297**: 2267-2270

Mastrorarde DN, McDonald KL, Ding R, McIntosh JR (1993) Interpolar spindle microtubules in PTK cells. *J Cell Biol* **123**: 1475-1489

Mather K (1939) Crossing over and Heterochromatin in the X Chromosome of *Drosophila Melanogaster*. *Genetics* **24**: 413-435

McAinsh AD, Tytell JD, Sorger PK (2003) Structure, function, and regulation of budding yeast kinetochores. *Annu Rev Cell Dev Biol* **19**: 519-539

McCarroll RM, Fangman WL (1988) Time of replication of yeast centromeres and telomeres. *Cell* **54**: 505-513

McCollum D (2002) First things first: spindle orientation and mitotic progression. *Nat Cell Biol* **4**: E225-226

McDonald KL, O'Toole ET, Mastrorarde DN, McIntosh JR (1992) Kinetochore microtubules in PTK cells. *J Cell Biol* **118**: 369-383

Mehta GD, Agarwal MP, Ghosh SK (2010) Centromere identity: a challenge to be faced. *Mol Genet Genomics* **284**: 75-94

Meraldi P, McAinsh AD, Rheinbay E, Sorger PK (2006) Phylogenetic and structural analysis of centromeric DNA and kinetochore proteins. *Genome Biol* **7**: R23

Miranda JJ, De Wulf P, Sorger PK, Harrison SC (2005) The yeast DASH complex forms closed rings on microtubules. *Nat Struct Mol Biol* **12**: 138-143

Mishra PK, Baum M, Carbon J (2007) Centromere size and position in *Candida albicans* are evolutionarily conserved independent of DNA sequence heterogeneity. *Mol Genet Genomics* **278**: 455-465

Mizuguchi G, Xiao H, Wisniewski J, Smith MM, Wu C (2007) Nonhistone Scm3 and histones CenH3-H4 assemble the core of centromere-specific nucleosomes. *Cell* **129**: 1153-1164

Monen J, Maddox PS, Hyndman F, Oegema K, Desai A (2005) Differential role of CENP-A in the segregation of holocentric *C. elegans* chromosomes during meiosis and mitosis. *Nat Cell Biol* **7**: 1248-1255

Moreno-Moreno O, Torras-Llort M, Azorín F (2006) Proteolysis restricts localization of CID, the centromere-specific histone H3 variant of *Drosophila*, to centromeres. *Nucleic Acids Res* **34**: 6247-6255

Morgenstern B (1999) DIALIGN 2: improvement of the segment-to-segment approach to multiple sequence alignment. *Bioinformatics* **15**: 211-218

Motamedi MR, Verdel A, Colmenares SU, Gerber SA, Gygi SP, Moazed D (2004) Two RNAi complexes, RITS and RDRC, physically interact and localize to noncoding centromeric RNAs. *Cell* **119**: 789-802

Musacchio A, Salmon ED (2007) The spindle-assembly checkpoint in space and time. *Nat Rev Mol Cell Biol* **8**: 379-393

Mythreye K, Bloom KS (2003) Differential kinetochore protein requirements for establishment versus propagation of centromere activity in *Saccharomyces cerevisiae*. *J Cell Biol* **160**: 833-843

Nagaki K, Cheng Z, Ouyang S, Talbert PB, Kim M, Jones KM, Henikoff S, Buell CR, Jiang J (2004) Sequencing of a rice centromere uncovers active genes. *Nat Genet* **36**: 138-145

Nasmyth K (2001) A prize for proliferation. *Cell* **107**: 689-701

Noble SM, Johnson AD (2005) Strains and strategies for large-scale gene deletion studies of the diploid human fungal pathogen *Candida albicans*. *Eukaryotic Cell* **4**: 298-309

Nogales E, Ramey VH (2009) Structure-function insights into the yeast Dam1 kinetochore complex. *Journal of Cell Science* **122**: 3831-3836

Notredame C, Higgins DG, Heringa J (2000) T-Coffee: A novel method for fast and accurate multiple sequence alignment. *J Mol Biol* **302**: 205-217

NOVITSKI E (1955) Genetic measures of centromere activity in *Drosophila melanogaster*. *J Cell Physiol Suppl* **45**: 151-169

Oegema K, Desai A, Rybina S, Kirkham M, Hyman AA (2001) Functional analysis of kinetochore assembly in *Caenorhabditis elegans*. *J Cell Biol* **153**: 1209-1226

Ohkuma M, Kobayashi K, Kawai S, Hwang CW, Ohta A, Takagi M (1995) Identification of a centromeric activity in the autonomously replicating TRA region allows improvement of the host-vector system for *Candida maltosa*. *Mol Gen Genet* **249**: 447-455

Ohzeki J, Nakano M, Okada T, Masumoto H (2002) CENP-B box is required for de novo centromere chromatin assembly on human alphoid DNA. *J Cell Biol* **159**: 765-775

Okada T, Ohzeki J, Nakano M, Yoda K, Brinkley WR, Larionov V, Masumoto H (2007) CENP-B controls centromere formation depending on the chromatin context. *Cell* **131**: 1287-1300

Oliferenko S, Balasubramanian MK (2002) Astral microtubules monitor metaphase spindle alignment in fission yeast. *Nat Cell Biol* **4**: 816-820

Palmer DK, O'Day K, Wener MH, Andrews BS, Margolis RL (1987) A 17-kD centromere protein (CENP-A) copurifies with nucleosome core particles and with histones. *J Cell Biol* **104**: 805-815

Palmer RE, Sullivan DS, Huffaker T, Koshland D (1992) Role of astral microtubules and actin in spindle orientation and migration in the budding yeast, *Saccharomyces cerevisiae*. *J Cell Biol* **119**: 583-593

Pearson CG, Yeh E, Gardner M, Odde D, Salmon ED, Bloom K (2004) Stable kinetochore-microtubule attachment constrains centromere positioning in metaphase. *Curr Biol* **14**: 1962-1967

Perepnikhatka V, Fischer FJ, Niimi M, Baker RA, Cannon RD, Wang YK, Sherman F, Rustchenko E (1999) Specific chromosome alterations in fluconazole-resistant mutants of *Candida albicans*. *J Bacteriol* **181**: 4041-4049

Pidoux AL, Richardson W, Allshire RC (2003) Sim4: a novel fission yeast kinetochore protein required for centromeric silencing and chromosome segregation. *J Cell Biol* **161**: 295-307

Polizzi C, Clarke L (1991) The chromatin structure of centromeres from fission yeast: differentiation of the central core that correlates with function. *J Cell Biol* **112**: 191-201

Poláková S, Blume C, Zárate JA, Mentel M, Jørck-Ramberg D, Stenderup J, Piskur J (2009) Formation of new chromosomes as a virulence mechanism in yeast *Candida glabrata*. *Proc Natl Acad Sci U S A* **106**: 2688-2693

Przewloka MR, Zhang W, Costa P, Archambault V, D'Avino PP, Lilley KS, Laue ED, McAinsh AD, Glover DM (2007) Molecular analysis of core kinetochore composition and assembly in *Drosophila melanogaster*. *PLoS One* **2**: e478

Pujol C, Daniels KJ, Lockhart SR, Srikantha T, Radke JB, Geiger J, Soll DR (2004) The closely related species *Candida albicans* and *Candida dubliniensis* can mate. *Eukaryot Cell* **3**: 1015-1027

Pâques F, Haber JE (1999) Multiple pathways of recombination induced by double-strand breaks in *Saccharomyces cerevisiae*. *Microbiol Mol Biol Rev* **63**: 349-404

Rhoades MM, Vilkomerson H (1942) On the Anaphase Movement of Chromosomes. *Proc Natl Acad Sci U S A* **28**: 433-436

Rockmill B, Voelkel-Meiman K, Roeder GS (2006) Centromere-proximal crossovers are associated with precocious separation of sister chromatids during meiosis in *Saccharomyces cerevisiae*. *Genetics* **174**: 1745-1754

Round EK, Flowers SK, Richards EJ (1997) *Arabidopsis thaliana* centromere regions: genetic map positions and repetitive DNA structure. *Genome Res* **7**: 1045-1053

Roy B, Burrack LS, Lone MA, Berman J, Sanyal K (2011) CaMtw1, a member of the evolutionarily conserved Mis12 kinetochore protein family, is required for efficient inner kinetochore assembly in the pathogenic yeast *Candida albicans*. *Mol Microbiol*

Régnier V, Vagnarelli P, Fukagawa T, Zerjal T, Burns E, Trouche D, Earnshaw W, Brown W (2005) CENP-A is required for accurate chromosome segregation and sustained kinetochore association of BubR1. *Mol Cell Biol* **25**: 3967-3981

Sanchez-Pulido L, Pidoux AL, Ponting CP, Allshire RC (2009) Common ancestry of the CENP-A chaperones Scm3 and HJURP. *Cell* **137**: 1173-1174

Sanyal K, Baum M, Carbon J (2004) Centromeric DNA sequences in the pathogenic yeast *Candida albicans* are all different and unique. *Proc Natl Acad Sci U S A* **101**: 11374-11379

Sanyal K, Carbon J (2002) The CENP-A homolog CaCse4p in the pathogenic yeast *Candida albicans* is a centromere protein essential for chromosome transmission. *Proc Natl Acad Sci U S A* **99**: 12969-12974

Sazer S (2005) Nuclear envelope: nuclear pore complexity. *Curr Biol* **15**: R23-26

Schueler MG, Higgins AW, Rudd MK, Gustashaw K, Willard HF (2001) Genomic and genetic definition of a functional human centromere. *Science* **294**: 109-115

Schueler MG, Sullivan BA (2006) Structural and functional dynamics of human centromeric chromatin. *Annu Rev Genomics Hum Genet* **7**: 301-313

Schuh M, Lehner CF, Heidmann S (2007) Incorporation of *Drosophila* CID/CENP-A and CENP-C into centromeres during early embryonic anaphase. *Curr Biol* **17**: 237-243

Sekulic N, Bassett EA, Rogers DJ, Black BE (2010) The structure of (CENP-A-H4)₂ reveals physical features that mark centromeres. *Nature* **467**: 347-351

Selmecki A, Forche A, Berman J (2006) Aneuploidy and isochromosome formation in drug-resistant *Candida albicans*. *Science* **313**: 367-370

Selmecki AM, Dulmage K, Cowen LE, Anderson JB, Berman J (2009) Acquisition of aneuploidy provides increased fitness during the evolution of antifungal drug resistance. *PLoS Genet* **5**: e1000705

Shelby RD, Vafa O, Sullivan KF (1997) Assembly of CENP-A into centromeric chromatin requires a cooperative array of nucleosomal DNA contact sites. *J Cell Biol* **136**: 501-513

Shi J, Wolf SE, Burke JM, Presting GG, Ross-Ibarra J, Dawe RK (2010) Widespread gene conversion in centromere cores. *PLoS Biol* **8**: e1000327

Siddharthan R (2006) Sigma: multiple alignment of weakly-conserved non-coding DNA sequence. *BMC Bioinformatics* **7**: 143

Slatis HM (1955) A Reconsideration of the Brown-Dominant Position Effect. *Genetics* **40**: 246-251

Soll DR (2002) *Candida* commensalism and virulence: the evolution of phenotypic plasticity. *Acta Trop* **81**: 101-110

Staib P, Morschhäuser J (1999) Chlamydospore formation on Staib agar as a species-specific characteristic of *Candida dubliniensis*. *Mycoses* **42**: 521-524

Steiner NC, Clarke L (1994) A novel epigenetic effect can alter centromere function in fission yeast. *Cell* **79**: 865-874

Straight AF, Marshall WF, Sedat JW, Murray AW (1997) Mitosis in living budding yeast: anaphase A but no metaphase plate. *Science* **277**: 574-578

Sugiyama T, Cam H, Verdel A, Moazed D, Grewal SI (2005) RNA-dependent RNA polymerase is an essential component of a self-enforcing loop coupling heterochromatin assembly to siRNA production. *Proc Natl Acad Sci U S A* **102**: 152-157

Sugiyama T, Cam HP, Sugiyama R, Noma K, Zofall M, Kobayashi R, Grewal SI (2007) SHREC, an effector complex for heterochromatic transcriptional silencing. *Cell* **128**: 491-504

Sullivan BA, Karpen GH (2004) Centromeric chromatin exhibits a histone modification pattern that is distinct from both euchromatin and heterochromatin. *Nat Struct Mol Biol* **11**: 1076-1083

Sullivan KF, Hechenberger M, Masri K (1994) Human CENP-A contains a histone H3 related histone fold domain that is required for targeting to the centromere. *J Cell Biol* **127**: 581-592

Sun X, Wahlstrom J, Karpen G (1997) Molecular structure of a functional *Drosophila* centromere. *Cell* **91**: 1007-1019

Symington LS, Petes TD (1988) Meiotic recombination within the centromere of a yeast chromosome. *Cell* **52**: 237-240

Takahashi K, Chen ES, Yanagida M (2000) Requirement of Mis6 centromere connector for localizing a CENP-A-like protein in fission yeast. *Science* **288**: 2215-2219

Takahashi K, Takayama Y, Masuda F, Kobayashi Y, Saitoh S (2005) Two distinct pathways responsible for the loading of CENP-A to centromeres in the fission yeast cell cycle. *Philos Trans R Soc Lond B Biol Sci* **360**: 595-606; discussion 606-597

Talbert PB, Henikoff S (2010) Centromeres convert but don't cross. *PLoS Biol* **8**: e1000326

Tanaka K, Kitamura E, Tanaka TU (2010) Live-cell analysis of kinetochore-microtubule interaction in budding yeast. *Methods* **51**: 206-213

Tanaka TU (2010) Kinetochore-microtubule interactions: steps towards bi-orientation. *EMBO J* **29**: 4070-4082

Thakur J, Sanyal K (2011) The essentiality of the fungal specific Dam1 complex is correlated with one kinetochore one microtubule interaction present throughout the cell cycle, independent of the nature of a centromere. *Eukaryot Cell*

Theesfeld CL, Irazoqui JE, Bloom K, Lew DJ (1999) The role of actin in spindle orientation changes during the *Saccharomyces cerevisiae* cell cycle. *J Cell Biol* **146**: 1019-1032

Thompson JD, Higgins DG, Gibson TJ (1994) CLUSTAL W: improving the sensitivity of progressive multiple sequence alignment through sequence weighting, position-specific gap penalties and weight matrix choice. *Nucleic Acids Res* **22**: 4673-4680

Tomonaga T, Matsushita K, Yamaguchi S, Oohashi T, Shimada H, Ochiai T, Yoda K, Nomura F (2003) Overexpression and mistargeting of centromere protein-A in human primary colorectal cancer. *Cancer Res* **63**: 3511-3516

Ventura M, Weigl S, Carbone L, Cardone MF, Misceo D, Teti M, D'Addabbo P, Wandall A, Björck E, de Jong PJ, She X, Eichler EE, Archidiacono N, Rocchi M (2004) Recurrent sites for new centromere seeding. *Genome Res* **14**: 1696-1703

Verdel A, Jia S, Gerber S, Sugiyama T, Gygi S, Grewal SI, Moazed D (2004) RNAi-mediated targeting of heterochromatin by the RITS complex. *Science* **303**: 672-676

Vernis L, Abbas A, Chasles M, Gaillardin CM, Brun C, Huberman JA, Fournier P (1997) An origin of replication and a centromere are both needed to establish a replicative plasmid in the yeast *Yarrowia lipolytica*. *Mol Cell Biol* **17**: 1995-2004

Vernis L, Poljak L, Chasles M, Uchida K, Casarégola S, Käs E, Matsuoka M, Gaillardin C, Fournier P (2001) Only centromeres can supply the partition system required for ARS function in the yeast *Yarrowia lipolytica*. *J Mol Biol* **305**: 203-217

Voullaire LE, Slater HR, Petrovic V, Choo KH (1993) A functional marker centromere with no detectable alpha-satellite, satellite III, or CENP-B protein: activation of a latent centromere? *Am J Hum Genet* **52**: 1153-1163

Waye JS, Durfy SJ, Pinkel D, Kenwrick S, Patterson M, Davies KE, Willard HF (1987) Chromosome-specific alpha satellite DNA from human chromosome 1: hierarchical structure and genomic organization of a polymorphic domain spanning several hundred kilobase pairs of centromeric DNA. *Genomics* **1**: 43-51

Weidtkamp-Peters S, Rahn HP, Cardoso MC, Hemmerich P (2006) Replication of centromeric heterochromatin in mouse fibroblasts takes place in early, middle, and late S phase. *Histochem Cell Biol* **125**: 91-102

Welburn JP, Grishchuk EL, Backer CB, Wilson-Kubalek EM, Yates JR, Cheeseman IM (2009) The human kinetochore Ska1 complex facilitates microtubule depolymerization-coupled motility. *Dev Cell* **16**: 374-385

Westermann S, Avila-Sakar A, Wang HW, Niederstrasser H, Wong J, Drubin DG, Nogales E, Barnes G (2005) Formation of a dynamic kinetochore-microtubule interface through assembly of the Dam1 ring complex. *Molecular Cell* **17**: 277-290

Westermann S, Cheeseman IM, Anderson S, Yates JR, Drubin DG, Barnes G (2003) Architecture of the budding yeast kinetochore reveals a conserved molecular core. *J Cell Biol* **163**: 215-222

Westermann S, Wang HW, Avila-Sakar A, Drubin DG, Nogales E, Barnes G (2006) The Dam1 kinetochore ring complex moves processively on depolymerizing microtubule ends. *Nature* **440**: 565-569

Wey SB, Mori M, Pfaller MA, Woolson RF, Wenzel RP (1988) Hospital-acquired candidemia. The attributable mortality and excess length of stay. *Arch Intern Med* **148**: 2642-2645

Wieland G, Orthaus S, Ohndorf S, Diekmann S, Hemmerich P (2004) Functional complementation of human centromere protein A (CENP-A) by Cse4p from *Saccharomyces cerevisiae*. *Mol Cell Biol* **24**: 6620-6630

Willard HF (1985) Chromosome-specific organization of human alpha satellite DNA. *Am J Hum Genet* **37**: 524-532

Willard HF (1990) Centromeres of mammalian chromosomes. *Trends Genet* **6**: 410-416

Williams BC, Murphy TD, Goldberg ML, Karpen GH (1998) Neocentromere activity of structurally acentric mini-chromosomes in *Drosophila*. *Nat Genet* **18**: 30-37

Williams JS, Hayashi T, Yanagida M, Russell P (2009) Fission yeast Scm3 mediates stable assembly of Cnp1/CENP-A into centromeric chromatin. *Mol Cell* **33**: 287-298

Wilson RB, Davis D, Mitchell AP (1999) Rapid hypothesis testing with *Candida albicans* through gene disruption with short homology regions. *J Bacteriol* **181**: 1868-1874

Winey M, Mamay CL, O'Toole ET, Mastrorarde DN, Giddings TH, McDonald KL, McIntosh JR (1995) Three-dimensional ultrastructural analysis of the *Saccharomyces cerevisiae* mitotic spindle. *J Cell Biol* **129**: 1601-1615

Wong AK, Rattner JB (1988) Sequence organization and cytological localization of the minor satellite of mouse. *Nucleic Acids Res* **16**: 11645-11661

Wong NC, Wong LH, Quach JM, Canham P, Craig JM, Song JZ, Clark SJ, Choo KH (2006) Permissive transcriptional activity at the centromere through pockets of DNA hypomethylation. *PLoS Genet* **2**: e17

Yamagata K, Yamazaki T, Miki H, Ogonuki N, Inoue K, Ogura A, Baba T (2007) Centromeric DNA hypomethylation as an epigenetic signature discriminates between germ and somatic cell lineages. *Dev Biol* **312**: 419-426

Yan H, Ito H, Nobuta K, Ouyang S, Jin W, Tian S, Lu C, Venu RC, Wang GL, Green PJ, Wing RA, Buell CR, Meyers BC, Jiang J (2006) Genomic and genetic characterization of rice Cen3 reveals extensive transcription and evolutionary implications of a complex centromere. *Plant Cell* **18**: 2123-2133

Zeitlin SG, Baker NM, Chapados BR, Soutoglou E, Wang JY, Berns MW, Cleveland DW (2009) Double-strand DNA breaks recruit the centromeric histone CENP-A. *Proc Natl Acad Sci U S A* **106**: 15762-15767

Zeng K, de las Heras JI, Ross A, Yang J, Cooke H, Shen MH (2004) Localisation of centromeric proteins to a fraction of mouse minor satellite DNA on a mini-chromosome in human, mouse and chicken cells. *Chromosoma* **113**: 84-91

Zhang W, Lee HR, Koo DH, Jiang J (2008) Epigenetic modification of centromeric chromatin: hypomethylation of DNA sequences in the CENH3-associated chromatin in *Arabidopsis thaliana* and maize. *Plant Cell* **20**: 25-34

Zhong CX, Marshall JB, Topp C, Mroczek R, Kato A, Nagaki K, Birchler JA, Jiang J, Dawe RK (2002) Centromeric retroelements and satellites interact with maize kinetochore protein CENH3. *Plant Cell* **14**: 2825-2836

Zwick ME, Salstrom JL, Langley CH (1999) Genetic variation in rates of nondisjunction: Association of two naturally occurring polymorphisms in the chromokinesin nod with increased rates of nondisjunction in *Drosophila melanogaster*. *Genetics* **152**: 1605-1614

List of publications

- 1.) Padmanabhan S*, Thakur J*, Siddharthan R, Sanyal K (2008) Rapid evolution of Cse4p-rich centromeric DNA sequences in closely related pathogenic yeasts, *Candida albicans* and *Candida dubliniensis*. *Proc Natl Acad Sci U S A* 105: 19797-19802.
- 2.) Thakur J, Sanyal K (2011) The essentiality of the fungal specific Dam1 complex is correlated with one kinetochore one microtubule interaction present throughout the cell cycle, independent of the nature of a centromere. *Eukaryot Cell*. In Press
- 3.) Thakur J, Sanyal K (2011) Dynamics of centromere and neocentromere formation in *C. albicans*. Manuscript under preparation.
- 4.) Thakur J, Sanyal K (2011) A coordinated interdependent protein circuitry stabilizes kinetochore ensemble that protects CENP-A in human pathogenic yeast *Candida albicans*. Manuscript under revision.

* Equal contribution